



Metrology Institute of the Republic of
Slovenia

University of Maribor
Faculty of Mechanical Engineering
Laboratory for Production Measurement

EUROMET Key Comparison, EUROMET.L-K7
(EUROMET Project 882)
Calibration of line scales
Final Report

Contents

| | | |
|-------------|--|-----|
| 1 | INTRODUCTION | 3 |
| 2 | ORGANISATION | 4 |
| 2.1 | Participants..... | 4 |
| 2.2 | Linking laboratories | 8 |
| 2.3 | Form of comparison..... | 8 |
| 2.4 | Circulation of the artefact and performance of the measurements | 8 |
| 2.5 | Transport of the artefacts | 10 |
| 3 | THE ARTEFACT | 11 |
| 3.1 | Description of the artefact..... | 11 |
| 3.2 | Fixing the artefact..... | 12 |
| 4 | MEASUREMENT INSTRUCTIONS | 13 |
| 4.1 | Traceability | 13 |
| 4.2 | Measurand..... | 13 |
| 4.3 | Measurement instructions | 14 |
| 4.4 | Measurement uncertainty | 14 |
| 5 | MEASUREMENT EQUIPMENT AND METHODS USED BY THE PARTICIPANTS..... | 17 |
| 6 | STABILITY OF THE STANDARDS..... | 20 |
| 6.1 | Stability of the total line scale length..... | 20 |
| 6.2 | Stability of single line centres | 21 |
| 6.3 | Impact of line scale instability | 24 |
| 7 | ANALYSIS OF THE RESULTS..... | 25 |
| 8 | MEASUREMENT RESULTS..... | 26 |
| 8.1 | Measurement results- Group 1 | 26 |
| 8.2 | Measurement results – Group 2 | 28 |
| 8.3 | Correction of the original results | 32 |
| 8.4 | Link between the groups | 33 |
| 8.5 | Intercomparison results for linked groups considering line scale stability... | 34 |
| 9 | CONCLUSIONS..... | 53 |
| 10 | ACKNOWLEDGMENT | 53 |
| 11 | REFERENCES | 53 |
| APPENDIX 1: | INTERCOMPARISON RESULTS FOR THE CASE OF SEPARATE TREATMENT OF GROUPS 1 AND 2 (WITHOUT LINK)..... | 54 |
| APPENDIX 2: | DESCRIPTIONS OF MEASUREMENT SETUPS AND METHODS AS REPORTED BY THE PARTICIPANTS..... | 75 |
| APPENDIX 3: | REPORTED UNCERTAINTY BUDGETS | 128 |

1 Introduction

- 1.1 At its meeting in October 2005, the TC for Length identified several EUROMET key comparisons in the field of dimensional metrology. In particular, it decided that a key comparison on line standards shall be carried out. This comparison follows the Nano3 comparison (WGDM-7 preliminary comparison on nanometrology).
- 1.2 Due to the large number of the participants, it has been decided to have 2 groups in the project. The participants for the 2 groups were chosen in accordance with their geographical position (in order to minimize travel times and expenses for the transportation of the standards). Linking laboratories between the groups were chosen among participants in Nano3 project.
- 1.3 The standards for the comparison were defined at the TCL meeting in October 2005. It was decided that only one line scale of 100 mm with line distance of 0,1 mm would be measured. The 2 groups have got equal standards offered (and produced) by NPL.
- 1.4 The pilot laboratory for both loops of the comparison was Metrology Institute of the Republic of Slovenia (MIRS/UM-FS). In addition, METAS (CH) and NPL (UK) were appointed as linking laboratories between the 2 groups.
- 1.5 A goal of the EUROMET key comparisons for topics in dimensional metrology is to demonstrate the equivalence of routine calibration services offered by NMIs to clients, as listed in Appendix C of the Mutual Recognition Agreement (MRA) [BIPM, 1999]. Therefore, participants in this comparison agreed to use the same apparatus and methods as routinely applied to client artefacts.

2 Organisation

2.1 Participants

The project began with 31 participants – 22 from EURAMET, 4 from SIM (3 NORAMET, 1 SURAMET), 2 from COOMET and 3 from APMP. Due to the large number of participants they were divided into two groups (Table 1 and Table 2). During the project, Norwegian Metrology Service (JV) and FPS Economy - DG Quality and Safety Metrology Division (SMD) from Belgium cancel their participation due to problems with equipment. In year 2006 Thailand sent a request to participate and the request was approved at the TCL meeting in October 2006. Thailand was placed in group 2.

Table 1: Participants in the group 1

| Laboratory | Address | Contact person/tel/fax/e-mail |
|------------|---|---|
| BEV | Bundesamt für Eich – und Vermessungswesen Arltgasse 35 AT-1160 Wien Austria | Michael Matus +43 1 49 110 540 +43 1 49 20 875 michael.matus@bev.gv.at |
| DZM-FSB | University of Zagreb Faculty of Mechanical Eng. and Naval Architecture Ivana Lucica 5 HR-10000 Zagreb Croatia | Vedran Mudronja +385 1 616 83 35 +385 1 616 85 99 vedran.mudronja@fsb.hr |
| GUM | Central Office of Measures ul. Elektoralna 2 PL-00950 Warszawa Poland | Zbigniew Ramotowski +48 22 581 9543 +48 22 620 8378 length@gum.gov.pl |
| INM | National Institute of Metrology Sos. Vitan-Barzesti 11 Sector 4 Bucharesti 042122-RO Romania | Alexandru Duta +40 21 334 55 20 +40 21 334 55 33 alexandru.duta@inm.ro |
| JV | Norwegian Metrology Service Fetvejen 99 NO-2007 Kjeller Norway | Helge Karlsson +47 64 84 84 84 +47 64 84 84 85 helge.karlsson@justervesenet.no |
| LNMC | Latvian National Metrology Centre 157, K. Valdemara Str. LV-1013 Riga Latvia | Edite Turka +371 7 362 086 +371 7 362 805 edite.turka@lnmc.lv |
| METAS | Bundesamt für Metrologie Lindenweg 50 CH-3084 Wabern Switzerland | Felix Meli +41 31 32 33 346 +41 31 32 33 210 felix.meli@metas.ch |
| MIKES | Centre for Metrology and Accreditation Tekniikantie 1 P.O. Box 9 FI-02151 Espoo Finland | Antti Lassila +358 10 6054 413 +358 10 6054 499 antti.lassila@mikes.fi |
| MIRS | University of Maribor Faculty of Mechanical Engineering Smetanova 17 SI-2000 Maribor Slovenia | Bojan Acko +386 2 220 7581 +386 2 220 7990 bojan.acko@uni-mb.si |

| Laboratory | Address | Contact person/tel/fax/e-mail |
|------------|--|---|
| NCM | National Centre of Metrology 52B G.M. Dimitrov Blvd. BG-1040 Sofia Bulgaria | Veselin Gavalyugov +359 2 97 02 760 +359 2 97 02 719 v.gavalyugov@bim.government.bg |
| NML | National Metrology Laboratory Enterprise Ireland Campus Glasnevin IE-Dublin 9 Ireland | Howard McQuoid +353 1 808 2657 +353 1 808 2026 howard.mcquoid@enterprise-ireland.com |
| NPL | National Physical Laboratory Hampton Road Teddington, Middlesex TW 11 OLW United Kingdom | Michael McCarthy +44 20 8943 6655 +44 20 8614 0453 michael.mccarthy@npl.co.uk |
| NSCIM | National Scientific Center "Institute of metrology" Myronosytskaja st., 42, Kharkov, 61002, Ukraine | Valentin Solovyov +380 57 704-98-77 +380 57 700-34-47 solovyov@metrology.kharkov.ua |
| OMH | National Office of Measures Németvölgyi út 37-39 H-1124 Budapest XII. Hungary | Edit Banreti +36 1 458 59 97 +36 1 458 59 27 e.banreti@omh.hu |
| PTB | Physikalisch-Technische Bundesanstalt Department 5.2, Length and Angle Metrology Bundesallee 100 DE-38116 Braunschweig Germany | Harald Bosse +49 531 5925200 +49 531 5925205 harald.bosse@ptb.de |
| SMU | Slovak Institute of Metrology Karloveská 63 SK-842 55 Bratislava Slovakia | Roman Fira +421 2 602 94 321 +421 2 654 29 592 fira@smu.gov.sk |
| ZMDM | Bureau of Measures and Precious Metals Mike Alasa 14 YU - 11 000 Beograd Serbia | Slobodan Zelenika +381 11 20 24 418 +381 11 21 81 668 zelenika@szmdm.sv.gov.yu |

Changes in group 1 during the project:

| | | |
|-----|--|--|
| JV | Norwegian Metrology Service Fetvejen 99 NO-2007 Kjeller Norway | Participation cancelled |
| CMI | Czech Metrology Institute V Botanice 4 CZ 150 72 Praha 5 Czech Republic | After measuring in Group 2 (October 06) they improved measurement capabilities. New measurements in Group 1 were approved by Euromet TCL. Results in group 2 were cancelled. |

Table 2: Participants in the group 2

| Laboratory | Address | Contact person/tel/fax/e-mail |
|---------------|---|--|
| CEM | Centro Espanol de Metrologia Alfar, 2 ES-28760 Tres Cantos (Madrid) Spain | Emilio Prieto +34 91 807 47 16 +34 91 807 48 07/809 eprieto@cem.mityc.es |
| CENAM | CENAM-Centro Nacional de Metrologia Division de Metrologia Dimensional Km 4,5 Carretera a Los Cues, El Marqués 76241 Queretaro Mexico | Carlos Colin Miguel Viliesid Alonso +52 442 211 05 74 +52 442 211 05 77 ccolin@cenam.mx mviliesi@cenam.mx |
| CMI | Czech Metrology Institute V Botanice 4 CZ 150 72 Praha 5 Czech Republic | Petr Balling +420 257 288 326 +420 257 328 077 pballing@cmi.cz |
| EIM | Hellenic Institute of Metrology Industrial Area of Thessaloniki Block 45 GR-57 022 Sindos Thessaloniki Greece | Christos Bandis +30 2310 56 99 99 +30 2310 56 99 96 bandis@eim.org.gr |
| INMETRO | Instituto Nacional de Metrologia, Normalização e Qualidade Industrial Laboratório de Metrologia Dimensional - Lamin - Prédio 3 Av. Nossa Senhora das Graças, 50 Xerém - 25250-020 Duque de Caxias Rio de Janeiro, Brazil | João Antônio Pires Alves +55 21 2679 9107 +55 21 2679 1505 jaalves@inmetro.gov.br |
| INRIM | Instituto Nazionale di Ricerca Metrologica (INRIM) Strada delle Cacce, 73 IT-10135 Torino Italy | Gian Bartolo Picotto +39 011 3977 469/473 +39 011 3977 459 g.picotto@inrim.it |
| METAS | Bundesamt für Metrologie Lindenweg 50 CH-3084 Wabern Switzerland | Felix Meli +41 31 32 33 346 +41 31 32 33 210 felix.meli@metas.ch |
| NIM | National Institute of Metrology Length Division Beisanhuandonglu 18 100013 Beijing China | Sitian Gao Tel: +86 10 84251574 Fax: +86 10 64218703 gaost@nim.ac.cn |
| NIST | National Institute of Standards and Technology Manufacturing Engineering Laboratory Precision Engineering Division Nano-Scale Metrology Group 100 Bureau Drive, Stop 8212 Bldg. 220, Rm A117 Gaithersburg, Maryland 20899-8212 USA | William B. Penzes +301 975 3477 +301 869 0822 william.penzes@nist.gov |
| NMi-VSL BV | NMi Van Swinden Laboratorium B.V. Thijssseweg 11 P.O. Box 654 NL-2600 AR Delft The Netherlands | Gerard Kotte +31 15 269 16 01 +31 15 261 29 71 gkotte@nmi.nl |

| Laboratory | Address | Contact person/tel/fax/e-mail |
|-----------------|---|--|
| NPL | National Physical Laboratory Hampton Road Teddington, Middlesex TW 11 OLW United Kingdom | Michael McCarthy +44 20 8943 6655 +44 20 8614 0453 michael.mccarthy@npl.co.uk |
| NPLI | National Physical Laboratory Physico-Mechanical Standards Length & Dimension Standards New Delhi -110012 India | R.P. Singhal +91-11-25732965 +91-11-25732965 singhal@mail.nplindia.ernet.in |
| NRC | Institute for National Measurement Standards (INMS) National Research Council Canada (NRC) 1200 Montreal Road Ottawa, ON, Canada K1A 0R6 | Jim Pekelsky +613 993 7578 +613 952 1394 jim.pekelsky@nrc.ca |
| SMD | FPS Economy DG Quality and Safety Metrology Division (SMD) Boulevard du Roi Albert II, 16 BE 1000 Brussels Belgium | Hugo Piree +32 2 277 7610 +32 2 277 5405 hugo.piree@mineco.fgov.be |
| A*Star - NMC | National Metrology Centre A*Star 1 Science Park Drive Singapore 118221 | Siew Leng Tan +65 6279 1938 +65 6279 1994 tan_siew_leng@nmc.a-star.edu.sg |
| VNIIM | VNIIM - All-Russian Institute for Metrology 19 Moscovsky prosp. RU - 198005 St. Petersburg Russia | Konstantin V.Chekirda +7 812 323 9664 +7 812 713 0114 K.V.Chekirda@vniim.ru |

Changes in group 2 during the project:

| | | |
|------|--|---|
| SMD | FPS Economy DG Quality and Safety Metrology Division (SMD) Boulevard du Roi Albert II, 16 BE 1000 Brussels Belgium | Participation cancelled |
| CMI | Czech Metrology Institute V Botanice 4 CZ 150 72 Praha 5 Czech Republic | Results in group 2 were cancelled New measurements in group 1 |
| NIMT | National Institute of Metrology Thailand Department of Dimensional Metrology 3/5 Moo 3, Klong 5, Klongluang, Pathumthani 12120 Thailand | NEW PARTICIPANT (approved at Euromet TCL meeting 2006) Contact: Anusorn Tonmueanwai +662 577 5100 ext 1216 +662 577 3658 / 662 5773659 anusorn@nimt.or.th |

2.2 *Linking laboratories*

Linking laboratories between the two groups were METAS – CH and NPL – UK. The linking laboratories measured both artefacts in the beginning and at the end of the loop. Their measurements were also used for evaluating the stability of the artefacts.

2.3 *Form of comparison*

2.3.1 The comparison was performed in a ‘circular’ form in both groups. The artefact was circulated within a group of laboratories. Before sending it to the non-EU participants (in the end of each loop), they were returned to the pilot laboratory in order to prepare the necessary ATA Carnet and other forms for the custom formalities.

2.3.2 All results were communicated directly to the pilot laboratory.

2.4 *Circulation of the artefact and performance of the measurements*

2.4.1 The participating laboratories were asked to specify a preferred timetable slot for their measurements of the artefact - the timetables given below have been drawn up taking these preferences into account.

Table 3: Time schedule for the group 1

| Laboratory | Country | Date |
|------------|----------------|----------------|
| MIRS | Slovenia | July 2006 |
| METAS | Switzerland | August 2006 |
| NPL | United kingdom | September 2006 |
| OMH | Hungary | October 2006 |
| BEV | Austria | November 2006 |
| SMU | Slovakia | December 2006 |
| PTB | Germany | January 2007 |
| GUM | Poland | February 2007 |
| MIKES | Finland | March 2007 |
| JV | Norway | April 2007 |
| LNMC | Latvia | May 2007 |
| NML | Ireland | June 2007 |
| NCM | Bulgaria | July 2007 |
| INM | Romania | August 2007 |
| ZMDM | Serbia | September 2007 |
| DZM-FSB | Croatia | October 2007 |
| NSCIM | Ukraine | November 2007 |
| METAS | Switzerland | December 2007 |
| NPL | United kingdom | January 2008 |

Table 4: Time schedule for the group 2

| Laboratory | Country | Date |
|------------|----------------|----------------|
| METAS | Switzerland | August 2006 |
| NPL | United kingdom | September 2006 |
| CMI | Czech Republic | October 2006 |
| EIM | Greece | November 2006 |
| INRIM | Italy | December 2006 |
| NMi-VSL | Netherlands | January 2007 |
| CEM | Spain | February 2007 |
| SMD | Belgium | March 2007 |
| INMETRO | Brazil | April 2007 |
| CENAM | Mexico | May 2007 |
| NIST | USA | June 2007 |
| NRC | Canada | July 2007 |
| A*Star-NMC | Singapore | August 2007 |
| NIM | China | September 2007 |
| NPLI | India | October 2007 |
| NPL | United kingdom | November 2007 |
| METAS | Switzerland | December 2007 |
| VNIIM | Russia | January 2008 |

2.4.2 Each laboratory had one month for calibration and transportation. With its confirmation to participate, each laboratory has confirmed that it was capable to perform the measurements in the time allocated to it. In this way it was assured, that the artefact arrived in the country of the next participant at the beginning of the next month. However, due to many customs problems (ATA not stamped, ATA lost, substitutional ATA, special arrangements – temporary imports for countries without ATA agreement, ...), cancellation of participation, new laboratory, additional measurement in another group, some measurements were not performed in the original time schedule. Changes are indicated in Table 5 and 6.

Table 5: Changes in measurement schedule in group 1

| Laboratory | Country | Date |
|------------|----------------|---------------|
| ZMDM | Serbia | October 2007 |
| DZM-FSB | Croatia | December 2007 |
| NSCIM | Ukraine | January 2007 |
| CMI | Czech Republic | March 2008 |
| METAS | Switzerland | July 2008 |
| NPL | United kingdom | June 2008 |

Table 6: Changes in measurement schedule in group 2

| Laboratory | Country | Date |
|------------|----------------|--------------------------|
| INMETRO | Brazil | May 2007 |
| CENAM | Mexico | June 2007 |
| NIST | USA | July – August 2007 |
| NRC | Canada | July 2008 |
| A*Star–NMC | Singapore | August – September 2007 |
| NIM | China | September – October 2007 |
| NPLI | India | Oct 2007 – Feb.2008 |
| NIMT | Thailand | March – April 2008 |
| NPL | United kingdom | September 2008 |
| METAS | Switzerland | June 2008 |
| VNIIM | Russia | December 2008 |

2.5 *Transport of the artefacts*

Transport of the artefacts was critical in some cases outside Europe. In most cases fast courier services were used. The ATA carnet, which was used for the majority of laboratories outside EU, was mostly handled correctly. Sometimes it was not stamped correctly and once it was lost in Asia. But a substitutional ATA was issued and the problem was successfully solved. Special customs arrangements (temporary import) were necessary for some countries.

Packaging for the artefact was robust to protect the artefacts from being deformed or damaged during transit. The artefact was in an original NPL wooden box, which was put into a robust transport box (See Fig. 1). The outer transport box was wrapped in a cardboard box, which was replaced each time when it was worn out.



Fig. 1: Scale containers

3 The artefact

3.1 Description of the artefact

At the Euromet TCL meeting in October 2005 in Bucharest it has been decided to measure a 100 mm quartz scale with 0.1 mm pitch. The artefact has been produced by NPL. Its basic purpose is to serve as a standard in precise industrial calibrations. The artefact is shown in Fig. 2.



Fig. 2: NPL line scale

The width of the scale lines is approx. 10 μm . The scale is provided by two parallel horizontal lines at the beginning and at the end of the scale. The distance between those 2 lines is approx. 50 μm . Some details of the scale can be seen in Fig. 3.

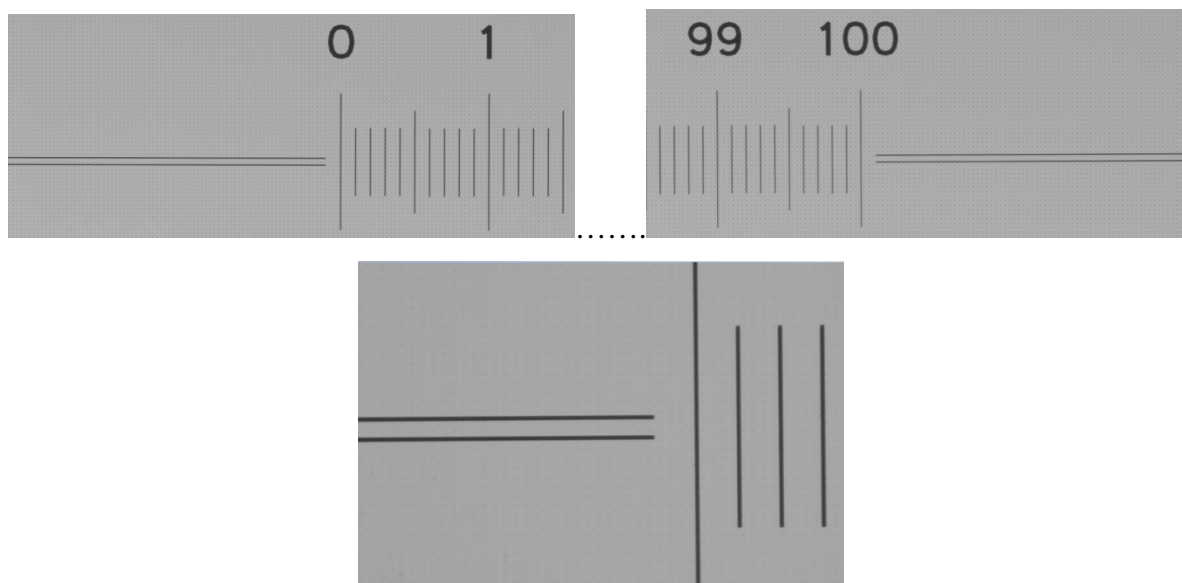


Fig. 3: Details of the scale

Equal artefacts were used in both groups. The artefact for group 1 was marked with engraved letter "A" and the artefact for group 2 with "B". The boxes were marked in the same manner with stickers.

Dimensions of the artefact are presented in Fig. 4.

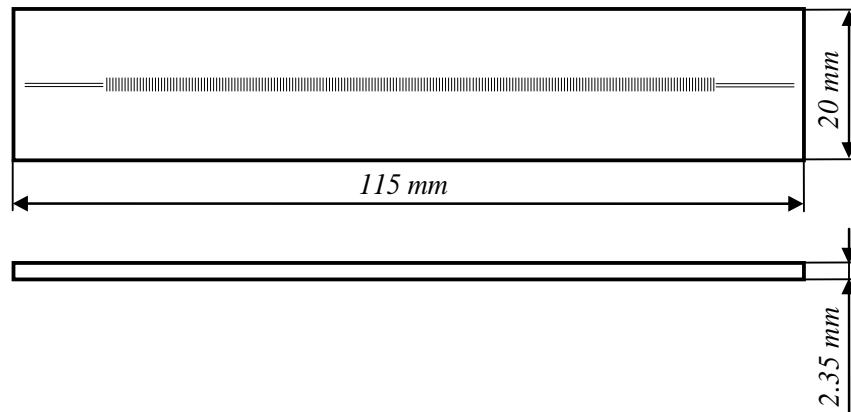


Fig. 4: Dimensions of the artefact

3.2 Fixing the artefact

The artefact was shipped without any special mounting fixtures. It was recommended to support the measurement objects at the Airy points (distance of $x = 0.2113 \cdot L$ from both ends), held only by their gravity forces. It was not allowed to use any type of glue or wax for mounting the scale. If additional clamping of the scale was required during measurement, e.g. because of a fast moving carriage, it was recommended to lightly pinch the scale on the sides at one of the Airy support points. If other support or clamping conditions were applied during measurement, it was the responsibility of the participant to refer his results to the Airy point support conditions.

4 Measurement instructions

4.1 Traceability

4.1.1 Length measurements should be traceable to the latest realisation of the metre as set out in the current “*Mise en Pratique*”.

4.1.2 Temperature measurements should be made using the International Temperature Scale of 1990 (ITS-90).

4.2 Measurand

Measurand was the distance between the centre line position of the reference line (position “0”) and the centre line position of the measured line (Fig. 5). To increase comparability of the results, all measurements were performed over the section between the two horizontal lines (at the beginning and at the end of the scale) with a width of approx. 50 µm. That is, it had to be tried to apply an effective slit height or CCD image window **height of 50 µm** for the analysis of measurements. If the effective height could not be set exactly to 50 µm, a value close to it should have been chosen.

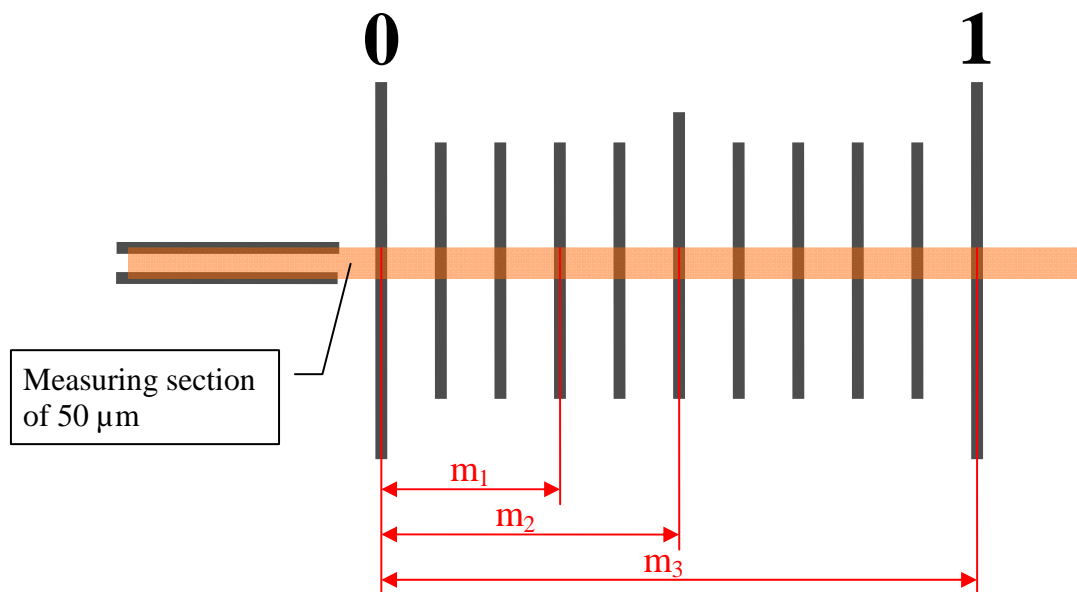


Fig. 5: Measurand (m_1 , m_2 , m_3) and measuring section

Table 7: The lines (distances) that were measured:

| Nominal lengths in mm | | | | | | | | | |
|-----------------------|-----|-----|-----|-----|-----|-----|-----|-----|-----|
| 0.1 | 0.2 | 0.3 | 0.4 | 0.5 | 0.6 | 0.7 | 0.8 | 0.9 | 1 |
| 5 | 10 | 15 | 20 | 25 | 30 | 35 | 40 | 45 | 50 |
| 55 | 60 | 65 | 70 | 75 | 80 | 85 | 90 | 95 | 100 |

Measurement conditions:

The positions of the lines had to be determined as the **centre line positions**¹ of every line, while the scale was lying on the Airy points (see 3.2). The participants were asked to describe the way the position of the line was determined.

For alignment purposes of the graduation lines the upper horizontal lines at the beginning and at the end of the scale should be used.

The measured values had to be referred to the following reference conditions:

- temperature of 20 °C (ITS-90),
- pressure of 1013,25 hPa (1013,25 mbar).

If necessary, corrections had to be applied based upon the following parameters:

Quartz:

- Thermal expansion coefficient: $\alpha = 5 \cdot 10^{-7} \text{ K}^{-1}$
- Length compressibility: $\kappa = - 8.9 \cdot 10^{-7} \text{ bar}^{-1}$

4.3 Measurement instructions

- 4.3.1 The calibration had to be carried out as for a normal customer. The participants were free to choose their own method of measurement. However, under the assumption that the value of the measurand is a true property of the material measure of length, only one result for a measurand had to be given irrespective of the number of different measurement methods used. For each method applied, a complete description of the method had to be given. A detailed estimation of the measurement uncertainty according to the *ISO Guide to the Expression of Uncertainty in Measurement (GUM)* had to be supplied.
- 4.3.2 The measurements had to be reported for measuring conditions, given in 4.2.
- 4.3.3 Before calibration, the scale had to be inspected for damages. Any scratches, dirty spots or other damages had to be documented
- 4.3.4 The measurement results (appropriately corrected to the reference conditions) had to be reported using forms, given in the protocol.

4.4 Measurement uncertainty

The uncertainty of measurement had to be estimated according to the *ISO Guide to the Expression of Uncertainty in Measurement*. In order to achieve a better comparability, some possible influence parameters and notations were given. The participants were encouraged to use all known and significant influence parameters for their applied methods. The following list could have been used as an indication of possible influence parameters:

Possible contributions from **line position sensing** technique:

- $\delta_{E_{res}}$ Resolution of edge detection
 s_E Repeatability of edge detection

¹ The key comparison guideline states, that the methods usually applied by the participants for calibrations should also be used within the comparison. Because different line center extraction algorithms will normally be used by the participants, it is essential that the different procedures are well described and that edge detection influences are accounted for in the uncertainty estimation. A possible edge detection algorithm e.g. is the arithmetic mean of left and right edge positions if those are explicitly measured (e.g. at 50% threshold) or the centroid of 2D image intensity data.

| | |
|---------------------|---|
| δ_{Edef} | Edge geometry influence (roughness, parallelism) |
| δ_{lpos} | Influence of adjustment of measurement line |
| δ_{lwin} | Influence of adjustment of measurement window or slit length |
| δ_{Efoc} | Influence of focal length variation |
| $\delta_{E\lambda}$ | Influence of detection light wavelength |
| δ_{Epol} | Influence of detection light polarization |
| δ_{Ecoh} | Influence of detection light coherence |
| <i>Mag</i> | Microscope magnification (or other position deviation sensing device) |
| δ_{Enon} | Nonlinearities of position sensing technique |
| δ_{Ealign} | Microscope axis alignment |
| δ_{Ealg} | Influence of line edge detection algorithm, possible asymmetry of line profiles, line shape |
| δ_{Erev} | Influence of measurement in reversed orientation |

Possible contributions from interferometric **displacement measurement** technique:

| | |
|------------------|--|
| λ_0 | vacuum wavelength of light source used for displacement measurement |
| n_{air} | Index of refraction of air ² |
| t_{air} | Air temperature |
| p_{air} | Air pressure |
| RH_{air} | Air humidity |
| c_{CO_2} | Air CO ₂ concentration |
| δ_{Res} | Interferometer resolution |
| δ_{NL} | Interferometer nonlinearity (polarisation mixing, etc.) |
| δ_{DP} | Interferometer dead path influences (temperature variation, etc.) |
| δ_{MP} | Variation of measurement path in one orientation (normal, meander, random, ..) |
| δ_{Drift} | Drift influence (forward, backward measurement) |
| δ_{Rev} | Influence of measurement in reversed orientation |
| δ_{Ai} | Errors due to Abbe offsets and pitch and yaw of translation stages |
| δ_{Si} | Errors of scale alignment |
| δ_{Ii} | Cosine errors of interferometer alignment |

Possible contributions from **scale properties**:

| | |
|------------------|--|
| $\alpha_{Z, Cr}$ | Linear coefficient of thermal expansion of scale material |
| Δt_s | = ($t_s - 20$) is the difference of the scale temperature t_s in °C during the measurement from the reference temperature of 20 °C |
| $\kappa_{Z, Cr}$ | Linear coefficient of compressibility of scale material |
| δh | Flatness deviation of scale graduation surface |
| δ_{supp} | Influence of support conditions |

² If the index of refraction is determined by the parameter method according to Edlen, the updated version of the formula should be applied as published in: G. Bönsch, E. Potulski, Metrologia, 1998, **35**, 133-139. The estimated combined standard uncertainty of the quoted formula itself is $1 \cdot 10^{-8}$.

The deviations dL from nominal length had to be measured and expressed as a function of input quantities x_i

$$dL = f(x_i), \quad (1)$$

The combined standard uncertainty $u_c(dL)$ is the quadratic sum of the standard uncertainties of the input quantities $u(x_i)$ each weighted by a sensitivity coefficient c_i

$$u_c^2(dL) = \sum_i c_i^2 u^2(x_i), \quad \text{with } c_i = \frac{\partial dL}{\partial x_i}. \quad (2)$$

The participants were required to report their measurement uncertainty budget in a prepared table (in Appendix A.2 of the technical protocol) with the format according to the scheme below. "Distrib." is the type of distribution of the input quantity (N=normal, R=rectangular, T=triangular, etc.), ν_i is the number of degrees of freedom of $u(x_i)$.

Example scheme:

| Input quantity x_i | Distrib. | $u(x_i)$ | ν_i | $c_i = \partial dL / \partial x_i$ | $u_i(dL) / \text{nm}$ |
|--|----------|---------------------|---------|------------------------------------|-----------------------|
| <i>Edge detection reproduc. s_E</i> | N | 3 nm | 10 | 1 | 3 |
| <i>Cosine error scale alignment</i> | R | 140 μrad | >100 | - | $10^{-8} L$ |
| ... | ... | ... | ... | ... | ... |

5 Measurement equipment and methods used by the participants

Detailed information on the equipment and method used by the participants is in Appendix 2. Short summary is presented in Table 8.

Table 8: Overview of instrumentation used by the participants

| Laboratory | Measuring instrument | Line detection |
|------------|---|---|
| MIRS | Zeiss ULM 01-600 C 1D measurement machine by using laser interferometer HP 5528A, fixed microscope, moving scale, hand driven | CCD microscope, in-house software |
| BEV | SIP 3002 length measuring machine with a standard HP 5529A laser interferometer; fixed scale, moving microscope, hand driven | Incident light CCD-microscope; two parallel reference lines |
| CMI | Interferometric comparator IK-1 (CMI design), fixed microscope, moving scale; motor driven | CCD microscope; in-house software |
| DZM-FSB | 500 mm 1D machine, in-house design and construction, Renishaw ML 10 laser interferometer, fixed microscope, moving scale, hand driven | CCD microscope, in-house software |
| GUM | 1000 mm 1D SIP measuring bench, laser interferometer HP-5528A, fixed microscope, moving scale, motor driven + precision piezo-electric actuator | CCD-microscope; two parallel reference lines |
| INM | Longitudinal comparator, He – Ne frequency stabilized laser interferometer, fixed microscope, moving scale, motor driven | Optical microscope |
| LNMC | Horizontal comparator IZA-7, longitudinal comparison, fixed scale, hand driven | 2 microscopes |
| METAS | 2D photomask measuring system 400 mm x 300 mm, differential two axis plane mirror interferometer (HP), fixed microscope, moving scale, motor driven, fully automated | CCD microscope, motorised focusing, in-house software |
| MIKES | MIKES' line scale interferometer, Michelson interferometer utilising a calibrated 633 nm Zeeman-stabilised He-Ne laser, dynamic method, moving microscope, motor driven | CCD microscope, synchronous data sampling |
| NCM | Comparator, HP 5529A laser interferometer, fixed scale, moving microscope, hand driven | Photoelectric microscope |
| NML | SIP horizontal measuring machine, Agilent 5519A laser, fixed microscope, moving scale, hand driven | Optical microscope |

| Laboratory | Measuring instrument | Line detection |
|------------|---|--|
| NPL | NPL 400mm range air-bearing stage (interferometrically monitored), two co-linear independent laser interferometers, (NPL differential Jamin type, HP Michelson), fixed microscope, moving scale (different conditions in 2006 and 2008), motor driven | NPL NanoVision image processing system |
| NSCIM | Horizontal comparator with Michelson dynamic laser interferometer, primary standard DETU 01-03-98, fixed scale, moving microscope, hand driven | Photoelectric microscope (PEM) |
| OMH | 3 m Zeiss universal length measuring machine, HP 5528 laser interferometer, hand driven | CCD microscope, reference screen lines |
| PTB | PTB Nanometer Comparator, vacuum interferometer (iodine-stabilized, frequency doubled Nd:YAG laser, fixed microscope, moving scale, motor driven | PTB optical microscope with CCD camera, in-house software |
| SMU | 1-D machine Abbe Zeiss (range up to 200 mm), laser interferometer HP 5529B, fixed microscope, moving scale, hand driven | Optical microscope |
| ZMDM | Zeiss ULM 3000 1-D measuring machine, laser interferometer HP 5526 A, fixed scale, moving microscope, hand driven | Zeiss optical microscope |
| CEM | Custom-built length comparator CEM-TEK 1200, laser-interferometer (Stabilized Laser Source HP 5517C) | In-house software |
| CENAM | Optical microscope brand Leitz Libra 200, moving scale, hand driven | CCD microscope, manual edge observation, Micro/Measure Microscope Software |
| EIM | Leitz universal measuring microscope, laser interferometer Renishaw, moving scale, hand driven | CCD microscope, analysis of digital images |
| INMETRO | Optical CMM SIP Trioptic, laser interferometer, fixed microscope, moving scale, hand driven | CCD microscope |
| INRIM | Moore Measuring Machine, laser interferometer HP 5518 fixed microscope, moving scale, motor driven | CCD microscope, in-house software |
| NIM | NIM comparator, , He-Ne laser interferometer | Optical-electronic microscope dual slit line position detection |
| NIST | NIST Line Scale Interferometer (LSI) - heterodyne interferometer, He-Ne laser, fixed microscope, moving scale, motor driven | Scanning electro-optical line detector, in-house software |
| NMi-VSL BV | SIP 400 measuring machine, laser interferometer HP, fixed microscope, moving scale, hand driven | CCD microscope, in-house software |

| Laboratory | Measuring instrument | Line detection |
|--------------|---|---|
| NPLI | Universal measuring machine SIP UMM – MUL -214 B, heterodyne laser interferometer HP 5529A, fixed microscope moving scale, hand driven | Optical microscope |
| NRC | NRC 4-metre Line Scale Comparator, HP heterodyne laser interferometer, fixed scale, moving microscope, motor driven | CCD microscope, in-house software |
| A*Star - NMC | Laser line width measurement system (base with two working stages, motor drives, He-Ne laser interferometer), fixed microscope moving scale, motor driven | Photoelectric microscope with single slit |
| NIMT | Line scale interferometer (stabilized He-Ne laser, fixed scale, moving edge sensor, motor (?) driven | Edge sensor using triple slits system |
| VNIIM | VNIIM comparator (carriage, laser polarization interferometer, refractometer) fixed scale, moving microscope, motor driven, measurements in dynamic mode | Microscope with laser diodes and photodiode |

6 Stability of the standards

The standards used for this comparison were made of quartz with expected good long term stability. However, no historical data were available, since the standards were new. The material properties (chapter 4) were not exactly determined, the values were obtained from general knowledge about the used material.

In order to check the long-term stability, measurements of two linking laboratories (METAS and NPL) were performed in the beginning of the project (year 2006) and close to the end of the project (2008).

The stability checks comprised the total length change during 2 years, as well as possible line centre shifts due to damages and dirtiness of single lines.

6.1 Stability of the total line scale length

Stability of the total line scale length (over 100 mm) is demonstrated in Figures 6 (Scale “A”, Group 1) and 7 (Scale “B”, Group 2). Deviations from nominal length, measured by the linking laboratories in years 2006 and 2008 are represented together with the standard uncertainties.

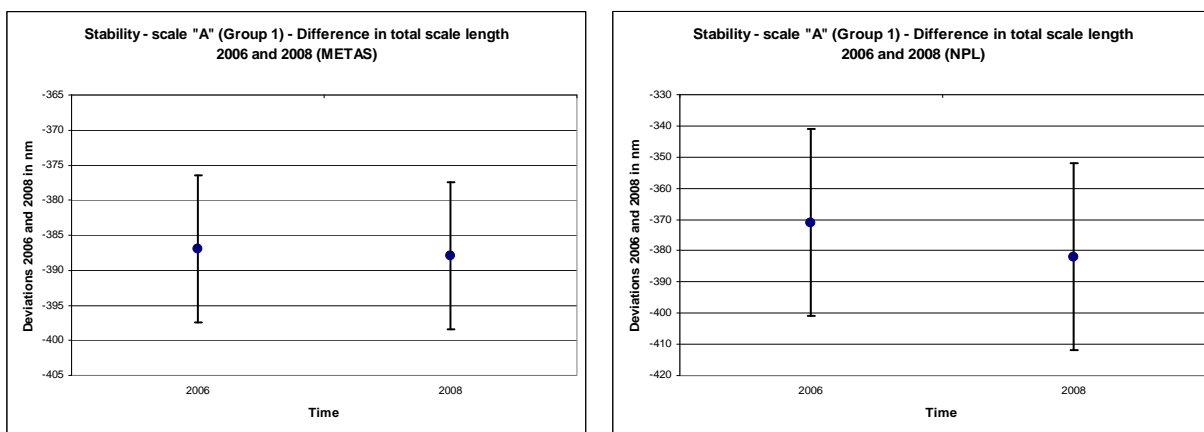


Fig. 6: Measured deviations of the scale “A” in years 2006 and 2008

The result for scale A in Fig. 6 shows a slight drift in negative direction, which is however much smaller than the standard uncertainties of both laboratories. Therefore, no drift correction was applied to the measurement values.

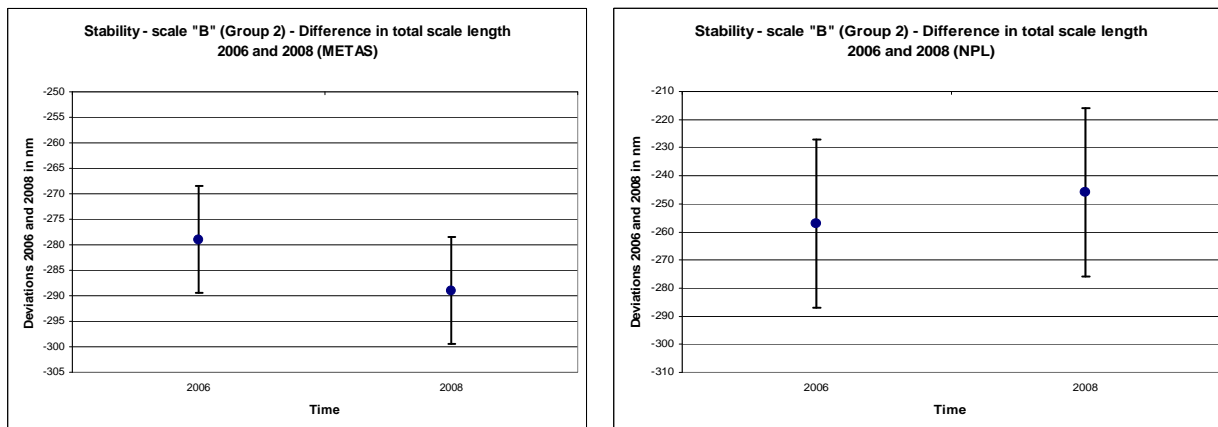


Fig. 7: Measured deviations of the scale “B” in years 2006 and 2008

The result for scale B in Fig. 7 shows drifts in different directions. Because no systematic drift was identified, no corrections were applied to the measurement values to compensate for drift.

6.2 Stability of single line centres

The participating laboratories were instructed how to clean the scale before measurement and to report possible damages. The following damages and dirt spots were reported:

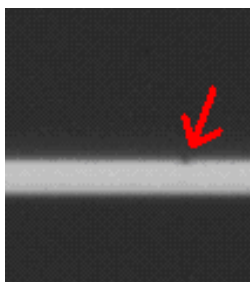
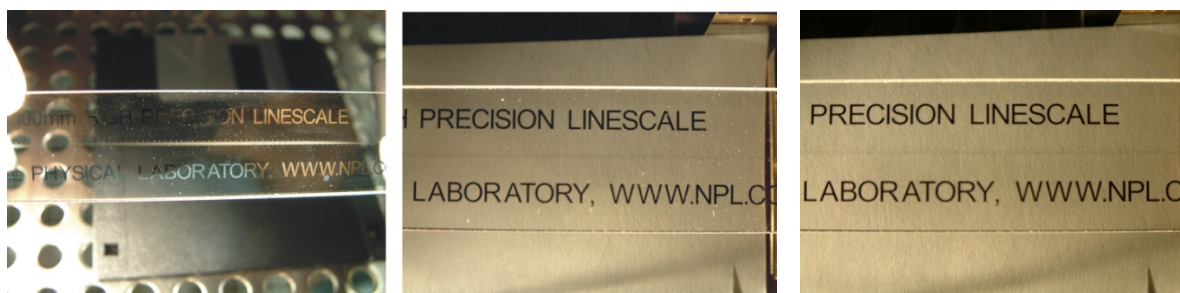
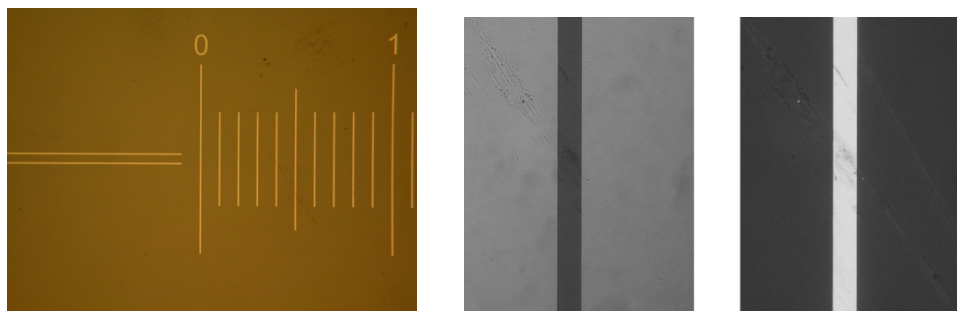


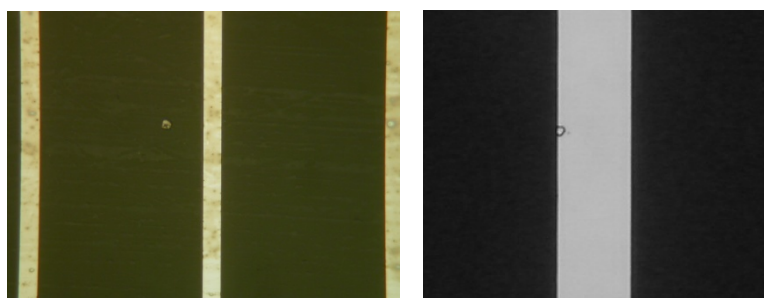
Fig. 8: MIKES reported small damage on the reference line (Scale “A”)



Dust on scale before and after cleaning



Spots on glass



Spots on a line

Fig. 9: Dirt and damages reported by PTB (scale “A”)

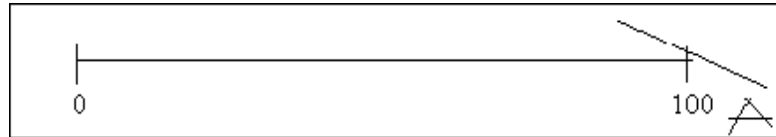


Fig. 10: Scratches reported by NCM (scale “A”)

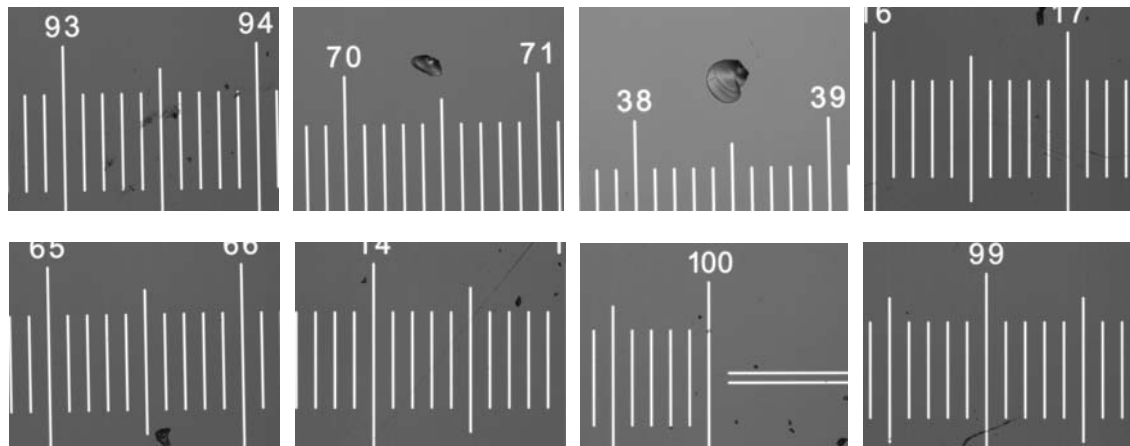


Fig. 11: Dirt and damages reported by A*Star–NMC Singapore (scale “B”)

After discussion between the pilot laboratory and both linking laboratories it was agreed that reported damages would not impact the majority of results and their uncertainties. The laboratories were also instructed in the technical protocol to perform the measurements as for their clients. So it was in their responsibility to consider disturbances in their uncertainty budget.

Single line centre shifts due to changes on lines can be evaluated from the diagrams in Figures 12 to 16. Results are presented in three different ways:

- as a comparison of measurements in 2006 and 2008 – Fig. 12 and 13
- as an absolute difference of two results (2008 – 2006) – Fig. 14
- as deviations of two measurements from calculated arithmetic mean (2006 and 2008) – Fig. 15 and 16

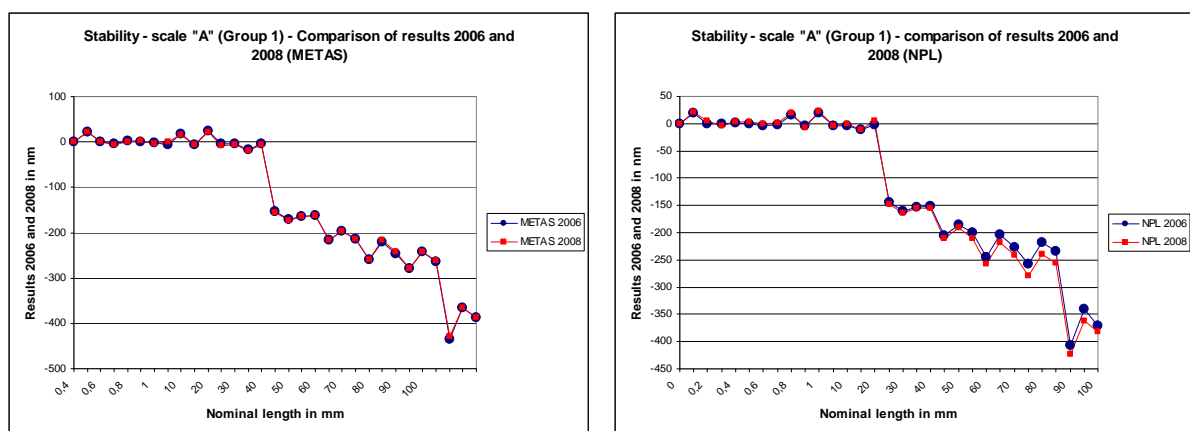


Fig. 12: Comparison of measurements, performed by METAS and NPL in 2006 and in 2008 on scale “A”

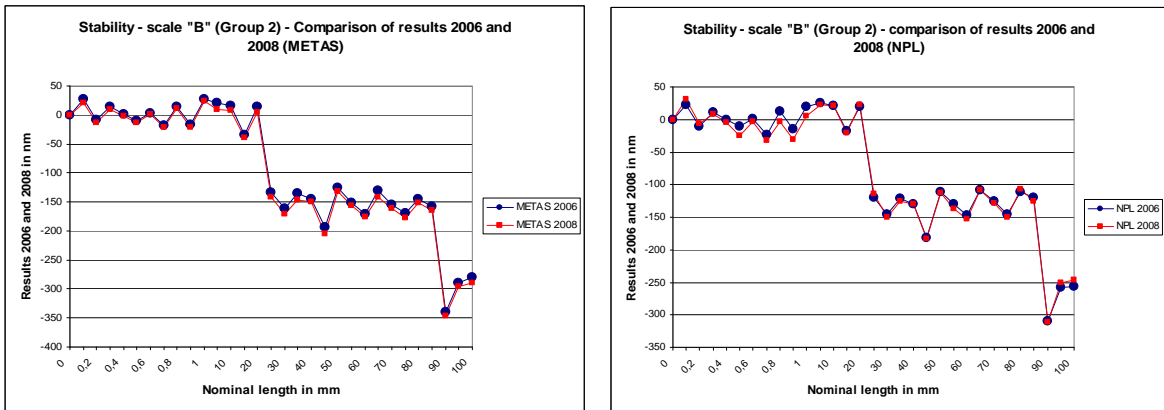


Fig. 13: Comparison of measurements, performed by METAS and NPL in 2006 and in 2008 on scale “B”

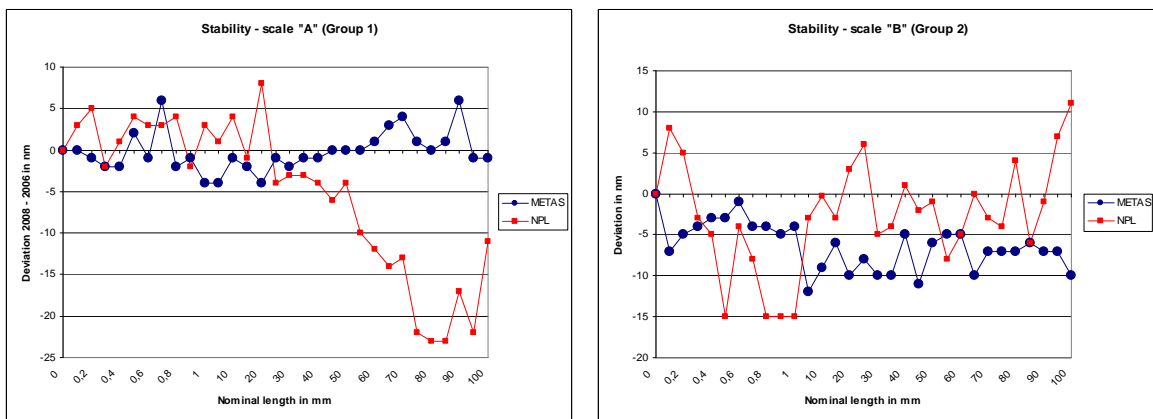


Fig. 14: Absolute difference of the results from 2006 and 2008 for scales “A” and “B”

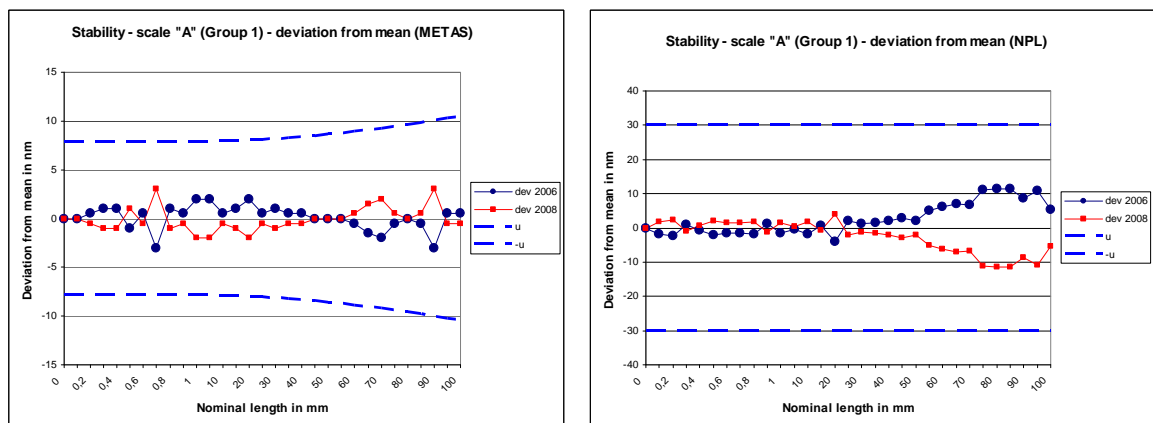


Fig. 15: Deviations of 2006 and 2008 measurements from the mean value (scale A) with indicated standard uncertainties

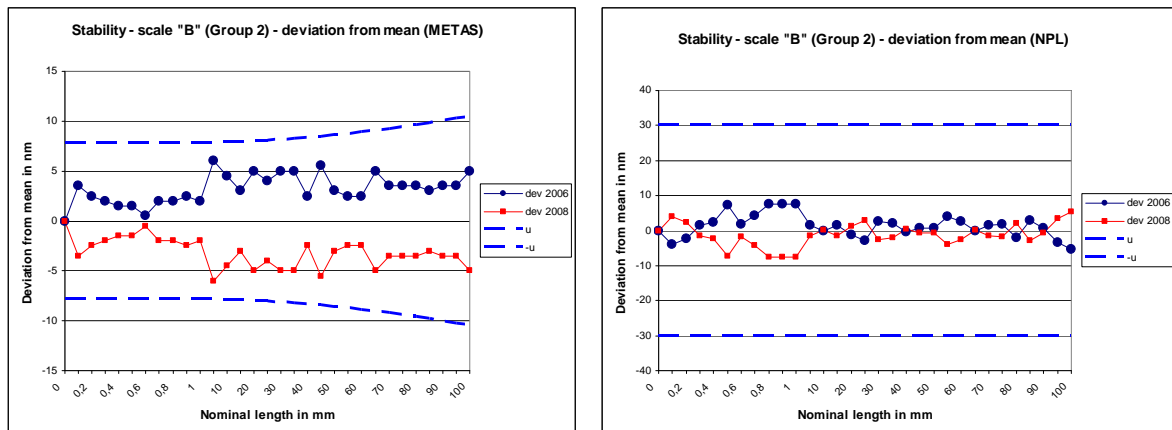


Fig. 16: Deviations of 2006 and 2008 measurements from the mean value (scale B) with indicated standard uncertainties

Figures 12 and 13 showing the deviations from the nominal values are not very useful, since the differences can hardly be seen. Fig. 14 shows for scale “A” the biggest difference of 23 nm measured by NPL, while the biggest difference in METAS results is 6 nm. For scale “B”, the biggest difference measured by NPL was 15 nm, while the biggest difference measured by METAS was 12 nm. Fig. 15 and 16 show, that all measured differences were within the standard uncertainty boundaries.

6.3 Impact of line scale instability

Although no systematic change in line scale length was detected, there are possible influences on measured results by random influences like dirt, damages, different cleaning approaches etc. These influences were taken into account by adding an additional uncertainty component before calculating the reference values and their uncertainties and consistency of the results (E_n). This uncertainty component derived from the stability measurements made by the linking laboratories. They measured the scale at the beginning and at the end of the comparison.

A time dependent contribution (stability uncertainty) has to be added to a calibration value because the value is used at a time considerably later than the measurement. So adding the stability contribution makes the calibration valid over the full time span of the comparison (which lasted more than 2 years).

7 Analysis of the results

The reference values (x_{ref}) were calculated as the weighted mean of all measurements (x_i), the weight factors being $u^{-2}(x_i)$. For each measurement point the reference value was calculated. In the second step, for the calculation of reference values from the largest consistent subset of measurements, some of the values with $|E_n| > 1$ were omitted one by one, beginning with the largest $|E_n|$, until the Birge criterion was met.

Reference value:

$$x_{ref} = \frac{\sum_{i=1}^n u^{-2}(x_i) \cdot x_i}{\sum_{i=1}^n u^{-2}(x_i)} \quad (3)$$

Combined standard uncertainty:

$$u_c(x_{ref}) = \frac{1}{\sqrt{\sum_{i=1}^n u^{-2}(x_i)}} \quad (4)$$

E_n -value:

$$E_n = \frac{x_{lab} - x_{ref}}{k \cdot \sqrt{u^2(x_{lab}) - u^2(x_{ref})}} ; k = 2 \quad (5)$$

The Birge ratio:

$$R_B = \frac{u_{ext}}{u_{int}} \quad (6)$$

$$u_{ext} = \sqrt{\frac{\left[\sum_{i=1}^n (x_i - x_{ref}) / u(x_i) \right]^2}{(n-1) \sum_{i=1}^n u^{-2}(x_i)}} \quad (7)$$

$$u_{int} = 1 / \sqrt{\sum_{i=1}^n u^{-2}(x_i)} \quad (8)$$

The Birge criterion:

$$R_B < \sqrt{1 + \frac{8}{n-1}} \quad (9)$$

8 Measurement results

8.1 Measurement results - Group 1

Measurement results of Group 1 are presented in Table 9. The first set of NPL measurements and the last set of METAS measurements were used only for scale stability evaluation. They were excluded from final evaluation of the participants.

Table 9: Measurement results – Group 1

| Meas. point | 0,1 mm | | 0,2 mm | | 0,3 mm | | 0,4 mm | | 0,5 mm | | 0,6 mm | |
|-------------|---------|------------|---------|------------|---------|------------|---------|------------|---------|------------|---------|------------|
| | dL / nm | u_c / nm |
| MIRS-SI | 20,0 | 61,1 | 0,0 | 61,2 | 0,0 | 61,4 | 20,0 | 61,5 | 30,0 | 61,6 | 30,0 | 61,7 |
| METAS-CH | 21,0 | 7,9 | 1,0 | 7,9 | -4,0 | 7,9 | 3,0 | 7,9 | 0,0 | 7,9 | -2,0 | 7,9 |
| NPL-GB | 18,6 | 30,0 | -0,6 | 30,0 | -1,3 | 30,0 | 2,3 | 30,0 | -1,0 | 30,0 | -3,6 | 30,0 |
| OMH-HU | -119,0 | 100,0 | -117,0 | 100,0 | -14,0 | 100,0 | -5,0 | 100,0 | 12,0 | 100,0 | 1,0 | 100,0 |
| BEV-AT | 14,0 | 23,0 | 10,0 | 23,0 | 10,0 | 23,0 | 20,0 | 23,0 | 14,0 | 23,0 | 12,0 | 23,0 |
| SMU-SK | 2,0 | 46,0 | -34,0 | 46,0 | -10,0 | 46,0 | -13,0 | 46,0 | -4,0 | 46,0 | 4,0 | 46,0 |
| PTB-DE | 35,2 | 13,0 | 5,4 | 32,0 | 9,0 | 13,0 | 55,5 | 32,0 | 32,0 | 32,0 | 10,5 | 13,0 |
| GUM-PL | 58,0 | 134,0 | 4,0 | 134,0 | 24,0 | 134,0 | 66,0 | 134,0 | 14,0 | 134,0 | 14,0 | 134,0 |
| MIKES-FI | 20,0 | 25,0 | 1,0 | 11,3 | -4,0 | 11,3 | 45,0 | 25,0 | 10,0 | 11,3 | -2,0 | 11,3 |
| LNMC-LV | -200,0 | 823,0 | -200,0 | 823,0 | -200,0 | 823,0 | 0,0 | 823,0 | 200,0 | 823,0 | 400,0 | 823,0 |
| NML-IE | -80,0 | 739,6 | -46,0 | 739,6 | -186,0 | 739,6 | 40,0 | 739,6 | -360,0 | 739,6 | -120,0 | 739,6 |
| NCM-BG | 24,0 | 78,0 | 0,0 | 78,0 | 1,0 | 78,0 | 2,0 | 78,0 | 41,0 | 78,0 | -2,0 | 78,0 |
| INM-RO | 40,0 | 101,0 | 60,0 | 101,0 | 60,0 | 101,0 | 40,0 | 101,0 | 10,0 | 101,0 | 10,0 | 101,0 |
| ZMDM-SR | -17,3 | 101,0 | -5,3 | 101,0 | 1,4 | 101,0 | 23,1 | 101,0 | 13,9 | 101,0 | -24,7 | 101,0 |
| DZM-HR | 3,0 | 75,1 | -1,0 | 75,1 | 3,0 | 75,2 | 14,0 | 75,2 | 26,0 | 75,3 | 8,0 | 75,3 |
| NSCIM-UA | 36,0 | 20,0 | 12,0 | 20,0 | -1,0 | 20,0 | 23,0 | 20,0 | 17,0 | 20,0 | -204,0 | 20,0 |
| CMi-CZ | 28,0 | 14,0 | 1,0 | 14,0 | -4,0 | 14,0 | 3,0 | 14,0 | 8,0 | 14,0 | 4,0 | 14,0 |
| METAS-CH | 21,0 | 7,9 | 0,0 | 7,9 | -6,0 | 7,9 | 1,0 | 7,9 | 2,0 | 7,9 | -3,0 | 7,9 |
| NPL-GB | 22,0 | 30,0 | 4,1 | 30,0 | -3,2 | 30,0 | 3,4 | 30,0 | 3,0 | 30,0 | -0,3 | 30,0 |

| Meas. point | 0,7 mm | | 0,8 mm | | 0,9 mm | | 1,0 mm | | 5,0 mm | | 10,0 mm | |
|-------------|---------|------------|---------|------------|---------|------------|---------|------------|---------|------------|---------|------------|
| | dL / nm | u_c / nm |
| MIRS-SI | 30,0 | 61,8 | 70,0 | 62,0 | 50,0 | 62,1 | 70,0 | 62,2 | 20,0 | 67,0 | 0,0 | 73,0 |
| METAS-CH | -6,0 | 7,9 | 17,0 | 7,9 | -6,0 | 7,9 | 25,0 | 7,9 | -4,0 | 7,9 | -5,0 | 7,9 |
| NPL-GB | -1,4 | 30,0 | 15,2 | 30,0 | -4,5 | 30,0 | 19,4 | 30,0 | -4,0 | 30,0 | -4,1 | 30,0 |
| OMH-HU | -49,0 | 100,0 | 28,0 | 100,0 | -61,0 | 100,0 | -45,0 | 100,0 | -57,0 | 100,0 | -91,0 | 100,0 |
| BEV-AT | 15,0 | 23,0 | 38,0 | 23,0 | 24,0 | 23,0 | 50,0 | 23,0 | -16,0 | 111,0 | -11,0 | 111,0 |
| SMU-SK | 3,0 | 46,0 | -14,0 | 46,0 | -8,0 | 46,0 | -3,0 | 46,0 | -26,0 | 46,0 | -30,0 | 46,0 |
| PTB-DE | 0,8 | 32,0 | 28,6 | 13,0 | -6,1 | 13,0 | 29,1 | 13,0 | 5,4 | 13,0 | 6,0 | 13,0 |
| GUM-PL | -15,0 | 134,0 | -47,0 | 134,0 | -43,0 | 134,0 | 6,0 | 134,0 | 135,0 | 134,1 | 135,0 | 134,4 |
| MIKES-FI | 1,0 | 11,3 | 25,0 | 11,3 | -13,0 | 11,3 | 5,0 | 11,3 | -4,0 | 11,3 | -6,0 | 11,3 |
| LNMC-LV | 300,0 | 823,0 | 100,0 | 823,0 | 100,0 | 823,0 | 50,0 | 823,0 | 420,0 | 823,0 | 360,0 | 823,0 |
| NML-IE | -60,0 | 739,6 | 140,0 | 739,6 | 340,0 | 739,6 | 320,0 | 739,6 | 240,0 | 739,6 | 200,0 | 739,6 |
| NCM-BG | 3,0 | 78,0 | 11,0 | 78,0 | 3,0 | 78,0 | 21,0 | 78,0 | -3,0 | 78,0 | 1,0 | 78,1 |
| INM-RO | 20,0 | 101,0 | 10,0 | 101,0 | 20,0 | 101,0 | -30,0 | 101,0 | 30,0 | 101,0 | 30,0 | 101,0 |
| ZMDM-SR | -31,8 | 101,0 | -64,8 | 101,0 | -50,9 | 101,0 | -42,0 | 101,0 | -3639,2 | 101,0 | -8219,0 | 101,0 |
| DZM-HR | 28,0 | 75,4 | 33,0 | 75,4 | 61,0 | 75,5 | 71,0 | 75,5 | 36,0 | 77,5 | 25,0 | 80,0 |
| NSCIM-UA | 27,0 | 20,0 | 41,0 | 20,0 | 17,0 | 20,0 | 48,0 | 20,0 | 68,0 | 20,0 | 92,0 | 20,1 |
| CMi-CZ | 0,0 | 14,0 | 20,0 | 14,0 | -8,0 | 14,0 | 20,0 | 14,0 | -5,0 | 14,0 | -6,0 | 14,1 |
| METAS-CH | 0,0 | 7,9 | 15,0 | 7,9 | -7,0 | 7,9 | 21,0 | 7,9 | -8,0 | 7,9 | -6,0 | 7,9 |
| NPL-GB | 1,5 | 30,0 | 19,0 | 30,0 | -6,9 | 30,0 | 22,5 | 30,0 | -3,3 | 30,0 | -0,3 | 30,0 |

| Meas. point | 15,0 mm | | 20,0 mm | | 25,0 mm | | 30,0 mm | | 35,0 mm | | 40,0 mm | |
|-------------|----------|---------------------|----------|---------------------|----------|---------------------|----------|---------------------|----------|---------------------|----------|---------------------|
| | dL / nm | u _c / nm | dL / nm | u _c / nm | dL / nm | u _c / nm | dL / nm | u _c / nm | dL / nm | u _c / nm | dL / nm | u _c / nm |
| MIRS-SI | 0,0 | 79,0 | 0,0 | 85,0 | -140,0 | 91,0 | -180,0 | 97,0 | -200,0 | 103,0 | -210,0 | 109,0 |
| METAS-CH | -17,0 | 8,0 | -3,0 | 8,0 | -154,0 | 8,1 | -171,0 | 8,2 | -164,0 | 8,3 | -162,0 | 8,4 |
| NPL-GB | -10,5 | 30,0 | -2,6 | 30,0 | -143,4 | 30,0 | -160,6 | 30,0 | -152,8 | 30,0 | -150,9 | 30,0 |
| OMH-HU | -50,0 | 100,0 | -28,0 | 100,0 | -263,0 | 100,0 | -159,0 | 100,0 | -89,0 | 100,1 | -322,0 | 100,1 |
| BEV-AT | -64,0 | 111,0 | -48,0 | 111,0 | -180,0 | 111,0 | -247,0 | 111,0 | -255,0 | 111,0 | -272,0 | 111,0 |
| SMU-SK | -21,0 | 46,0 | -34,0 | 46,0 | -83,0 | 46,1 | -87,0 | 46,1 | -90,0 | 46,1 | -102,0 | 46,2 |
| PTB-DE | 17,6 | 13,0 | 5,7 | 13,0 | -134,1 | 13,0 | -158,5 | 13,0 | -149,7 | 13,0 | -149,1 | 13,0 |
| GUM-PL | 174,0 | 134,8 | 81,0 | 135,5 | -66,0 | 136,3 | -15,0 | 137,3 | -126,0 | 138,5 | -45,0 | 139,8 |
| MIKES-FI | -1,0 | 11,3 | -9,0 | 11,3 | -144,0 | 11,4 | -171,0 | 11,4 | -161,0 | 11,4 | -159,0 | 11,4 |
| LNMC-LV | 270,0 | 823,0 | 510,0 | 823,0 | 230,0 | 823,0 | 970,0 | 823,0 | -150,0 | 823,0 | 320,0 | 823,0 |
| NML-IE | 480,0 | 739,6 | 400,0 | 739,6 | 760,0 | 739,6 | 340,0 | 739,6 | 680,0 | 739,6 | 900,0 | 739,6 |
| NCM-BG | -21,0 | 78,2 | -13,0 | 78,3 | -154,0 | 78,5 | -176,0 | 78,7 | -150,0 | 78,9 | -179,0 | 79,2 |
| INM-RO | 10,0 | 101,1 | -10,0 | 101,1 | -40,0 | 101,2 | -20,0 | 101,3 | -20,0 | 101,4 | -10,0 | 101,6 |
| ZMDM-SR | -10837,1 | 101,0 | -14582,3 | 101,1 | -18716,9 | 101,1 | -22493,0 | 101,2 | -25864,6 | 101,2 | -29161,2 | 101,3 |
| DZM-HR | -7,0 | 82,5 | 14,0 | 85,0 | -238,0 | 87,5 | -276,0 | 90,0 | -299,0 | 92,5 | -167,0 | 95,0 |
| NSCIM-UA | 116,0 | 20,2 | 162,0 | 20,3 | 62,0 | 20,4 | 124,0 | 20,6 | 134,0 | 20,9 | 162,0 | 21,1 |
| CMI-CZ | -12,0 | 14,3 | -3,0 | 14,5 | -153,0 | 14,8 | -174,0 | 15,1 | -161,0 | 15,5 | -168,0 | 16,0 |
| METAS-CH | -19,0 | 8,0 | -7,0 | 8,0 | -155,0 | 8,1 | -173,0 | 8,2 | -165,0 | 8,3 | -163,0 | 8,4 |
| NPL-GB | -11,9 | 30,0 | 5,7 | 30,0 | -147,2 | 30,0 | -163,2 | 30,0 | -155,7 | 30,0 | -155,0 | 30,0 |

| Meas. point | 45,0 mm | | 50,0 mm | | 55,0 mm | | 60,0 mm | | 65,0 mm | | 70,0 mm | |
|-------------|----------|---------------------|----------|---------------------|----------|---------------------|----------|---------------------|----------|---------------------|----------|---------------------|
| | dL / nm | u _c / nm | dL / nm | u _c / nm | dL / nm | u _c / nm | dL / nm | u _c / nm | dL / nm | u _c / nm | dL / nm | u _c / nm |
| MIRS-SI | -290,0 | 115,0 | -220,0 | 121,0 | -270,0 | 127,0 | -310,0 | 133,0 | -250,0 | 139,0 | -280,0 | 145,0 |
| METAS-CH | -216,0 | 8,5 | -196,0 | 8,6 | -214,0 | 8,8 | -260,0 | 8,9 | -220,0 | 9,1 | -246,0 | 9,3 |
| NPL-GB | -205,0 | 30,0 | -186,4 | 30,0 | -200,1 | 30,0 | -245,1 | 30,0 | -203,9 | 30,0 | -227,5 | 30,0 |
| OMH-HU | -282,0 | 100,1 | -261,0 | 100,1 | -351,0 | 100,1 | -318,0 | 100,2 | -232,0 | 100,2 | -329,0 | 100,2 |
| BEV-AT | -351,0 | 111,0 | -290,0 | 111,0 | -342,0 | 111,0 | -418,0 | 111,0 | -377,0 | 111,0 | -444,0 | 111,0 |
| SMU-SK | -109,0 | 46,2 | -107,0 | 46,2 | -124,0 | 46,3 | -142,0 | 46,3 | -144,0 | 46,4 | -162,0 | 46,5 |
| PTB-DE | -200,9 | 13,0 | -180,6 | 13,0 | -201,5 | 13,0 | -244,2 | 13,0 | -200,4 | 13,0 | -236,4 | 13,0 |
| GUM-PL | -236,0 | 141,4 | -259,0 | 143,0 | -312,0 | 144,8 | -422,0 | 146,8 | -335,0 | 148,9 | -479,0 | 151,2 |
| MIKES-FI | -220,0 | 11,5 | -195,0 | 11,5 | -210,0 | 11,6 | -257,0 | 11,6 | -213,0 | 11,7 | -245,0 | 11,7 |
| LNMC-LV | 140,0 | 823,0 | 670,0 | 823,0 | 120,0 | 823,0 | 580,0 | 823,0 | -220,0 | 823,0 | -110,0 | 823,0 |
| NML-IE | 760,0 | 739,6 | 920,0 | 739,6 | 880,0 | 739,6 | 1600,0 | 739,6 | 1860,0 | 739,6 | 1780,0 | 739,6 |
| NCM-BG | -231,0 | 79,5 | -225,0 | 79,8 | -243,0 | 80,2 | -294,0 | 80,6 | -249,0 | 81,1 | -282,0 | 81,6 |
| INM-RO | -50,0 | 101,7 | -50,0 | 101,9 | -20,0 | 102,1 | -20,0 | 102,3 | -40,0 | 102,5 | -40,0 | 102,8 |
| ZMDM-SR | -33155,7 | 101,4 | -37149,2 | 101,4 | -40400,0 | 101,5 | -43905,1 | 101,6 | -48228,9 | 101,8 | -50952,6 | 101,9 |
| DZM-HR | -200,0 | 97,5 | -168,0 | 100,0 | -222,0 | 102,5 | -266,0 | 105,0 | -201,0 | 107,5 | -255,0 | 110,0 |
| NSCIM-UA | -69,0 | 21,4 | 221,0 | 21,7 | 214,0 | 22,1 | 209,0 | 22,5 | 236,0 | 22,8 | 230,0 | 23,3 |
| CMI-CZ | -229,0 | 16,5 | -213,0 | 17,0 | -218,0 | 17,5 | -276,0 | 18,1 | -224,0 | 18,8 | -259,0 | 19,4 |
| METAS-CH | -216,0 | 8,5 | -196,0 | 8,6 | -214,0 | 8,8 | -259,0 | 8,9 | -217,0 | 9,1 | -242,0 | 9,3 |
| NPL-GB | -210,7 | 30,0 | -190,6 | 30,0 | -210,5 | 30,0 | -257,5 | 30,0 | -217,9 | 30,0 | -240,9 | 30,0 |

| Meas. point | 75,0 mm | | 80,0 mm | | 85,0 mm | | 90,0 mm | | 95,0 mm | | 100,0 mm | |
|-------------|----------|---------------------|----------|---------------------|----------|---------------------|----------|---------------------|----------|---------------------|----------|---------------------|
| | dL / nm | u _c / nm | dL / nm | u _c / nm | dL / nm | u _c / nm | dL / nm | u _c / nm | dL / nm | u _c / nm | dL / nm | u _c / nm |
| MIRS-SI | -290,0 | 151,0 | -280,0 | 157,0 | -320,0 | 163,0 | -510,0 | 169,0 | -420,0 | 175,0 | -440,0 | 181,0 |
| METAS-CH | -280,0 | 9,4 | -242,0 | 9,6 | -263,0 | 9,8 | -434,0 | 10,0 | -365,0 | 10,3 | -387,0 | 10,5 |
| NPL-GB | -257,0 | 30,0 | -217,4 | 30,0 | -234,0 | 30,0 | -406,3 | 30,0 | -340,6 | 30,0 | -371,0 | 30,0 |
| OMH-HU | -559,0 | 100,2 | -456,0 | 100,3 | -531,0 | 100,3 | -639,0 | 100,4 | -466,0 | 100,4 | -486,0 | 100,4 |
| BEV-AT | -465,0 | 111,0 | -475,0 | 111,0 | -516,0 | 111,0 | -657,0 | 111,0 | -615,0 | 111,0 | -709,0 | 111,0 |
| SMU-SK | -191,0 | 46,5 | -201,0 | 46,6 | -197,0 | 46,7 | -222,0 | 46,8 | -211,0 | 46,9 | -250,0 | 47,0 |
| PTB-DE | -273,6 | 13,0 | -231,1 | 13,0 | -230,7 | 13,0 | -410,3 | 13,0 | -352,8 | 13,0 | -387,9 | 13,0 |
| GUM-PL | -451,0 | 153,6 | -533,0 | 156,1 | -562,0 | 158,7 | -605,0 | 161,4 | -551,0 | 164,3 | -588,0 | 167,2 |
| MIKES-FI | -284,0 | 11,8 | -235,0 | 11,9 | -292,0 | 25,0 | -399,0 | 25,0 | -342,0 | 25,0 | -388,0 | 12,2 |
| LNMC-LV | 250,0 | 823,0 | -230,0 | 823,0 | -950,0 | 823,0 | -1420,0 | 823,0 | -1210,0 | 823,0 | -1720,0 | 823,0 |
| NML-IE | 2500,0 | 739,6 | 2020,0 | 739,6 | 2060,0 | 739,6 | 2340,0 | 739,6 | 2840,0 | 739,6 | 2840,0 | 739,6 |
| NCM-BG | -324,0 | 82,1 | -289,0 | 82,6 | -313,0 | 83,2 | -485,0 | 83,8 | -423,0 | 84,4 | -443,0 | 85,1 |
| INM-RO | -50,0 | 103,0 | -40,0 | 103,3 | -20,0 | 103,6 | -30,0 | 103,9 | -60,0 | 104,3 | -30,0 | 104,6 |
| ZMDM-SR | -55368,7 | 102,0 | -58869,3 | 102,1 | -62248,0 | 102,3 | -66038,9 | 102,4 | -69011,4 | 102,6 | -73278,6 | 102,8 |
| DZM-HR | -310,0 | 112,5 | -262,0 | 115,0 | -310,0 | 117,5 | -391,0 | 120,0 | -321,0 | 122,5 | -312,0 | 125,0 |
| NSCIM-UA | 187,0 | 23,7 | 235,0 | 24,2 | 226,0 | 24,7 | 74,0 | 25,2 | 182,0 | 25,7 | 135,0 | 26,2 |
| CMI-CZ | -295,0 | 20,1 | -259,0 | 20,8 | -280,0 | 21,5 | -459,0 | 22,2 | -382,0 | 23,0 | -412,0 | 23,8 |
| METAS-CH | -279,0 | 9,4 | -242,0 | 9,6 | -262,0 | 9,8 | -428,0 | 10,0 | -366,0 | 10,3 | -388,0 | 10,5 |
| NPL-GB | -279,3 | 30,0 | -240,0 | 30,0 | -256,6 | 30,0 | -423,7 | 30,0 | -362,4 | 30,0 | -381,6 | 30,0 |

Figure 17 presents measurement results (deviations from nominal values) for measurement ranges 0,1 mm to 1 mm and 1 mm to 100 mm.

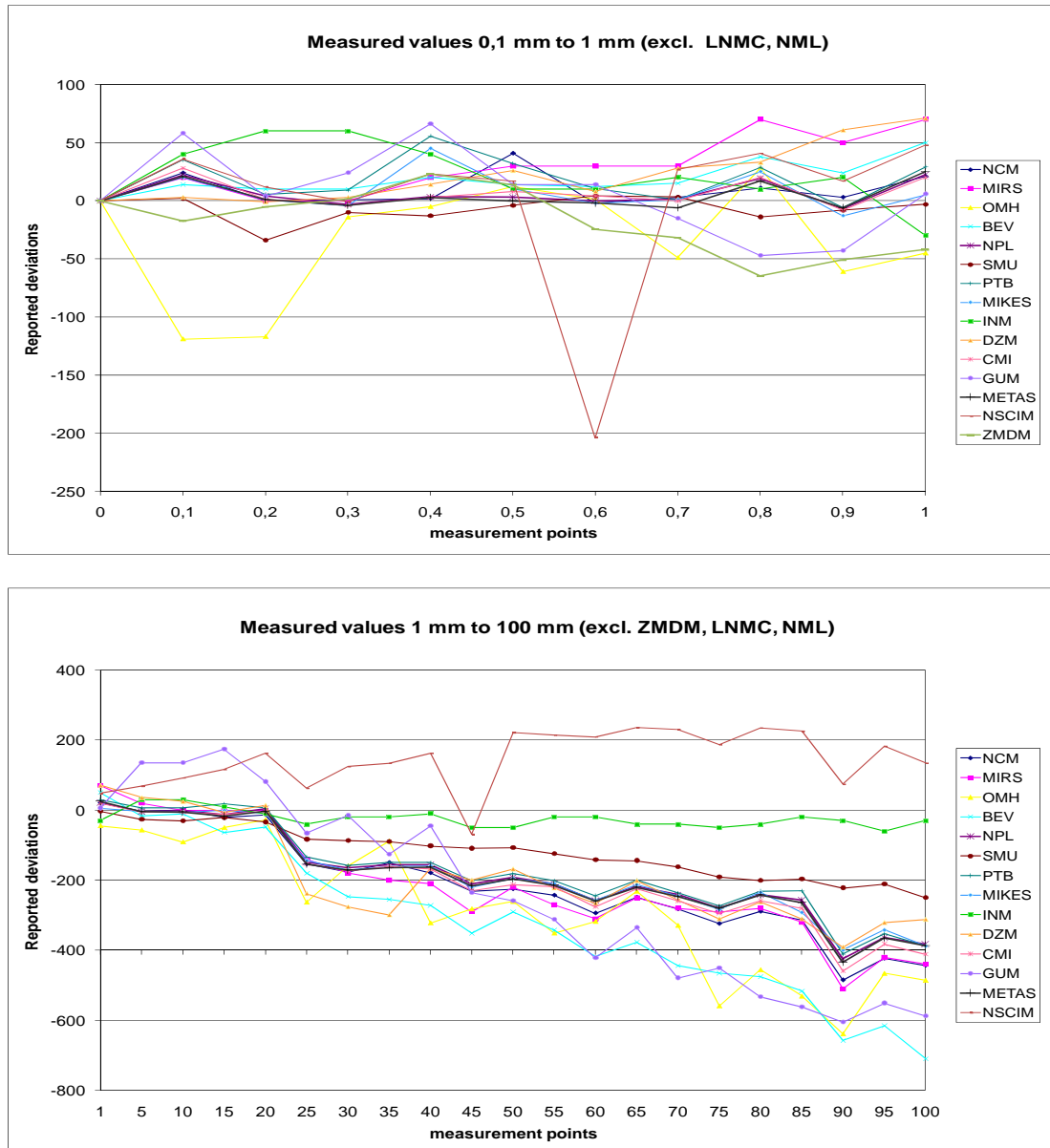


Figure 17: Deviations from nominal values - group 1

Graphical illustration of deviations from the reference values, which were calculated separately for group 1 (without linking the groups) are presented in Appendix 1.

8.2 Measurement results – Group 2

Measurement results of Group 2 are presented in Table 10. The first set of NPL measurements and the last set of METAS measurements were used only for scale stability evaluation. They were excluded from final evaluation of the participants.

Table 10: Measurement results – Group 2

| Meas. point | 0,1 mm | | 0,2 mm | | 0,3 mm | | 0,4 mm | | 0,5 mm | | 0,6 mm | |
|---------------|---------|---------------------|---------|---------------------|---------|---------------------|---------|---------------------|---------|---------------------|---------|---------------------|
| | dL / nm | u _c / nm | dL / nm | u _c / nm | dL / nm | u _c / nm | dL / nm | u _c / nm | dL / nm | u _c / nm | dL / nm | u _c / nm |
| METAS-CH | 28,0 | 7,9 | -8,0 | 7,9 | 14,0 | 7,9 | 1,0 | 7,9 | -10,0 | 7,9 | 3,0 | 7,9 |
| NPL-GB | 22,9 | 30,0 | -10,7 | 30,0 | 11,4 | 30,0 | -0,5 | 30,0 | -9,9 | 30,0 | 0,6 | 30,0 |
| EIM-GR | 29,0 | 566,0 | 22,0 | 566,0 | 48,0 | 566,0 | 34,0 | 566,0 | 20,0 | 566,0 | 17,0 | 566,0 |
| INRIM-IT | 31,0 | 45,0 | -4,0 | 45,0 | 21,0 | 45,0 | 7,0 | 45,0 | -2,0 | 45,0 | 6,0 | 45,0 |
| Nmi-VSL-NL | 22,0 | 21,0 | -13,0 | 21,0 | 10,0 | 21,0 | -8,0 | 21,0 | -15,0 | 21,0 | -40,0 | 21,1 |
| CEM-ES | 35,0 | 28,4 | -12,0 | 28,4 | 15,0 | 28,4 | 9,0 | 28,4 | -7,0 | 28,4 | 3,0 | 28,4 |
| INMETRO-BR | 30,0 | 63,0 | 42,0 | 63,0 | 62,0 | 63,0 | 21,0 | 63,0 | 11,0 | 63,0 | 23,0 | 63,0 |
| CENAM-MX | 0,0 | 137,8 | 0,0 | 137,8 | 0,0 | 137,8 | 0,0 | 137,8 | 0,0 | 137,8 | -100,0 | 137,8 |
| NIST-US | 36,0 | 3,1 | 1,2 | 3,1 | 16,7 | 3,1 | 4,4 | 3,1 | -11,2 | 3,1 | 4,9 | 3,1 |
| NRC-CA | 26,8 | 40,0 | -11,3 | 40,0 | 13,6 | 40,0 | 2,3 | 40,0 | -13,7 | 40,0 | 5,3 | 40,0 |
| A*Star-NMC-SG | 50,0 | 115,0 | 0,0 | 115,0 | 0,0 | 115,0 | 25,0 | 115,0 | 0,0 | 115,0 | 0,0 | 115,0 |
| NIM-CN | 11,0 | 49,0 | -28,0 | 49,0 | -12,0 | 49,0 | -26,0 | 49,0 | -33,0 | 49,0 | -16,0 | 49,0 |
| NPLI-IN | 26,0 | 236,0 | -32,0 | 236,0 | 92,0 | 236,0 | -144,0 | 236,0 | -76,0 | 236,0 | -114,0 | 236,0 |
| NIMT-THA | 25,8 | 20,5 | -8,8 | 20,5 | 18,7 | 20,5 | 20,5 | 20,5 | 5,1 | 20,5 | 4,0 | 20,5 |
| NPL-GB | 30,9 | 30,0 | -5,8 | 30,0 | 8,6 | 30,0 | -5,1 | 30,0 | -24,6 | 30,0 | -3,3 | 30,0 |
| METAS-CH | 21,0 | 7,9 | -13,0 | 7,9 | 10,0 | 7,9 | -2,0 | 7,9 | -13,0 | 7,9 | 2,0 | 7,9 |
| VNIIM-RU | 27,0 | 10,0 | -13,0 | 10,0 | 10,0 | 10,0 | -5,0 | 10,1 | -16,0 | 10,1 | -1,0 | 10,1 |

| Meas. point | 0,7 mm | | 0,8 mm | | 0,9 mm | | 1,0 mm | | 5,0 mm | | 10,0 mm | |
|---------------|---------|---------------------|---------|---------------------|---------|---------------------|---------|---------------------|---------|---------------------|---------|---------------------|
| | dL / nm | u _c / nm | dL / nm | u _c / nm | dL / nm | u _c / nm | dL / nm | u _c / nm | dL / nm | u _c / nm | dL / nm | u _c / nm |
| METAS-CH | -18,0 | 7,9 | 15,0 | 7,9 | -16,0 | 7,9 | 28,0 | 7,9 | 21,0 | 7,9 | 16,0 | 7,9 |
| NPL-GB | -23,9 | 30,0 | 12,2 | 30,0 | -15,5 | 30,0 | 20,3 | 30,0 | 24,9 | 30,0 | 20,9 | 30,0 |
| EIM-GR | -39,0 | 566,0 | -50,0 | 566,0 | -35,0 | 566,0 | 31,0 | 566,0 | -29,0 | 566,0 | -37,0 | 566,1 |
| INRIM-IT | -20,0 | 45,0 | 17,0 | 45,0 | -19,0 | 45,0 | 30,0 | 45,0 | 21,0 | 45,0 | 23,0 | 45,0 |
| Nmi-VSL-NL | -22,0 | 21,1 | 20,0 | 21,1 | -23,0 | 21,1 | 29,0 | 21,1 | 16,0 | 21,5 | 12,0 | 21,9 |
| CEM-ES | -13,0 | 28,4 | 33,0 | 28,4 | 1,0 | 28,4 | 27,0 | 28,4 | 40,0 | 28,4 | 60,0 | 28,5 |
| INMETRO-BR | 16,0 | 63,0 | 23,0 | 63,0 | -12,0 | 63,0 | 19,0 | 63,0 | -4,0 | 63,0 | -4,0 | 63,0 |
| CENAM-MX | -100,0 | 137,8 | -100,0 | 137,8 | -100,0 | 137,8 | 0,0 | 137,8 | -100,0 | 138,2 | 0,0 | 139,2 |
| NIST-US | -15,1 | 3,1 | 18,2 | 3,1 | -11,3 | 3,1 | 30,3 | 3,1 | 20,7 | 3,7 | 24,9 | 3,7 |
| NRC-CA | -17,6 | 40,0 | 17,4 | 40,0 | -13,6 | 40,0 | 31,8 | 40,0 | 21,5 | 40,0 | 22,9 | 40,0 |
| A*Star-NMC-SG | 0,0 | 115,0 | 0,0 | 115,0 | 25,0 | 115,0 | 75,0 | 115,0 | -25,0 | 115,0 | -50,0 | 115,1 |
| NIM-CN | -40,0 | 49,0 | -23,0 | 49,0 | -32,0 | 49,0 | 6,0 | 49,0 | 9,0 | 49,0 | 1,0 | 49,0 |
| NPLI-IN | 43,0 | 236,0 | 78,0 | 236,0 | -59,0 | 236,0 | -96,0 | 236,0 | 12,0 | 236,0 | -76,0 | 236,0 |
| NIMT-THA | -32,2 | 20,5 | 11,8 | 20,5 | -6,7 | 20,5 | 40,0 | 20,5 | 20,8 | 20,7 | 16,1 | 21,1 |
| NPL-GB | -32,3 | 30,0 | -2,9 | 30,0 | -30,7 | 30,0 | 5,2 | 30,0 | 22,0 | 30,0 | 21,2 | 30,0 |
| METAS-CH | -22,0 | 7,9 | 11,0 | 7,9 | -21,0 | 7,9 | 24,0 | 7,9 | 9,0 | 7,9 | 7,0 | 7,9 |
| VNIIM-RU | -24,0 | 10,1 | 8,0 | 10,1 | -24,0 | 10,1 | 22,0 | 10,2 | 8,0 | 10,8 | 10,0 | 11,5 |

| Meas. point | 15,0 mm | | 20,0 mm | | 25,0 mm | | 30,0 mm | | 35,0 mm | | 40,0 mm | |
|---------------|---------|---------------------|---------|---------------------|---------|---------------------|---------|---------------------|---------|---------------------|---------|---------------------|
| | dL / nm | u _c / nm | dL / nm | u _c / nm | dL / nm | u _c / nm | dL / nm | u _c / nm | dL / nm | u _c / nm | dL / nm | u _c / nm |
| METAS-CH | -34,0 | 8,0 | 15,0 | 8,0 | -133,0 | 8,1 | -161,0 | 8,2 | -136,0 | 8,3 | -145,0 | 8,4 |
| NPL-GB | -17,9 | 30,0 | 20,0 | 30,0 | -119,4 | 30,0 | -145,6 | 30,0 | -121,8 | 30,0 | -130,5 | 30,0 |
| EIM-GR | -75,0 | 566,2 | -126,0 | 566,4 | -269,0 | 566,6 | -422,0 | 566,8 | -396,0 | 567,1 | -522,0 | 567,4 |
| INRIM-IT | -23,0 | 45,1 | 22,0 | 45,2 | -126,0 | 45,3 | -154,0 | 45,4 | -131,0 | 45,5 | -136,0 | 45,7 |
| Nmi-VSL-NL | -29,0 | 22,4 | 28,0 | 22,8 | -101,0 | 23,3 | -142,0 | 23,7 | -128,0 | 24,2 | -112,0 | 24,6 |
| CEM-ES | 16,0 | 28,5 | 43,0 | 28,6 | -79,0 | 28,7 | -131,0 | 28,8 | -77,0 | 28,9 | -79,0 | 29,1 |
| INMETRO-BR | -23,0 | 63,0 | 16,0 | 63,0 | -69,0 | 63,0 | -95,0 | 63,0 | -84,0 | 63,0 | -80,0 | 63,0 |
| CENAM-MX | 0,0 | 140,9 | -100,0 | 143,2 | -300,0 | 146,2 | 0,0 | 149,7 | -200,0 | 153,8 | 0,0 | 158,3 |
| NIST-US | -19,4 | 3,8 | 27,3 | 3,8 | -116,6 | 3,9 | -145,8 | 4,0 | -119,3 | 4,1 | -119,3 | 4,2 |
| NRC-CA | -24,2 | 40,1 | 23,1 | 40,2 | -115,0 | 40,3 | -139,9 | 40,4 | -120,8 | 40,6 | -121,1 | 40,8 |
| A*Star-NMC-SG | -75,0 | 115,1 | 0,0 | 115,2 | -150,0 | 115,3 | -150,0 | 115,5 | -150,0 | 115,7 | -150,0 | 115,8 |
| NIM-CN | -12,0 | 49,0 | 28,0 | 49,0 | -91,0 | 49,0 | -97,0 | 49,0 | -75,0 | 49,0 | -73,0 | 49,0 |
| NPLI-IN | -68,0 | 236,0 | -23,0 | 236,1 | -344,0 | 236,1 | -261,0 | 236,2 | -176,0 | 236,3 | -212,0 | 236,3 |
| NIMT-THA | -19,7 | 21,9 | 1,2 | 23,0 | -119,6 | 24,2 | -151,3 | 25,7 | -137,1 | 27,3 | -127,9 | 29,1 |
| NPL-GB | -20,7 | 30,0 | 22,7 | 30,0 | -113,3 | 30,0 | -150,7 | 30,0 | -126,2 | 30,0 | -129,5 | 30,0 |
| METAS-CH | -40,0 | 8,0 | 5,0 | 8,0 | -141,0 | 8,1 | -171,0 | 8,2 | -146,0 | 8,3 | -150,0 | 8,4 |
| VNIIM-RU | -38,0 | 12,3 | 6,0 | 13,0 | -140,0 | 13,8 | -167,0 | 14,5 | -146,0 | 15,3 | -151,0 | 16,0 |

| Meas. point | 45,0 mm | | 50,0 mm | | 55,0 mm | | 60,0 mm | | 65,0 mm | | 70,0 mm | |
|---------------|---------|---------------------|---------|---------------------|---------|---------------------|---------|---------------------|---------|---------------------|---------|---------------------|
| | dL / nm | u _c / nm | dL / nm | u _c / nm | dL / nm | u _c / nm | dL / nm | u _c / nm | dL / nm | u _c / nm | dL / nm | u _c / nm |
| METAS-CH | -194,0 | 8,5 | -126,0 | 8,6 | -151,0 | 8,8 | -171,0 | 8,9 | -131,0 | 9,1 | -155,0 | 9,3 |
| NPL-GB | -181,4 | 30,0 | -110,9 | 30,0 | -129,4 | 30,0 | -147,5 | 30,0 | -107,8 | 30,0 | -125,3 | 30,0 |
| EIM-GR | -582,0 | 567,8 | -561,0 | 568,2 | -547,0 | 568,7 | -547,0 | 569,2 | -474,0 | 569,7 | -520,0 | 570,3 |
| INRIM-IT | -180,0 | 45,9 | -106,0 | 46,1 | -138,0 | 46,3 | -156,0 | 46,6 | -117,0 | 46,8 | -143,0 | 47,1 |
| Nmi-VSL-NL | -159,0 | 25,1 | -59,0 | 25,5 | -101,0 | 26,0 | -124,0 | 26,4 | -84,0 | 26,9 | -89,0 | 27,3 |
| CEM-ES | -151,0 | 29,2 | -101,0 | 29,4 | -128,0 | 29,6 | -134,0 | 29,8 | -113,0 | 30,1 | -128,0 | 30,3 |
| INMETRO-BR | -98,0 | 63,0 | -84,0 | 63,0 | -87,0 | 63,0 | -77,0 | 92,0 | -140,0 | 92,0 | -77,0 | 92,0 |
| CENAM-MX | 100,0 | 163,4 | -100,0 | 168,8 | -100,0 | 174,6 | -100,0 | 180,8 | -200,0 | 187,2 | -300,0 | 193,9 |
| NIST-US | -183,1 | 4,3 | -110,8 | 4,5 | -131,7 | 4,6 | -153,1 | 4,8 | -111,2 | 4,9 | -129,0 | 5,1 |
| NRC-CA | -171,5 | 41,0 | -99,7 | 41,2 | -127,5 | 41,5 | -145,6 | 41,8 | -106,9 | 42,1 | -133,0 | 42,4 |
| A*Star-NMC-SG | -200,0 | 116,1 | -150,0 | 116,3 | -175,0 | 116,6 | -200,0 | 116,9 | -175,0 | 117,2 | -175,0 | 117,6 |
| NIM-CN | -116,0 | 49,0 | -32,0 | 49,0 | -53,0 | 49,0 | -48,0 | 49,0 | -5,0 | 49,0 | -27,0 | 49,0 |
| NPLI-IN | -238,0 | 236,4 | -163,0 | 236,5 | -252,0 | 236,7 | -271,0 | 236,8 | -129,0 | 236,9 | -56,0 | 237,1 |
| NIMT-THA | -192,0 | 31,0 | -121,9 | 33,0 | -147,7 | 35,1 | -150,9 | 37,2 | -131,1 | 39,4 | -206,0 | 41,6 |
| NPL-GB | -183,0 | 30,0 | -112,3 | 30,0 | -137,5 | 30,0 | -152,5 | 30,0 | -107,8 | 30,0 | -128,5 | 30,0 |
| METAS-CH | -205,0 | 8,5 | -132,0 | 8,6 | -156,0 | 8,8 | -176,0 | 8,9 | -141,0 | 9,1 | -162,0 | 9,3 |
| VNIIM-RU | -202,0 | 16,8 | -133,0 | 17,5 | -157,0 | 18,3 | -177,0 | 19,0 | -138,0 | 19,8 | -161,0 | 20,5 |

| Meas. point | 75,0 mm | | 80,0 mm | | 85,0 mm | | 90,0 mm | | 95,0 mm | | 100,0 mm | |
|---------------|---------|---------------------|---------|---------------------|---------|---------------------|---------|---------------------|---------|---------------------|----------|---------------------|
| | dL / nm | u _c / nm | dL / nm | u _c / nm | dL / nm | u _c / nm | dL / nm | u _c / nm | dL / nm | u _c / nm | dL / nm | u _c / nm |
| METAS-CH | -170,0 | 9,4 | -145,0 | 9,6 | -158,0 | 9,8 | -340,0 | 10,0 | -289,0 | 10,3 | -279,0 | 10,5 |
| NPL-GB | -146,3 | 30,0 | -110,6 | 30,0 | -120,5 | 30,0 | -310,3 | 30,0 | -258,1 | 30,0 | -256,7 | 30,0 |
| EIM-GR | -541,0 | 570,9 | -505,0 | 571,6 | -570,0 | 572,3 | -641,0 | 573,1 | -562,0 | 573,9 | -497,0 | 574,8 |
| INRIM-IT | -151,0 | 47,4 | -123,0 | 47,8 | -139,0 | 48,1 | -315,0 | 48,5 | -262,0 | 48,8 | -255,0 | 49,2 |
| Nmi-VSL-NL | -112,0 | 27,8 | -99,0 | 28,2 | -109,0 | 28,7 | -273,0 | 29,1 | -216,0 | 29,6 | -187,0 | 30,0 |
| CEM-ES | -156,0 | 30,6 | -105,0 | 30,9 | -144,0 | 31,2 | -307,0 | 31,5 | -257,0 | 31,8 | -261,0 | 32,1 |
| INMETRO-BR | -80,0 | 92,0 | 9,0 | 92,0 | -59,0 | 92,0 | -308,0 | 92,0 | -263,0 | 92,0 | -342,0 | 92,0 |
| CENAM-MX | -400,0 | 200,9 | -400,0 | 208,1 | -400,0 | 215,5 | -500,0 | 223,1 | -500,0 | 230,8 | -500,0 | 238,7 |
| NIST-US | -146,2 | 5,3 | -125,3 | 5,4 | -125,4 | 5,6 | -313,4 | 5,8 | -266,3 | 6,0 | -249,6 | 6,2 |
| NRC-CA | -143,6 | 42,7 | -118,2 | 43,1 | -125,4 | 43,5 | -312,9 | 43,9 | -261,8 | 44,3 | -256,8 | 44,7 |
| A*Star-NMC-SG | -225,0 | 118,0 | -150,0 | 118,4 | -162,0 | 118,8 | -338,0 | 119,2 | -238,0 | 119,7 | -212,0 | 120,2 |
| NIM-CN | -31,0 | 49,0 | 8,0 | 49,0 | -2,0 | 49,0 | -167,0 | 49,0 | -115,0 | 49,0 | -101,0 | 49,0 |
| NPLI-IN | -106,0 | 237,2 | -190,0 | 237,4 | -294,0 | 237,6 | -364,0 | 237,8 | -592,0 | 237,9 | -713,0 | 238,2 |
| NIMT-THA | -158,0 | 43,9 | -124,5 | 46,2 | -151,7 | 48,5 | -314,1 | 50,8 | -279,4 | 53,2 | -259,4 | 55,6 |
| NPL-GB | -149,8 | 30,0 | -106,3 | 30,0 | -126,2 | 30,0 | -311,5 | 30,0 | -251,2 | 30,0 | -246,2 | 30,0 |
| METAS-CH | -177,0 | 9,4 | -152,0 | 9,6 | -164,0 | 9,8 | -347,0 | 10,0 | -296,0 | 10,3 | -289,0 | 10,5 |
| VNIIM-RU | -179,0 | 21,3 | -147,0 | 22,0 | -161,0 | 22,8 | -345,0 | 23,5 | -292,0 | 24,3 | -286,0 | 25,0 |

Figure 18 presents measurement results (deviations from nominal values) for measurement ranges 0,1 mm to 1 mm and 1 mm to 100 mm.

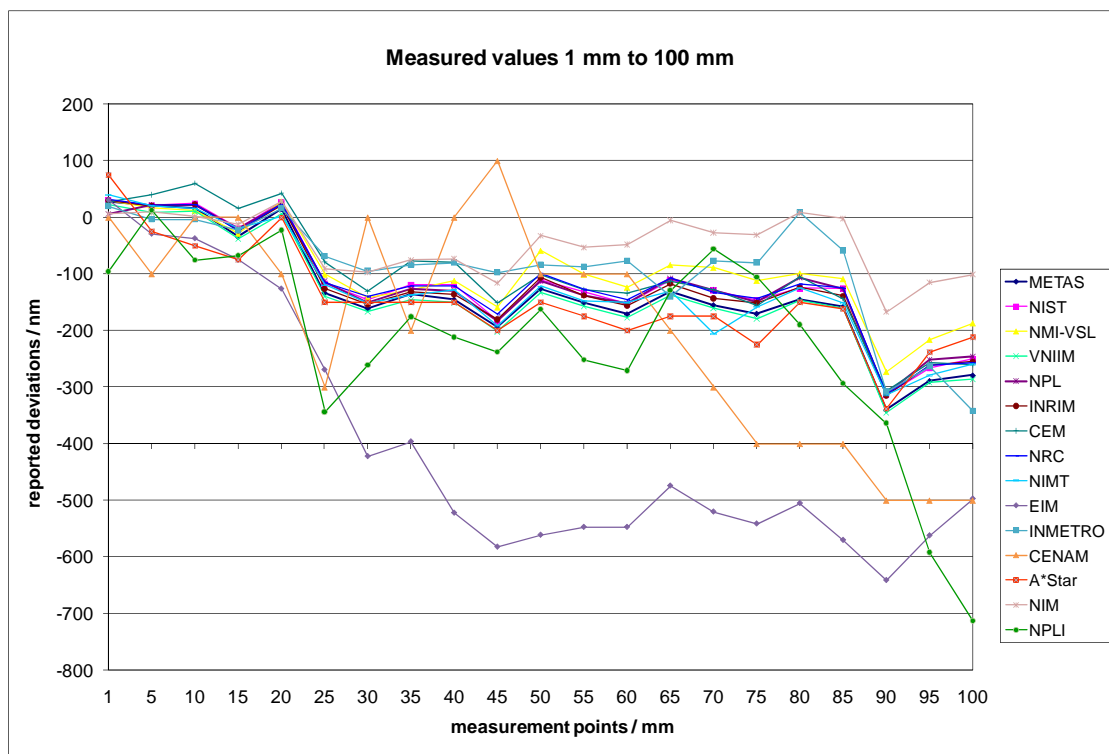
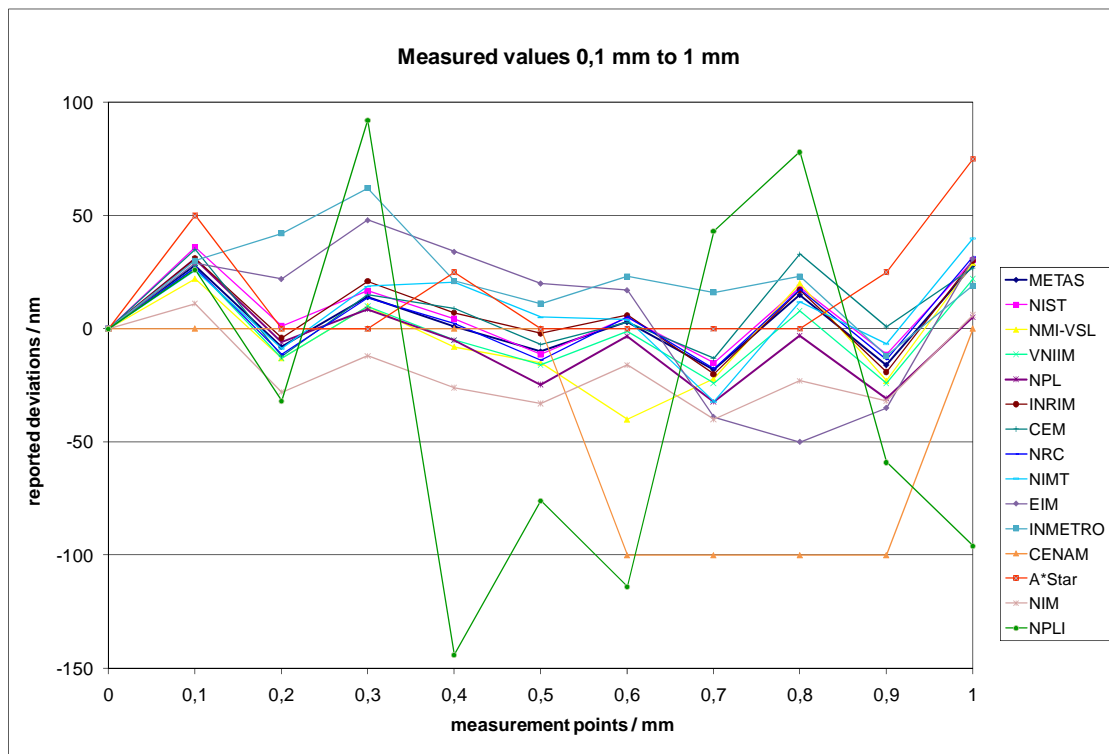


Figure 18: Deviations from nominal values – group 2

Graphical illustration of deviations from the reference values, which were calculated separately for group 2 (without linking the groups) are presented in Appendix 1.

8.3 Correction of the original results

After issuing draft A report, one laboratory (SMU from Group 1) requested to correct its results due to wrong thermal expansion correction, and one laboratory (A*Star from group 2) requested to correct its uncertainty budget due to obvious error in calculating standard uncertainties of input quantities.

After the two laboratories had sent their technical explanations, the requested changes were approved, because clear mistakes were shown. The explanations are attached below:

SMU Slovakia:

“SMU used Abbe Zeiss length measuring machine combined with HP 5529B laser interferometer. The computer was working permanently during the measurement period (December 2006), i.e. it ran approximately 3 weeks without switch off. The external sensors have been used and the actualized values of the line measure temperature and atmosphere parameters were being inserted into the system before each measurement cycle (10 lines within each measurement cycle). Of course, the thermal dilatation coefficient (in the form $x.xxx \text{ ppm}/^\circ\text{C}$) was inserted once at the beginning of SMU measurements and thus its value remained untouched during the whole measurement period.

The most frequently used values while measuring steel or glass artifacts are therefore $11.500 \text{ ppm}/^\circ\text{C}$ or $8.500 \text{ ppm}/^\circ\text{C}$ respectively. Unfortunately, only after receipt of the first draft I realized that the value I saw displayed was $5.000 \text{ ppm}/^\circ\text{C}$ (instead of $0.500 \text{ ppm}/^\circ\text{C}$). Nevertheless, I must admit that after almost 3 years I am not quite sure (i.e. 100%) what I actually saw on the display, but it is much more probable that 0.5 ppm was not displayed there.

The average temperature corresponding to the larger nominal lengths was $19,63 \text{ }^\circ\text{C}$, therefore the temperature compensation according to the value of $5 \times 10^{-6} \text{ K}^{-1}$ was 10 times larger and hence it shifted the measured values towards the nominal ones (of course, just those lying below the nominal, but in fact it seems that for entirely all larger values it is the case). For example, in the corrected set of SMU results, the deviation corresponding to 100 mm has changed from -84 nm to -250 nm , etc.

Paradoxically, I always kept in mind that the thermal expansion coefficient of quartz is low and thus I did not care for the temperature as usually, not in terms of the temperature measurement itself, but in terms of the communication with the air condition centre. The air conditioning system of the institute is old, expensive and not as effective as in many other institutes, therefore we have always problem to keep the temperature close to $20 \text{ }^\circ\text{C}$, even if it is relatively stable. It was December and thus the temperature in lab was below $20 \text{ }^\circ\text{C}$. Just three weeks I had for measurements (we have obliged holiday from Christmas to New Year at the SMU) and there was not enough time to wait until the ambient temperature is closer to $20 \text{ }^\circ\text{C}$.

The microscope magnification I used was 125x and the line edge was of high quality; according to my experience, I can hardly believe that I could be wrong by roughly $0.5 \text{ } \mu\text{m}$ as it looks from the first submitted set of measurements. I am aware that some people could take the explanation given above as the clear speculation, because of the subjective feeling of “what I saw on the display 2.5 years ago” can be hardly taken as the rigid proof in this case.”

A*Star Singapore:

*“A*Star-NMC-SG has requested a change in two uncertainty components being the errors due to horizontal and vertical Abbe offsets. The initial values of the two components were given at 2 sigma level with rectangular distribution and should be divided by $\text{SQRT}(3)$ for the conversion to standard uncertainty. The miss-calculations were corrected and updated in the uncertainty budget table.”*

8.4 Link between the groups

The results in the previous chapter were shown for each group separately. This chapter is presenting the results after linking the groups by using Bayesian statistics [2].

In order to make statistical formulas more clear, Group 1 is indexed with “A” and Group 2 with “B” as shown in Figure 19. Index “C” is assigned to the intersection of sets “A” and “B”, which contains 2 elements (linking laboratories NPL and METAS).

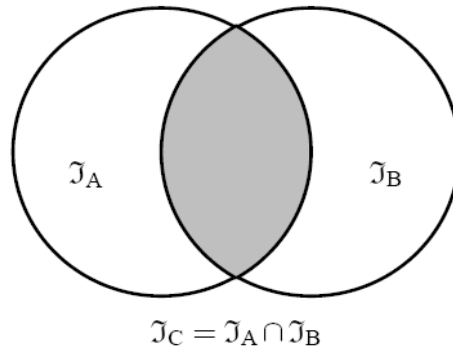


Figure 19: Group 1 and Group 2 are presented by 2 sets of elements “A” and “B”

The results are calculated by the following formulas:

Reference values:

$$y_A = \frac{bS_1 + cS_2}{ab - c^2} \quad (10)$$

$$y_B = \frac{cS_1 + aS_2}{ab - c^2} \quad (11)$$

Standard uncertainties of the reference values:

$$u(y_A) = \sqrt{\frac{b}{ab - c^2}} \quad (12)$$

$$u(y_B) = \sqrt{\frac{a}{ab - c^2}} \quad (13)$$

Covariance:

$$u(y_A, y_B) = \frac{c}{ab - c^2} \quad (14)$$

Where:

$$a = \sum_{i \in (I_A \setminus I_B)} \frac{1}{u^2(x_{A,i})} + \sum_{i \in (I_A \cap I_B)} \frac{u^2(x_{B,i})}{u^2(x_{A,i})u^2(x_{B,i}) - u^2(x_{A,i}, x_{B,i})} \quad (15)$$

$$b = \sum_{i \in (I_B \setminus I_A)} \frac{1}{u^2(x_{B,i})} + \sum_{i \in (I_A \cap I_B)} \frac{u^2(x_{A,i})}{u^2(x_{A,i})u^2(x_{B,i}) - u^2(x_{A,i}, x_{B,i})} \quad (16)$$

$$c = \sum_{i \in (\mathfrak{S}_A \cap \mathfrak{S}_B)} \frac{u(x_{A,i}, x_{B,i})}{u^2(x_{A,i})u^2(x_{B,i}) - u^2(x_{A,i}, x_{B,i})} \quad (17)$$

$$S_1 = \sum_{i \in (\mathfrak{S}_A \setminus \mathfrak{S}_B)} \frac{x_{A,i}}{u^2(x_{A,i})} + \sum_{i \in (\mathfrak{S}_A \cap \mathfrak{S}_B)} \frac{u^2(x_{B,i})x_{A,i} - u(x_{A,i}, x_{B,i})x_{B,i}}{u^2(x_{A,i})u^2(x_{B,i}) - u^2(x_{A,i}, x_{B,i})} \quad (18)$$

$$S_2 = \sum_{i \in (\mathfrak{S}_A \setminus \mathfrak{S}_B)} \frac{x_{B,i}}{u^2(x_{B,i})} + \sum_{i \in (\mathfrak{S}_A \cap \mathfrak{S}_B)} \frac{u^2(x_{A,i})x_{B,i} - u(x_{A,i}, x_{B,i})x_{A,i}}{u^2(x_{A,i})u^2(x_{B,i}) - u^2(x_{A,i}, x_{B,i})} \quad (19)$$

Values x are reported results of participating laboratories ($x_{A,i}$ for Group 1 and $x_{B,i}$ for Group 2), while $u(x)$ are reported standard uncertainties.

8.5 Intercomparison results for linked groups considering line scale stability

The results are shown in Table 12. Linking laboratories are in the middle of the table and are marked with green colour. Above them are laboratories from Group 1, while the laboratories from Group 2 are in the bottom part of the table.

The results given in Table 12 were calculated from the largest consistent subset. This subset was created by eliminating laboratories with the greatest E_n values until the Birge criterion (Ch. 7) was met and Chi-test passed. E_n values $|E_n| > 1$ are marked with yellow colour. Eliminated laboratories for single measurement points are shown in Table 11.

Table 11: Laboratories that were excluded from calculation of the reference values:

| Measuring point (mm) | No. of excl. labs | Excluded laboratories | Measuring point (mm) | No. of excl. labs | Excluded laboratories |
|----------------------|-------------------|-----------------------|----------------------|-------------------|---|
| 0,6 | 1 | NSCIM-UA | 55 | 2 | ZMDM-SR, NSCIM-UA |
| 5 | 1 | ZMDM-SR | 60 | 3 | ZMDM-SR, NSCIM-UA, NML-IE |
| 10 | 1 | ZMDM-SR | 65 | 2 | ZMDM-SR, NSCIM-UA |
| 15 | 2 | ZMDM-SR, NSCIM-UA | 70 | 2 | ZMDM-SR, NSCIM-UA |
| 20 | 2 | ZMDM-SR, NSCIM-UA | 75 | 3 | ZMDM-SR, NSCIM-UA, NML-IE |
| 25 | 2 | ZMDM-SR, NSCIM-UA | 80 | 3 | ZMDM-SR, NSCIM-UA, NML-IE |
| 30 | 2 | ZMDM-SR, NSCIM-UA | 85 | 5 | ZMDM-SR, NSCIM-UA, NML-IE, OMH-HU, BEV-AT, NIM-CN |
| 35 | 2 | ZMDM-SR, NSCIM-UA | 90 | 5 | ZMDM-SR, NSCIM-UA, NML-IE, SMU-SK, INM-RO |
| 40 | 2 | ZMDM-SR, NSCIM-UA | 95 | 4 | ZMDM-SR, NSCIM-UA, NML-IE, SMU-SK |
| 45 | 2 | ZMDM-SR, NSCIM-UA | 100 | 5 | ZMDM-SR, NSCIM-UA, NML-IE, BEV-AT, INM-RO, NIM-CN |
| 50 | 2 | ZMDM-SR, NSCIM-UA | | | |

Table 12: Reference values and uncertainties for all lines of scale A and scale B. Additionally, the deviations and the consistency with the reference values (E_n) are given for each participant

| Meas. Point | 0,1 mm | | 0,2 mm | | 0,3 mm | | 0,4 mm | | 0,5 mm | | 0,6 mm | |
|------------------------|-----------------|-------|-----------------|-------|-----------------|-------|-----------------|-------|-----------------|-------|-----------------|-------|
| $X_{ref, scale A}$ | 24,3 nm | | 2,0 nm | | -0,4 nm | | 13,4 nm | | 8,8 nm | | 2,9 nm | |
| $X_{ref, scale B}$ | 29,9 nm | | -6,4 nm | | 14,2 nm | | 1,7 nm | | -11,3 nm | | -0,6 nm | |
| $U_{c(xref), scale A}$ | 7,2 nm | | 7,1 nm | | 6,7 nm | | 7,7 nm | | 7,1 nm | | 7,0 nm | |
| $U_{c(xref), scale B}$ | 6,2 nm | |
| | $X_i - X_{ref}$ | E_n |
| MIRS-SI | -4,3 | 0,03 | -2,0 | 0,02 | 0,4 | 0,00 | 6,6 | 0,05 | 21,2 | 0,17 | 27,1 | 0,22 |
| OMH-HU | -143,3 | 0,71 | -119,0 | 0,59 | -13,6 | 0,07 | -18,4 | 0,09 | 3,2 | 0,02 | -1,9 | 0,01 |
| BEV-AT | -10,3 | 0,21 | 8,0 | 0,16 | 10,4 | 0,21 | 6,6 | 0,14 | 5,2 | 0,11 | 9,1 | 0,19 |
| SMU-SK | -22,3 | 0,24 | -36,0 | 0,39 | -9,6 | 0,10 | -26,4 | 0,28 | -12,8 | 0,14 | 1,1 | 0,01 |
| PTB-DE | 10,9 | 0,36 | 3,4 | 0,05 | 9,4 | 0,30 | 42,1 | 0,64 | 23,2 | 0,35 | 7,6 | 0,25 |
| GUM-PL | 33,7 | 0,13 | 2,0 | 0,01 | 24,4 | 0,09 | 52,6 | 0,20 | 5,2 | 0,02 | 11,1 | 0,04 |
| MIKES-FI | -4,3 | 0,08 | -1,0 | 0,03 | -3,6 | 0,13 | 31,6 | 0,60 | 1,2 | 0,04 | -4,9 | 0,18 |
| LNMC-LV | -224,3 | 0,14 | -202,0 | 0,12 | -199,6 | 0,12 | -13,4 | 0,01 | 191,2 | 0,12 | 397,1 | 0,24 |
| NML-IE | -104,3 | 0,07 | -48,0 | 0,03 | -185,6 | 0,13 | 26,6 | 0,02 | -368,8 | 0,25 | -122,9 | 0,08 |
| NCM-BG | -0,3 | 0,00 | -2,0 | 0,01 | 1,4 | 0,01 | -11,4 | 0,07 | 32,2 | 0,21 | -4,9 | 0,03 |
| INM-RO | 15,7 | 0,08 | 58,0 | 0,29 | 60,4 | 0,30 | 26,6 | 0,13 | 1,2 | 0,01 | 7,1 | 0,03 |
| ZMDM-SR | -41,6 | 0,21 | -7,3 | 0,04 | 1,8 | 0,01 | 9,7 | 0,05 | 5,1 | 0,03 | -27,6 | 0,14 |
| DZM-HR | -21,3 | 0,14 | -3,0 | 0,02 | 3,4 | 0,02 | 0,6 | 0,00 | 17,2 | 0,11 | 5,1 | 0,03 |
| NSCIM-UA | 11,7 | 0,27 | 10,0 | 0,23 | -0,6 | 0,01 | 9,6 | 0,22 | 8,2 | 0,19 | -206,9 | 4,35 |
| CMI-CZ | 3,7 | 0,11 | -1,0 | 0,03 | -3,6 | 0,11 | -10,4 | 0,33 | -0,8 | 0,03 | 1,1 | 0,03 |
| NPL-GB | -2,3 | 0,04 | 2,2 | 0,03 | -2,8 | 0,05 | -10,0 | 0,16 | -5,8 | 0,09 | -3,2 | 0,05 |
| METAS-CH | -3,3 | 0,15 | -1,0 | 0,04 | -3,6 | 0,16 | -10,4 | 0,47 | -8,8 | 0,39 | -4,9 | 0,22 |
| NPL-GB | 1,0 | 0,02 | 0,5 | 0,01 | -5,6 | 0,09 | -6,8 | 0,11 | -13,2 | 0,21 | -2,6 | 0,04 |
| METAS-CH | -1,9 | 0,08 | -1,6 | 0,07 | -0,2 | 0,01 | -0,7 | 0,03 | 1,3 | 0,06 | 3,6 | 0,15 |
| EIM-GR | -0,9 | 0,00 | 28,4 | 0,03 | 33,8 | 0,03 | 32,3 | 0,03 | 31,3 | 0,03 | 17,6 | 0,02 |
| INRIM-IT | 1,1 | 0,01 | 2,4 | 0,03 | 6,8 | 0,07 | 5,3 | 0,06 | 9,3 | 0,10 | 6,6 | 0,07 |
| Nmi-VSL-NL | -7,9 | 0,17 | -6,6 | 0,15 | -4,2 | 0,09 | -9,7 | 0,21 | -3,7 | 0,08 | -39,4 | 0,86 |
| CEM-ES | 5,1 | 0,09 | -5,6 | 0,09 | 0,8 | 0,01 | 7,3 | 0,12 | 4,3 | 0,07 | 3,6 | 0,06 |
| INMETRO-BR | 0,1 | 0,00 | 48,4 | 0,38 | 47,8 | 0,38 | 19,3 | 0,15 | 22,3 | 0,18 | 23,6 | 0,19 |
| CENAM-MX | -29,9 | 0,11 | 6,4 | 0,02 | -14,2 | 0,05 | -1,7 | 0,01 | 11,3 | 0,04 | -99,4 | 0,36 |
| NIST-US | 6,1 | 0,33 | 7,6 | 0,40 | 2,5 | 0,14 | 2,7 | 0,14 | 0,1 | 0,01 | 5,5 | 0,29 |
| NRC-CA | -3,1 | 0,04 | -4,9 | 0,06 | -0,5 | 0,01 | 0,6 | 0,01 | -2,4 | 0,03 | 5,9 | 0,07 |
| A*Star-NMC-SG | 20,1 | 0,09 | 6,4 | 0,03 | -14,2 | 0,06 | 23,3 | 0,10 | 11,3 | 0,05 | 0,6 | 0,00 |
| NIM-CN | -18,9 | 0,19 | -21,6 | 0,22 | -26,2 | 0,26 | -27,7 | 0,28 | -21,7 | 0,22 | -15,4 | 0,15 |
| NPL-IN | -3,9 | 0,01 | -25,6 | 0,05 | 77,8 | 0,16 | -145,7 | 0,31 | -64,7 | 0,14 | -113,4 | 0,24 |
| NIMT-THA | -4,1 | 0,09 | -2,4 | 0,05 | 4,5 | 0,10 | 18,7 | 0,42 | 16,4 | 0,37 | 4,6 | 0,10 |
| VNIM-RU | -2,9 | 0,11 | -6,6 | 0,25 | -4,2 | 0,16 | -6,7 | 0,25 | -4,7 | 0,17 | -0,4 | 0,01 |

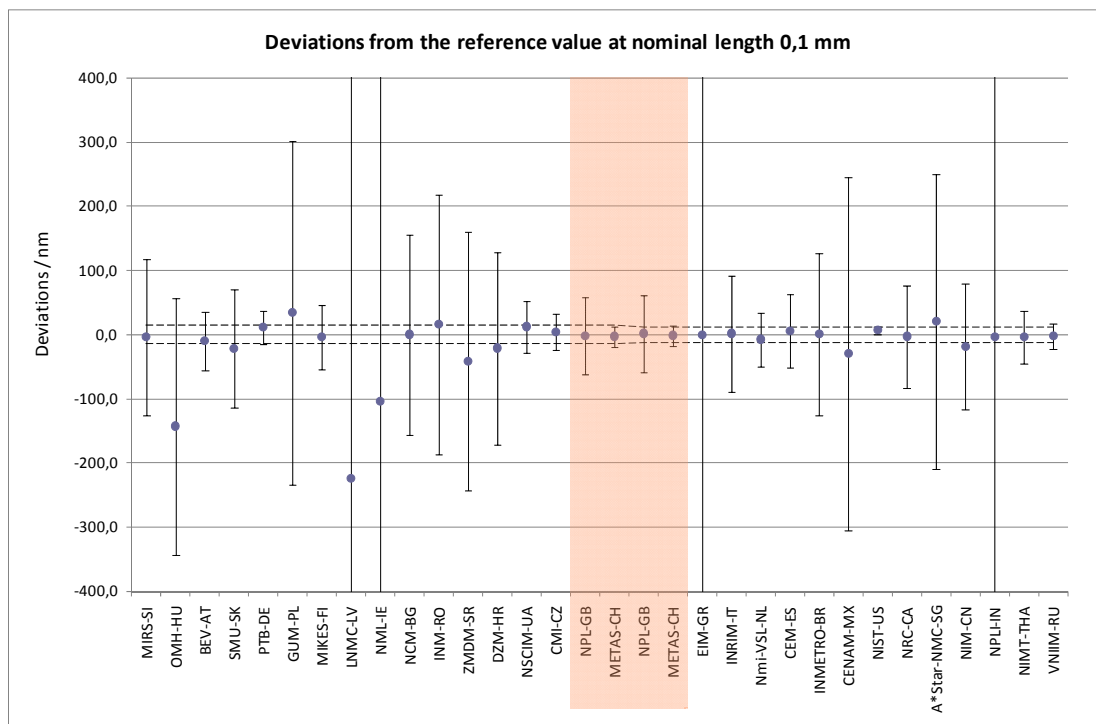
| Meas. Point | 0,7 mm | | 0,8 mm | | 0,9 mm | | 1 mm | | 5 mm | | 10 mm | |
|------------------------|-----------------|-------|-----------------|-------|-----------------|-------|-----------------|-------|-----------------|-------|-----------------|-------|
| $X_{ref, scale A}$ | 2,9 nm | | 23,9 nm | | -2,7 nm | | 24,3 nm | | 4,6 nm | | 5,8 nm | |
| $X_{ref, scale B}$ | -20,2 nm | | 14,2 nm | | -15,9 nm | | 27,3 nm | | 18,3 nm | | 19,3 nm | |
| $U_{c(xref), scale A}$ | 7,1 nm | | 6,7 nm | | 6,7 nm | | 6,7 nm | | 7,0 nm | | 7,0 nm | |
| $U_{c(xref), scale B}$ | 6,2 nm | | 6,2 nm | | 6,2 nm | | 6,2 nm | | 6,3 nm | | 6,4 nm | |
| | $X_i - X_{ref}$ | E_n |
| MIRS-SI | 27,1 | 0,22 | 46,1 | 0,37 | 52,7 | 0,42 | 45,7 | 0,36 | 15,4 | 0,11 | -5,8 | 0,04 |
| OMH-HU | -51,9 | 0,26 | 4,1 | 0,02 | -58,3 | 0,29 | -69,3 | 0,35 | -61,6 | 0,31 | -96,8 | 0,48 |
| BEV-AT | 12,1 | 0,25 | 14,1 | 0,29 | 26,7 | 0,55 | 25,7 | 0,52 | -20,6 | 0,09 | -16,8 | 0,08 |
| SMU-SK | 0,1 | 0,00 | -37,9 | 0,41 | -5,3 | 0,06 | -27,3 | 0,29 | -30,6 | 0,33 | -35,8 | 0,38 |
| PTB-DE | -2,1 | 0,03 | 4,7 | 0,15 | -3,4 | 0,11 | 4,8 | 0,16 | 0,8 | 0,03 | 0,2 | 0,01 |
| GUM-PL | -17,9 | 0,07 | -70,9 | 0,26 | -40,3 | 0,15 | -18,3 | 0,07 | 130,4 | 0,49 | 129,2 | 0,48 |
| MIKES-FI | -1,9 | 0,07 | 1,1 | 0,04 | -10,3 | 0,36 | -19,3 | 0,68 | -8,6 | 0,31 | -11,8 | 0,42 |
| LNMC-LV | 297,1 | 0,18 | 76,1 | 0,05 | 102,7 | 0,06 | 25,7 | 0,02 | 415,4 | 0,25 | 354,2 | 0,22 |
| NML-IE | -62,9 | 0,04 | 116,1 | 0,08 | 342,7 | 0,23 | 295,7 | 0,20 | 235,4 | 0,16 | 194,2 | 0,13 |
| NCM-BG | 0,1 | 0,00 | -12,9 | 0,08 | 5,7 | 0,04 | -3,3 | 0,02 | -7,6 | 0,05 | -4,8 | 0,03 |
| INM-RO | 17,1 | 0,08 | -13,9 | 0,07 | 22,7 | 0,11 | -54,3 | 0,27 | 25,4 | 0,13 | 24,2 | 0,12 |
| ZMDM-SR | -34,7 | 0,17 | -88,7 | 0,44 | -48,2 | 0,24 | -66,3 | 0,33 | -3643,8 | 17,89 | -8224,8 | 40,38 |
| DZM-HR | 25,1 | 0,17 | 9,1 | 0,06 | 63,7 | 0,42 | 46,7 | 0,31 | 31,4 | 0,20 | 19,2 | 0,12 |
| NSCIM-UA | 24,1 | 0,56 | 17,1 | 0,39 | 19,7 | 0,45 | 23,7 | 0,55 | 63,4 | 1,46 | 86,2 | 1,98 |
| CMI-CZ | -2,9 | 0,09 | -3,9 | 0,12 | -5,3 | 0,16 | -4,3 | 0,13 | -9,6 | 0,30 | -11,8 | 0,36 |
| NPL-GB | -1,4 | 0,02 | -5,0 | 0,08 | -4,2 | 0,07 | -1,8 | 0,03 | -7,9 | 0,13 | -6,1 | 0,10 |
| METAS-CH | -8,9 | 0,39 | -6,9 | 0,30 | -3,3 | 0,14 | 0,7 | 0,03 | -8,6 | 0,38 | -10,8 | 0,47 |
| NPL-GB | -12,0 | 0,19 | -17,1 | 0,27 | -14,8 | 0,24 | -22,2 | 0,35 | 3,7 | 0,06 | 1,9 | 0,03 |
| METAS-CH | 2,2 | 0,09 | 0,8 | 0,03 | -0,1 | 0,00 | 0,7 | 0,03 | 2,7 | 0,11 | -3,3 | 0,14 |
| EIM-GR | -18,8 | 0,02 | -64,2 | 0,06 | -19,1 | 0,02 | 3,7 | 0,00 | -47,3 | 0,04 | -56,3 | 0,05 |
| INRIM-IT | 0,2 | 0,00 | 2,8 | 0,03 | -3,1 | 0,03 | 2,7 | 0,03 | 2,7 | 0,03 | 3,7 | 0,04 |
| Nmi-VSL-NL | -1,8 | 0,04 | 5,8 | 0,13 | -7,1 | 0,16 | 1,7 | 0,04 | -2,3 | 0,05 | -7,3 | 0,15 |
| CEM-ES | 7,2 | 0,12 | 18,8 | 0,32 | 16,9 | 0,28 | -0,3 | 0,01 | 21,7 | 0,36 | 40,7 | 0,68 |
| INMETRO-BR | 36,2 | 0,28 | 8,8 | 0,07 | 3,9 | 0,03 | -8,3 | 0,07 | -22,3 | 0,18 | -23,3 | 0,18 |
| CENAM-MX | -79,8 | 0,29 | -114,2 | 0,41 | -84,1 | 0,30 | -27,3 | 0,10 | -118,3 | 0,43 | -19,3 | 0,07 |
| NIST-US | 5,1 | 0,27 | 4,0 | 0,21 | 4,6 | 0,25 | 3,0 | 0,16 | 2,4 | 0,12 | 5,6 | 0,29 |
| NRC-CA | 2,6 | 0,03 | 3,2 | 0,04 | 2,3 | 0,03 | 4,5 | 0,05 | 3,1 | 0,04 | 3,6 | 0,04 |
| A*Star-NMC-SG | 20,2 | 0,09 | -14,2 | 0,06 | 40,9 | 0,18 | 47,7 | 0,21 | -43,3 | 0,19 | -69,3 | 0,30 |
| NIM-CN | -19,8 | 0,20 | -37,2 | 0,37 | -16,1 | 0,16 | -21,3 | 0,21 | -9,3 | 0,09 | -18,3 | 0,18 |
| NPL-IN | 63,2 | 0,13 | 63,8 | 0,14 | -43,1 | 0,09 | -123,3 | 0,26 | -6,3 | 0,01 | -95,3 | 0,20 |
| NIMT-THA | -12,0 | 0,27 | -2,4 | 0,05 | 9,2 | 0,21 | 12,6 | 0,28 | 2,4 | 0,05 | -3,2 | 0,07 |
| VNIM-RU | -3,8 | 0,14 | -6,2 | 0,23 | -8,1 | 0,30 | -5,3 | 0,20 | -10,3 | 0,37 | -9,3 | 0,32 |

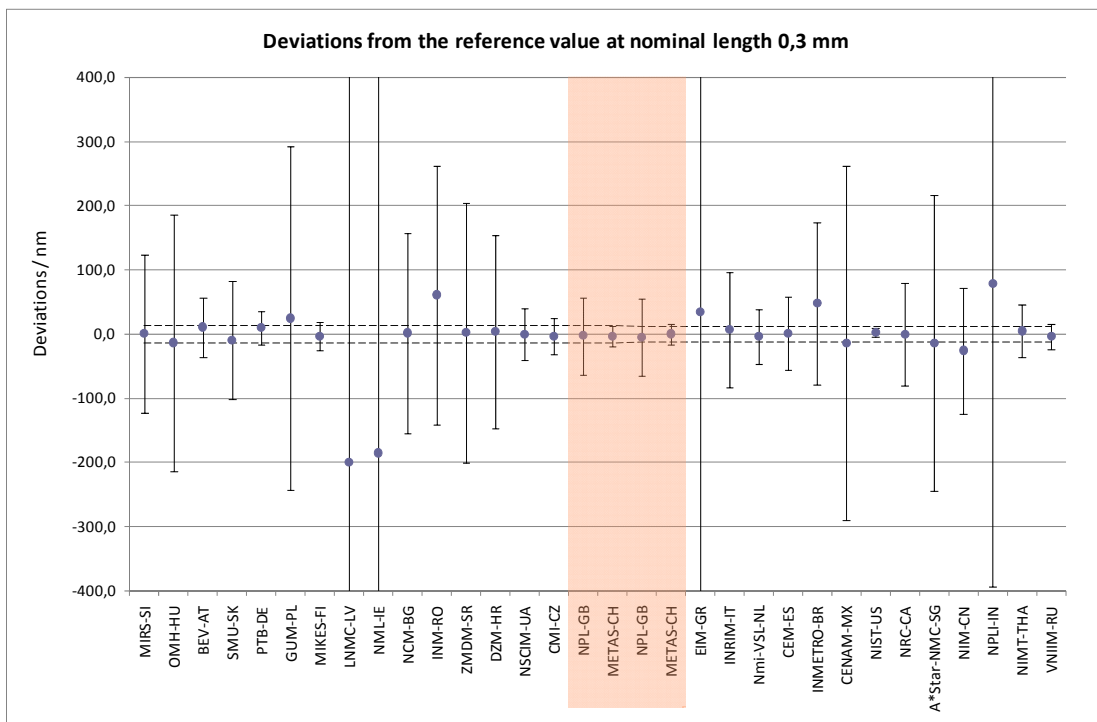
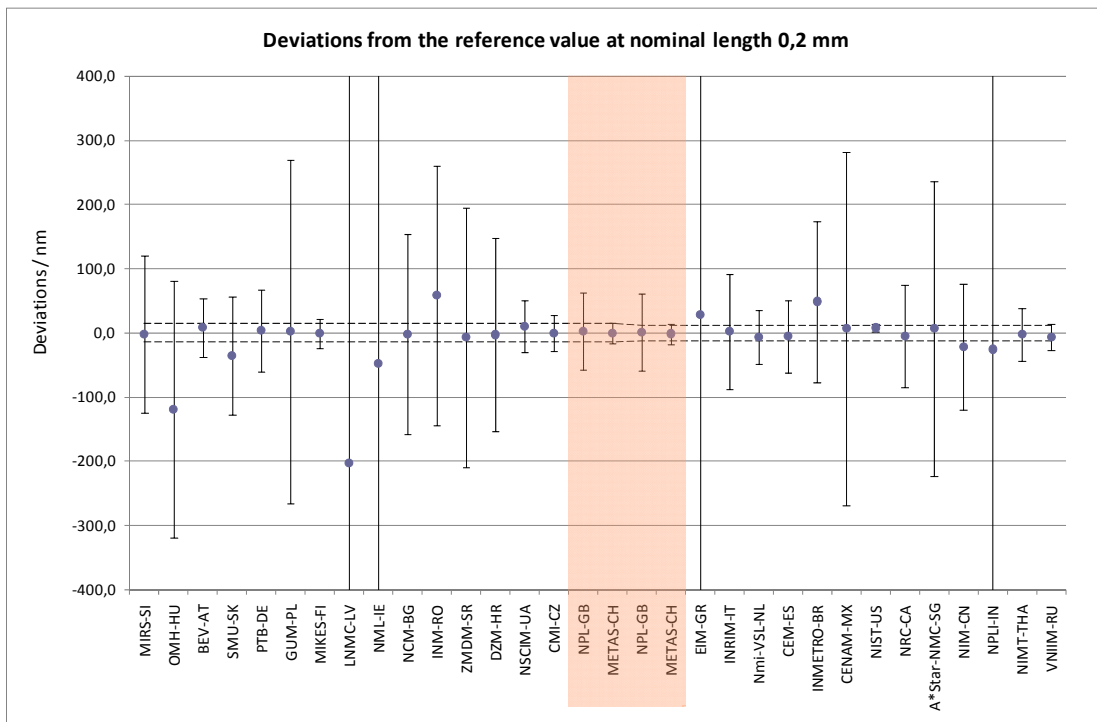
| Meas. Point | 15 mm | | 20 mm | | 25 mm | | 30 mm | | 35 mm | | 40 mm | |
|------------------------|-----------------|-------|-----------------|-------|-----------------|-------|-----------------|--------|-----------------|--------|-----------------|--------|
| $X_{ref, scale A}$ | -5,1 nm | | -2,8 nm | | -145,3 nm | | -165,8 nm | | -157,3 nm | | -157,5 nm | |
| $X_{ref, scale B}$ | -24,8 nm | | 19,4 nm | | -120,6 nm | | -150,2 nm | | -125,9 nm | | -127,0 nm | |
| $U_{c(xref), scale A}$ | 7,4 nm | | 7,4 nm | | 7,5 nm | | 7,5 nm | | 7,6 nm | | 7,7 nm | |
| $U_{c(xref), scale B}$ | 6,5 nm | | 6,5 nm | | 6,6 nm | | 6,7 nm | | 6,9 nm | | 7,0 nm | |
| | $X_i - X_{ref}$ | E_n | $X_i - X_{ref}$ | E_n | $X_i - X_{ref}$ | E_n |
| MIRS-SI | 5,1 | 0,03 | 2,8 | 0,02 | 5,3 | 0,03 | -14,2 | 0,07 | -42,7 | 0,21 | -52,5 | 0,24 |
| OMH-HU | -44,9 | 0,22 | -25,2 | 0,13 | -117,7 | 0,59 | 6,8 | 0,03 | 68,3 | 0,34 | -164,5 | 0,82 |
| BEV-AT | -58,9 | 0,26 | -45,2 | 0,20 | -34,7 | 0,16 | -81,2 | 0,06 | -97,7 | 0,44 | -114,5 | 0,51 |
| SMU-SK | -15,9 | 0,17 | -31,2 | 0,33 | 62,3 | 0,67 | 78,8 | 0,84 | 67,3 | 0,72 | 55,5 | 0,59 |
| PTB-DE | 22,7 | 0,74 | 8,5 | 0,28 | 11,2 | 0,36 | 7,3 | 0,24 | 7,6 | 0,25 | 8,4 | 0,27 |
| GUM-PL | 179,1 | 0,66 | 83,8 | 0,31 | 79,3 | 0,29 | 150,8 | 0,55 | 31,3 | 0,11 | 112,5 | 0,40 |
| MIKES-FI | 4,1 | 0,15 | -6,2 | 0,22 | 1,3 | 0,05 | -5,2 | 0,18 | -3,7 | 0,13 | -1,5 | 0,05 |
| LNMC-LV | 275,1 | 0,17 | 512,8 | 0,31 | 375,3 | 0,23 | 1135,8 | 0,69 | 7,3 | 0,00 | 477,5 | 0,29 |
| NML-IE | 485,1 | 0,33 | 402,8 | 0,27 | 905,3 | 0,61 | 505,8 | 0,34 | 837,3 | 0,57 | 1057,5 | 0,71 |
| NCM-BG | -15,9 | 0,10 | -10,2 | 0,06 | -8,7 | 0,06 | -10,2 | 0,06 | 7,3 | 0,05 | -21,5 | 0,14 |
| INM-RO | 15,1 | 0,07 | -7,2 | 0,04 | 105,3 | 0,52 | 145,8 | 0,72 | 137,3 | 0,67 | 147,5 | 0,72 |
| ZMDM-SR | -10832,0 | 53,15 | -14579,5 | 71,51 | -18571,6 | 91,05 | -22327,2 | 109,39 | -25707,3 | 125,86 | -29003,7 | 141,88 |
| DZM-HR | -1,9 | 0,01 | 16,8 | 0,10 | -92,7 | 0,53 | -110,2 | 0,61 | -141,7 | 0,76 | -9,5 | 0,05 |
| NSCIM-UA | 121,1 | 2,51 | 164,8 | 3,40 | 207,3 | 4,25 | 289,8 | 5,88 | 291,3 | 5,85 | 319,5 | 6,34 |
| CMI-CZ | -6,9 | 0,21 | -0,2 | 0,01 | -7,7 | 0,23 | -8,2 | 0,24 | -3,7 | 0,10 | -10,5 | 0,29 |
| NPL-GB | -6,9 | 0,11 | 8,5 | 0,14 | -1,9 | 0,03 | 2,6 | 0,04 | 1,7 | 0,03 | 2,5 | 0,04 |
| METAS-CH | -11,9 | 0,53 | -0,2 | 0,01 | -8,7 | 0,38 | -5,2 | 0,22 | -6,7 | 0,28 | -4,5 | 0,19 |
| NPL-GB | 4,1 | 0,07 | 3,3 | 0,05 | 7,3 | 0,12 | -0,4 | 0,01 | -0,3 | 0,00 | -2,5 | 0,04 |
| METAS-CH | -9,2 | 0,39 | -4,4 | 0,18 | -12,4 | 0,52 | -10,8 | 0,45 | -10,1 | 0,42 | -18,0 | 0,73 |
| EIM-GR | -50,2 | 0,04 | -145,4 | 0,13 | -148,4 | 0,13 | -271,8 | 0,24 | -270,1 | 0,24 | -395,0 | 0,35 |
| INRIM-IT | 1,8 | 0,02 | 2,6 | 0,03 | -5,4 | 0,06 | -3,8 | 0,04 | -5,1 | 0,06 | -9,0 | 0,10 |
| Nmi-VSL-NL | -4,2 | 0,09 | 8,6 | 0,18 | 19,6 | 0,39 | 8,2 | 0,16 | -2,1 | 0,04 | 15,0 | 0,29 |
| CEM-ES | 40,8 | 0,68 | 23,6 | 0,40 | 41,6 | 0,69 | 19,2 | 0,32 | 48,9 | 0,81 | 48,0 | 0,79 |
| INMETRO-BR | 1,8 | 0,01 | -3,4 | 0,03 | 51,6 | 0,41 | 55,2 | 0,43 | 41,9 | 0,33 | 47,0 | 0,37 |
| CENAM-MX | 24,8 | 0,09 | -119,4 | 0,42 | -179,4 | 0,61 | 150,2 | 0,50 | -74,1 | 0,24 | 127,0 | 0,40 |
| NIST-US | 5,4 | 0,28 | 7,9 | 0,41 | 4,0 | 0,21 | 4,4 | 0,23 | 6,6 | 0,33 | 7,7 | 0,39 |
| NRC-CA | 0,6 | 0,01 | 3,7 | 0,05 | 5,6 | 0,07 | 10,3 | 0,12 | 5,1 | 0,06 | 5,9 | 0,07 |
| A*Star-NMC-SG | -50,2 | 0,22 | -19,4 | 0,08 | -29,4 | 0,13 | 0,2 | 0,00 | -24,1 | 0,10 | -23,0 | 0,10 |
| NIM-CN | 12,8 | 0,13 | 8,6 | 0,09 | 29,6 | 0,30 | 53,2 | 0,53 | 50,9 | 0,51 | 54,0 | 0,54 |
| NPL-IN | -43,2 | 0,09 | -42,4 | 0,09 | -223,4 | 0,47 | -110,8 | 0,23 | -50,1 | 0,11 | -85,0 | 0,18 |
| NIMT-THA | 5,2 | 0,11 | -18,1 | 0,37 | 1,1 | 0,02 | -1,1 | 0,02 | -11,2 | 0,19 | -9,9 | 0,01 |
| VNIM-RU | -13,2 | 0,44 | -13,4 | 0,43 | -19,4 | 0,59 | -16,8 | 0,49 | -20,1 | 0,57 | -24,0 | 0,65 |

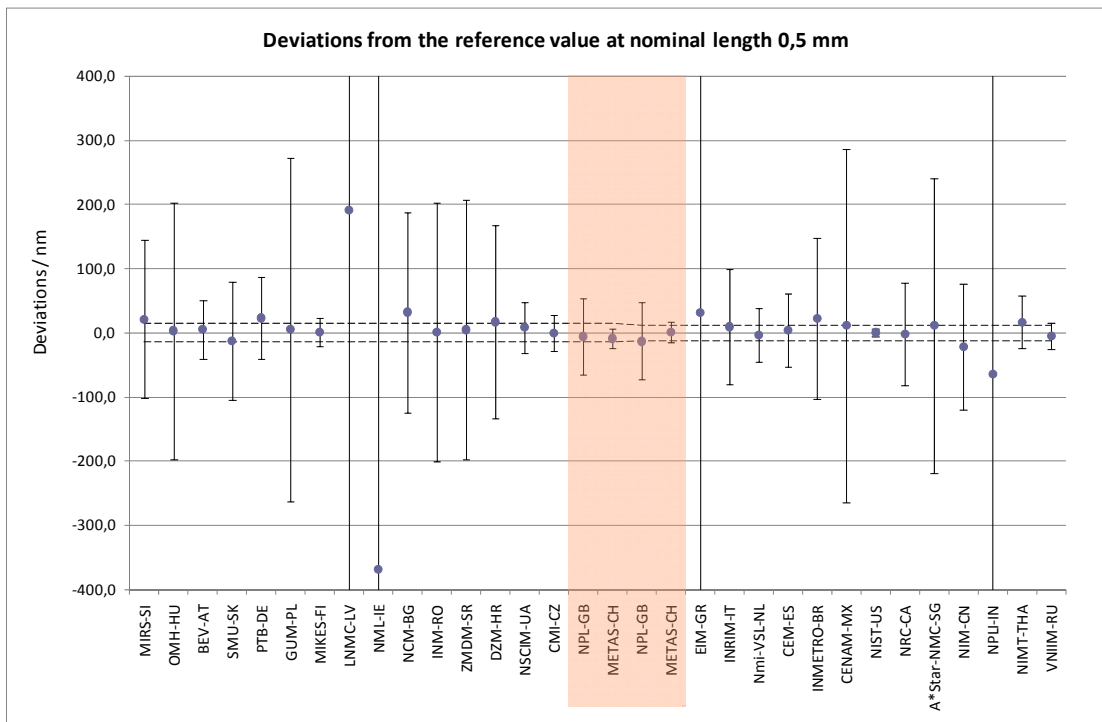
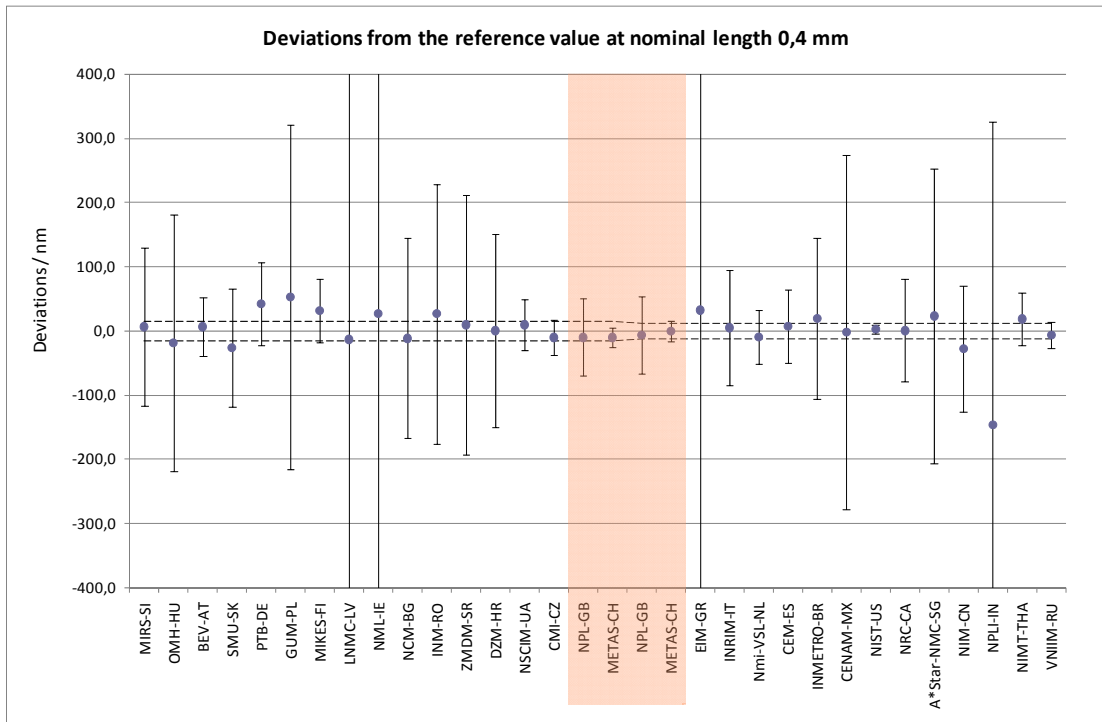
| Meas. Point | 45 mm | | 50 mm | | 55 mm | | 60 mm | | 65 mm | | 70 mm | |
|------------------------|-----------------|--------|-----------------|--------|-----------------|--------|-----------------|--------|-----------------|--------|-----------------|--------|
| $X_{ref, scale A}$ | -212,8 nm | | -192,2 nm | | -209,1 nm | | -255,1 nm | | -212,4 nm | | -243,2 nm | |
| $X_{ref, scale B}$ | -182,1 nm | | -111,6 nm | | -136,1 nm | | -154,4 nm | | -116,0 nm | | -136,8 nm | |
| $U_{c(xref), scale A}$ | 7,8 nm | | 7,9 nm | | 8,0 nm | | 8,1 nm | | 8,2 nm | | 8,3 nm | |
| $U_{c(xref), scale B}$ | 7,1 nm | | 7,2 nm | | 7,4 nm | | 7,5 nm | | 7,7 nm | | 7,8 nm | |
| | $X_i - X_{ref}$ | E_n |
| MIRS-SI | -77,2 | 0,33 | -27,8 | 0,11 | -60,9 | 0,24 | -54,9 | 0,21 | -37,6 | 0,14 | -36,8 | 0,13 |
| OMH-HU | -69,2 | 0,34 | -68,8 | 0,34 | -141,9 | 0,71 | -62,9 | 0,31 | -19,6 | 0,10 | -85,8 | 0,43 |
| BEV-AT | -138,2 | 0,62 | -97,8 | 0,44 | -132,9 | 0,60 | -162,9 | 0,73 | -164,6 | 0,74 | -200,8 | 0,90 |
| SMU-SK | 103,8 | 1,10 | 85,2 | 0,91 | 85,1 | 0,90 | 113,1 | 1,20 | 68,4 | 0,72 | 81,2 | 0,86 |
| PTB-DE | 11,9 | 0,38 | 11,6 | 0,37 | 7,6 | 0,24 | 10,9 | 0,35 | 12,0 | 0,38 | 6,8 | 0,21 |
| GUM-PL | -23,2 | 0,08 | -66,8 | 0,23 | -102,9 | 0,35 | -166,9 | 0,57 | -122,6 | 0,41 | -235,8 | 0,78 |
| MIKES-FI | -7,2 | 0,25 | -2,8 | 0,10 | -0,9 | 0,03 | -1,9 | 0,06 | -0,6 | 0,02 | -1,8 | 0,06 |
| LNMC-LV | 352,8 | 0,21 | 862,2 | 0,52 | 329,1 | 0,20 | 835,1 | 0,51 | -7,6 | 0,00 | 133,2 | 0,08 |
| NML-IE | 972,8 | 0,66 | 1112,2 | 0,75 | 1089,1 | 0,74 | 1855,1 | 1,25 | 2072,4 | 1,40 | 2023,2 | 1,37 |
| NCM-BG | -18,2 | 0,11 | -32,8 | 0,20 | -33,9 | 0,21 | -38,9 | 0,24 | -36,6 | 0,22 | -38,8 | 0,24 |
| INM-RO | 162,8 | 0,80 | 142,2 | 0,70 | 189,1 | 0,92 | 235,1 | 1,14 | 172,4 | 0,84 | 203,2 | 0,98 |
| ZMDM-SR | -32942,9 | 160,99 | -36957,0 | 180,41 | -40190,9 | 195,97 | -43650,0 | 212,56 | -48016,5 | 233,50 | -50709,4 | 246,23 |
| DZM-HR | 12,8 | 0,07 | 24,2 | 0,12 | -12,9 | 0,06 | -10,9 | 0,05 | 11,4 | 0,05 | -11,8 | 0,05 |
| NSCIM-UA | 143,8 | 2,81 | 413,2 | 7,97 | 423,1 | 8,04 | 464,1 | 8,67 | 448,4 | 8,24 | 473,2 | 8,54 |
| CMI-CZ | -16,2 | 0,44 | -20,8 | 0,55 | -8,9 | 0,23 | -20,9 | 0,52 | -11,6 | 0,28 | -15,8 | 0,37 |
| NPL-GB | 2,1 | 0,03 | 1,6 | 0,03 | -1,3 | 0,02 | -2,3 | 0,04 | -5,6 | 0,09 | 2,2 | 0,04 |
| METAS-CH | -3,2 | 0,13 | -3,8 | 0,16 | -4,9 | 0,20 | -4,9 | 0,19 | -7,6 | 0,30 | -2,8 | 0,11 |
| NPL-GB | -0,9 | 0,01 | -0,8 | 0,01 | -1,4 | 0,02 | 1,9 | 0,03 | 8,2 | 0,13 | 8,3 | 0,13 |
| METAS-CH | -11,9 | 0,48 | -14,4 | 0,57 | -14,9 | 0,58 | -16,6 | 0,64 | -15,0 | 0,57 | -18,2 | 0,68 |
| EIM-GR | -399,9 | 0,35 | -449,4 | 0,40 | -410,9 | 0,36 | -392,6 | 0,34 | -358,0 | 0,31 | -383,2 | 0,34 |
| INRIM-IT | 2,1 | 0,02 | 5,6 | 0,06 | -1,9 | 0,02 | -1,6 | 0,02 | -1,0 | 0,01 | -6,2 | 0,06 |
| Nmi-VSL-NL | 23,1 | 0,43 | 52,6 | 0,97 | 35,1 | 0,64 | 30,4 | 0,54 | 32,0 | 0,56 | 47,8 | 0,82 |
| CEM-ES | 31,1 | 0,51 | 10,6 | 0,17 | 8,1 | 0,13 | 20,4 | 0,33 | 3,0 | 0,05 | 8,8 | 0,14 |
| INMETRO-BR | 84,1 | 0,66 | 27,6 | 0,22 | 49,1 | 0,39 | 77,4 | 0,42 | -24,0 | 0,13 | 59,8 | 0,32 |
| CENAM-MX | 282,1 | 0,86 | 11,6 | 0,03 | 36,1 | 0,10 | 54,4 | 0,15 | -84,0 | 0,22 | -163,2 | 0,42 |
| NIST-US | -1,0 | 0,05 | 0,8 | 0,04 | 4,4 | 0,21 | 1,3 | 0,06 | 4,8 | 0,22 | 7,8 | 0,35 |
| NRC-CA | 10,6 | 0,13 | 11,9 | 0,14 | 8,6 | 0,10 | 8,8 | 0,10 | 9,1 | 0,11 | 3,8 | 0,04 |
| A*Star-NMC-SG | -17,9 | 0,08 | -38,4 | 0,16 | -38,9 | 0,17 | -45,6 | 0,19 | -59,0 | 0,25 | -38,2 | 0,16 |
| NIM-CN | 66,1 | 0,66 | 79,6 | 0,80 | 83,1 | 0,83 | 106,4 | 1,07 | 111,0 | 1,11 | 109,8 | 1,10 |
| NPL-IN | -55,9 | 0,12 | -51,4 | 0,11 | -115,9 | 0,24 | -116,6 | 0,25 | -13,0 | 0,03 | 80,8 | 0,17 |
| NIMT-THA | -9,9 | 0,15 | -10,3 | 0,15 | -11,6 | 0,16 | 3,5 | 0,05 | -15,1 | 0,19 | -69,2 | 0,81 |
| VNIM-RU | -19,9 | 0,52 | -21,4 | 0,54 | -20,9 | 0,51 | -22,6 | 0,53 | -22,0 | 0,50 | -24,2 | 0,53 |

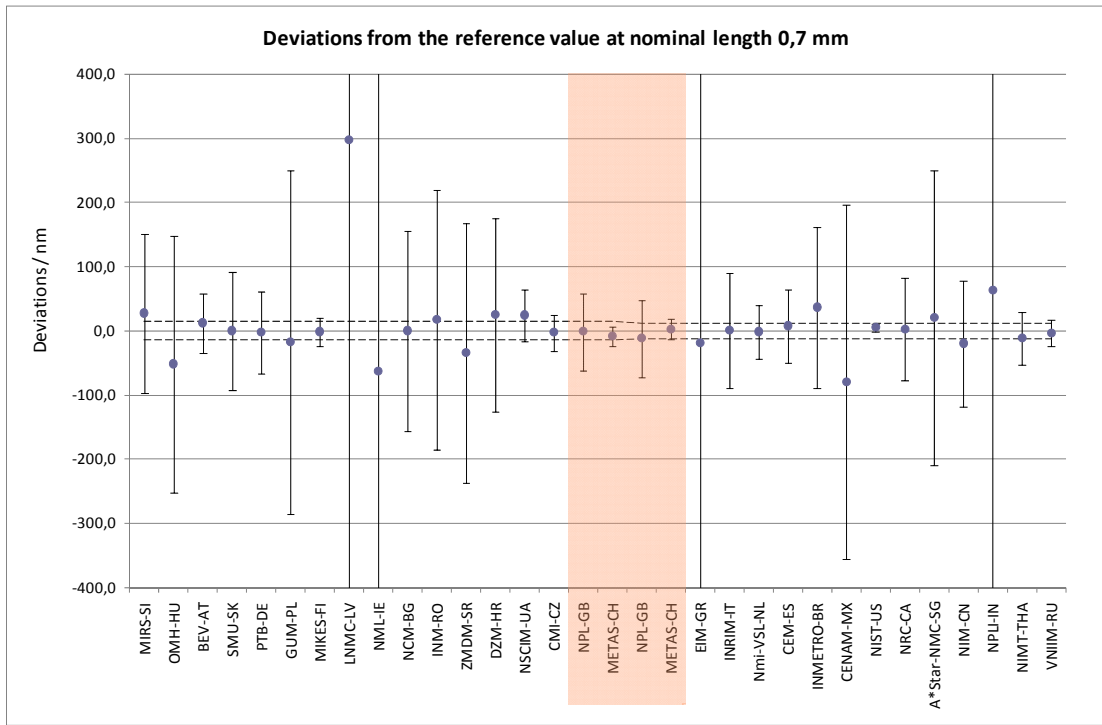
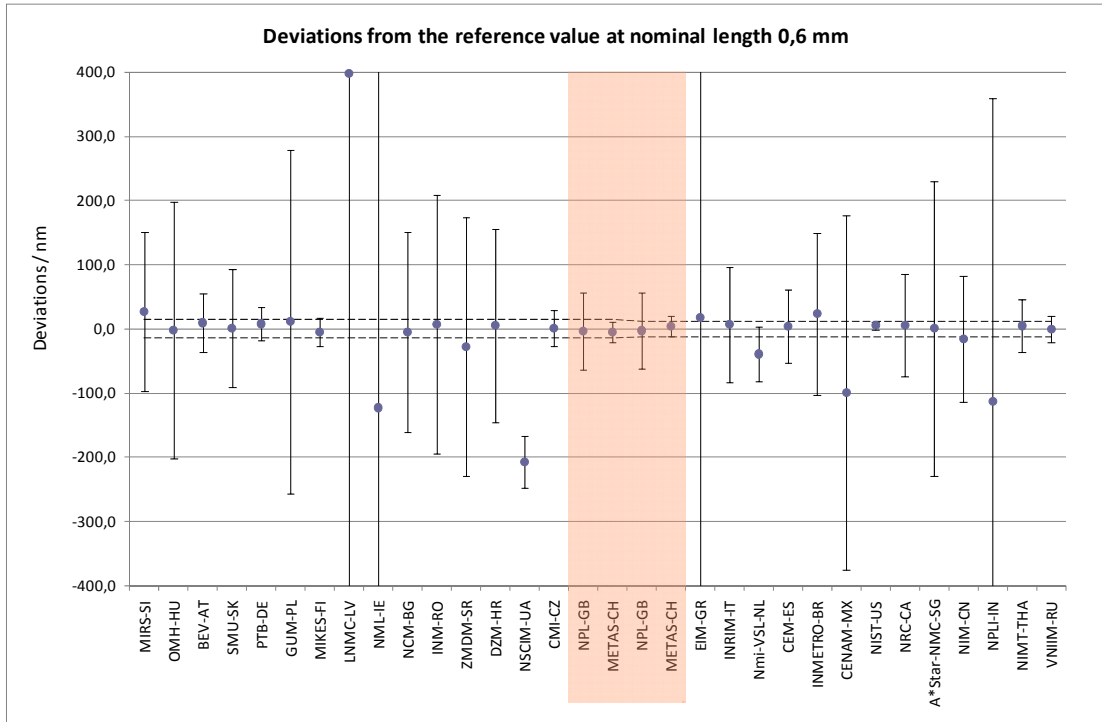
| Meas. Point | 75 mm | | 80 mm | | 85 mm | | 90 mm | | 95 mm | | 100 mm | |
|------------------------|-----------------|--------|-----------------|--------|-----------------|--------|-----------------|--------|-----------------|--------|-----------------|--------|
| $X_{ref, scale A}$ | -281,2 nm | | -241,3 nm | | -256,3 nm | | -429,0 nm | | -362,1 nm | | -386,2 nm | |
| $X_{ref, scale B}$ | -151,9 nm | | -124,2 nm | | -138,7 nm | | -316,4 nm | | -265,7 nm | | -259,0 nm | |
| $U_{c(jref), scale A}$ | 8,4 nm | | 8,6 nm | | 9,4 nm | | 9,7 nm | | 9,9 nm | | 9,1 nm | |
| $U_{c(jref), scale B}$ | 8,0 nm | | 8,1 nm | | 8,3 nm | | 8,4 nm | | 8,6 nm | | 8,8 nm | |
| | $x_j - X_{ref}$ | E_n |
| MIRS-SI | -8,8 | 0,03 | -38,7 | 0,12 | -63,7 | 0,19 | -81,0 | 0,24 | -57,9 | 0,17 | -53,8 | 0,15 |
| OMH-HU | -277,8 | 1,38 | -214,7 | 1,07 | -274,7 | 1,35 | -210,0 | 1,04 | -103,9 | 0,52 | -99,8 | 0,49 |
| BEV-AT | -183,8 | 0,82 | -233,7 | 1,05 | -259,7 | 1,16 | -228,0 | 1,02 | -252,9 | 1,14 | -322,8 | 1,44 |
| SMU-SK | 90,2 | 0,95 | 40,3 | 0,42 | 59,3 | 0,62 | 207,0 | 2,09 | 151,1 | 1,52 | 136,2 | 1,41 |
| PTB-DE | 7,6 | 0,24 | 10,2 | 0,31 | 25,6 | 0,80 | 18,7 | 0,58 | 9,3 | 0,29 | -1,7 | 0,05 |
| GUM-PL | -169,8 | 0,55 | -291,7 | 0,93 | -305,7 | 0,96 | -176,0 | 0,54 | -188,9 | 0,57 | -201,8 | 0,60 |
| MIKES-FI | -2,8 | 0,09 | 6,3 | 0,21 | -35,7 | 0,67 | 30,0 | 0,56 | 20,1 | 0,37 | -1,8 | 0,06 |
| LNMC-LV | 531,2 | 0,32 | 11,3 | 0,01 | -693,7 | 0,42 | -991,0 | 0,60 | -847,9 | 0,52 | -1333,8 | 0,81 |
| NMI-IE | 2781,2 | 1,88 | 2261,3 | 1,53 | 2316,3 | 1,57 | 2769,0 | 1,87 | 3202,1 | 2,16 | 3226,2 | 2,18 |
| NCM-BG | -42,8 | 0,26 | -47,7 | 0,29 | -56,7 | 0,34 | -56,0 | 0,33 | -60,9 | 0,36 | -56,8 | 0,33 |
| INM-RO | 231,2 | 1,12 | 201,3 | 0,97 | 236,3 | 1,14 | 399,0 | 1,90 | 302,1 | 1,44 | 366,2 | 1,68 |
| ZMDM-SR | -55087,5 | 267,05 | -58628,0 | 283,74 | -61991,7 | 299,29 | -65609,9 | 316,12 | -68649,3 | 330,10 | -72892,4 | 350,03 |
| DZM-HR | -28,8 | 0,13 | -20,7 | 0,09 | -53,7 | 0,23 | 38,0 | 0,16 | 41,1 | 0,17 | 74,2 | 0,30 |
| NSCIM-UA | 468,2 | 8,30 | 476,3 | 8,28 | 482,3 | 8,16 | 503,0 | 8,34 | 544,1 | 8,84 | 521,2 | 8,37 |
| CMH-CZ | -13,8 | 0,31 | -17,7 | 0,38 | -23,7 | 0,51 | -30,0 | 0,62 | -19,9 | 0,40 | -25,8 | 0,50 |
| NPL-GB | 1,9 | 0,03 | 1,3 | 0,02 | -0,2 | 0,00 | 5,3 | 0,08 | -0,4 | 0,01 | 4,6 | 0,07 |
| METAS-CH | 1,2 | 0,05 | -0,7 | 0,02 | -6,7 | 0,25 | -5,0 | 0,18 | -2,9 | 0,10 | -0,8 | 0,03 |
| NPL-GB | 2,1 | 0,03 | 17,9 | 0,28 | 12,6 | 0,20 | 4,9 | 0,08 | 14,5 | 0,23 | 12,9 | 0,20 |
| METAS-CH | -18,1 | 0,66 | -20,8 | 0,74 | -19,3 | 0,68 | -23,6 | 0,81 | -23,3 | 0,78 | -20,0 | 0,66 |
| EIM-GR | -389,1 | 0,34 | -380,8 | 0,33 | -431,3 | 0,38 | -324,6 | 0,28 | -296,3 | 0,26 | -238,0 | 0,21 |
| INRIM-IT | 0,9 | 0,01 | 1,2 | 0,01 | -0,3 | 0,00 | 1,4 | 0,01 | 3,7 | 0,04 | 4,0 | 0,04 |
| Nmi-VSL-NL | 39,9 | 0,68 | 25,2 | 0,42 | 29,7 | 0,49 | 43,4 | 0,70 | 49,7 | 0,79 | 72,0 | 1,13 |
| CEM-ES | -4,1 | 0,06 | 19,2 | 0,30 | -5,3 | 0,08 | 9,4 | 0,14 | 8,7 | 0,13 | -2,0 | 0,03 |
| INMETRO-BR | 71,9 | 0,39 | 133,2 | 0,72 | 79,7 | 0,43 | 8,4 | 0,05 | 2,7 | 0,01 | -83,0 | 0,45 |
| CENAM-MX | -248,1 | 0,62 | -275,8 | 0,66 | -261,3 | 0,61 | -183,6 | 0,41 | -234,3 | 0,51 | -241,0 | 0,50 |
| NIST-US | 5,7 | 0,25 | -1,1 | 0,05 | 13,3 | 0,57 | 3,0 | 0,13 | -0,6 | 0,02 | 9,4 | 0,38 |
| NRC-CA | 8,3 | 0,09 | 6,1 | 0,07 | 13,4 | 0,15 | 3,6 | 0,04 | 3,9 | 0,04 | 2,2 | 0,02 |
| A*Star-NMC-SG | -73,1 | 0,31 | -25,8 | 0,11 | -23,3 | 0,10 | -21,6 | 0,09 | 27,7 | 0,12 | 47,0 | 0,19 |
| NIM-CN | 120,9 | 1,21 | 132,2 | 1,32 | 136,7 | 1,33 | 149,4 | 1,49 | 150,7 | 1,50 | 158,0 | 1,53 |
| NPL-IN | 45,9 | 0,10 | -65,8 | 0,14 | -155,3 | 0,33 | -47,6 | 0,10 | -326,3 | 0,68 | -454,0 | 0,95 |
| NIMT-THA | -6,1 | 0,07 | -0,3 | 0,00 | -13,0 | 0,13 | 2,4 | 0,02 | -13,7 | 0,13 | -0,3 | 0,00 |
| VNIM-RU | -27,1 | 0,58 | -22,8 | 0,47 | -22,3 | 0,45 | -28,6 | 0,55 | -26,3 | 0,50 | -27,0 | 0,49 |

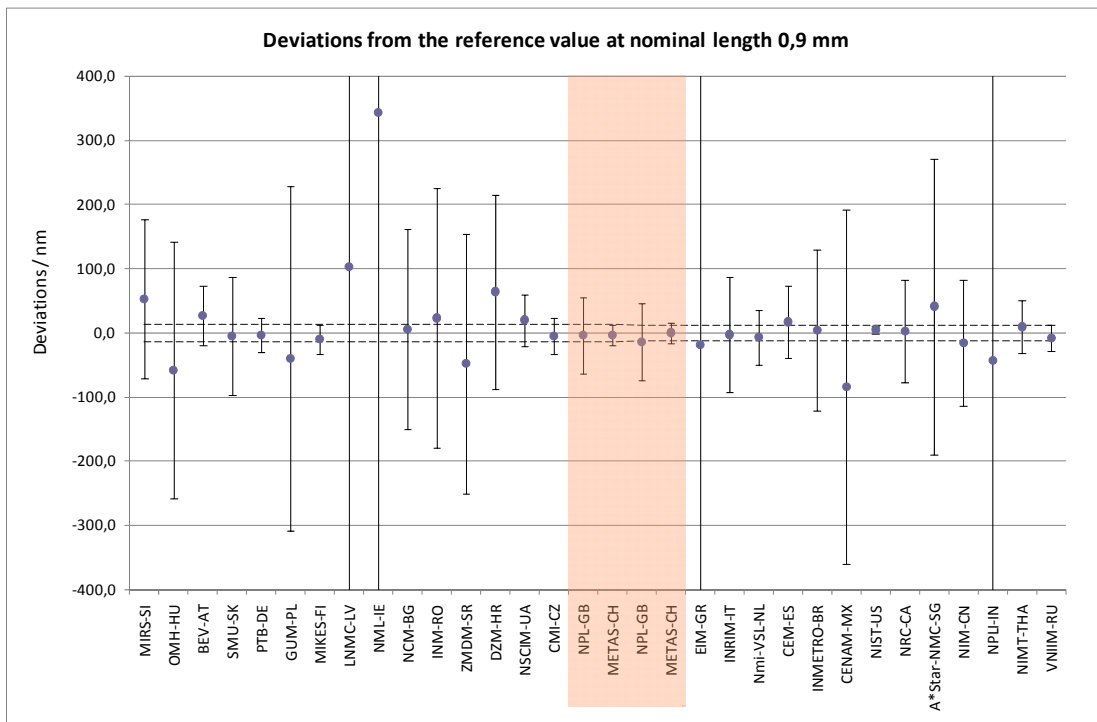
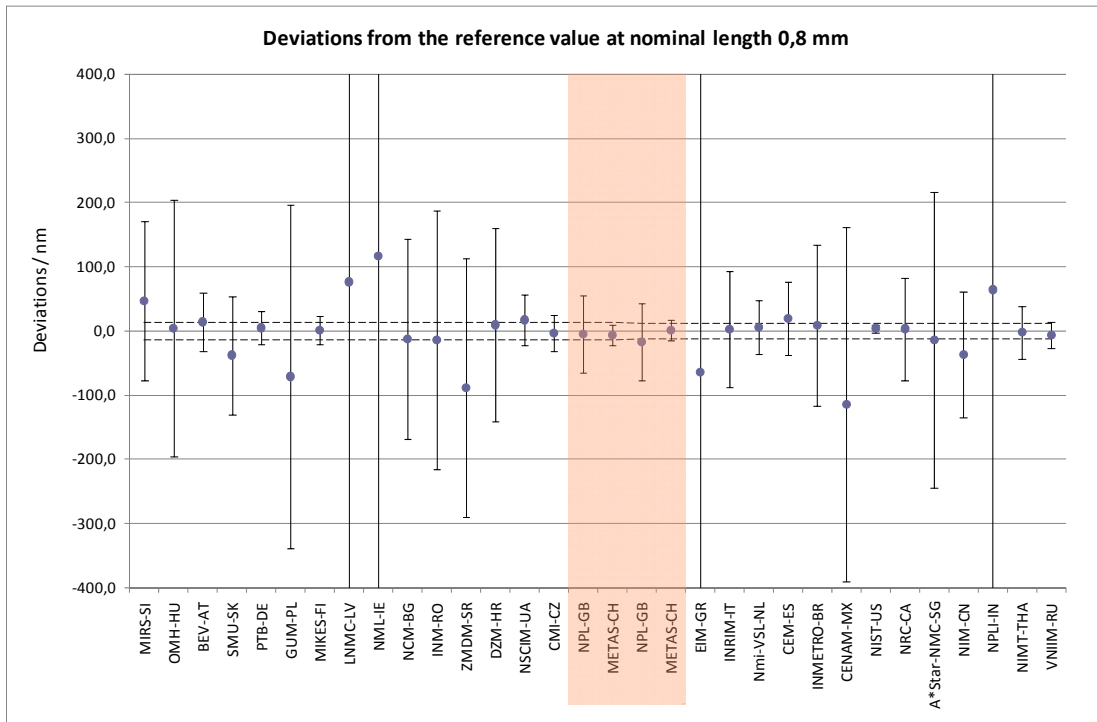
Graphical presentations of measured results indicated as deviations from calculated reference values follow in the next 30 diagrams. The dotted lines indicate the uncertainties of the reference values. Uncertainty bars in the diagrams represent expanded uncertainty $U (k = 2)$.

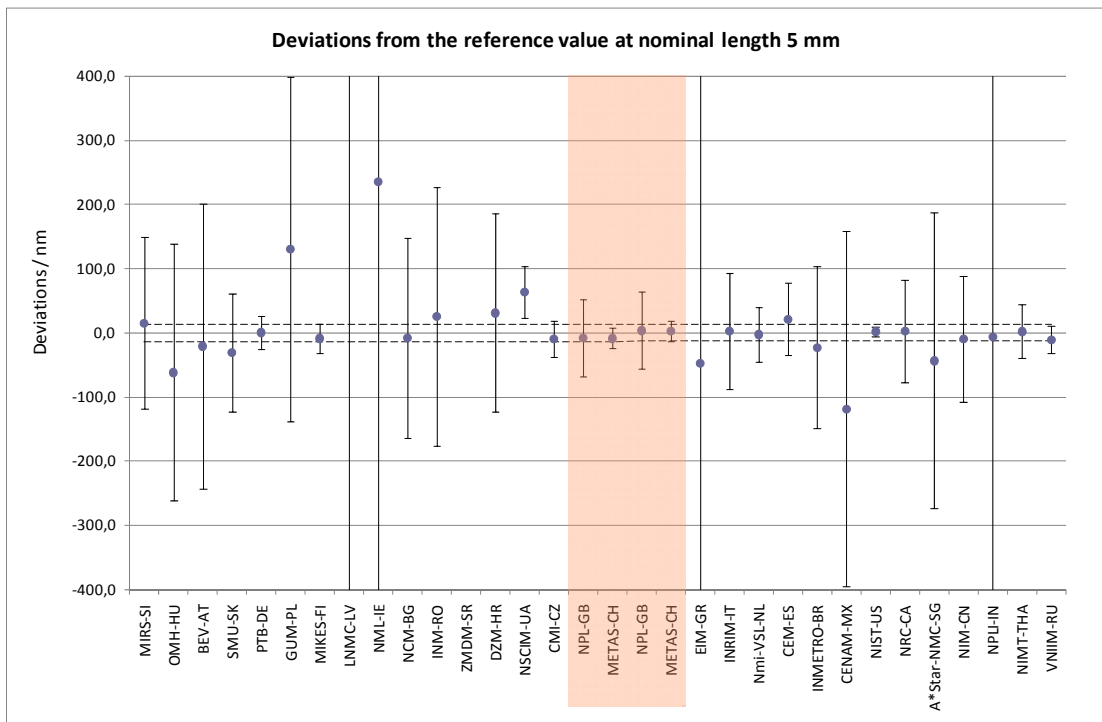
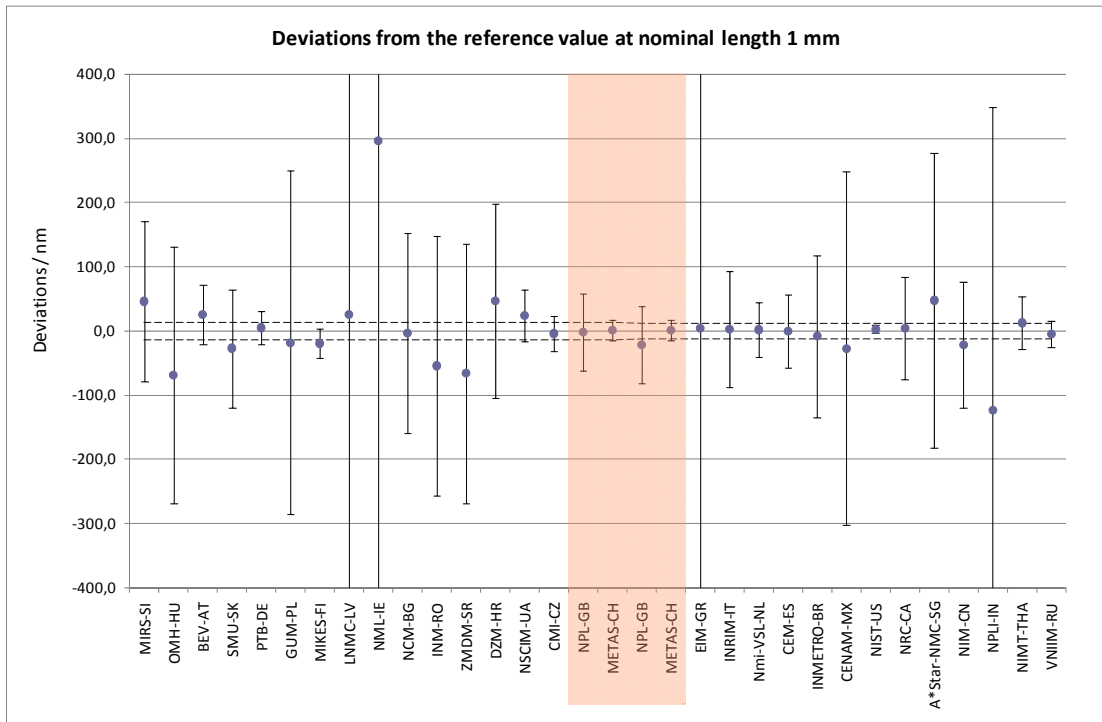


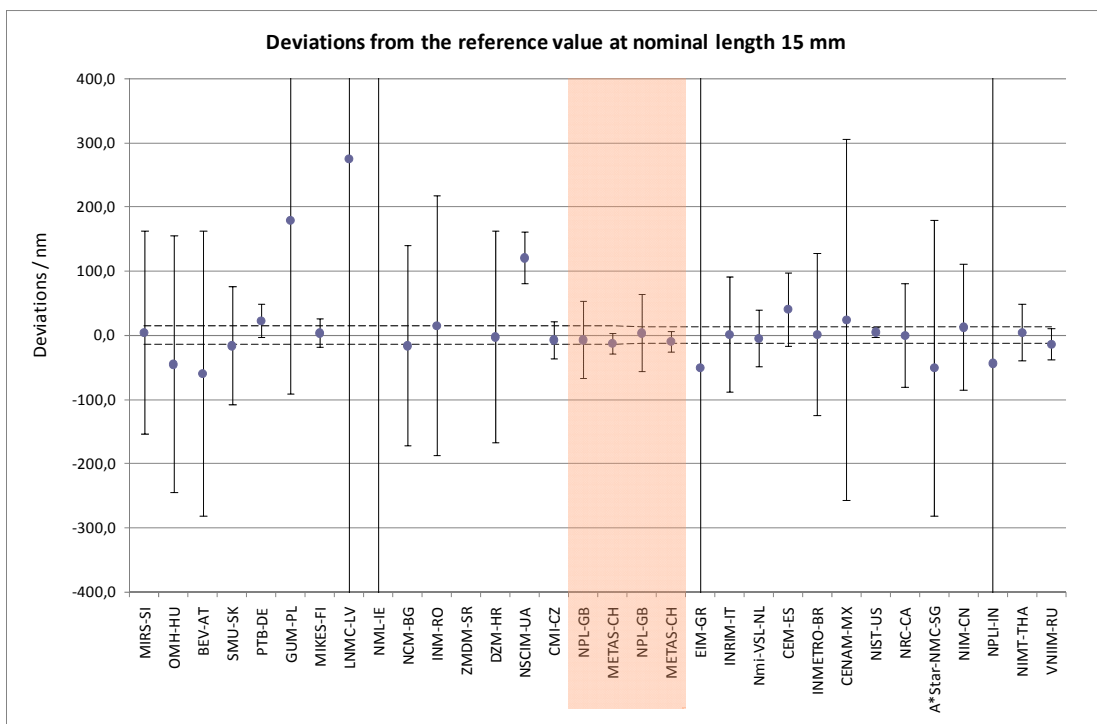
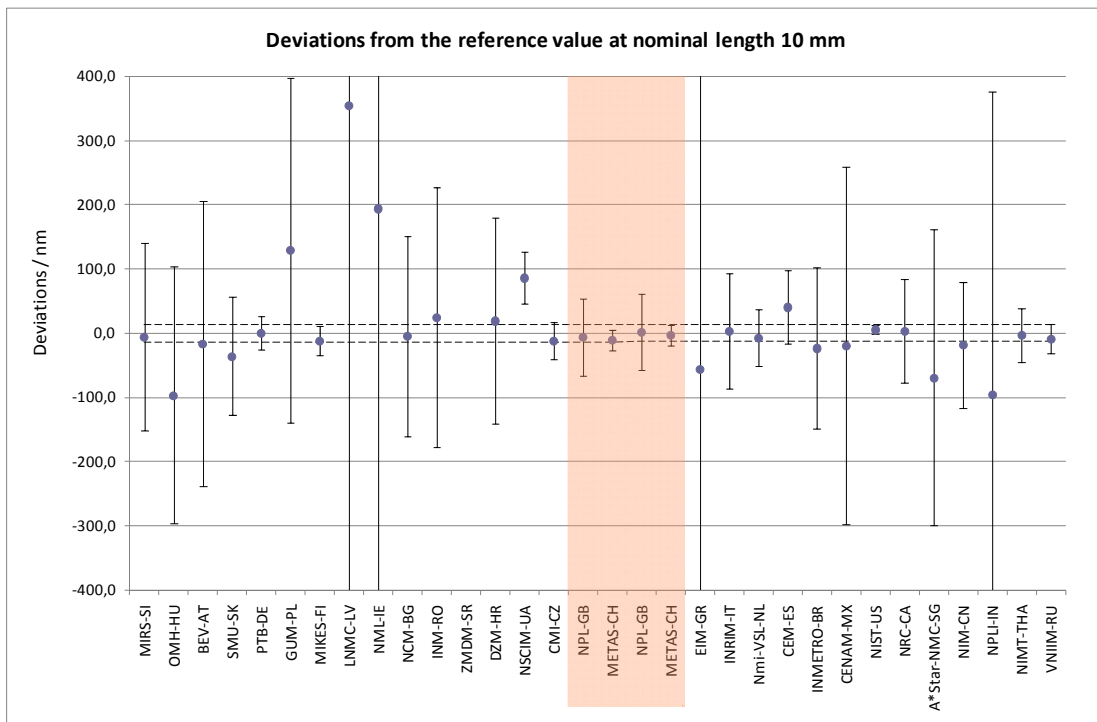


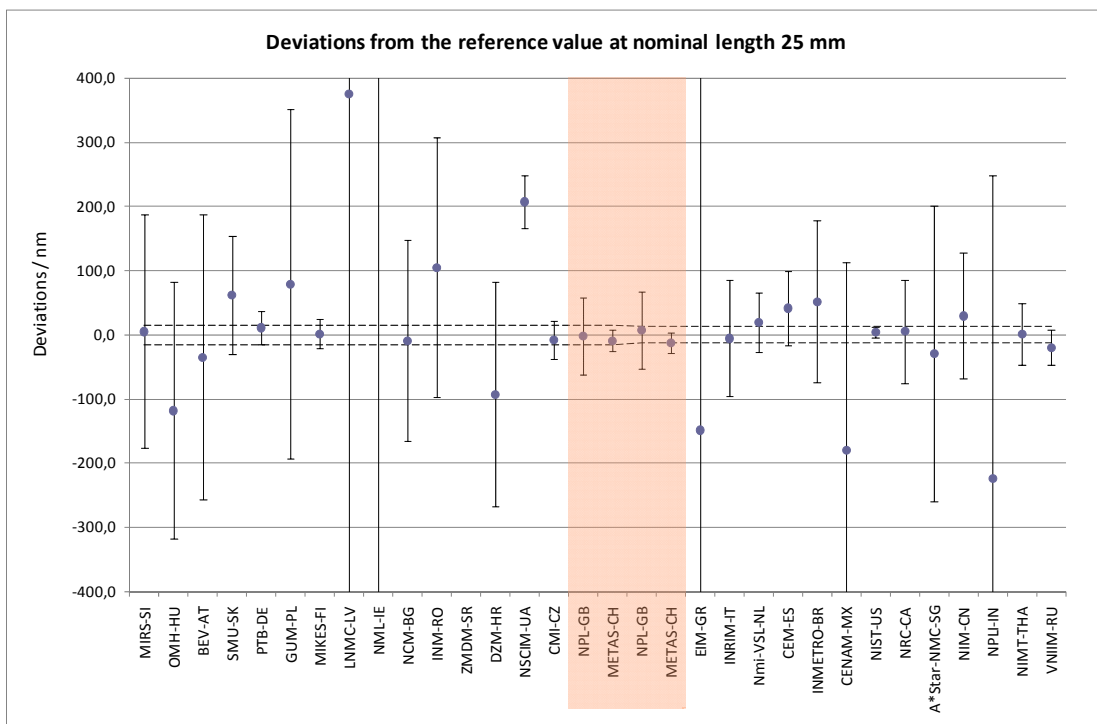
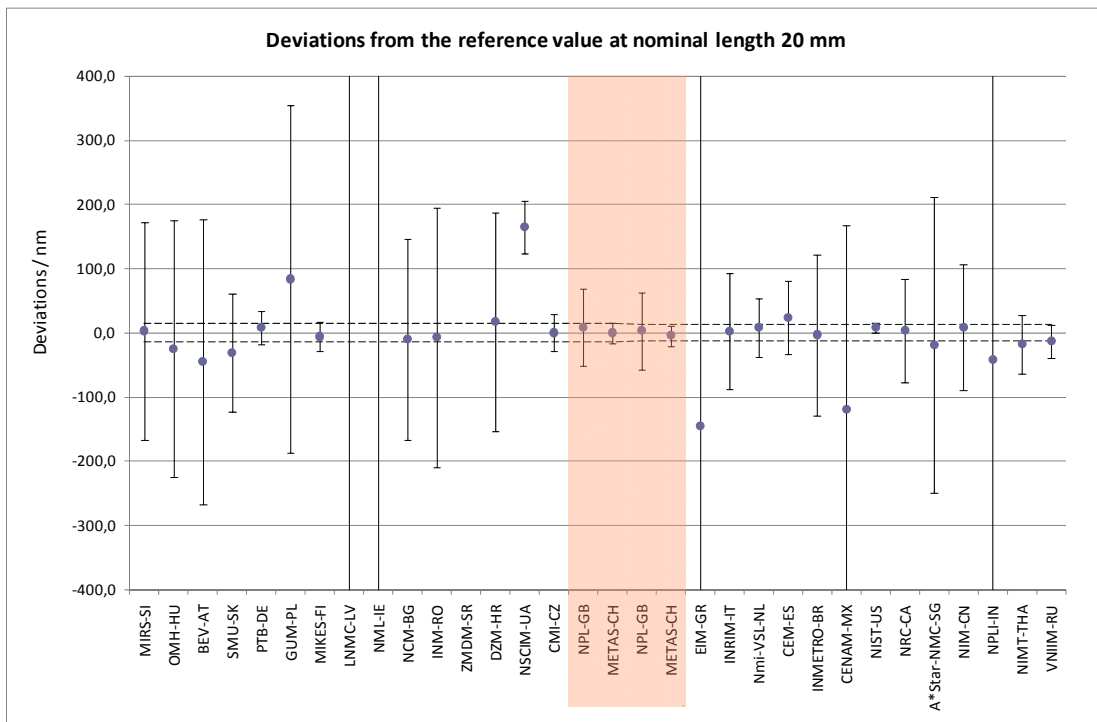


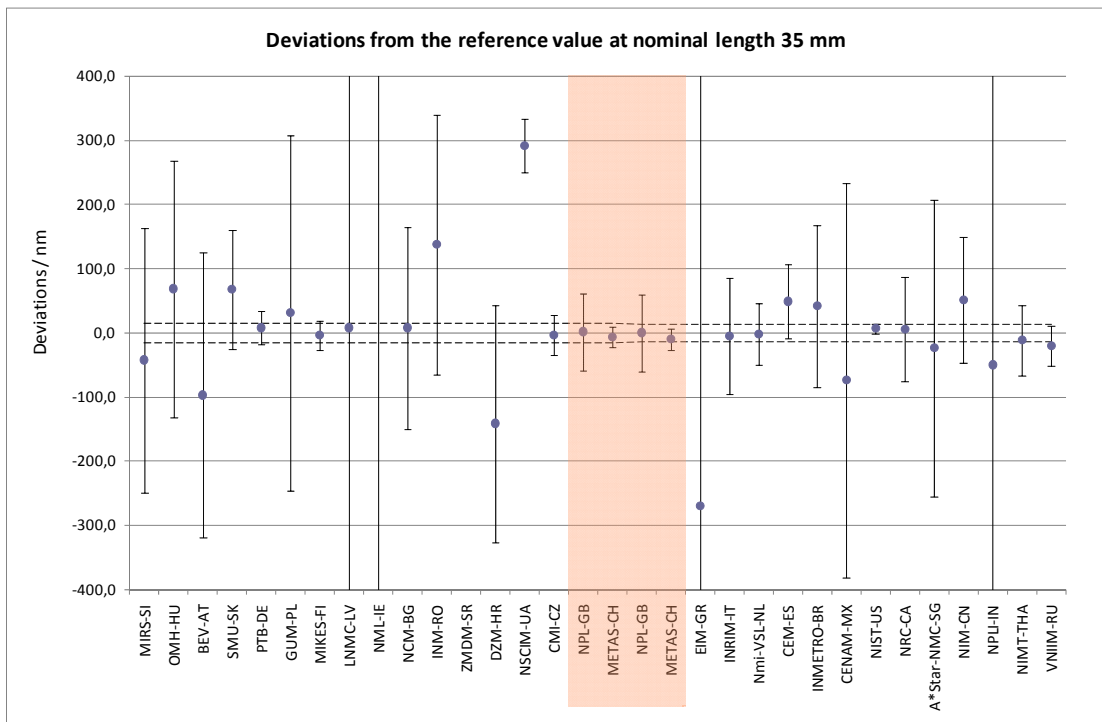
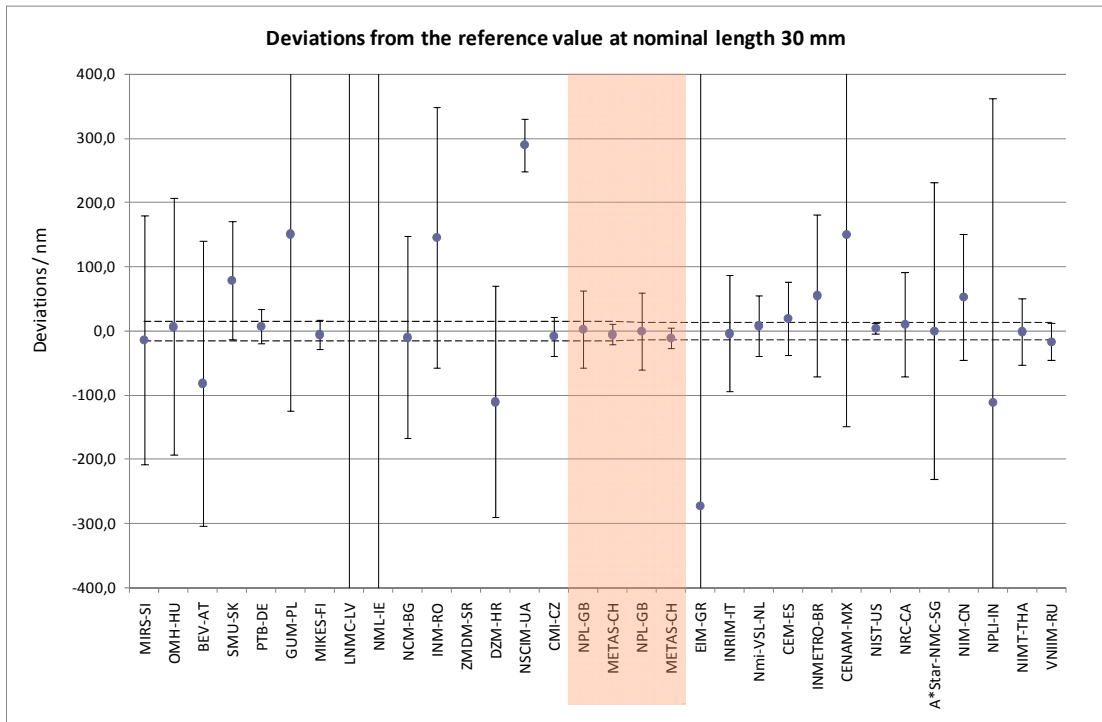


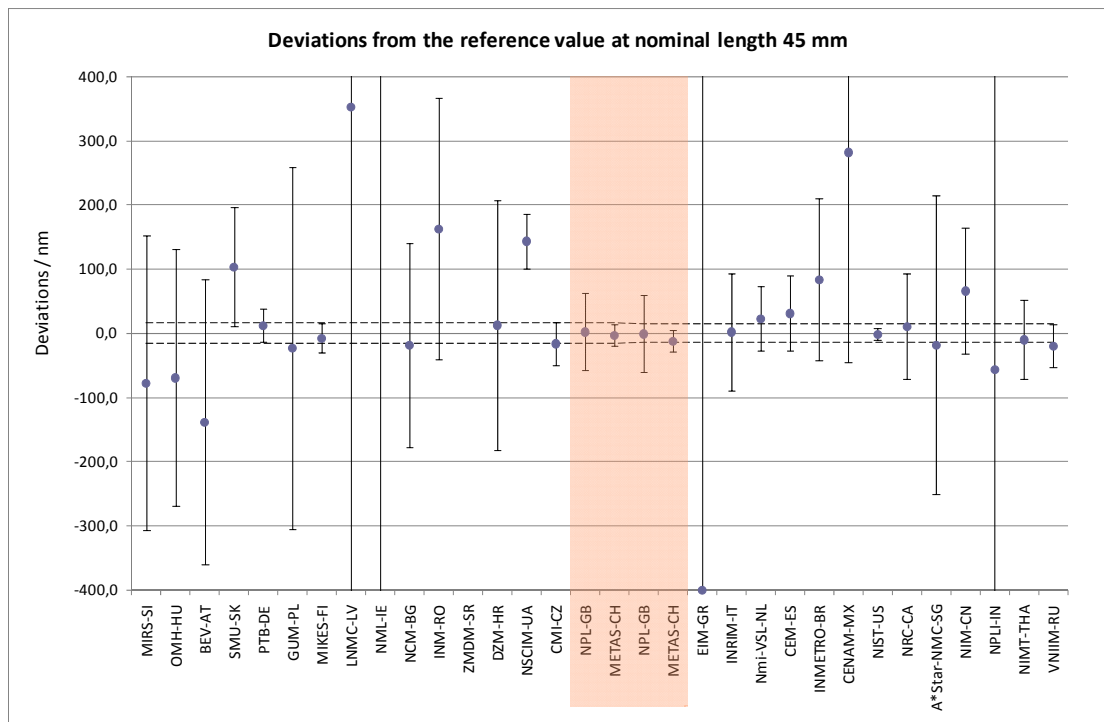
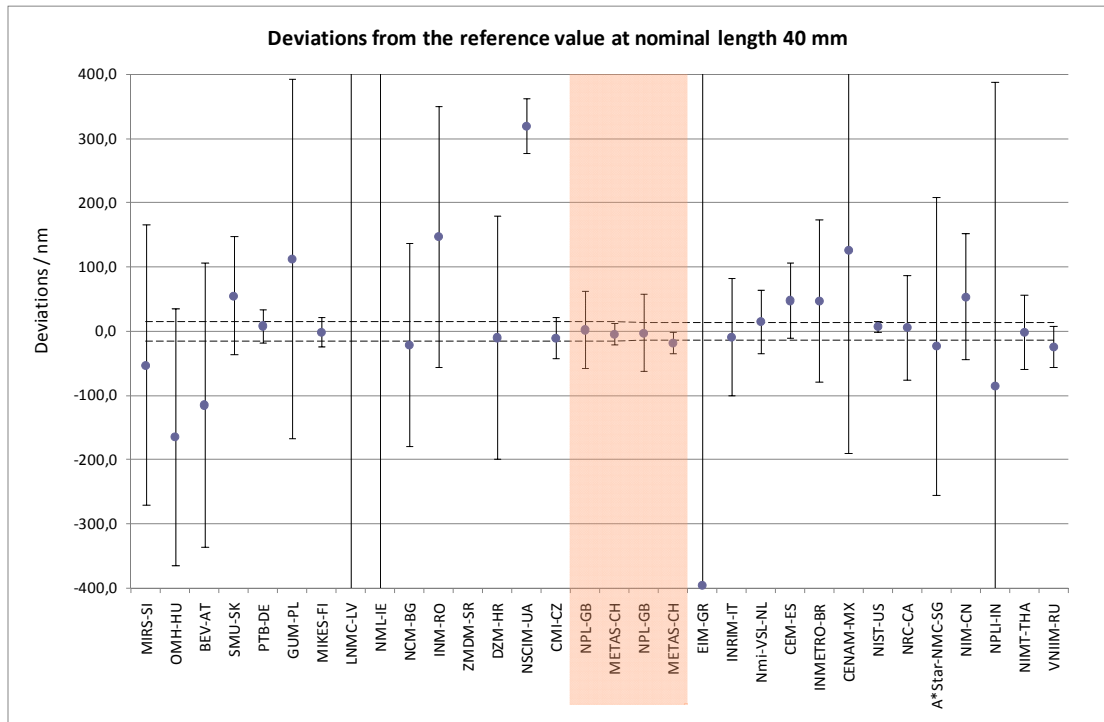


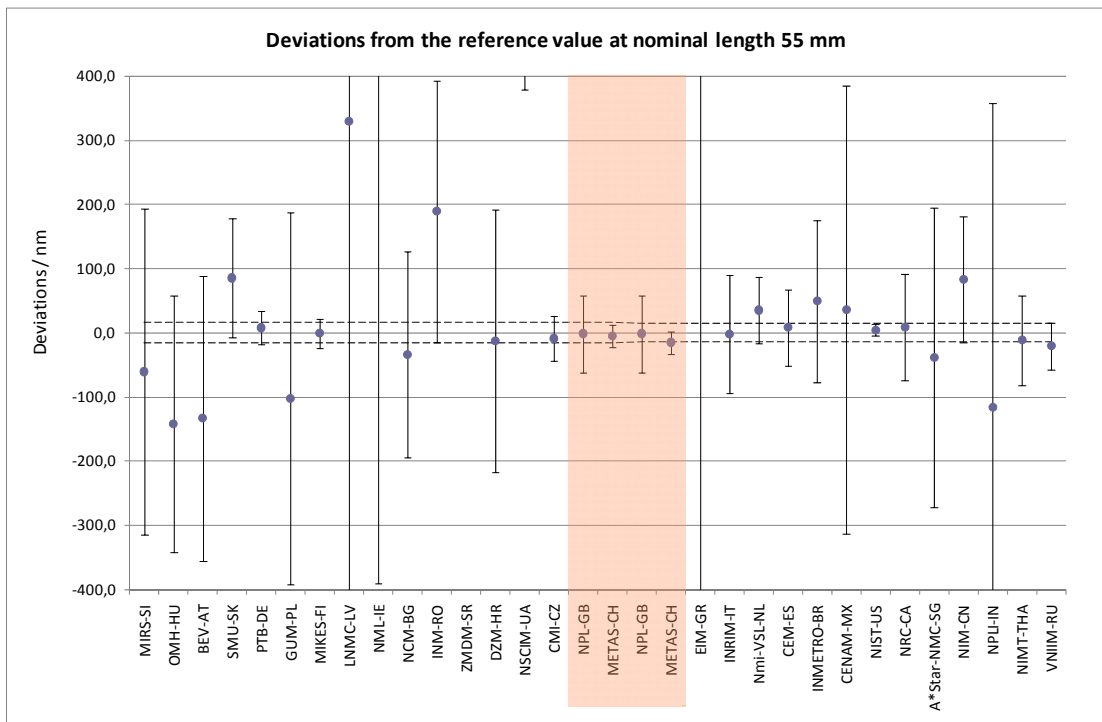
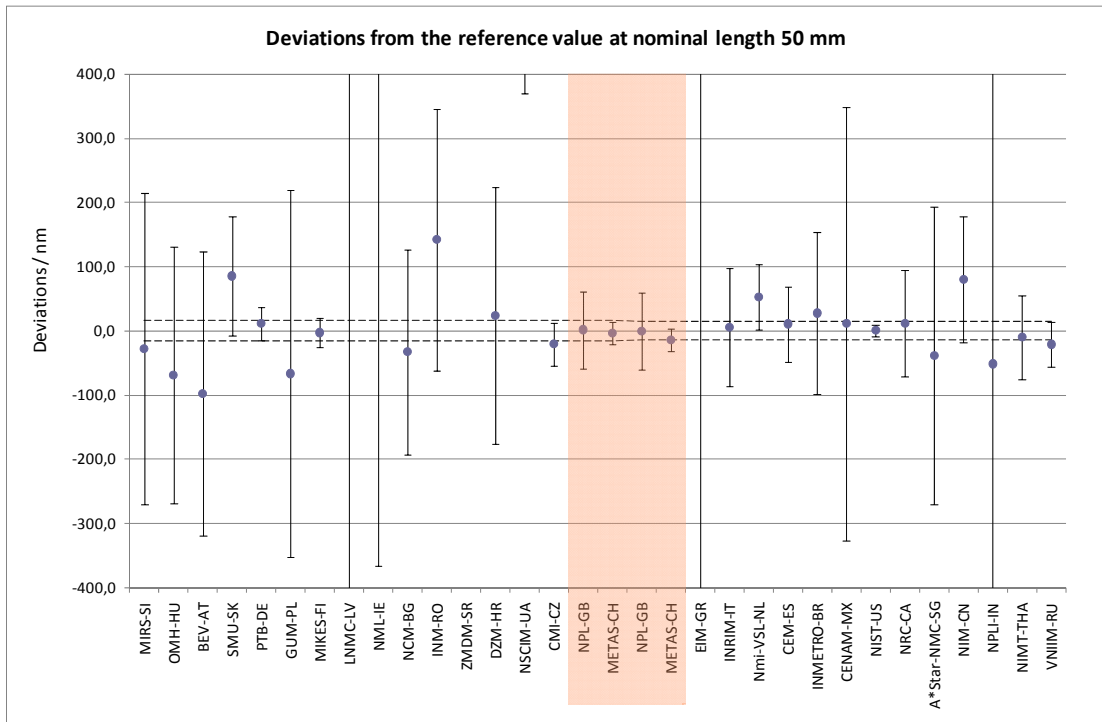


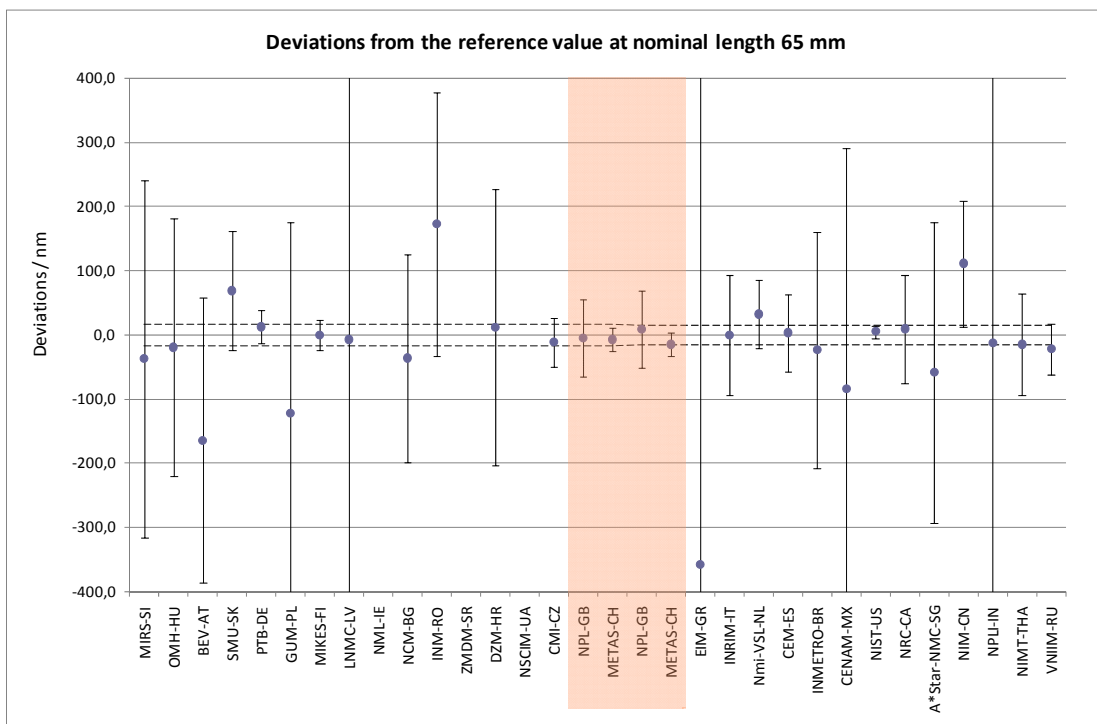
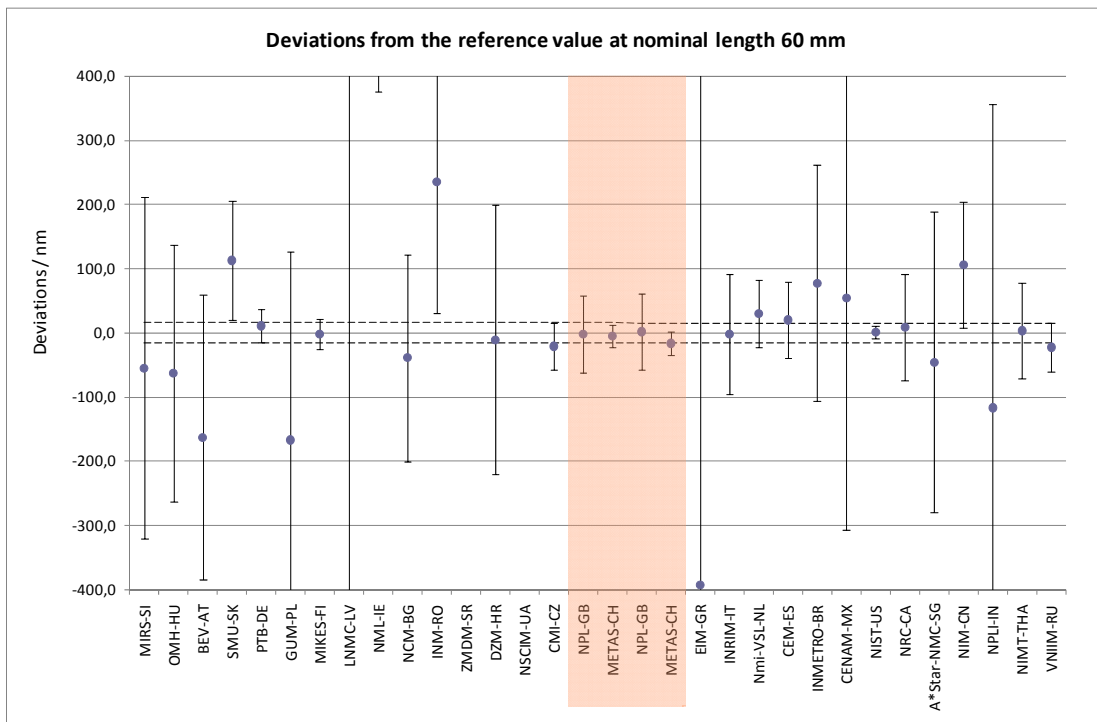


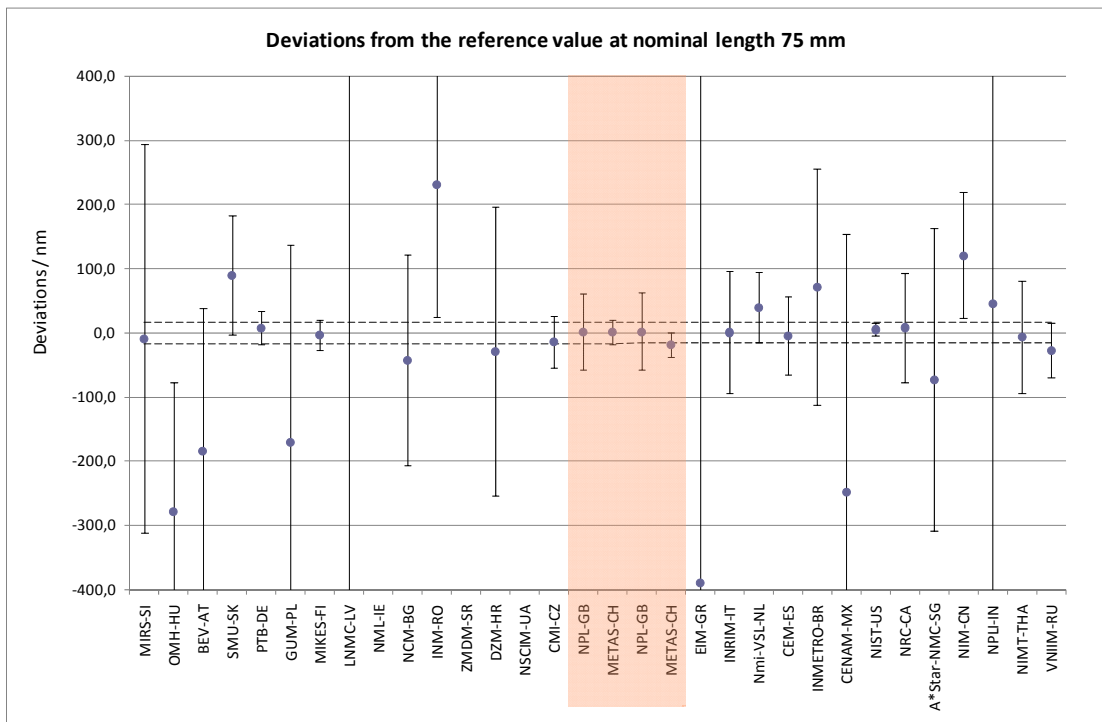
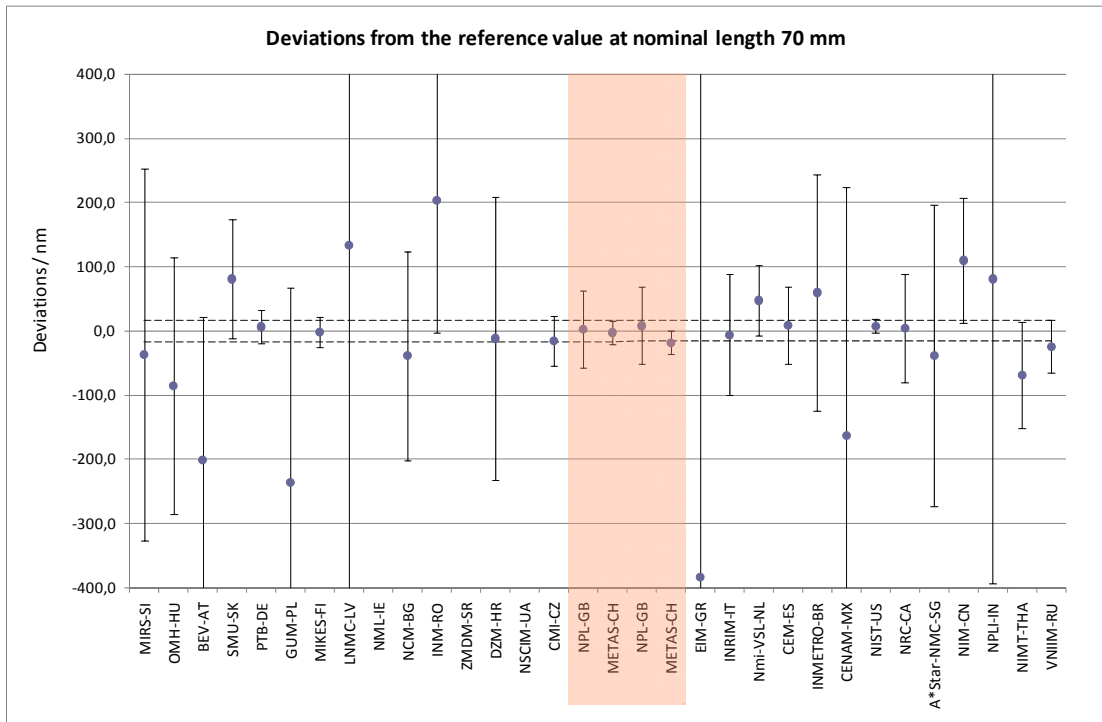


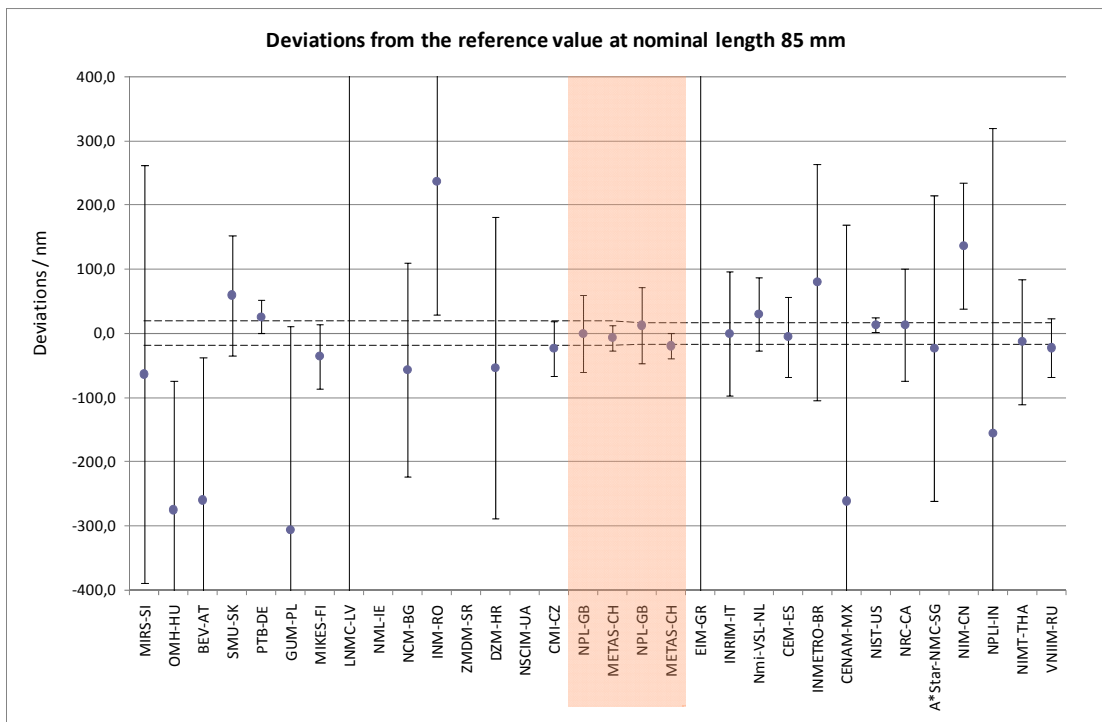
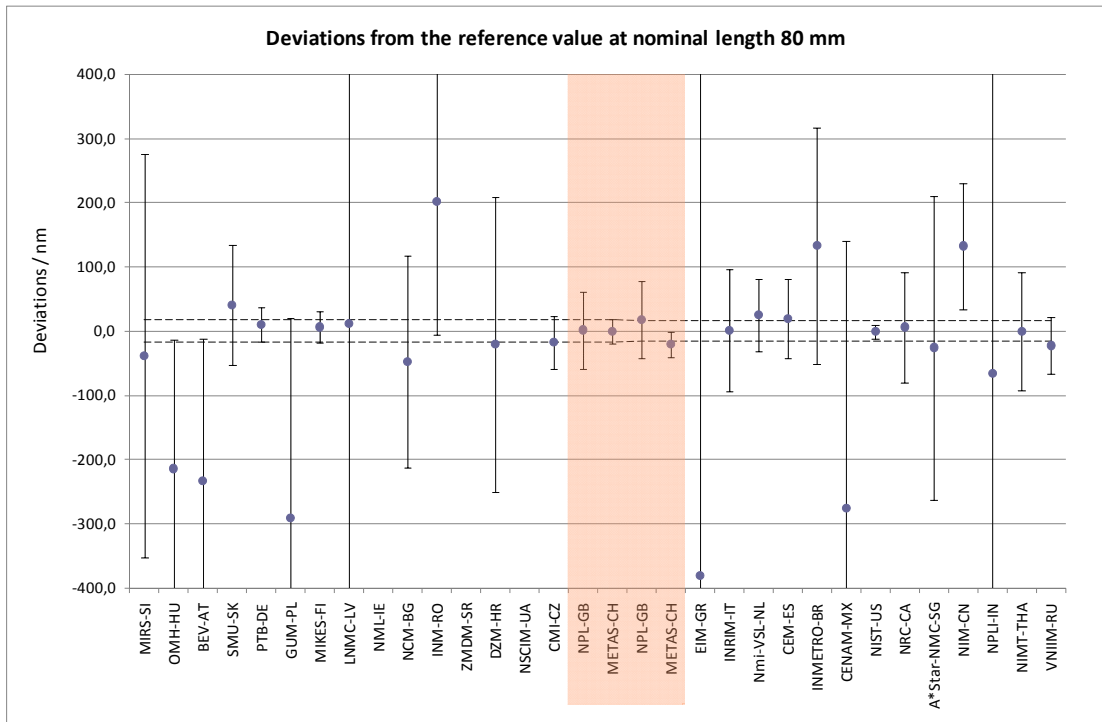


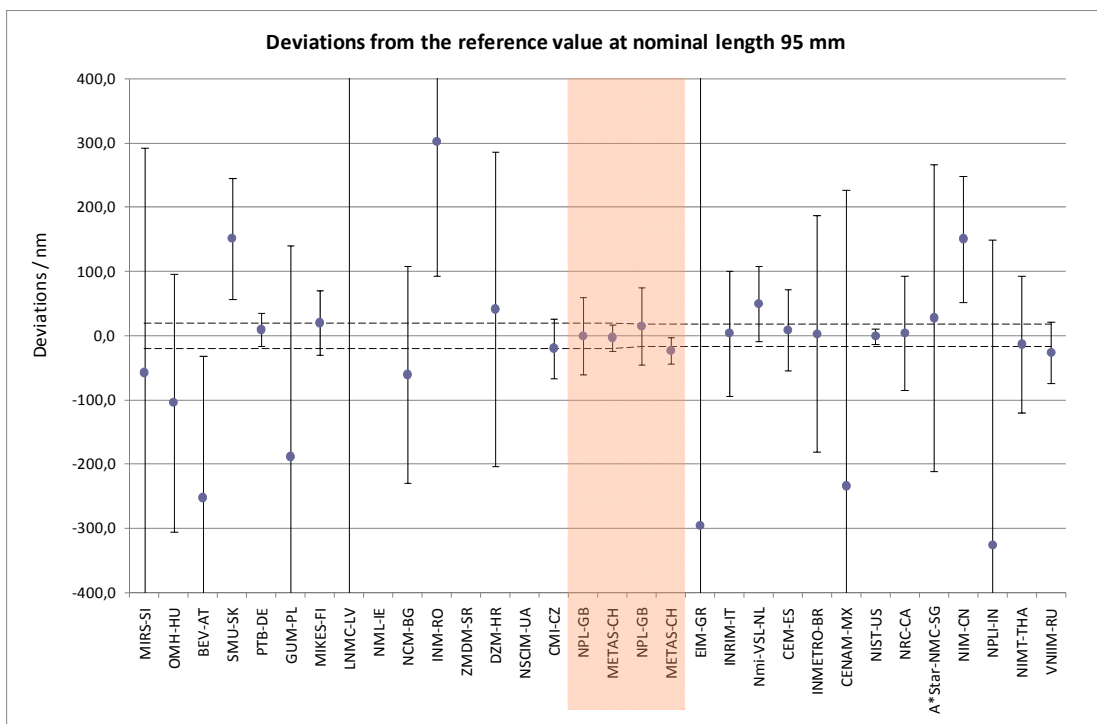
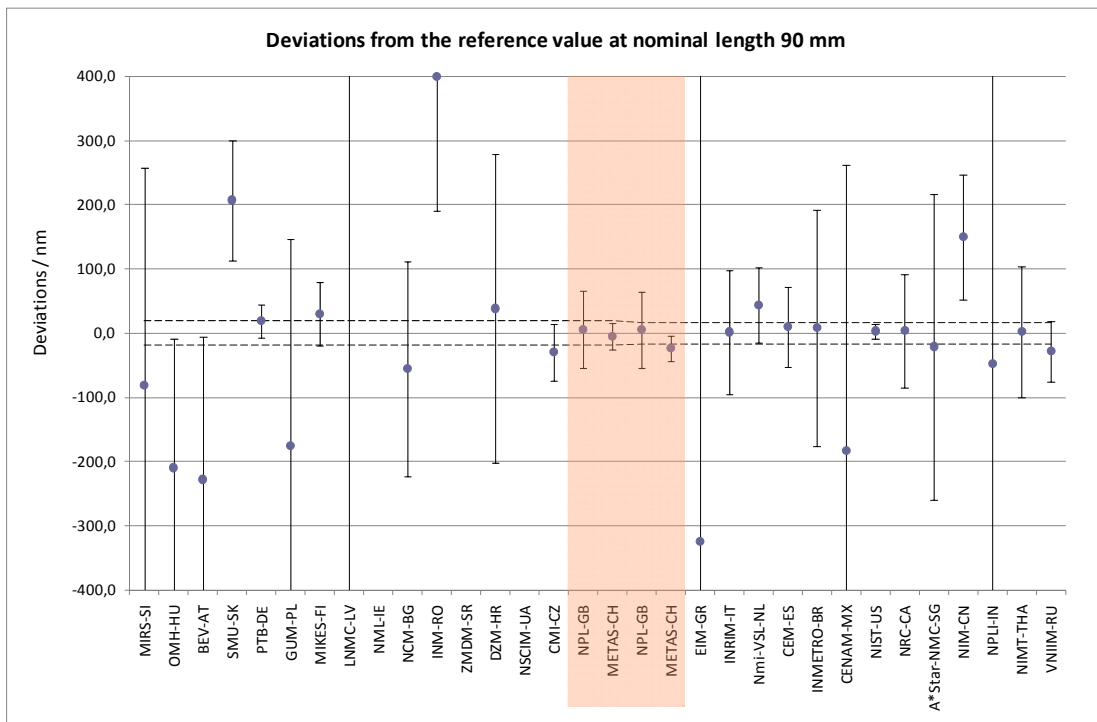


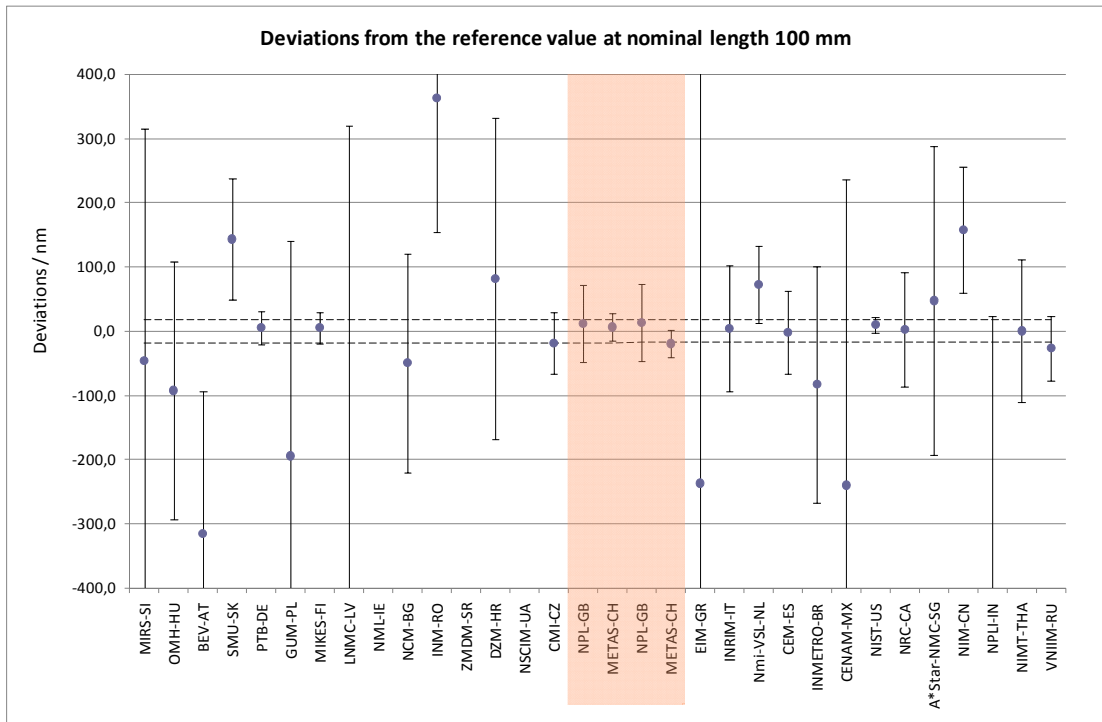












9 Conclusions

The intention of this comparison was to determine and to document capabilities of the participating NMIs to carry out line scale calibrations on high quality line scales produced for industrial purposes. The line scales used for the comparison were designed and produced by NPL in UK. Two scales of same design and very similar quality were kindly donated by NPL.

The idea for the comparison arised at the Euramet TCL meeting in October 2005. The comparison started in July 2006 and the last measurement was performed in December 2008. Originally, 31 NMIs expressed interest for participating in the comparison. During the comparison, two laboratories decided not to perform measurements due to technical reasons and one new laboratory was approved to take part. At the end 30 laboratories reported their results.

Participating laboratories were divided into 2 groups in accordance with their geographical position (in order to minimize travel times and expenses for the transportation of the standards). Linking laboratories between the groups were chosen among participants in Nano3 project (NPL and METAS).

Although the standards traveled through a large number of laboratories, no significant damages were noticed. Some laboratories reported some dirt and scratches, but no significant influence on the results were indicated. The comparison ran quite well within the schedule in spite of some customs problems. Changes in the schedule are indicated in chapter 2.4.

Results were evaluated for each group separately and also after linking groups by using Bayesian statistics [2]. The performance of the participants was evaluated by using E_n value as the acceptance criterion. The reference value was calculated as the weighted mean of reported results for each measuring point. The Birge criterion and Chi-test were used for approving calculated reference values.

In the conclusion it can be summarised that the comparison was successful and has shown realistic picture about calibration and measurement capabilities of participating laboratories.

10 Acknowledgment

The pilot laboratory would like to thank all involved experts and other staff from the participating NMIs for their co-operation and performed technical and formal work. Special thanks should be addressed to the linking laboratories NPL-UK and METAS-CH for offering technical support through extensive discussions about the analysis of the results.

However, the comparison would not be possible without the generous support of the producer and owner of the line scales – NPL from UK. At this occasion the pilot laboratory is expressing very special thanks to NPL and to Dr. Michael McCarthy personally.

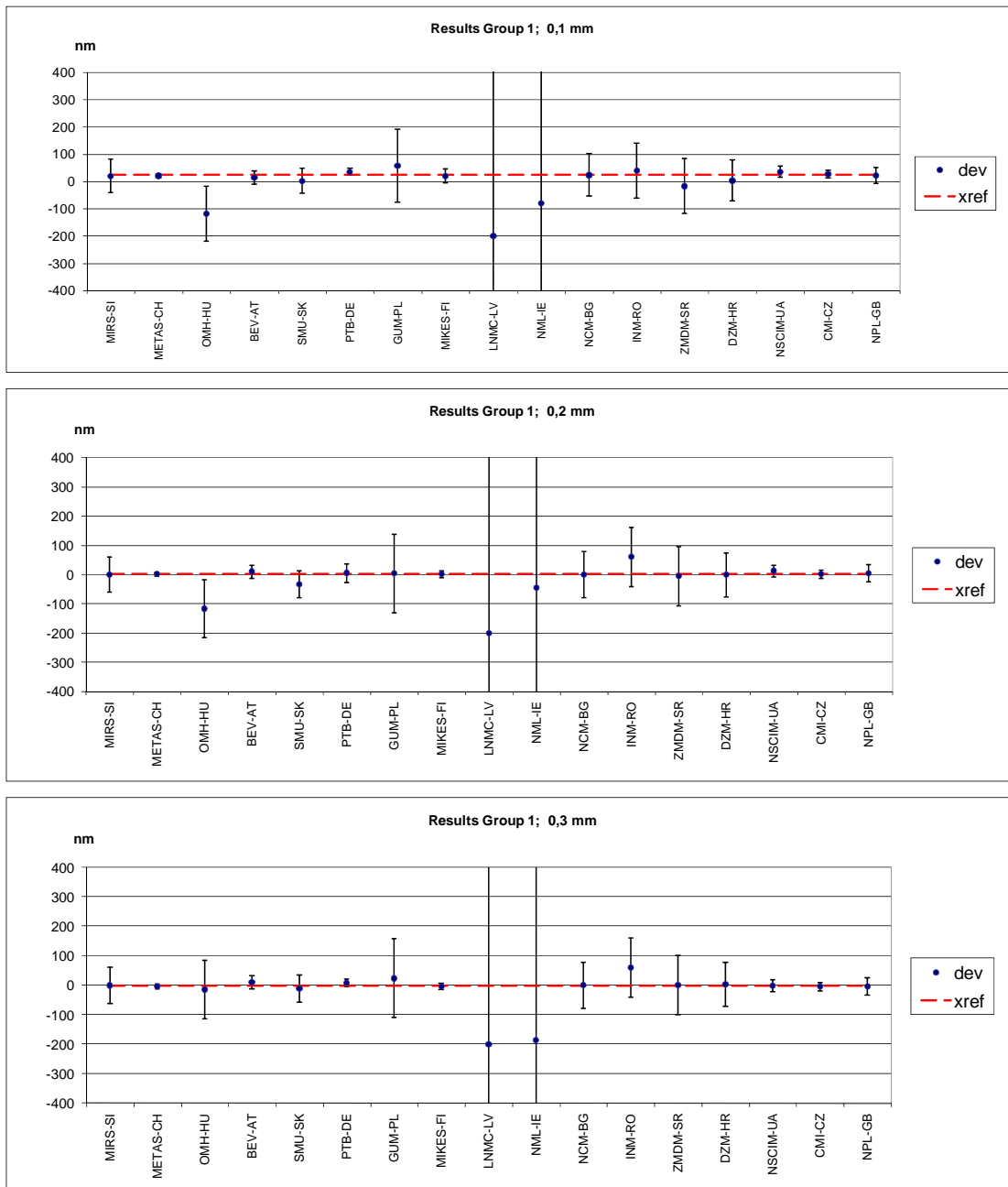
11 References

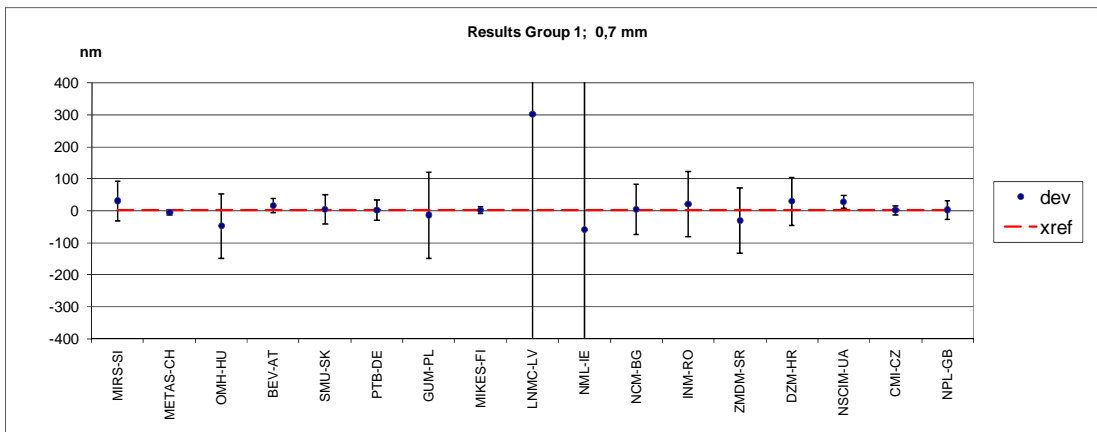
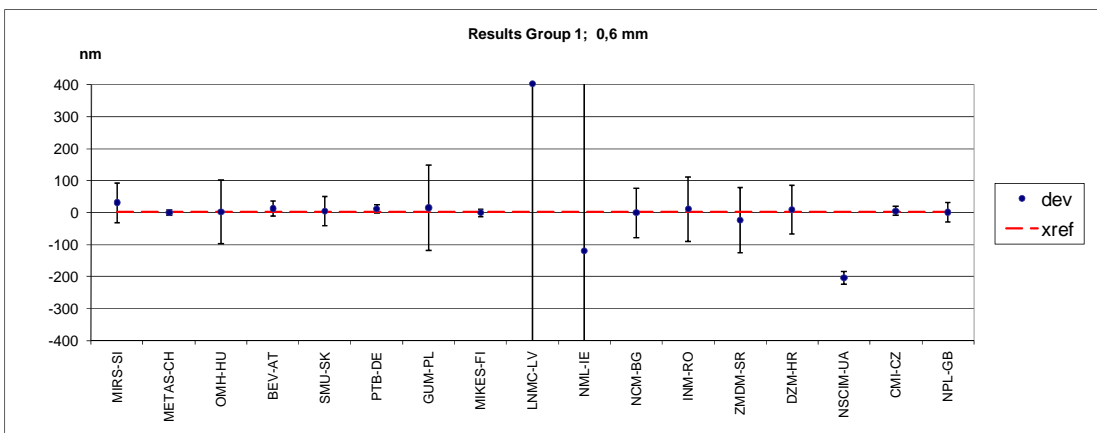
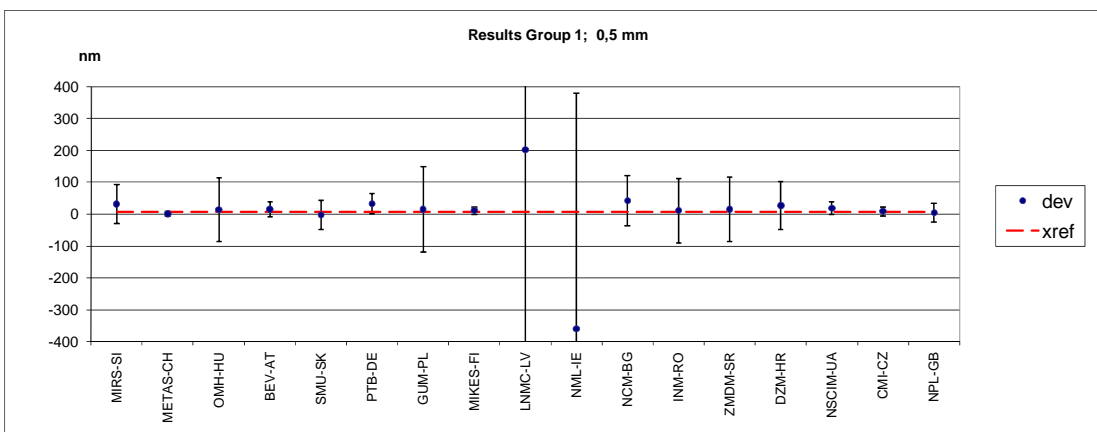
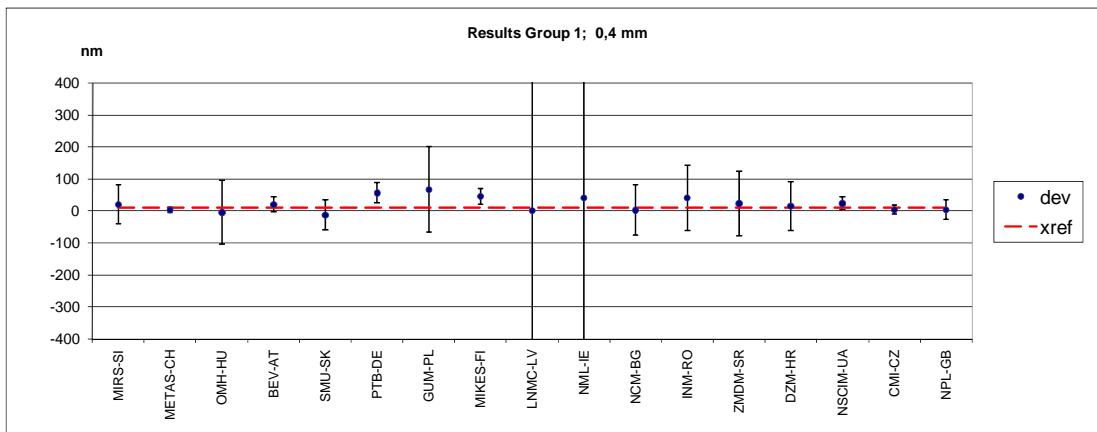
- [1] M. G. Cox. The evaluation of key comparison data, *Metrologia* 39, 589–595 (2002)
- [2] M. Krystek; personal communication
- [3] H. Bose. Nano 3 – Line Scale Standards; WGDM-7 Preliminary comparison on nanometrology, *Final report* (2003)
- [4] R. Thalmann. EUROMET 677- Steel Tape Measures, *Final report* (2004)
- [5] Guidelines for CIPM key comparisons, (2003), <http://www.bipm.org/utis/en/pdf/guidelines.pdf>

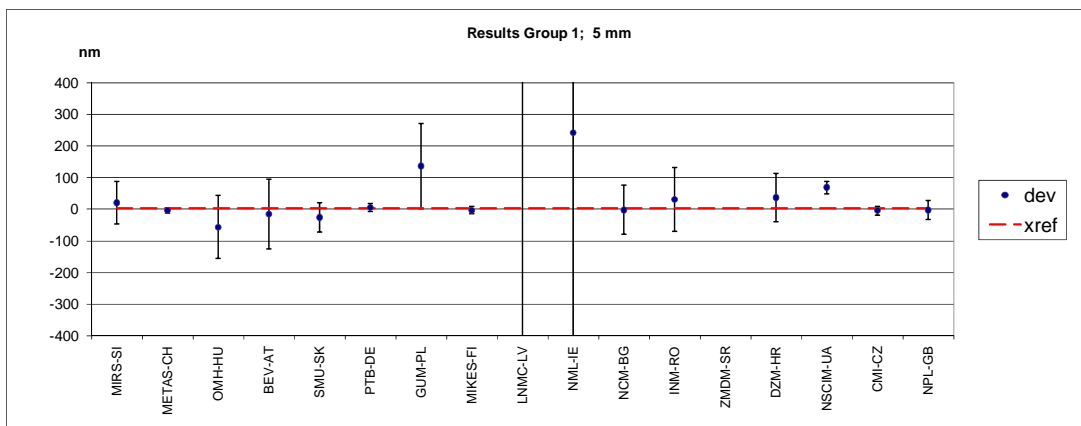
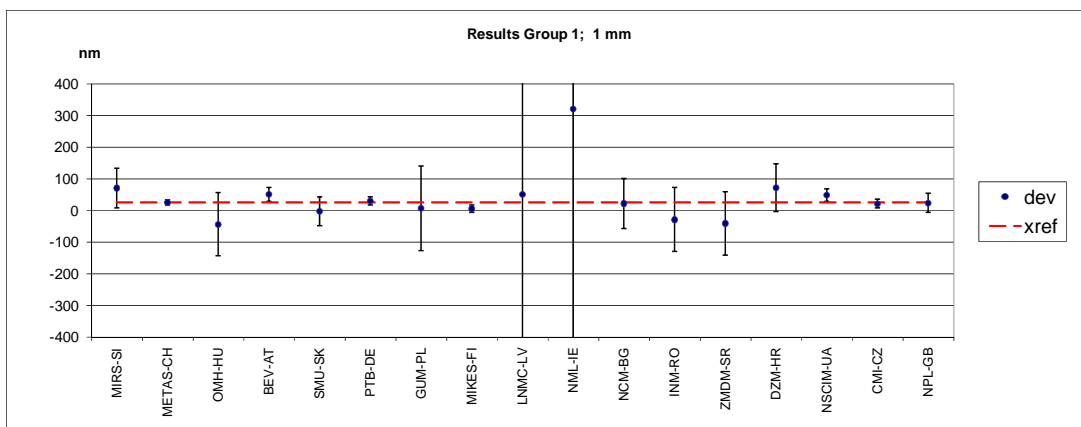
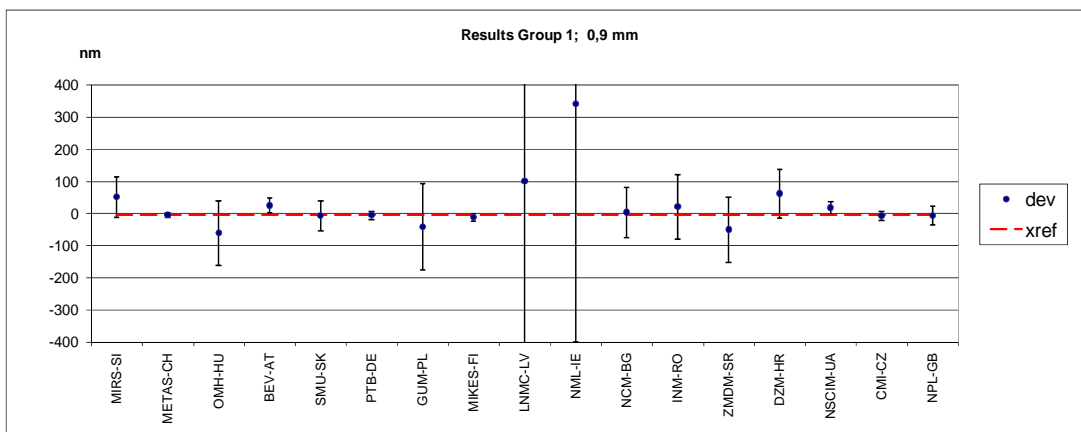
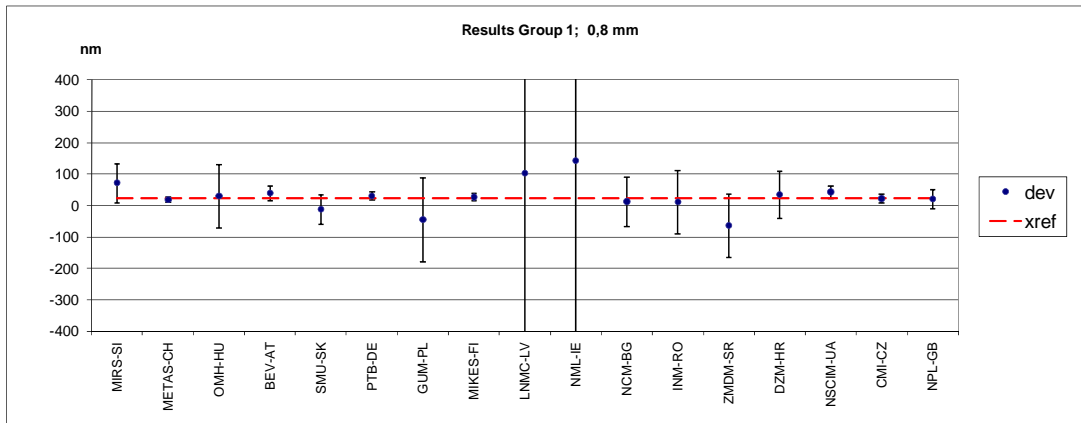
Appendix 1: Intercomparison results for the case of separate treatment of groups 1 and 2 (without link)

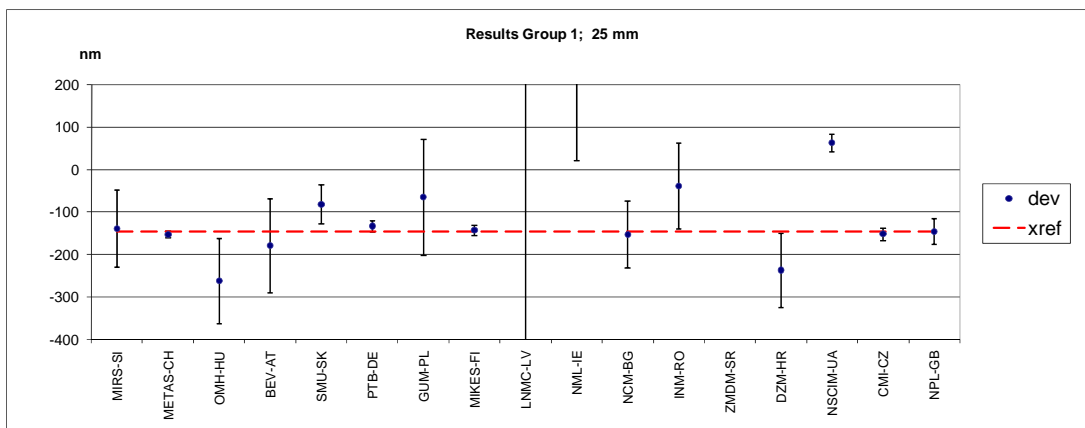
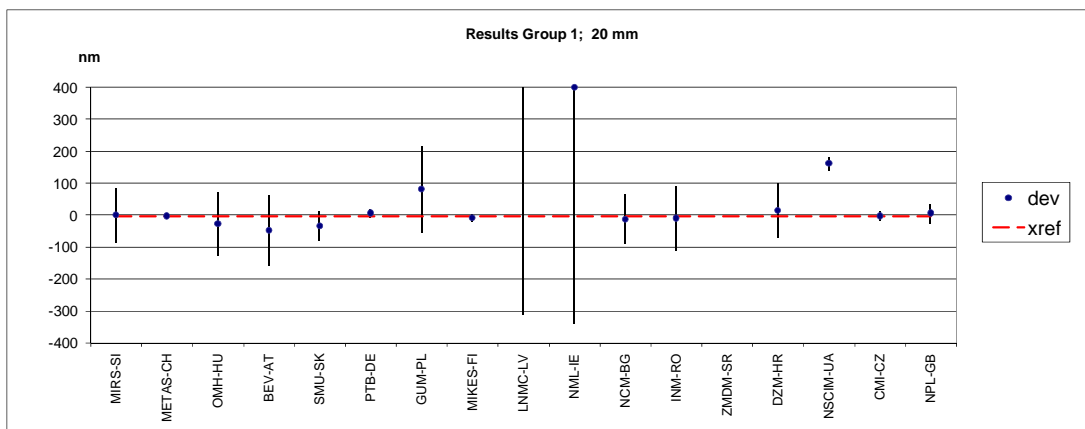
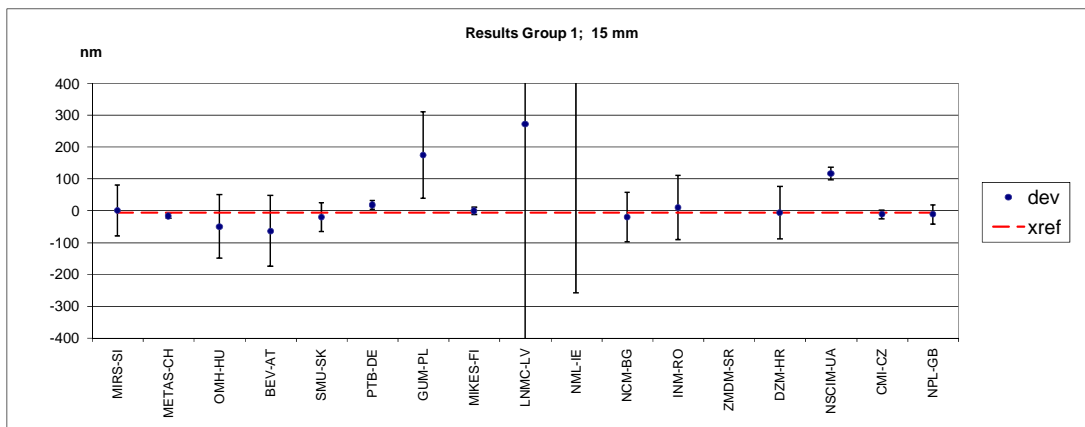
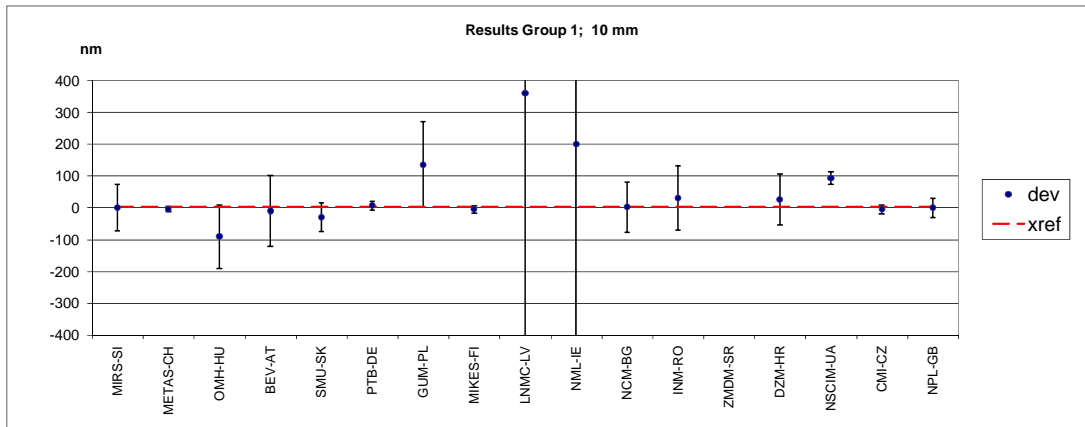
1.1 Group 1 – deviations from reference value

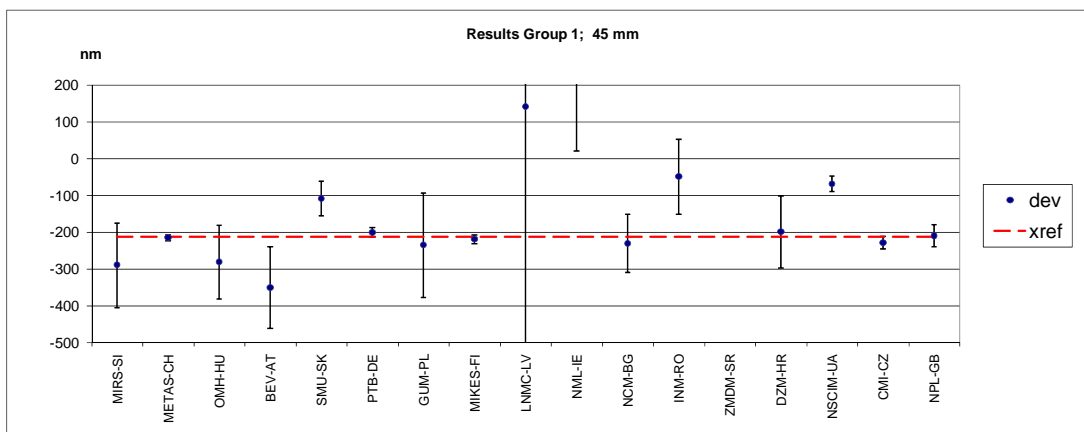
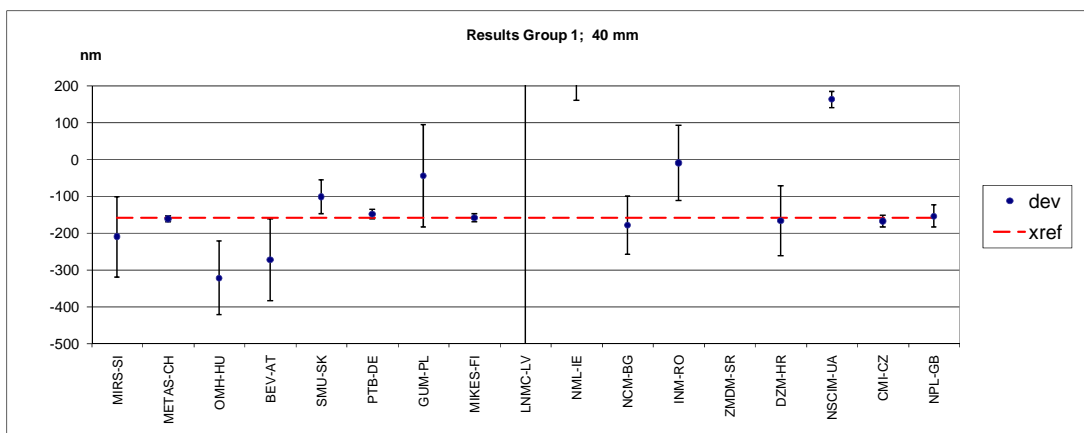
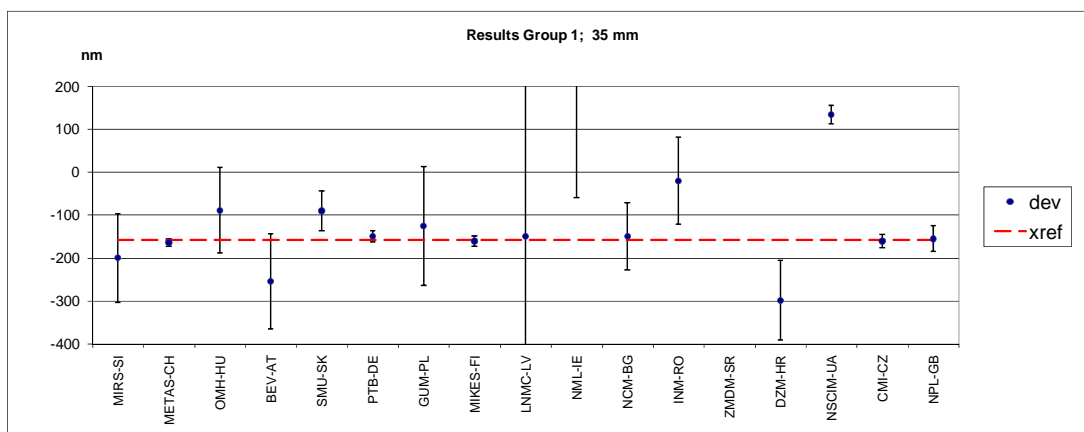
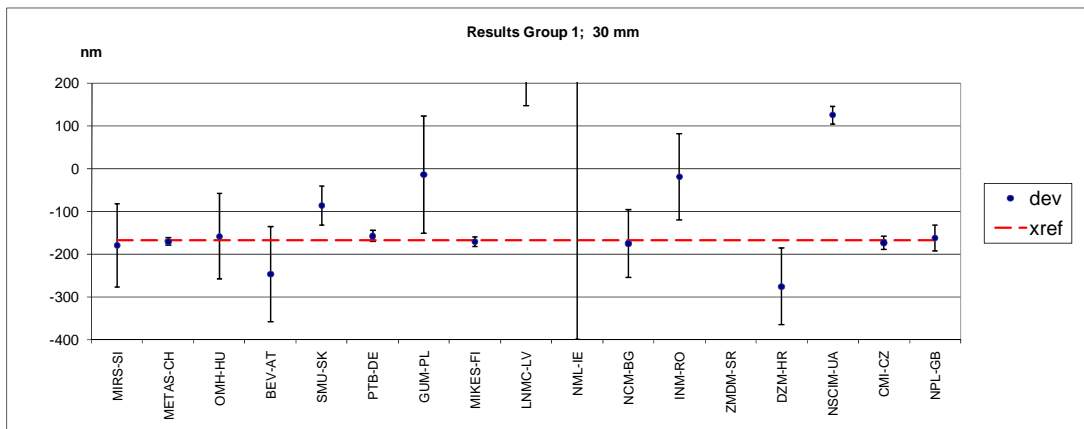
Graphical presentation of measurement results follows in 30 diagrams. Uncertainty bars in the diagrams for single measuring points represent standard uncertainty u ($k = 1$).

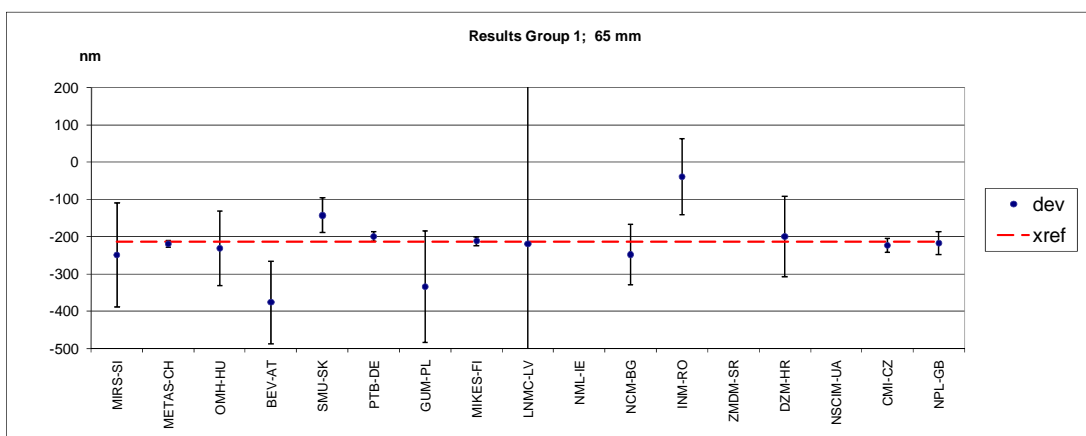
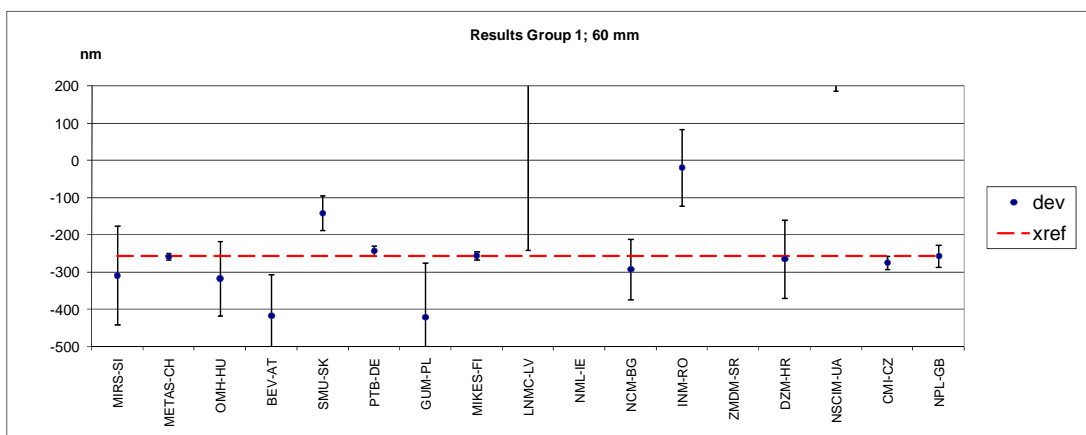
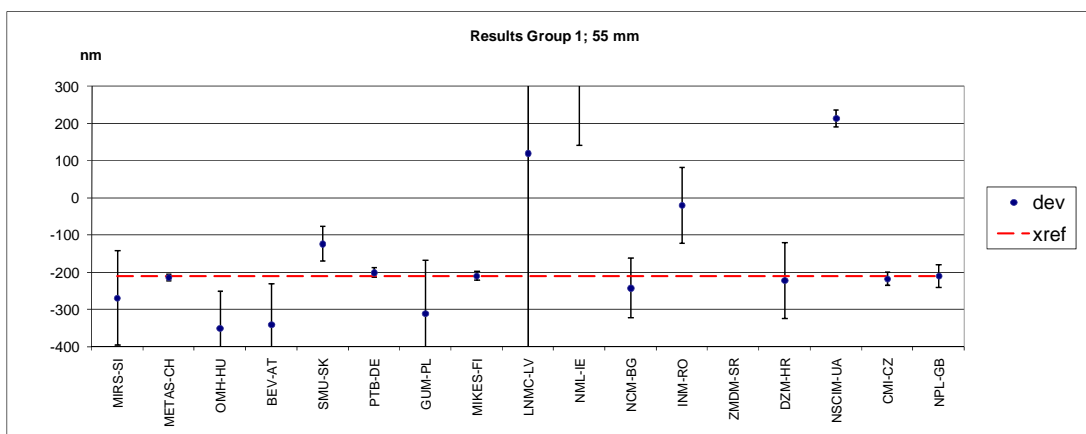
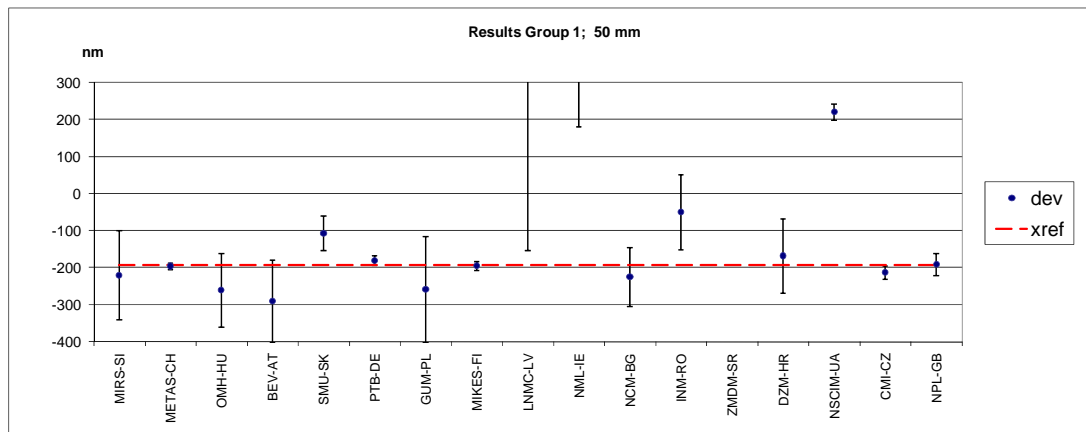


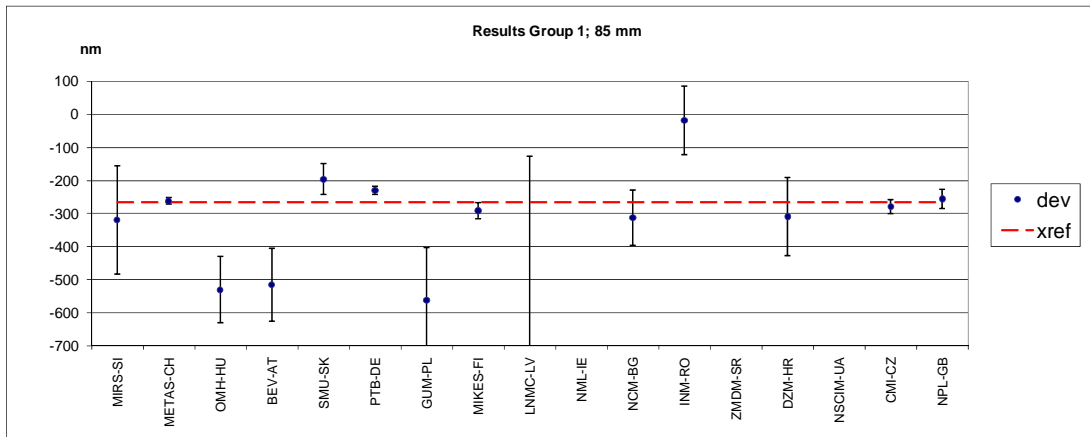
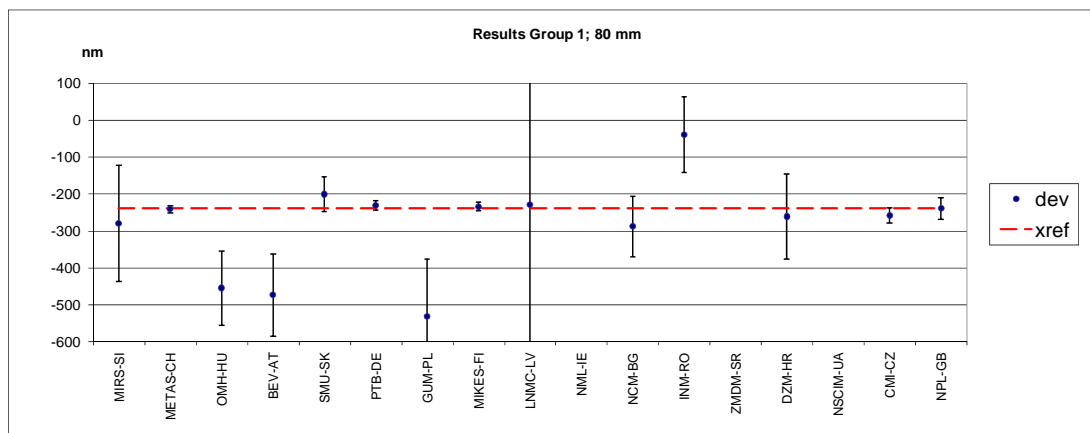
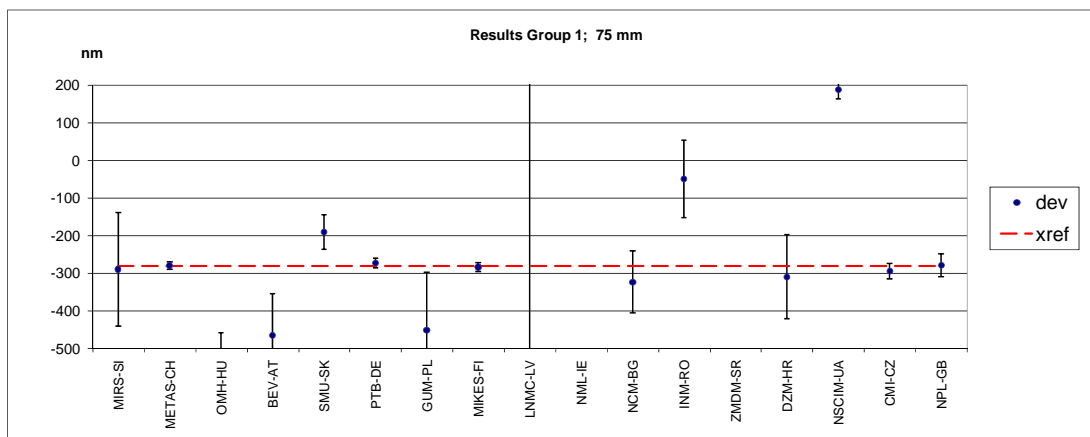
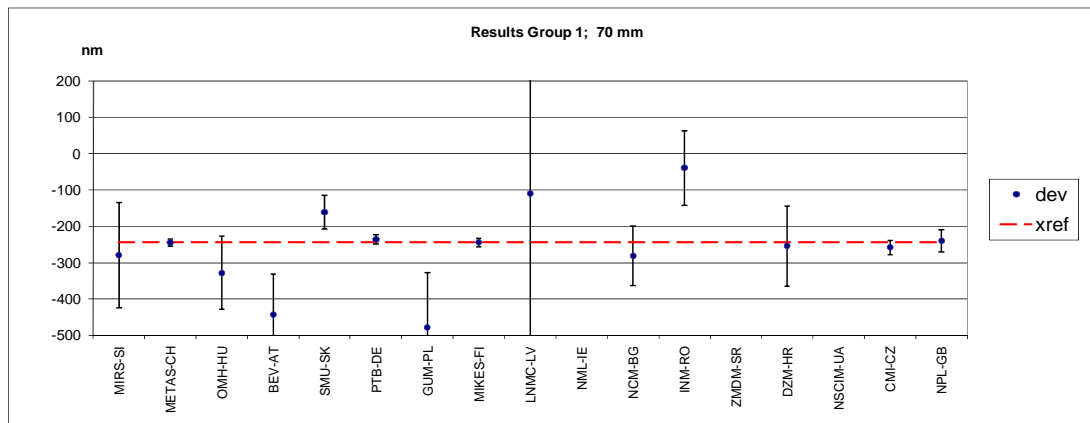


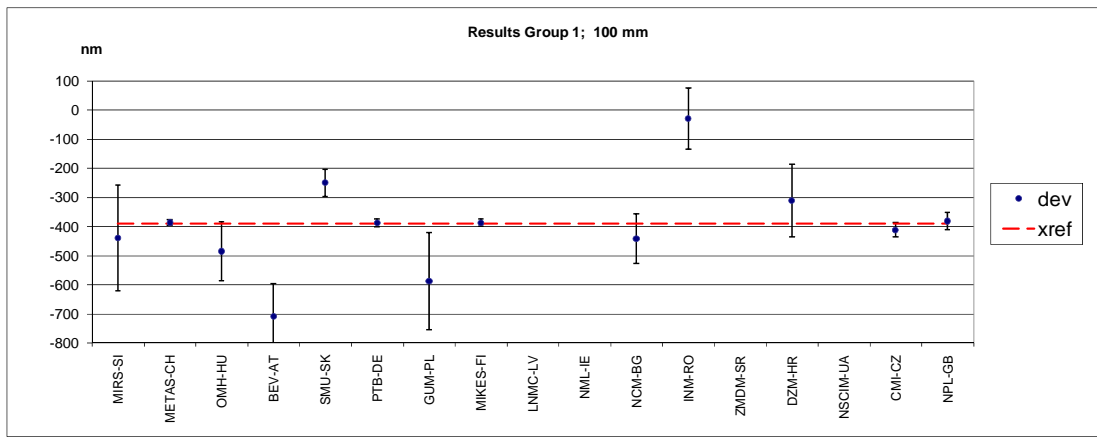
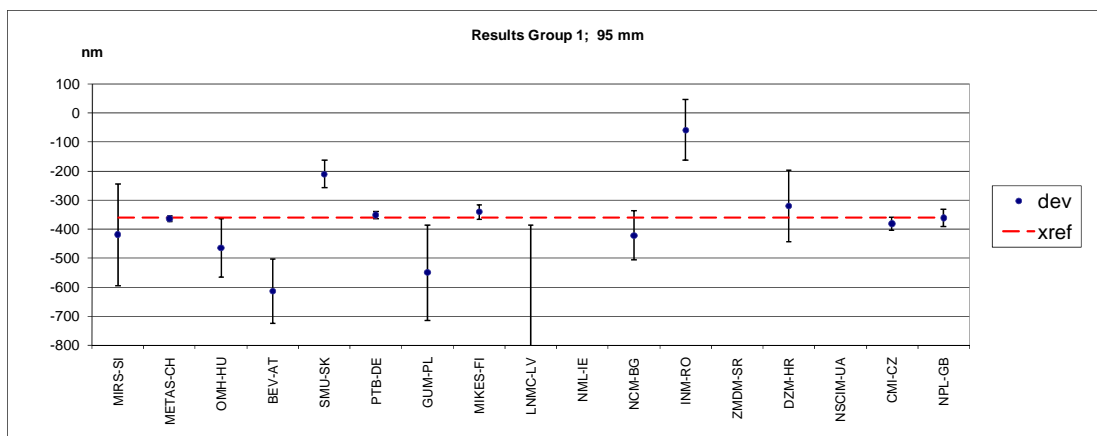
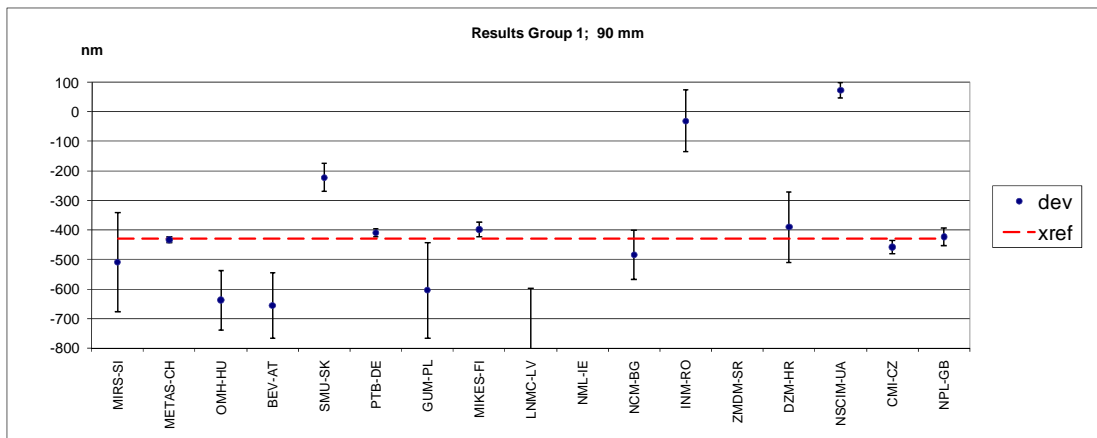












1.2 Group 1 - Calculated values

The results given in Table 1.2 were calculated from the largest consistent subset. This subset was created by eliminating laboratories with the greatest E_n values until the Birge criterion (Ch. 7) was met. E_n values $|E_n| > 1$ are marked with yellow colour. Eliminated laboratories for single measurement points are shown in Table 1.1.

Table 1.1: Laboratories that were excluded from calculation of the reference values

| Measuring point (mm) | No. of excl. labs | Excluded laboratories | Measuring point (mm) | No. of excl. labs | Excluded laboratories |
|----------------------|-------------------|-----------------------|----------------------|-------------------|---|
| 0,6 | 1 | NSCIM-UA | 55 | 2 | ZMDM-SR, NSCIM-UA |
| 5 | 1 | ZMDM-SR | 60 | 3 | ZMDM-SR, NSCIM-UA, NML-IE |
| 10 | 1 | ZMDM-SR | 65 | 2 | ZMDM-SR, NSCIM-UA |
| 15 | 2 | ZMDM-SR, NSCIM-UA | 70 | 2 | ZMDM-SR, NSCIM-UA |
| 20 | 2 | ZMDM-SR, NSCIM-UA | 75 | 3 | ZMDM-SR, NSCIM-UA, NML-IE |
| 25 | 2 | ZMDM-SR, NSCIM-UA | 80 | 3 | ZMDM-SR, NSCIM-UA, NML-IE |
| 30 | 2 | ZMDM-SR, NSCIM-UA | 85 | 5 | ZMDM-SR, NSCIM-UA, NML-IE, SMU-SK, INM-RO |
| 35 | 2 | ZMDM-SR, NSCIM-UA | 90 | 5 | ZMDM-SR, NSCIM-UA, NML-IE, SMU-SK, INM-RO |
| 40 | 2 | ZMDM-SR, NSCIM-UA | 95 | 4 | ZMDM-SR, NSCIM-UA, NML-IE, SMU-SK |
| 45 | 2 | ZMDM-SR, NSCIM-UA | 100 | 5 | ZMDM-SR, NSCIM-UA, NML-IE, SMU-SK, INM-RO |
| 50 | 2 | ZMDM-SR, NSCIM-UA | | | |

Table 1.2: Results calculated from the given values – Group 1

| Meas. Point | 0,1 mm | | 0,2 mm | | 0,3 mm | | 0,4 mm | | 0,5 mm | | 0,6 mm | |
|--------------------|-----------------|-------|-----------------|-------|-----------------|-------|-----------------|-------|-----------------|-------|-----------------|--------------|
| X_{ref} | 24,3 nm | | 1,8 nm | | -1,2 nm | | 9,8 nm | | 6,6 nm | | 1,7 nm | |
| $U_c(X_{ref})$ | 5,3 nm | | 5,2 nm | | 4,9 nm | | 5,7 nm | | 5,2 nm | | 5,0 nm | |
| U_{ext} | 2,7 nm | | 2,2 nm | | 1,6 nm | | 3,6 nm | | 2,1 nm | | 1,6 nm | |
| No of participants | 17 | | 17 | | 17 | | 17 | | 17 | | 16 | |
| R_B | 0,52 | | 0,42 | | 0,32 | | 0,63 | | 0,40 | | 0,32 | |
| $R_{B,crit}$ | 1,31 | | 1,31 | | 1,31 | | 1,31 | | 1,31 | | 1,32 | |
| | $x_i - X_{ref}$ | E_n |
| MIRS-SI | -4,29 | -0,04 | -1,76 | -0,01 | 1,16 | 0,01 | 10,21 | 0,08 | 23,38 | 0,19 | 28,28 | 0,23 |
| METAS-CH | -3,29 | -0,28 | -0,76 | -0,06 | -2,84 | -0,23 | -6,79 | -0,62 | -6,62 | -0,56 | -3,72 | -0,31 |
| OMH-HU | -143,29 | -0,72 | -118,76 | -0,59 | -12,84 | -0,06 | -14,79 | -0,07 | 5,38 | 0,03 | -0,72 | 0,00 |
| BEV-AT | -10,29 | -0,23 | 8,24 | 0,18 | 11,16 | 0,25 | 10,21 | 0,23 | 7,38 | 0,16 | 10,28 | 0,23 |
| SMU-SK | -22,29 | -0,24 | -35,76 | -0,39 | -8,84 | -0,10 | -22,79 | -0,25 | -10,62 | -0,12 | 2,28 | 0,02 |
| PTB-DE | 10,91 | 0,46 | 3,64 | 0,06 | 10,16 | 0,42 | 45,71 | 0,73 | 25,38 | 0,40 | 8,78 | 0,37 |
| GUM-PL | 33,71 | 0,13 | 2,24 | 0,01 | 25,16 | 0,09 | 56,21 | 0,21 | 7,38 | 0,03 | 12,28 | 0,05 |
| MIKES-FI | -4,29 | -0,09 | -0,76 | -0,04 | -2,84 | -0,14 | 35,21 | 0,72 | 3,38 | 0,17 | -3,72 | -0,18 |
| LNMC-LV | -224,29 | -0,14 | -201,76 | -0,12 | -198,84 | -0,12 | -9,79 | -0,01 | 193,38 | 0,12 | 398,28 | 0,24 |
| NML-IE | -104,29 | -0,07 | -47,76 | -0,03 | -184,84 | -0,12 | 30,21 | 0,02 | -366,62 | -0,25 | -121,72 | -0,08 |
| NCM-BG | -0,29 | 0,00 | -1,76 | -0,01 | 2,16 | 0,01 | -7,79 | -0,05 | 34,38 | 0,22 | -3,72 | -0,02 |
| INM-RO | 15,71 | 0,08 | 58,24 | 0,29 | 61,16 | 0,30 | 30,21 | 0,15 | 3,38 | 0,02 | 8,28 | 0,04 |
| ZMDM-SR | -41,59 | -0,21 | -7,06 | -0,04 | 2,56 | 0,01 | 13,31 | 0,07 | 7,28 | 0,04 | -26,42 | -0,13 |
| DZM-HR | -21,29 | -0,14 | -2,76 | -0,02 | 4,16 | 0,03 | 4,21 | 0,03 | 19,38 | 0,13 | 6,28 | 0,04 |
| NSCIM-UA | 11,71 | 0,30 | 10,24 | 0,27 | 0,16 | 0,00 | 13,21 | 0,34 | 10,38 | 0,27 | -205,72 | -5,31 |
| CMI-CZ | 3,71 | 0,14 | -0,76 | -0,03 | -2,84 | -0,11 | -6,79 | -0,27 | 1,38 | 0,05 | 2,28 | 0,09 |
| NPL-GB | -2,29 | -0,04 | 2,38 | 0,04 | -2,01 | -0,03 | -6,39 | -0,11 | -3,60 | -0,06 | -2,06 | -0,03 |

| Meas. Point | 0,7 mm | | 0,8 mm | | 0,9 mm | | 1,0 mm | | 5,0 mm | | 10,0 mm | |
|--------------------|-----------------|-------|-----------------|-------|-----------------|-------|-----------------|-------|-----------------|---------------|-----------------|---------------|
| X_{ref} | 0,5 nm | | 22,7 nm | | -4,4 nm | | 23,3 nm | | 2,0 nm | | 2,5 nm | |
| $U_c(X_{ref})$ | 5,2 nm | | 4,9 nm | | 4,9 nm | | 4,9 nm | | 5,0 nm | | 5,0 nm | |
| U_{ext} | 2,5 nm | | 2,6 nm | | 3,0 nm | | 3,6 nm | | 4,9 nm | | 6,4 nm | |
| No of participants | 17 | | 17 | | 17 | | 17 | | 16 | | 16 | |
| R_B | 0,48 | | 0,53 | | 0,60 | | 0,73 | | 0,98 | | 1,28 | |
| $R_{B,crit}$ | 1,31 | | 1,31 | | 1,31 | | 1,31 | | 1,32 | | 1,32 | |
| | $x_i - X_{ref}$ | E_n | $x_i - X_{ref}$ | E_n |
| MIRS-SI | 29,51 | 0,24 | 47,29 | 0,38 | 54,43 | 0,44 | 46,66 | 0,38 | 18,00 | 0,13 | -2,48 | -0,02 |
| METAS-CH | -6,49 | -0,55 | -5,71 | -0,46 | -1,57 | -0,13 | 1,66 | 0,13 | -6,00 | -0,49 | -7,48 | -0,61 |
| OMH-HU | -49,49 | -0,25 | 5,29 | 0,03 | -56,57 | -0,28 | -68,34 | -0,34 | -59,00 | -0,30 | -93,48 | -0,47 |
| BEV-AT | 14,51 | 0,32 | 15,29 | 0,34 | 28,43 | 0,63 | 26,66 | 0,59 | -18,00 | -0,08 | -13,48 | -0,06 |
| SMU-SK | 2,51 | 0,03 | -36,71 | -0,40 | -3,57 | -0,04 | -26,34 | -0,29 | -28,00 | -0,31 | -32,48 | -0,36 |
| PTB-DE | 0,31 | 0,00 | 5,89 | 0,24 | -1,67 | -0,07 | 5,76 | 0,24 | 3,40 | 0,14 | 3,52 | 0,15 |
| GUM-PL | -15,49 | -0,06 | -69,71 | -0,26 | -38,57 | -0,14 | -17,34 | -0,06 | 133,00 | 0,50 | 132,52 | 0,49 |
| MIKES-FI | 0,51 | 0,03 | 2,29 | 0,11 | -8,57 | -0,42 | -18,34 | -0,90 | -6,00 | -0,30 | -8,48 | -0,42 |
| LNMC-LV | 299,51 | 0,18 | 77,29 | 0,05 | 104,43 | 0,06 | 26,66 | 0,02 | 418,00 | 0,25 | 357,52 | 0,22 |
| NML-IE | -60,49 | -0,04 | 117,29 | 0,08 | 344,43 | 0,23 | 296,66 | 0,20 | 238,00 | 0,16 | 197,52 | 0,13 |
| NCM-BG | 2,51 | 0,02 | -11,71 | -0,08 | 7,43 | 0,05 | -2,34 | -0,02 | -5,00 | -0,03 | -1,48 | -0,01 |
| INM-RO | 19,51 | 0,10 | -12,71 | -0,06 | 24,43 | 0,12 | -53,34 | -0,26 | 28,00 | 0,14 | 27,52 | 0,14 |
| ZMDM-SR | -32,29 | -0,16 | -87,51 | -0,43 | -46,47 | -0,23 | -65,34 | -0,32 | -3641,20 | -18,05 | -8221,48 | -40,74 |
| DZM-HR | 27,51 | 0,18 | 10,29 | 0,07 | 65,43 | 0,43 | 47,66 | 0,32 | 34,00 | 0,22 | 22,52 | 0,14 |
| NSCIM-UA | 26,51 | 0,69 | 18,29 | 0,47 | 21,43 | 0,55 | 24,66 | 0,64 | 66,00 | 1,70 | 89,52 | 2,30 |
| CMI-CZ | -0,49 | -0,02 | -2,71 | -0,10 | -3,57 | -0,14 | -3,34 | -0,13 | -7,00 | -0,27 | -8,48 | -0,32 |
| NPL-GB | 1,01 | 0,02 | -3,71 | -0,06 | -2,51 | -0,04 | -0,86 | -0,01 | -5,30 | -0,09 | -2,78 | -0,05 |

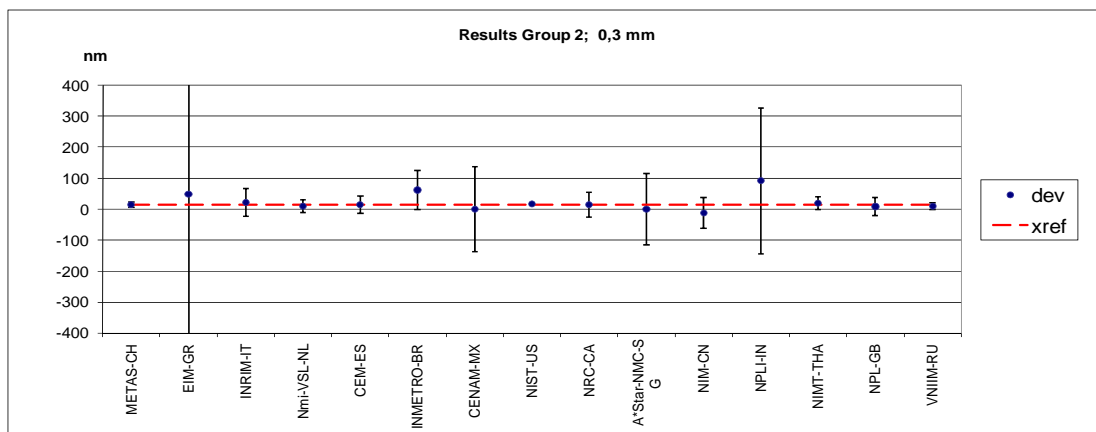
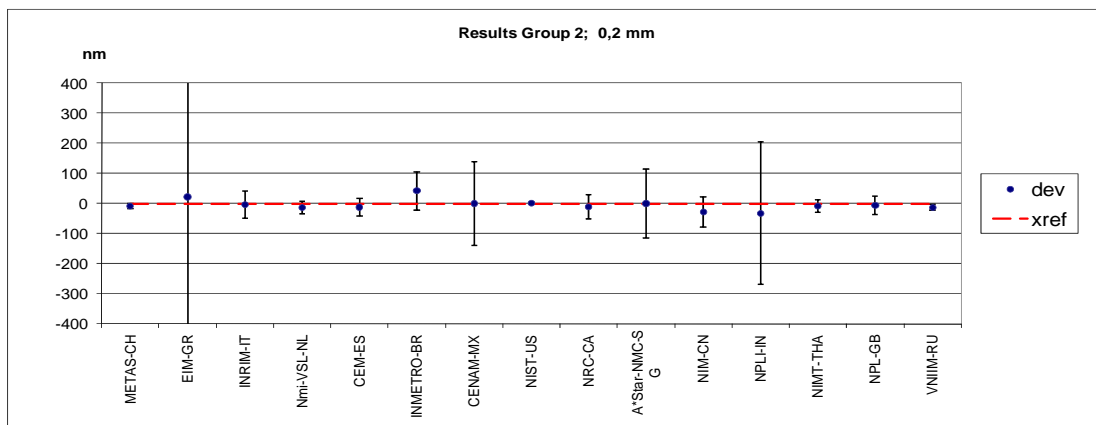
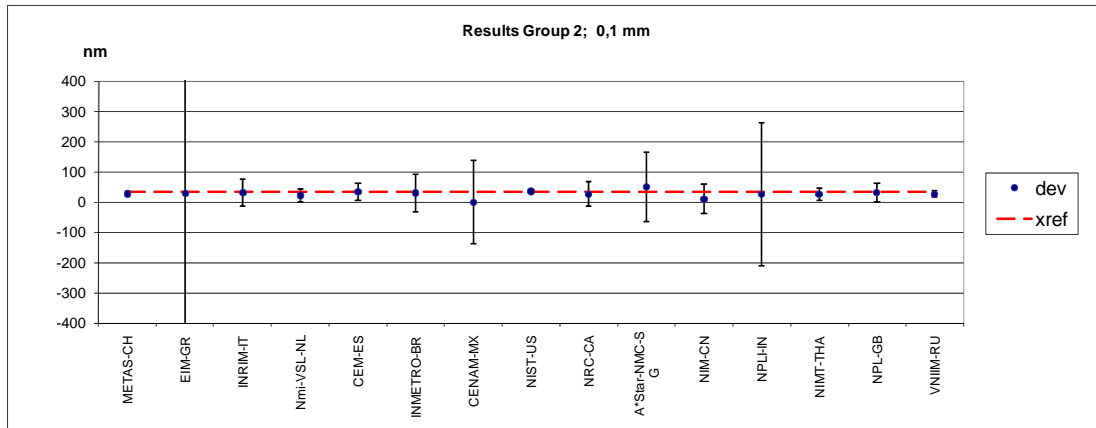
| Meas. Point | 15.0 mm | | 20.0 mm | | 25.0 mm | | 30.0 mm | | 35.0 mm | | 40.0 mm | |
|--------------------|------------------|---------------|------------------|---------------|------------------|---------------|------------------|----------------|------------------|----------------|------------------|----------------|
| X_{ref} | -7.0 nm | | -2.7 nm | | -147.4 nm | | -167.7 nm | | -159.2 nm | | -159.0 nm | |
| $u_c(X_{ref})$ | 5.2 nm | | 5.2 nm | | 5.3 nm | | 5.3 nm | | 5.4 nm | | 5.4 nm | |
| u_{ext} | 4.1 nm | | 2.1 nm | | 4.4 nm | | 4.9 nm | | 4.6 nm | | 5.0 nm | |
| No of participants | 15 | | 15 | | 15 | | 15 | | 15 | | 15 | |
| R_B | 0,78 | | 0,40 | | 0,83 | | 0,92 | | 0,85 | | 0,92 | |
| $R_{B,oit}$ | 1,33 | | 1,33 | | 1,33 | | 1,33 | | 1,33 | | 1,33 | |
| | $X_j - X_{ref}$ | E_n | $X_j - X_{ref}$ | E_n | $X_j - X_{ref}$ | E_n |
| MIRS-SI | 6,97 | 0,04 | 2,71 | 0,02 | 7,40 | 0,04 | -12,26 | -0,06 | -40,75 | -0,20 | -51,02 | -0,23 |
| METAS-CH | -10,03 | -0,83 | -0,29 | -0,02 | -6,60 | -0,54 | -3,26 | -0,26 | -4,75 | -0,38 | -3,02 | -0,24 |
| OMH-HU | -43,03 | -0,22 | -25,29 | -0,13 | -115,60 | -0,58 | 8,74 | 0,04 | 70,25 | 0,35 | -163,02 | -0,82 |
| BEV-AT | -57,03 | -0,26 | -45,29 | -0,20 | -32,60 | -0,15 | -79,26 | -0,36 | -95,75 | -0,43 | -113,02 | -0,51 |
| SMU-SK | -14,03 | -0,15 | -9,29 | -0,10 | 64,40 | 0,70 | 80,74 | 0,88 | 69,25 | 0,76 | 56,98 | 0,62 |
| PTB-DE | 24,57 | 1,03 | 8,41 | 0,35 | 13,30 | 0,56 | 9,24 | 0,39 | 9,55 | 0,40 | 9,88 | 0,42 |
| GUM-PL | 180,97 | 0,67 | 83,71 | 0,31 | 81,40 | 0,30 | 152,74 | 0,56 | 33,25 | 0,12 | 113,98 | 0,41 |
| MIKES-FI | 5,97 | 0,30 | -6,29 | -0,31 | 3,40 | 0,17 | -3,26 | -0,16 | -1,75 | -0,09 | -0,02 | 0,00 |
| LNMC-LV | 276,97 | 0,17 | 512,71 | 0,31 | 377,40 | 0,23 | 1137,74 | 0,69 | 9,25 | 0,01 | 478,98 | 0,29 |
| NML-IE | 486,97 | 0,33 | 402,71 | 0,27 | 907,40 | 0,61 | 507,74 | 0,34 | 839,25 | 0,57 | 1058,98 | 0,72 |
| NCM-BG | -14,03 | -0,09 | -10,29 | -0,07 | -6,60 | -0,04 | -8,26 | -0,05 | 9,25 | 0,06 | -20,02 | -0,13 |
| INM-RO | 16,97 | 0,08 | -7,29 | -0,04 | 107,40 | 0,53 | 147,74 | 0,73 | 139,25 | 0,69 | 148,98 | 0,73 |
| ZMDM-SR | -10830,13 | -53,66 | -14579,59 | -72,22 | -18569,50 | -91,95 | -22325,26 | -110,50 | -25705,35 | -127,16 | -29002,22 | -143,38 |
| DZM-HR | -0,03 | 0,00 | 16,71 | 0,10 | -90,60 | -0,52 | -108,26 | -0,60 | -139,75 | -0,76 | -8,02 | -0,04 |
| NSCIM-UA | 122,97 | 3,16 | 164,71 | 4,20 | 209,40 | 5,30 | 291,74 | 7,31 | 293,25 | 7,27 | 320,98 | 7,86 |
| CMI-CZ | -5,03 | -0,19 | -0,29 | -0,01 | -5,60 | -0,20 | -6,26 | -0,22 | -1,75 | -0,06 | -9,02 | -0,30 |
| NPL-GB | -4,97 | -0,08 | 8,38 | 0,14 | 0,18 | 0,00 | 4,52 | 0,08 | 3,58 | 0,06 | 3,99 | 0,07 |

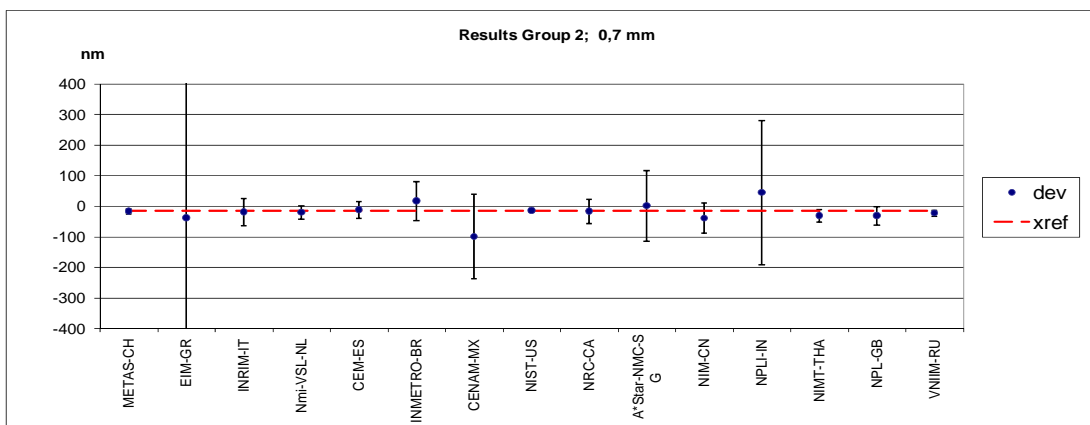
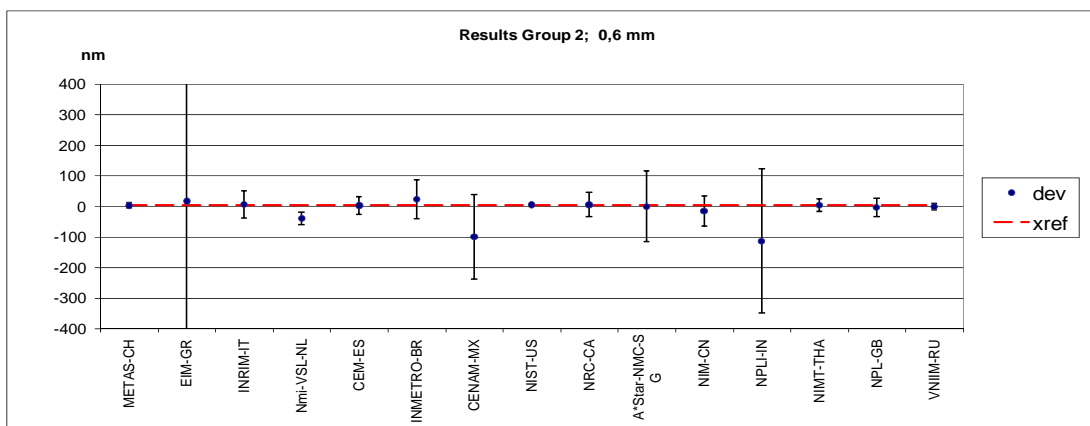
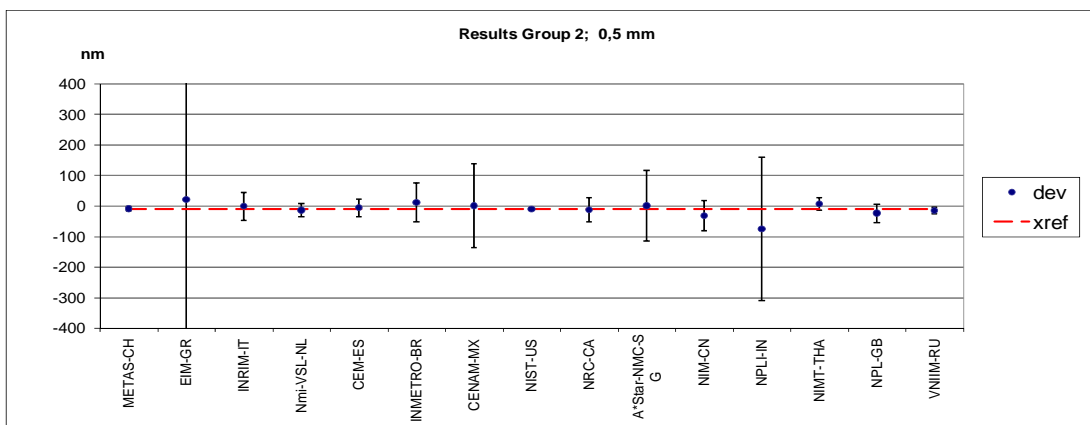
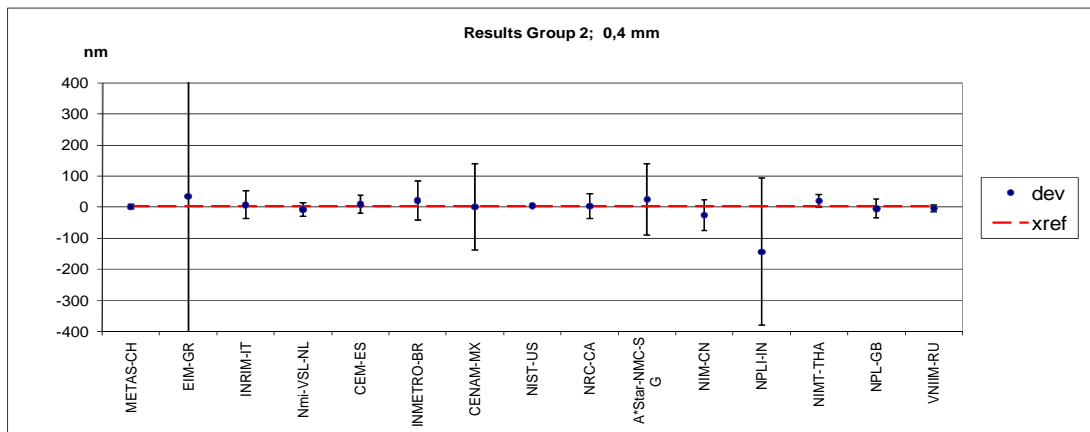
| Meas. Point | 45.0 mm | | 50.0 mm | | 55.0 mm | | 60.0 mm | | 65.0 mm | | 70.0 mm | |
|--------------------|------------------|----------------|------------------|----------------|------------------|----------------|------------------|----------------|------------------|----------------|------------------|----------------|
| X_{ref} | -214.2 nm | | -193.4 nm | | -211.5 nm | | -258.0 nm | | -214.8 nm | | -245.4 nm | |
| $u_c(X_{ref})$ | 5.5 nm | | 5.5 nm | | 5.6 nm | | 5.7 nm | | 5.8 nm | | 5.9 nm | |
| u_{ext} | 5.6 nm | | 5.3 nm | | 5.2 nm | | 6.9 nm | | 6.3 nm | | 7.1 nm | |
| No of participants | 15 | | 15 | | 14 | | 14 | | 14 | | 14 | |
| R_B | 1,01 | | 0,96 | | 0,91 | | 1,21 | | 1,10 | | 1,21 | |
| $R_{B,oit}$ | 1,33 | | 1,33 | | 1,34 | | 1,34 | | 1,34 | | 1,34 | |
| | $X_j - X_{ref}$ | E_n |
| MIRS-SI | -75,81 | -0,33 | -26,58 | -0,11 | -59,78 | -0,24 | -53,67 | -0,20 | -36,28 | -0,13 | -35,86 | -0,12 |
| METAS-CH | -1,81 | -0,14 | -2,58 | -0,20 | -3,78 | -0,28 | -3,67 | -0,27 | -6,28 | -0,45 | -1,86 | -0,13 |
| OMH-HU | -67,81 | -0,34 | -67,58 | -0,34 | -140,78 | -0,70 | -61,67 | -0,31 | -18,28 | -0,09 | -84,86 | -0,42 |
| BEV-AT | -136,81 | -0,62 | -96,58 | -0,44 | -131,78 | -0,59 | -161,67 | -0,73 | -163,28 | -0,74 | -199,86 | -0,90 |
| SMU-SK | 105,19 | 1,15 | 86,42 | 0,94 | 86,22 | 0,94 | 114,33 | 1,24 | 69,72 | 0,76 | 82,14 | 0,89 |
| PTB-DE | 13,29 | 0,56 | 12,82 | 0,54 | 8,72 | 0,37 | 12,13 | 0,52 | 13,32 | 0,57 | 7,74 | 0,33 |
| GUM-PL | -21,81 | -0,08 | -65,58 | -0,23 | -101,78 | -0,35 | -165,67 | -0,56 | -121,28 | -0,41 | -234,86 | -0,78 |
| MIKES-FI | -5,81 | -0,29 | -1,58 | -0,08 | 0,22 | 0,01 | -0,67 | -0,03 | 0,72 | 0,04 | -0,86 | -0,04 |
| LNMC-LV | 354,19 | 0,22 | 863,42 | 0,52 | 330,22 | 0,20 | 836,33 | 0,51 | -6,28 | 0,00 | 134,14 | 0,08 |
| NML-IE | 974,19 | 0,66 | 1113,42 | 0,75 | 1090,22 | 0,74 | 1856,33 | 1,26 | 2073,72 | 1,40 | 2024,14 | 1,37 |
| NCM-BG | -16,81 | -0,11 | -31,58 | -0,20 | -32,78 | -0,20 | -37,67 | -0,23 | -35,28 | -0,22 | -37,86 | -0,23 |
| INM-RO | 164,19 | 0,81 | 143,42 | 0,70 | 190,22 | 0,93 | 236,33 | 1,16 | 173,72 | 0,85 | 204,14 | 0,99 |
| ZMDM-SR | -32941,51 | -162,73 | -36955,78 | -182,42 | -40189,78 | -198,20 | -43648,77 | -215,05 | -48015,18 | -236,32 | -50708,46 | -249,29 |
| DZM-HR | 14,19 | 0,07 | 25,42 | 0,13 | -11,78 | -0,06 | -9,67 | -0,05 | 12,72 | 0,06 | -10,86 | -0,05 |
| NSCIM-UA | 145,19 | 3,51 | 414,42 | 9,86 | 424,22 | 9,93 | 465,33 | 10,71 | 449,72 | 10,17 | 474,14 | 10,52 |
| CMI-CZ | -14,81 | -0,48 | -19,58 | -0,61 | -7,78 | -0,23 | -19,67 | -0,57 | -10,28 | -0,29 | -14,86 | -0,40 |
| NPL-GB | 3,44 | 0,06 | 2,84 | 0,05 | -0,25 | 0,00 | -1,12 | -0,02 | -4,23 | -0,07 | 3,21 | 0,05 |

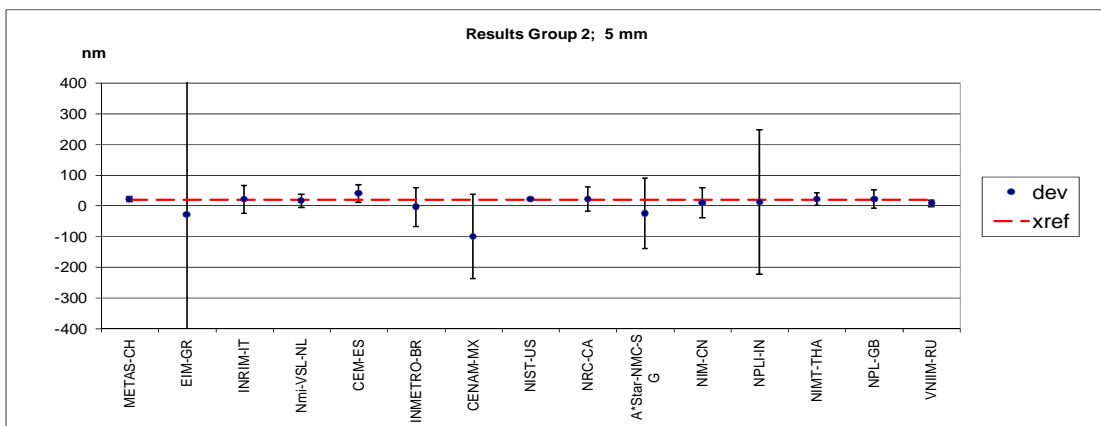
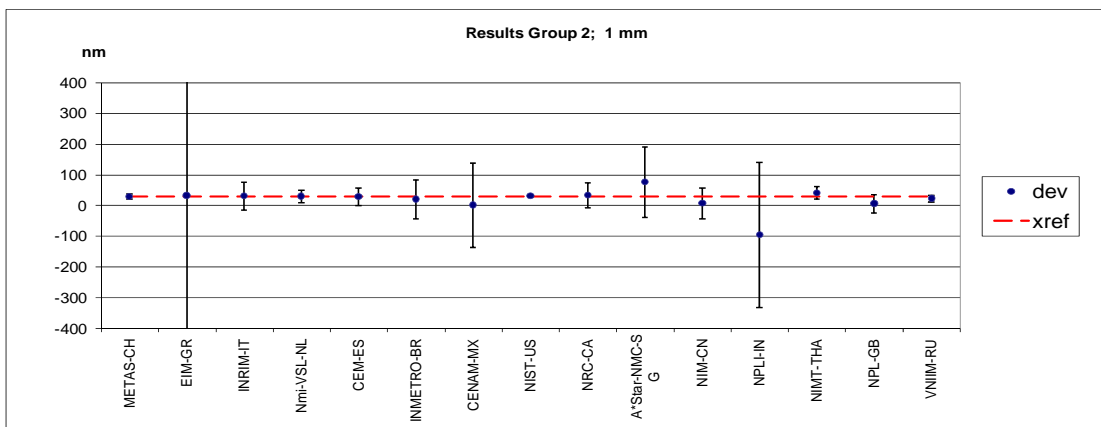
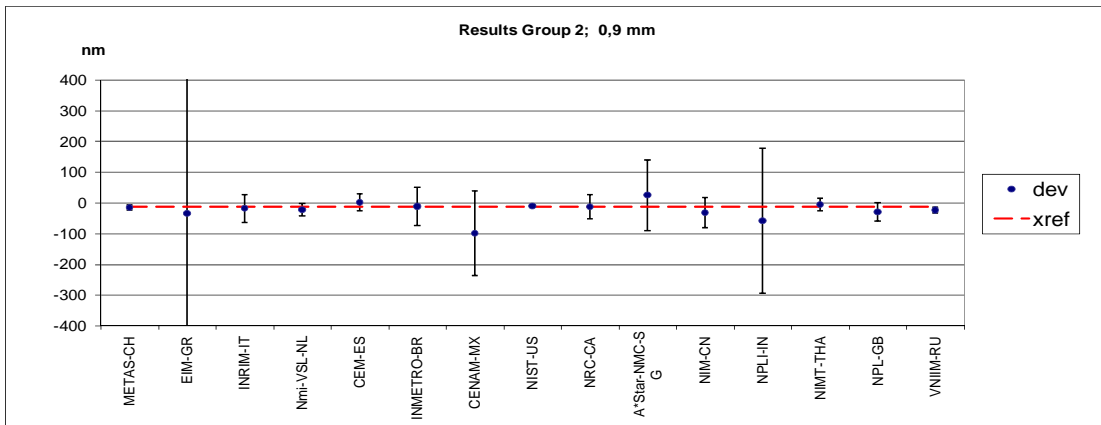
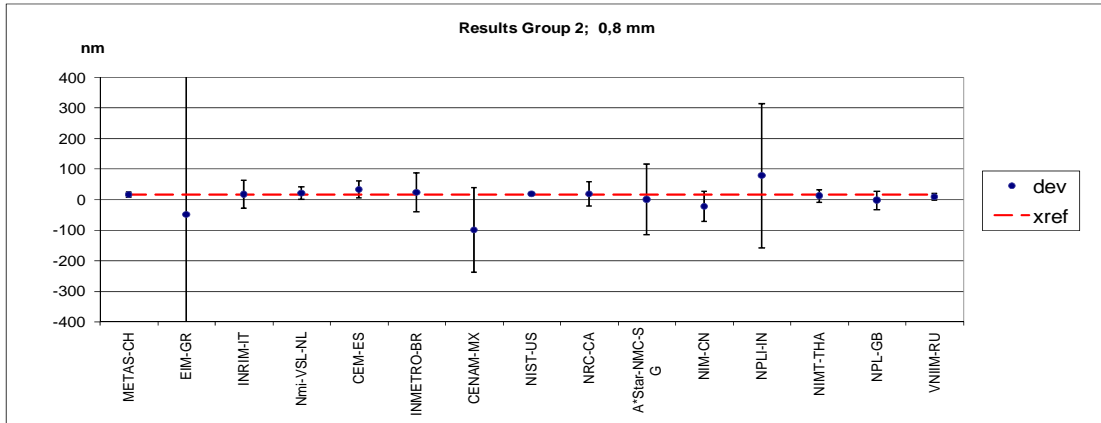
| Meas. Point | 75.0 mm | | 80.0 mm | | 85.0 mm | | 90.0 mm | | 95.0 mm | | 100.0 mm | |
|--------------------|------------------|----------------|------------------|----------------|------------------|----------------|------------------|----------------|------------------|----------------|------------------|----------------|
| X_{ref} | -282.3 nm | | -240.8 nm | | -269.4 nm | | -429.1 nm | | -362.0 nm | | -391.0 nm | |
| $u_c(X_{ref})$ | 5.9 nm | | 6.0 nm | | 8.0 nm | | 6.9 nm | | 7.0 nm | | 6.3 nm | |
| u_{ext} | 7.3 nm | | 7.4 nm | | 10.4 nm | | 8.7 nm | | 9.0 nm | | 7.4 nm | |
| No of participants | 13 | | 13 | | 11 | | 12 | | 13 | | 12 | |
| R_B | 1,23 | | 1,24 | | 1,30 | | 1,27 | | 1,28 | | 1,17 | |
| $R_{B,oit}$ | 1,35 | | 1,35 | | 1,38 | | 1,36 | | 1,35 | | 1,36 | |
| | $X_j - X_{ref}$ | E_n |
| MIRS-SI | -9,20 | -0,03 | -39,87 | -0,13 | -52,70 | -0,16 | -80,93 | -0,24 | -58,03 | -0,17 | -49,01 | -0,14 |
| METAS-CH | 0,80 | 0,05 | -1,87 | -0,12 | 4,30 | 0,36 | -4,93 | -0,34 | -3,03 | -0,20 | 3,99 | 0,24 |
| OMH-HU | -278,20 | -1,39 | -215,87 | -1,08 | -263,70 | -1,32 | -209,93 | -1,05 | -104,03 | -0,52 | -95,01 | -0,47 |
| BEV-AT | -184,20 | -0,83 | -234,87 | -1,06 | -248,70 | -1,12 | -227,93 | -1,03 | -253,03 | -1,14 | -318,01 | -1,43 |
| SMU-SK | 89,80 | 0,97 | 39,13 | 0,42 | 70,30 | 0,76 | 207,07 | 2,24 | 150,97 | 1,63 | 140,99 | 1,52 |
| PTB-DE | 7,20 | 0,31 | 9,03 | 0,39 | 36,60 | 1,77 | 18,77 | 0,85 | 9,17 | 0,42 | 3,09 | 0,14 |
| GUM-PL | -170,20 | -0,55 | -292,87 | -0,94 | -294,70 | -0,93 | -175,93 | -0,55 | -189,03 | -0,58 | -197,01 | -0,59 |
| MIKES-FI | -3,20 | -0,16 | 5,13 | 0,25 | -24,70 | -0,52 | 30,07 | 0,63 | 19,97 | 0,42 | 2,99 | 0,14 |
| LNMC-LV | 530,80 | 0,32 | 10,13 | 0,01 | -682,70 | -0,41 | -990,93 | -0,60 | -848,03 | -0,52 | -1329,01 | -0,81 |
| NML-IE | 2780,80 | 1,88 | 2260,13 | 1,53 | 2327,30 | 1,57 | 2769,07 | 1,87 | 3201,97 | 2,16 | 3230,99 | 2,18 |
| NCM-BG | -43,20 | -0,26 | -48,87 | -0,30 | -45,70 | -0,28 | -55,93 | -0,33 | -61,03 | -0,36 | -52,01 | -0,31 |
| INM-RO | 230,80 | 1,12 | 200,13 | 0,97 | 247,30 | 1,20 | 399,07 | 1,92 | 301,97 | 1,45 | 360,99 | 1,73 |
| ZMDM-SR | -55087,90 | -270,49 | -58629,17 | -287,50 | -61980,70 | -303,89 | -65609,83 | -320,97 | -68649,43 | -335,32 | -72887,61 | -355,28 |
| DZM-HR | -29,20 | -0,13 | -21,87 | -0,10 | -42,70 | -0,18 | 38,07 | 0,16 | 40,97 | 0,17 | 78,99 | 0,32 |
| NSCIM-UA | 467,80 | 10,18 | 475,13 | 10,13 | 493,30 | 10,55 | 503,07 | 10,39 | 543,97 | 10,99 | 525,99 | 10,32 |
| CMI-CZ | -14,20 | -0,37 | -18,87 | -0,47 | -12,70 | -0,32 | -29,93 | -0,71 | -20,03 | -0,46 | -21,01 | -0,46 |
| NPL-GB | 1,47 | 0,03 | 0,12 | 0,00 | 10,72 | 0,19 | 5,33 | 0,09 | -0,47 | -0,01 | 9,37 | 0,16 |

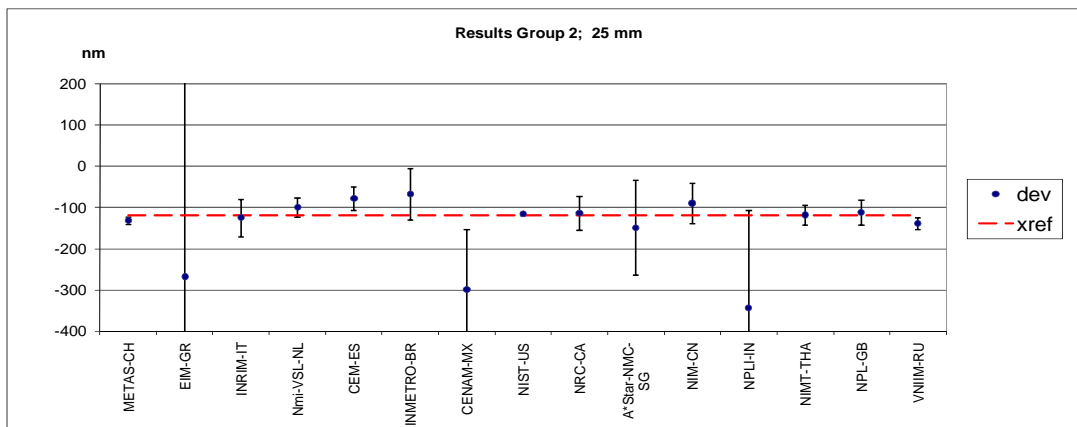
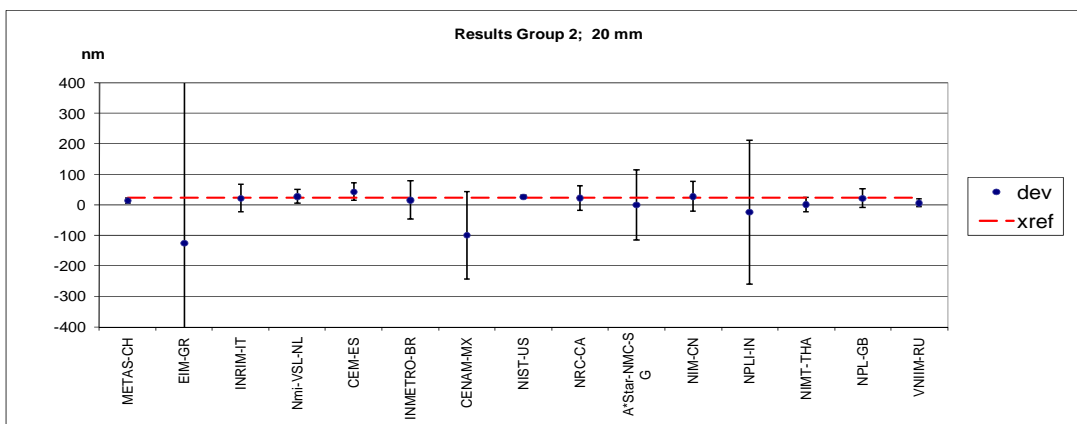
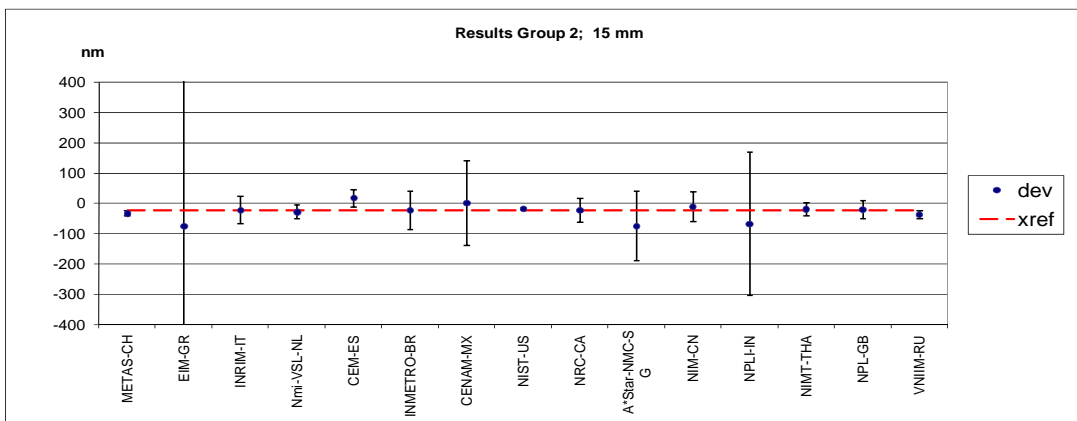
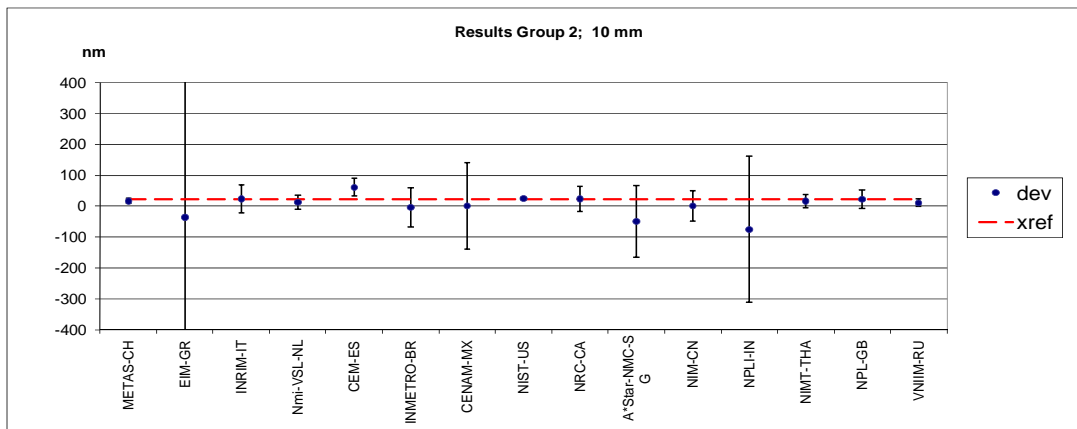
1.3 Group 2 – deviations from reference value

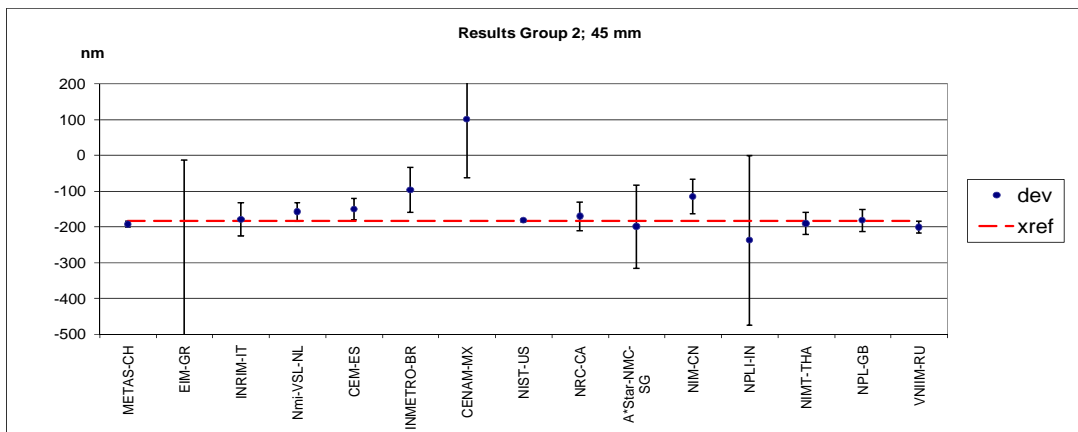
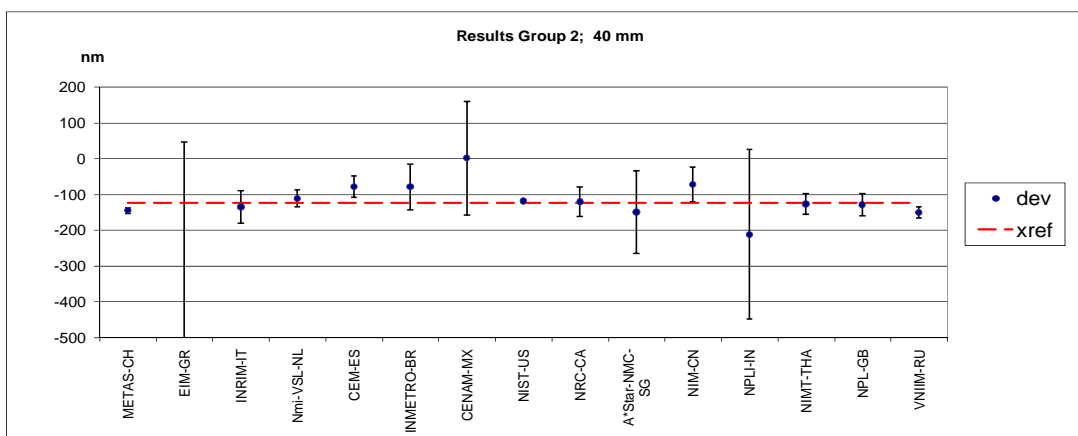
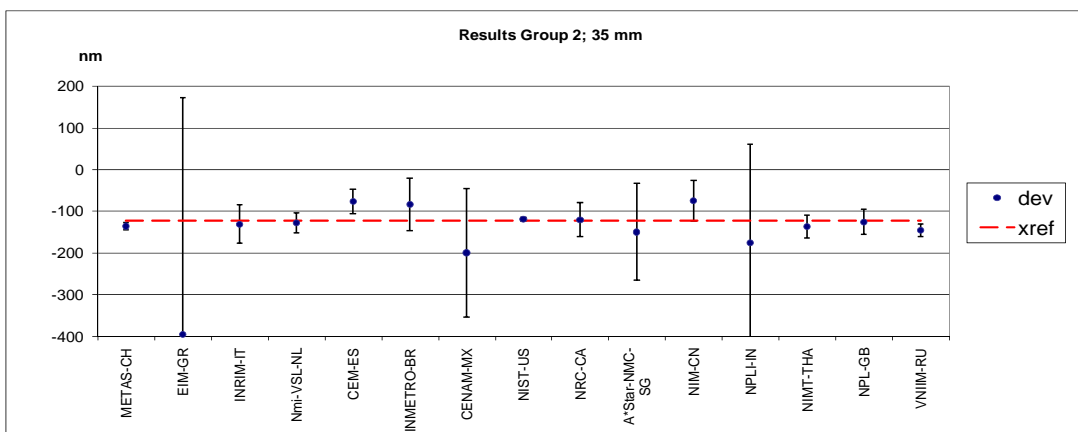
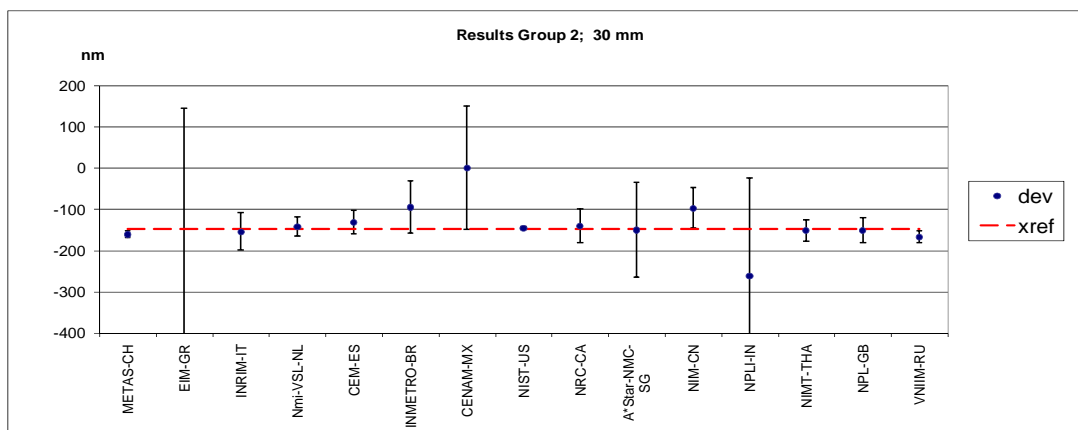
Graphical presentation of measurement results follows in 30 diagrams. Uncertainty bars in the diagrams for single measuring points represent standard uncertainty u ($k = 1$).

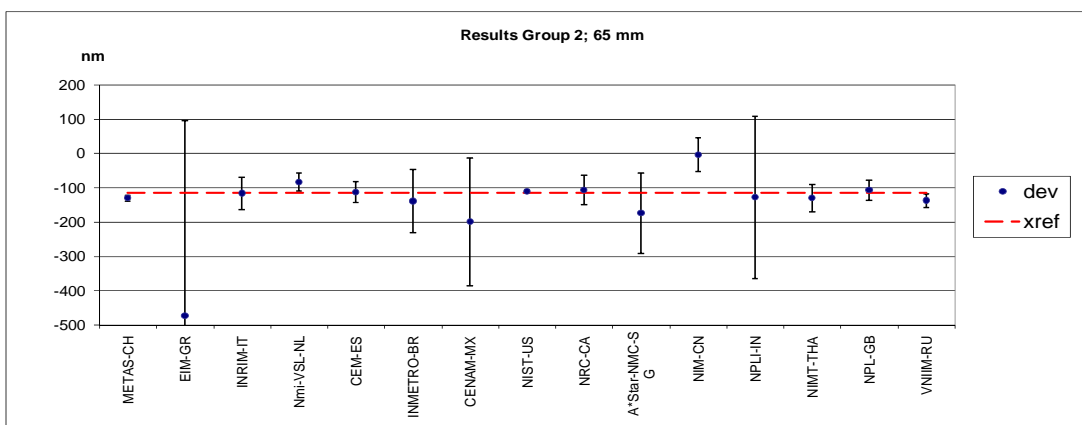
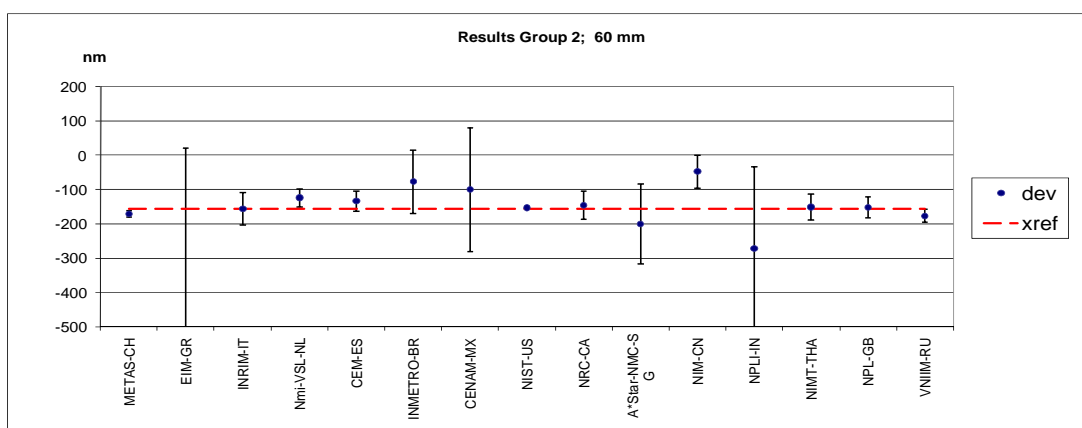
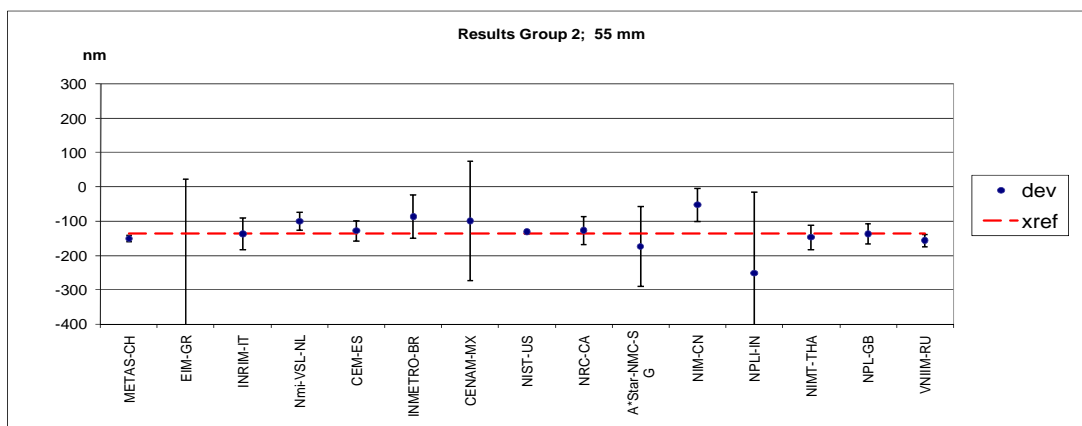
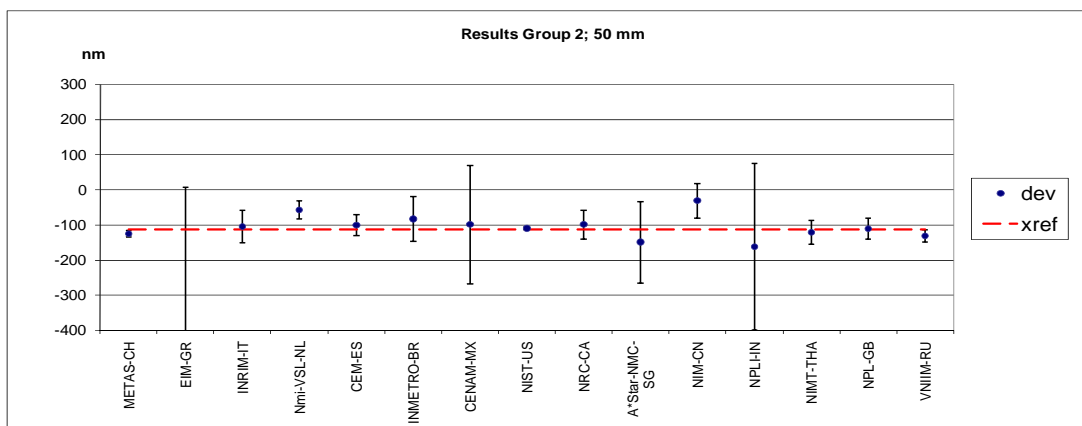


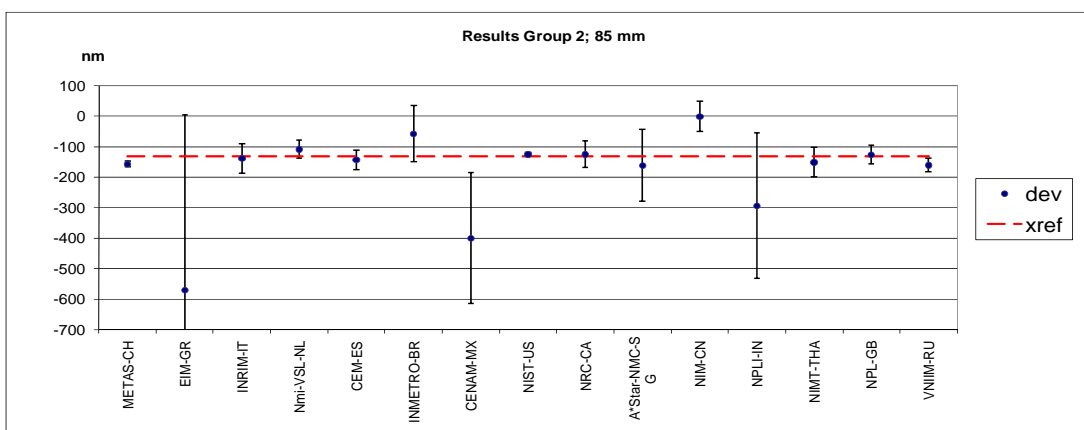
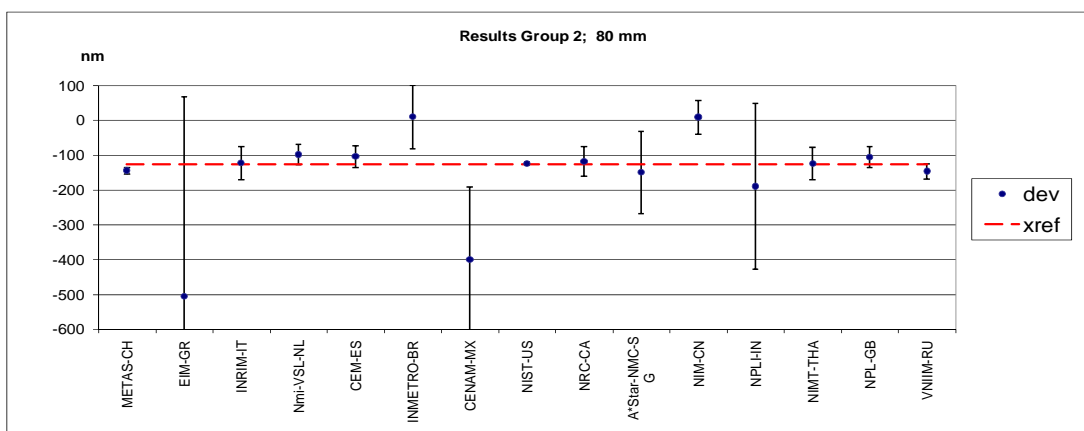
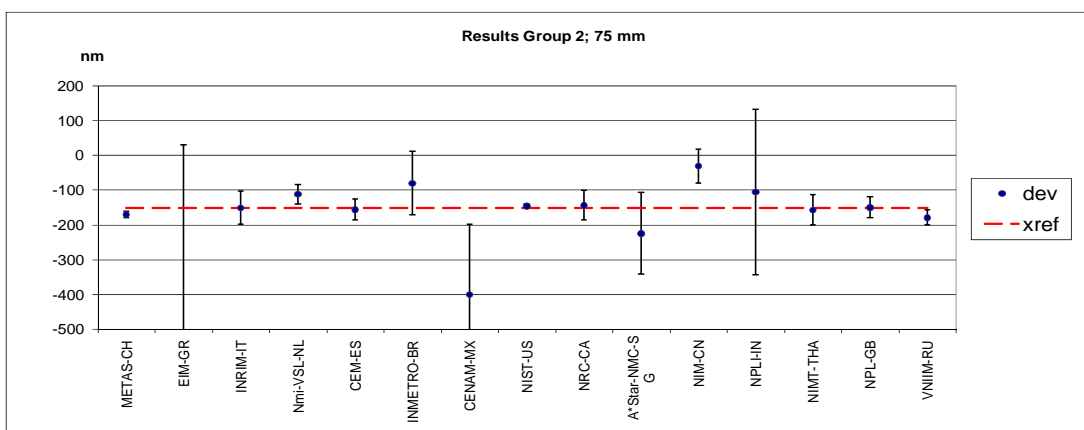
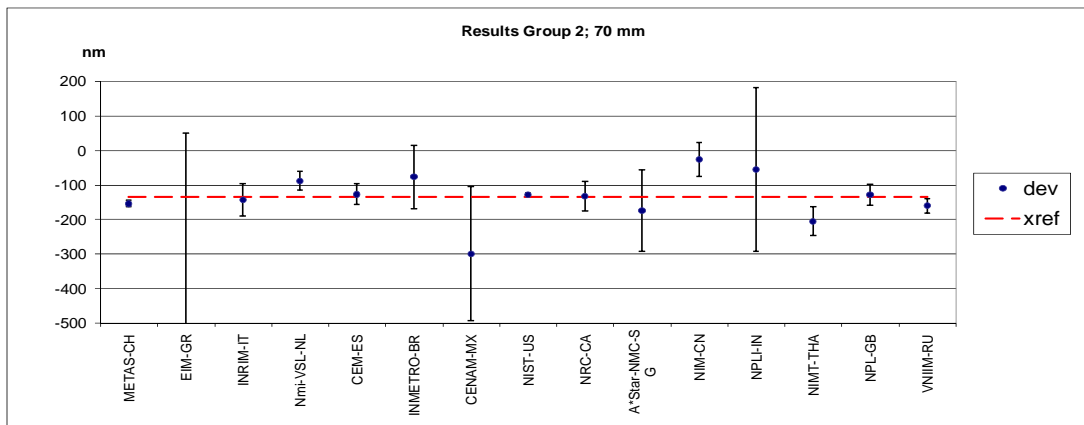


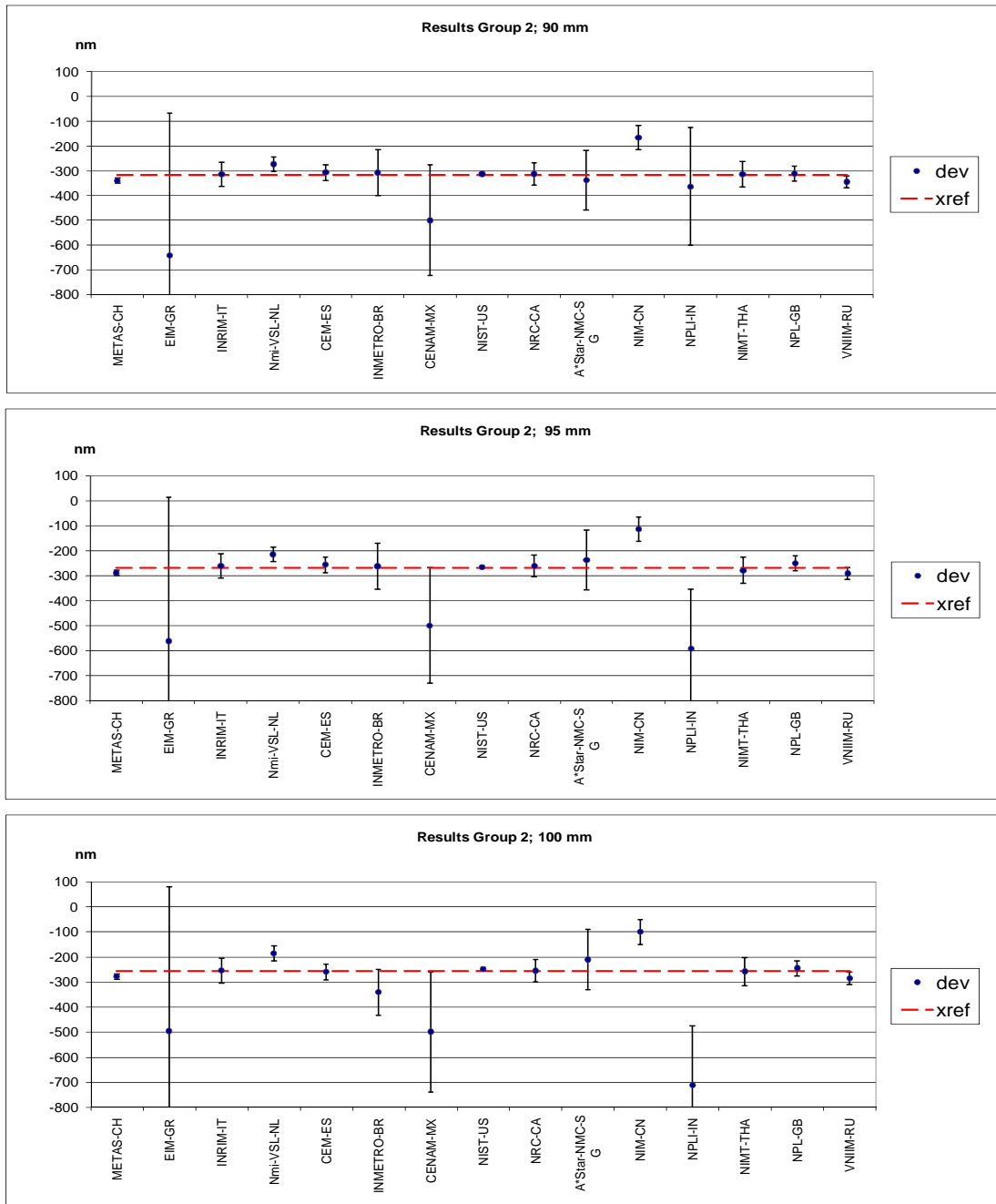












1.4 Group 2 - Calculated values

The results given in Table 1.4 were calculated from the largest consistent subset. This subset was created by eliminating laboratories with the greatest E_n values until the Birge criterion (Ch. 7) was met. E_n values $|E_n| > 1$ are marked with yellow colour. Eliminated laboratories for single measurement points are shown in Table 1.3.

Table 1.3: Laboratories that were excluded from calculation of the reference values

| Measuring point (mm) | No. of excluded laboratories | Excluded laboratories |
|----------------------|------------------------------|-----------------------|
| 100 | 1 | NIM-CN |

Table 1.4: Results calculated from the given values – Group 2

| Meas. Point | 0,1 mm | | 0,2 mm | | 0,3 mm | | 0,4 mm | | 0,5 mm | | 0,6 mm | |
|--------------------|---------------|-------|---------------|-------|---------------|-------|---------------|-------|---------------|-------|---------------|-------|
| x_{ref} | 33,8 nm | | -1,5 nm | | 15,7 nm | | 3,3 nm | | -11,3 nm | | 3,4 nm | |
| $u_c(x_{ref})$ | 2,7 nm | |
| u_{exit} | 1,1 nm | | 1,5 nm | | 0,9 nm | | 1,2 nm | | 0,9 nm | | 1,7 nm | |
| No of participants | 15 | | 15 | | 15 | | 15 | | 15 | | 15 | |
| R_B | 0,41 | | 0,55 | | 0,34 | | 0,45 | | 0,34 | | 0,64 | |
| $R_{B,crit}$ | 1,33 | | 1,33 | | 1,33 | | 1,33 | | 1,33 | | 1,33 | |
| | x_i-x_{ref} | E_n |
| METAS-CH | -5,8 | -0,39 | -6,5 | -0,43 | -1,7 | -0,12 | -2,3 | -0,16 | 1,3 | 0,08 | -0,4 | -0,02 |
| EIM-GR | -4,8 | 0,00 | 23,5 | 0,02 | 32,3 | 0,03 | 30,7 | 0,03 | 31,3 | 0,03 | 13,6 | 0,01 |
| INRIM-IT | -2,8 | -0,03 | -2,5 | -0,03 | 5,3 | 0,06 | 3,7 | 0,04 | 9,3 | 0,10 | 2,6 | 0,03 |
| Nmi-VSL-NL | -11,8 | -0,28 | -11,5 | -0,27 | -5,7 | -0,14 | -11,3 | -0,27 | -3,7 | -0,09 | -43,4 | -1,04 |
| CEM-ES | 1,2 | 0,02 | -10,5 | -0,18 | -0,7 | -0,01 | 5,7 | 0,10 | 4,3 | 0,08 | -0,4 | -0,01 |
| INMETRO-BR | -3,8 | -0,03 | 43,5 | 0,35 | 46,3 | 0,37 | 17,7 | 0,14 | 22,3 | 0,18 | 19,6 | 0,16 |
| CENAM-MX | -33,8 | -0,12 | 1,5 | 0,01 | -15,7 | -0,06 | -3,3 | -0,01 | 11,3 | 0,04 | -103,4 | -0,38 |
| NIST-US | 2,2 | 0,70 | 2,7 | 0,88 | 1,0 | 0,31 | 1,1 | 0,35 | 0,1 | 0,02 | 1,5 | 0,50 |
| NRC-CA | -7,0 | -0,09 | -9,7 | -0,12 | -2,1 | -0,03 | -1,0 | -0,01 | -2,5 | -0,03 | 1,9 | 0,02 |
| A*Star-NMC-SG | 16,2 | 0,07 | 1,5 | 0,01 | -15,7 | -0,07 | 21,7 | 0,09 | 11,3 | 0,05 | -3,4 | -0,01 |
| NIM-CN | -22,8 | -0,23 | -26,5 | -0,27 | -27,7 | -0,28 | -29,3 | -0,30 | -21,7 | -0,22 | -19,4 | -0,20 |
| NPLI-IN | -7,8 | -0,02 | -30,5 | -0,06 | 76,3 | 0,16 | -147,3 | -0,31 | -64,7 | -0,14 | -117,4 | -0,25 |
| NIMT-THA | -8,1 | -0,20 | -7,2 | -0,18 | 2,9 | 0,07 | 17,1 | 0,42 | 16,3 | 0,40 | 0,6 | 0,02 |
| NPL-GB | -2,9 | -0,05 | -4,3 | -0,07 | -7,2 | -0,12 | -8,4 | -0,14 | -13,3 | -0,22 | -6,6 | -0,11 |
| VNIIM-RU | -6,8 | -0,35 | -11,5 | -0,59 | -5,7 | -0,30 | -8,3 | -0,43 | -4,7 | -0,24 | -4,4 | -0,22 |

| Meas. Point | 0,7 mm | | 0,8 mm | | 0,9 mm | | 1 mm | | 5 mm | | 10 mm | |
|--------------------|---------------|-------|---------------|-------|---------------|-------|---------------|-------|---------------|-------|---------------|-------|
| x_{ref} | -16,7 nm | | 16,8 nm | | -13,0 nm | | 29,3 nm | | 19,7 nm | | 22,1 nm | |
| $u_c(x_{ref})$ | 2,7 nm | | 2,7 nm | | 2,7 nm | | 2,7 nm | | 3,1 nm | | 3,1 nm | |
| u_{exit} | 1,2 nm | | 1,3 nm | | 1,3 nm | | 1,1 nm | | 1,4 nm | | 1,9 nm | |
| No of participants | 15 | | 15 | | 15 | | 15 | | 15 | | 15 | |
| R_B | 0,44 | | 0,49 | | 0,48 | | 0,41 | | 0,46 | | 0,61 | |
| $R_{B,crit}$ | 1,33 | | 1,33 | | 1,33 | | 1,33 | | 1,33 | | 1,33 | |
| | x_i-x_{ref} | E_n |
| METAS-CH | -1,3 | -0,09 | -1,8 | -0,12 | -3,0 | -0,20 | -1,3 | -0,09 | 1,3 | 0,09 | -6,1 | -0,42 |
| EIM-GR | -22,3 | -0,02 | -66,8 | -0,06 | -22,0 | -0,02 | 1,7 | 0,00 | -48,7 | -0,04 | -59,1 | -0,05 |
| INRIM-IT | -3,3 | -0,04 | 0,2 | 0,00 | -6,0 | -0,07 | 0,7 | 0,01 | 1,3 | 0,01 | 0,9 | 0,01 |
| Nmi-VSL-NL | -5,3 | -0,13 | 3,2 | 0,08 | -10,0 | -0,24 | -0,3 | -0,01 | -3,7 | -0,09 | -10,1 | -0,23 |
| CEM-ES | 3,7 | 0,06 | 16,2 | 0,29 | 14,0 | 0,25 | -2,3 | -0,04 | 20,3 | 0,36 | 37,9 | 0,67 |
| INMETRO-BR | 32,7 | 0,26 | 6,2 | 0,05 | 1,0 | 0,01 | -10,3 | -0,08 | -23,7 | -0,19 | -26,1 | -0,21 |
| CENAM-MX | -83,3 | -0,30 | -116,8 | -0,42 | -87,0 | -0,32 | -29,3 | -0,11 | -119,7 | -0,43 | -22,1 | -0,08 |
| NIST-US | 1,6 | 0,50 | 1,4 | 0,44 | 1,7 | 0,55 | 1,0 | 0,33 | 1,0 | 0,25 | 2,8 | 0,67 |
| NRC-CA | -0,9 | -0,01 | 0,6 | 0,01 | -0,6 | -0,01 | 2,5 | 0,03 | 1,8 | 0,02 | 0,8 | 0,01 |
| A*Star-NMC-SG | 16,7 | 0,07 | -16,8 | -0,07 | 38,0 | 0,17 | 45,7 | 0,20 | -44,7 | -0,19 | -72,1 | -0,31 |
| NIM-CN | -23,3 | -0,24 | -39,8 | -0,41 | -19,0 | -0,19 | -23,3 | -0,24 | -10,7 | -0,11 | -21,1 | -0,22 |
| NPLI-IN | 59,7 | 0,13 | 61,2 | 0,13 | -46,0 | -0,10 | -125,3 | -0,27 | -7,7 | -0,02 | -98,1 | -0,21 |
| NIMT-THA | -15,6 | -0,38 | -5,0 | -0,12 | 6,3 | 0,16 | 10,7 | 0,26 | 1,1 | 0,03 | -6,0 | -0,14 |
| NPL-GB | -15,6 | -0,26 | -19,7 | -0,33 | -17,7 | -0,30 | -24,1 | -0,40 | 2,3 | 0,04 | -0,9 | -0,02 |
| VNIIM-RU | -7,3 | -0,38 | -8,8 | -0,45 | -11,0 | -0,56 | -7,3 | -0,37 | -11,7 | -0,57 | -12,1 | -0,55 |

| Meas. Point | 15 mm | | 20 mm | | 25 mm | | 30 mm | | 35 mm | | 40 mm | |
|--------------------|-----------------|-------|-----------------|-------|-----------------|-------|-----------------|-------|-----------------|-------|-----------------|-------|
| x_{ref} | -22,8 nm | | 23,5 nm | | -119,8 nm | | -148,9 nm | | -123,3 nm | | -124,6 nm | |
| $u_c(x_{ref})$ | 3,1 nm | | 3,2 nm | | 3,3 nm | | 3,3 nm | | 3,4 nm | | 3,5 nm | |
| u_{ext} | 2,2 nm | | 2,1 nm | | 3,0 nm | | 2,6 nm | | 2,9 nm | | 3,7 nm | |
| No of participants | 15 | | 15 | | 15 | | 15 | | 15 | | 15 | |
| R_B | 0,69 | | 0,67 | | 0,92 | | 0,77 | | 0,86 | | 1,07 | |
| $R_{B,crit}$ | 1,33 | | 1,33 | | 1,33 | | 1,33 | | 1,33 | | 1,33 | |
| | $x_i - x_{ref}$ | E_n |
| METAS-CH | -11,2 | -0,77 | -8,5 | -0,58 | -13,2 | -0,89 | -12,1 | -0,81 | -12,7 | -0,85 | -20,4 | -1,34 |
| EIM-GR | -52,2 | -0,05 | -149,5 | -0,13 | -149,2 | -0,13 | -273,1 | -0,24 | -272,7 | -0,24 | -397,4 | -0,35 |
| INRIM-IT | -0,2 | 0,00 | -1,5 | -0,02 | -6,2 | -0,07 | -5,1 | -0,06 | -7,7 | -0,08 | -11,4 | -0,13 |
| Nmi-VSL-NL | -6,2 | -0,14 | 4,5 | 0,10 | 18,8 | 0,41 | 6,9 | 0,15 | -4,7 | -0,10 | 12,6 | 0,26 |
| CEM-ES | 38,8 | 0,68 | 19,5 | 0,34 | 40,8 | 0,72 | 17,9 | 0,31 | 46,3 | 0,81 | 45,6 | 0,79 |
| INMETRO-BR | -0,2 | 0,00 | -7,5 | -0,06 | 50,8 | 0,40 | 53,9 | 0,43 | 39,3 | 0,31 | 44,6 | 0,35 |
| CENAM-MX | 22,8 | 0,08 | -123,5 | -0,43 | -180,2 | -0,62 | 148,9 | 0,50 | -76,7 | -0,25 | 124,6 | 0,39 |
| NIST-US | 3,4 | 0,80 | 3,8 | 0,90 | 3,2 | 0,74 | 3,1 | 0,71 | 4,0 | 0,88 | 5,3 | 1,13 |
| NRC-CA | -1,5 | -0,02 | -0,4 | -0,01 | 4,7 | 0,06 | 9,1 | 0,11 | 2,5 | 0,03 | 3,5 | 0,04 |
| A*Star-NMC-SG | -52,2 | -0,23 | -23,5 | -0,10 | -30,2 | -0,13 | -1,1 | 0,00 | -26,7 | -0,12 | -25,4 | -0,11 |
| NIM-CN | 10,8 | 0,11 | 4,5 | 0,05 | 28,8 | 0,29 | 51,9 | 0,53 | 48,3 | 0,49 | 51,6 | 0,53 |
| NPLI-IN | -45,2 | -0,10 | -46,5 | -0,10 | -224,2 | -0,47 | -112,1 | -0,24 | -52,7 | -0,11 | -87,4 | -0,18 |
| NIMT-THA | 3,1 | 0,07 | -22,3 | -0,49 | 0,2 | 0,00 | -2,3 | -0,05 | -13,8 | -0,25 | -3,3 | -0,06 |
| NPL-GB | 2,1 | 0,03 | -0,9 | -0,01 | 6,4 | 0,11 | -1,7 | -0,03 | -2,9 | -0,05 | -4,9 | -0,08 |
| VNIIM-RU | -15,2 | -0,64 | -17,5 | -0,70 | -20,2 | -0,76 | -18,1 | -0,64 | -22,7 | -0,76 | -26,4 | -0,85 |

| Meas. Point | 45 mm | | 50 mm | | 55 mm | | 60 mm | | 65 mm | | 70 mm | |
|--------------------|-----------------|-------|-----------------|-------|-----------------|-------|-----------------|-------|-----------------|-------|-----------------|-------|
| x_{ref} | -184,2 nm | | -112,9 nm | | -135,4 nm | | -155,8 nm | | -115,2 nm | | -134,8 nm | |
| $u_c(x_{ref})$ | 3,6 nm | | 3,7 nm | | 3,8 nm | | 3,9 nm | | 4,0 nm | | 4,1 nm | |
| u_{ext} | 3,4 nm | | 3,5 nm | | 3,4 nm | | 3,8 nm | | 3,8 nm | | 5,0 nm | |
| No of participants | 15 | | 15 | | 15 | | 15 | | 15 | | 15 | |
| R_B | 0,94 | | 0,94 | | 0,91 | | 0,97 | | 0,95 | | 1,20 | |
| $R_{B,crit}$ | 1,33 | | 1,33 | | 1,33 | | 1,33 | | 1,33 | | 1,33 | |
| | $x_i - x_{ref}$ | E_n |
| METAS-CH | -9,8 | -0,64 | -13,1 | -0,84 | -15,6 | -0,99 | -15,2 | -0,95 | -15,8 | -0,97 | -20,2 | -1,22 |
| EIM-GR | -397,8 | -0,35 | -448,1 | -0,39 | -411,6 | -0,36 | -391,2 | -0,34 | -358,8 | -0,31 | -385,2 | -0,34 |
| INRIM-IT | 4,2 | 0,05 | 6,9 | 0,08 | -2,6 | -0,03 | -0,2 | 0,00 | -1,8 | -0,02 | -8,2 | -0,09 |
| Nmi-VSL-NL | 25,2 | 0,51 | 53,9 | 1,07 | 34,4 | 0,67 | 31,8 | 0,61 | 31,2 | 0,59 | 45,8 | 0,85 |
| CEM-ES | 33,2 | 0,57 | 11,9 | 0,20 | 7,4 | 0,13 | 21,8 | 0,37 | 2,2 | 0,04 | 6,8 | 0,11 |
| INMETRO-BR | 86,2 | 0,69 | 28,9 | 0,23 | 48,4 | 0,39 | 78,8 | 0,43 | -24,8 | -0,13 | 57,8 | 0,31 |
| CENAM-MX | 284,2 | 0,87 | 12,9 | 0,04 | 35,4 | 0,10 | 55,8 | 0,15 | -84,8 | -0,23 | -165,2 | -0,43 |
| NIST-US | 1,1 | 0,23 | 2,1 | 0,42 | 3,7 | 0,71 | 2,7 | 0,49 | 4,0 | 0,71 | 5,8 | 0,97 |
| NRC-CA | 12,7 | 0,16 | 13,2 | 0,16 | 8,0 | 0,10 | 10,2 | 0,12 | 8,3 | 0,10 | 1,8 | 0,02 |
| A*Star-NMC-SG | -15,8 | -0,07 | -37,1 | -0,16 | -39,6 | -0,17 | -44,2 | -0,19 | -59,8 | -0,26 | -40,2 | -0,17 |
| NIM-CN | 68,2 | 0,70 | 80,9 | 0,83 | 82,4 | 0,84 | 107,8 | 1,10 | 110,2 | 1,13 | 107,8 | 1,10 |
| NPLI-IN | -53,8 | -0,11 | -50,1 | -0,11 | -116,6 | -0,25 | -115,2 | -0,24 | -13,8 | -0,03 | 78,8 | 0,17 |
| NIMT-THA | -7,7 | -0,13 | -8,9 | -0,14 | -12,3 | -0,18 | 4,9 | 0,07 | -15,9 | -0,20 | -71,2 | -0,86 |
| NPL-GB | 1,2 | 0,02 | 0,6 | 0,01 | -2,1 | -0,03 | 3,3 | 0,06 | 7,4 | 0,12 | 6,3 | 0,11 |
| VNIIM-RU | -17,8 | -0,54 | -20,1 | -0,59 | -21,6 | -0,60 | -21,2 | -0,57 | -22,8 | -0,59 | -26,2 | -0,65 |

| Meas. Point | 75 mm | | 80 mm | | 85 mm | | 90 mm | | 95 mm | | 100 mm | |
|--------------------|-----------------|-------|-----------------|-------|-----------------|-------|-----------------|-------|-----------------|-------|-----------------|-------|
| x_{ref} | -151,2 nm | | -127,5 nm | | -133,1 nm | | -317,9 nm | | -269,1 nm | | -256,7 nm | |
| $u_c(x_{ref})$ | 4,3 nm | | 4,4 nm | | 4,5 nm | | 4,6 nm | | 4,8 nm | | 4,9 nm | |
| u_{ext} | 4,8 nm | | 5,0 nm | | 5,6 nm | | 5,5 nm | | 5,9 nm | | 5,9 nm | |
| No of participants | 15 | | 15 | | 15 | | 15 | | 15 | | 14 | |
| R_B | 1,12 | | 1,15 | | 1,23 | | 1,19 | | 1,25 | | 1,20 | |
| $R_{B,crit}$ | 1,33 | | 1,33 | | 1,33 | | 1,33 | | 1,33 | | 1,34 | |
| | $x_i - x_{ref}$ | E_n |
| METAS-CH | -18,8 | -1,12 | -17,5 | -1,02 | -24,9 | -1,43 | -22,1 | -1,24 | -19,9 | -1,10 | -22,3 | -1,20 |
| EIM-GR | -389,8 | -0,34 | -377,5 | -0,33 | -436,9 | -0,38 | -323,1 | -0,28 | -292,9 | -0,26 | -240,3 | -0,21 |
| INRIM-IT | 0,2 | 0,00 | 4,5 | 0,05 | -5,9 | -0,06 | 2,9 | 0,03 | 7,1 | 0,07 | 1,7 | 0,02 |
| Nmi-VSL-NL | 39,2 | 0,71 | 28,5 | 0,51 | 24,1 | 0,43 | 44,9 | 0,78 | 53,1 | 0,91 | 69,7 | 1,18 |
| CEM-ES | -4,8 | -0,08 | 22,5 | 0,37 | -10,9 | -0,18 | 10,9 | 0,18 | 12,1 | 0,19 | -4,3 | -0,07 |
| INMETRO-BR | 71,2 | 0,39 | 136,5 | 0,74 | 74,1 | 0,40 | 9,9 | 0,05 | 6,1 | 0,03 | -85,3 | -0,46 |
| CENAM-MX | -248,8 | -0,62 | -272,5 | -0,65 | -266,9 | -0,62 | -182,1 | -0,41 | -230,9 | -0,50 | -243,3 | -0,51 |
| NIST-US | 5,0 | 0,80 | 2,2 | 0,34 | 7,7 | 1,13 | 4,5 | 0,64 | 2,8 | 0,38 | 7,1 | 0,94 |
| NRC-CA | 7,6 | 0,09 | 9,4 | 0,11 | 7,7 | 0,09 | 5,1 | 0,06 | 7,2 | 0,08 | -0,1 | 0,00 |
| A*Star-NMC-SG | -73,8 | -0,31 | -22,5 | -0,10 | -28,9 | -0,12 | -20,1 | -0,08 | 31,1 | 0,13 | 44,7 | 0,19 |
| NIM-CN | 120,2 | 1,23 | 135,5 | 1,39 | 131,1 | 1,34 | 150,9 | 1,55 | 154,1 | 1,58 | 256,7 | 2,63 |
| NPLI-IN | 45,2 | 0,10 | -62,5 | -0,13 | -160,9 | -0,34 | -46,1 | -0,10 | -322,9 | -0,68 | -456,3 | -0,96 |
| NIMT-THA | -6,9 | -0,08 | 3,0 | 0,03 | -18,7 | -0,19 | 3,9 | 0,04 | -10,3 | -0,10 | -2,6 | -0,02 |
| NPL-GB | 1,3 | 0,02 | 21,2 | 0,36 | 6,9 | 0,12 | 6,4 | 0,11 | 17,9 | 0,30 | 10,6 | 0,18 |
| VNIIM-RU | -27,8 | -0,67 | -19,5 | -0,45 | -27,9 | -0,63 | -27,1 | -0,59 | -22,9 | -0,48 | -29,3 | -0,60 |

Appendix 2: Descriptions of measurement setups and methods as reported by the participants

GROUP 1

BEV Austria

SIP 3002 length measuring machine with a standard HP 5529A laser interferometer only (i.e. no internal scale.) A standard linear interferometer, an Agilent 10751D air sensor, and 3 material temperature sensors were used. All systems calibrated by the BEV. The instrument is equipped with an incident light CCD-microscope. A special holder was constructed to ensure that the scale axis and the measurement axis of the laser interferometer coincide to within 0.1 mm.

For these measurements a 100× NA 0.55 objective with LED illumination was used. The image of the scale marks (as seen on a video monitor) were placed between two fixed lines (produced by a line generator) by manually moving the carriage together with the microscope. This visual technique together with residual straightness errors causes the most important uncertainty contribution.

To evaluate this uncertainty contributions measurements were performed by 4 different operators and on 5 diverse locations (orientation) on the machine. The stated results are the mean of this 5 measurements which are themselves the means of the observer-specific values. Because of instrumental boundary conditions the actual measurements were performed in two steps: 1 mm all 0.1 mm and 100 mm all 5 mm, respectively. The uncertainty for this two configurations is significantly different mainly of relocking effects.

Thermal drift was compensated by a time symmetrical measurement scheme. The scale temperature was estimated by measuring the table temperature some 5 cm away from the artefact. The scale support was near the end of the artefact (i.e. not at the Airy points).



CMI Czech Republic

CMI uses interferometric comparator IK-1 (CMI design) with static CCD microscope (objective 20x, ~130nm/pixel), transmission illumination by adjustable green or red LED, adjustable moving stage with linescale and interferometer retro-reflector.

Image processing:

line image is parallel to CCD rows: all pixels from selected range of one row are first added, then positions of both edges is found by linear interpolation of row sums, average of this two edge positions is taken as line position.

The stage automatically moves to predefined positions with about $\pm 4\mu\text{m}$ precision (each line always close to the centre of the field of view). The readings of interferometer and CCD residual deviation are taken in synchronization. Resolution, noise and vibrations are bellow 10 nm. The stage returns to reference (zero) line after each movement.

DZM Croatia

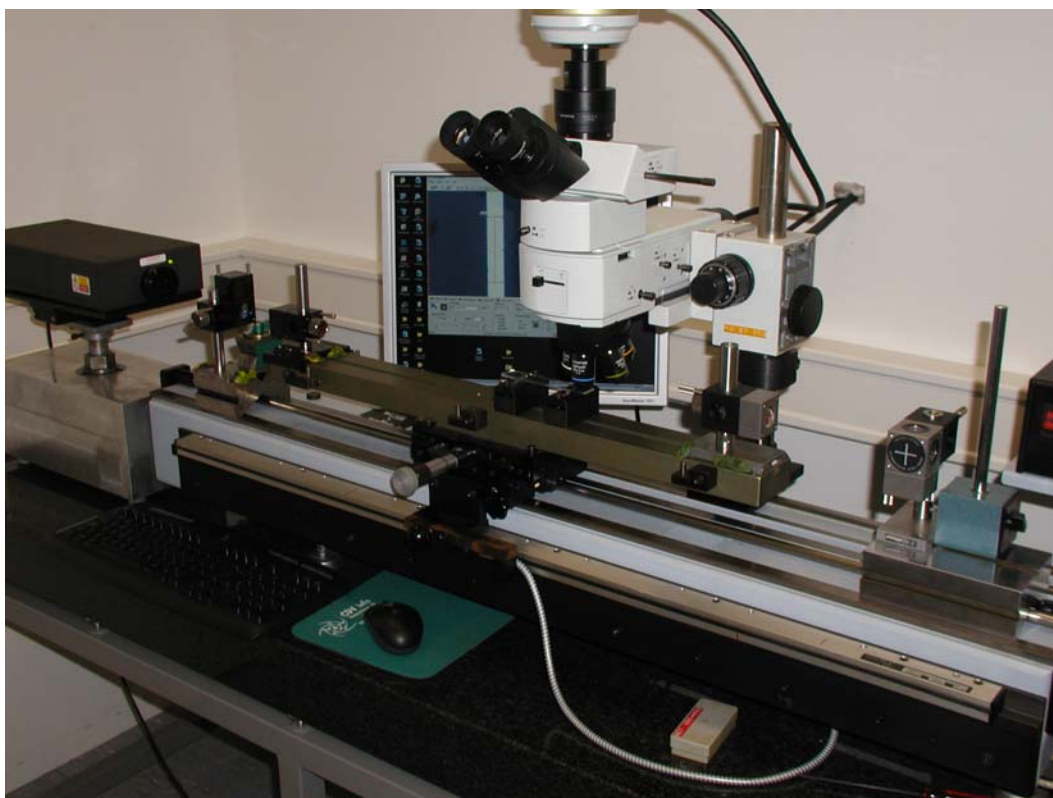
The measuring range of the device is 500 mm and it is primarily intended for the calibration of precise line scales. Device is fully constructed and produced at our Laboratory.

Stage movement is done manually.

The sighting process is done by means of a microscope with a digital CCD camera Olympus DP 70 with 12, 5 Megapixels with objective magnification of 50X.

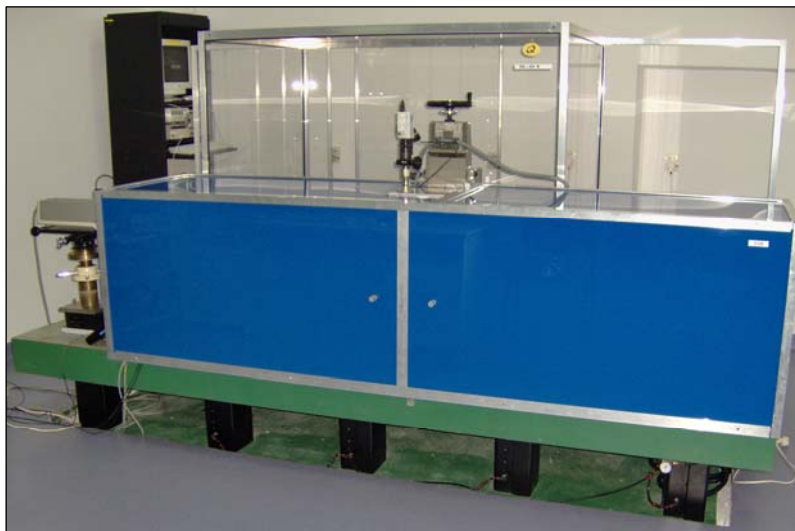
The measuring system used is the laser interferometer (Renishaw ML 10). The basis of the Renishaw Laser Interferometer system is HeNe Laser operating at a wavelength of 0,663 μm . The EC 10 Environmental Compensation unit automatically measures the three critical environmental parameters (temperature, pressure and relative humidity) and passes the data to the CS 10 Control Unit of which will compensate for any resultant change in wavelength.

The image processing is static, which means that it is necessary to process images and not the "live" signal of the display provided by a CCD camera. The software solution functions in such a way that all the pixels of a certain image are transmitted into a black&white combination and then the position of the line centre is calculated by arithmetic algorithms. The software solution provides the exact position of the line centre in pixels. In order to convert the values in pixels into the length values, it is necessary to calibrate the pixels size, i.e. to find out the length amount of every pixel. Calibration of the pixels is done absolutely by taking two images of the same line, which are shifted by the distance read on the laser interferometer.



GUM Poland

The 1-D measuring bench (SIP) with total length of one meter is the base of the line scale measurement set-up. The set-up is located in the air-conditioned lab, housed and mounted on the concrete plate supported by the pneumatic vibroisolation system. The scale lines are detected using the microscope and the CCD-camera, mounted on the fixed column. The lines are observed on the monitor equipped with two parallel lines generated electronically. The distance of the generated lines can be adjusted for the artifact to be measured. The scale lines are aligned between this two lines by eye in a symmetrical manner with precision piezo-electric actuator. The line spacing is measured with the laser interferometer HP-5528A. The line scale was placed on the moving, remote controlled carriage. The linear reflector of the interferometer is mounted on the carriage. The measurement data are collected with PC computer through the HP-IB interface.



The line scale was supported, during the measurement, at the Airy points using gauge blocks. The measurements were carried out in normal and reversed orientation (0° and 180°). There was applied the image window height close to $50\ \mu\text{m}$, the microscope with 20x objective and total magnification of 770x for the analysis of measurements.



The environmental parameters (material and air temperature) were measured by interferometer sensors. Humidity was measured with thermo-hygrometer LB-706. The refractive index of air was calculated from the modified Edlen formula [G. Bönsch and E. Potulski, *Metrologia*, 1998, 35] with sensors corrections.

INM Romania

Instrument:

- longitudinal comparator, equipped with an optical microscope and a laser interferometer with laser source He – Ne stabilized in frequency, having a resolution equal to 0,01 μm .

The longitudinal comparator is based on the cinematic method, according to Abbe principle: the line scale must be aligned on the same longitudinal axis with laser beam on the measurement direction, in the scope to eliminate the first order errors. Because the line scale was short, it was supported with the whole surface on the special carriage of the comparator.

Measurement method:

Method of measurement consists in the displacement of the reference line measure along the measurement direction. Speed of displacement is about maxim 10 mm/min. Marks' viewing of line measure is made using an optical microscope. The line is put on the mobile arm of the interferometer and the distance between marks is directly measured in length units.

The appearance of a fringe in the field of view of interferometer is determined by a deviation of optical path from measurement arm of interferometer equal with $\lambda/2$, where λ is the wavelength in the propagating medium at medium's temperature, pressure and humidity of the laser He-Ne radiation, used as monochromatic source of light.

During one measurement between the beginning and the end of the measurement, difference between the thermometer readings was equal to $\Delta t_g = 0,01$ $^{\circ}\text{C}$. The difference between the temperature of the room and the reference temperature was 0,4 $^{\circ}\text{C}$...0,8 $^{\circ}\text{C}$ during all measurements.

LNMC Latvia

Action principle of horizontal comparator IZA-7 is based on optical viewfinder method.

Comparator IZA-7 design maintains adhering to principle of longitudinal comparison.

Measured item is possible to set up on the bedplate so that its axis could be the longitudinal extension of scale line axis. Scale line axis alignment with line of moving bedplate.

Measurement of length (line) is performed by method of comparison measured item line with comparator line scale using 2 microscopes with steadily span and parallel optical axis.

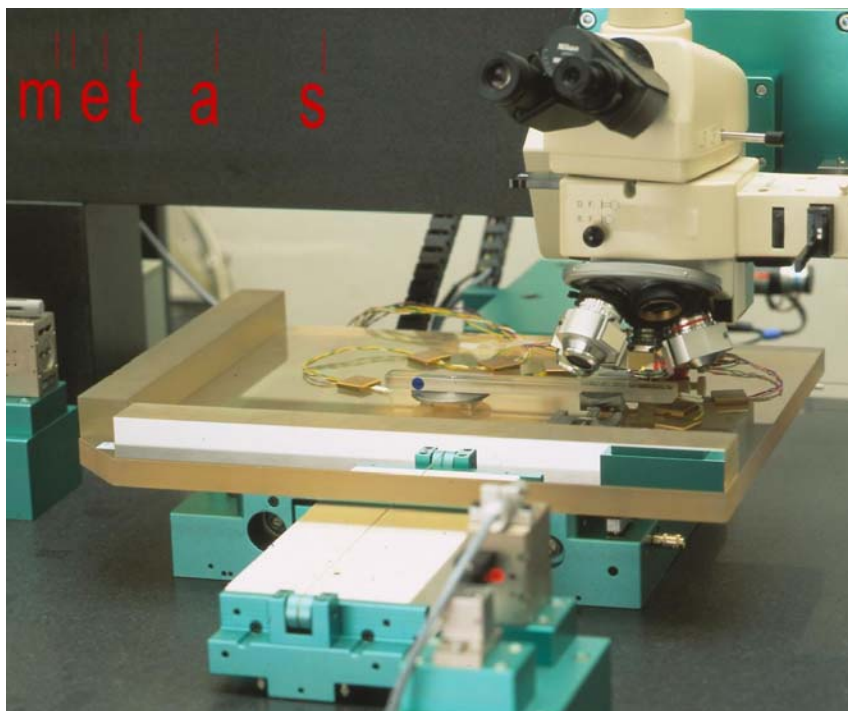
One microscope is used for aiming line, the other for reading on comparator scale.

METAS Switzerland

Measuring system:

The measurements were performed on a 2D photomask measuring system with a measurement range of 400 mm x 300 mm. The system has an xy-stage with unique vacuum air-bearings featuring very small errors of motion. Two speed controlled servo motors move the table by means of fine strings. Once positioned, the stage is clamped to the granite base table by a vacuum brake. A differential two axis plane mirror interferometer (HP) measures the position of the stage. The moving mirrors are attached to a Zerodur base plate and the reference mirrors are fixed to the microscope objectives. Air pressure, temperature, humidity and CO₂ content are on line accessed to determine the refraction index of the air by the Edlen formula. A microscope with a CCD camera and an episcopic illumination is used to localise structure positions. The microscope has a motorised turret and focus. For automatic focussing the image contrast is maximised.

The machine is located in a temperature stabilised clean room cabin of class 100 (US) within the clean room section here at METAS.



Scale mounting:

The line scales were aligned parallel to the x- or y-axis of the 2D photomask measuring system. They were supported at the Airy points, with a distance of 66.4 mm, by 4 spheres, two on a pivot. The scales were aligned using piezoelectric actuators. Vertically to better than 10 $\mu\text{m}/100\text{ mm}$. Additionally, as a 2D measuring system is used, the x-axis of the object coordinate system is placed through the alignment marks by a numerical coordinate transformation to better than 4 $\mu\text{m}/100\text{ mm}$.

Line evaluation:

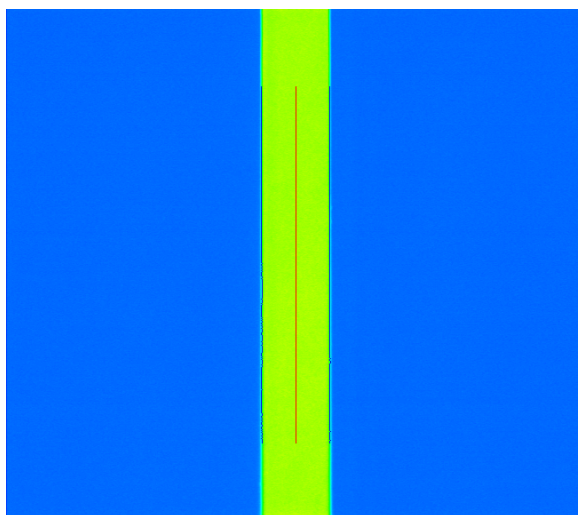
Each vertical line in the video image is analysed within the region of interest (ROI). The centre of a line profile is the average of the left and the right edge. The edge locations are determined

with a moment based edge operator. A line is fitted through all individual profile centres using only points within 2σ . The intersection of the fitted line with the reference line is used as the scale line position. The reference line was determined using the right and left pair of the horizontal alignment marks. Each line was evaluated within a length of $50\ \mu\text{m}$ (height of the ROI).

Table: Image size and evaluation range.

| Magnification | | 20x | 50x |
|-------------------|---|---------------|---------------|
| | | μm | μm |
| Image size: | x | 244 | 98 |
| | y | 182 | 73 |
| Evaluation range: | x | 30 | 40 |
| | y | 50 | 50 |

Typical line at 50x magnification with edge and line centre indication:



Measurement strategy:

The 2D photomask measuring system can operate fully automatically, therefore always a complete set of measurements was made lasting for about 2 hours. Such a set consisted of the following measurements:

| Scale (mm) | Lines | Repetitions |
|---|-------|-------------|
| 0, 0.1 .. 1 | 11 | 10 |
| 0, 5 .. 100 | 21 | 10 |
| 0 .. 100 (for verification only) | 2 | 10 |

Both line scales were measured in four orientations 0° , 90° , 180° and 270° with the 20x objective and additionally at 0° and 180° with the 50x objective. For the final result all these measurements were averaged. There was no systematic difference.

Corrections:

For the final results all known corrections were applied. In particular, the thermal expansion was corrected using the given thermal expansion coefficients of $5E-07/K$ for quartz. The temperature deviations from $20^{\circ}C$ were within $\pm 0.1 K$ (average $20.06^{\circ}C$). Furthermore, as the measuring system is located 550 m above sea level, the average barometric pressure during the measurements was only around (945 .. 950) mbar. The results were reduced to the standard pressure of 1013 mbar with the given compressibility coefficient of $-8.90E-07/bar$ for quartz. This correction was $-5.9 nm$ for 100 mm.

Uncertainty contributions:

For the total uncertainty 30 contributions were considered. The largest contributions at 100 mm were for both scales, the repeatability, the air temperature and the scale support. For quartz scales also the material temperature is critical because glass has a low thermal conductivity and a small thermal capacity therefore it is difficult to measure its temperature. The accuracy of the thermistors itself is not the problem.

MIKES Finland



Figure 1. MIKES' line scale interferometer

MIKES' line scale interferometer (fig 1) uses a dynamic method of measurement with a moving microscope for speed, simplicity, and considerations of space requirements. The graduation line distances are measured during continuous motion, which makes the system fast and the interferometer insensitive to minor turbulence in the interferometer beam path. Possible problems with speed fluctuations and time delay in observing the lines are avoided by using an electrically shuttered CCD camera as a line detector and synchronous data sampling.

The interferometer is constructed on a vibration isolated stone table to eliminate mechanical disturbances. The interferometer is situated in a laboratory room with air temperature 20 ± 0.05 °C and humidity $46 \pm 2\%$ RH. The microscope is fixed on one side of a carriage and the CCD camera on the top of the microscope, axis of which is adjusted perpendicularly to the scale plane.

The displacement of the microscope is followed by a Michelson interferometer utilising a calibrated 633 nm Zeeman-stabilised He-Ne laser. The light of laser is coupled via single mode fibre to the interferometer and adjusted parallel with the carriage movement by using a quadrant detector. Abbé error is eliminated with a large cube corner, making it possible to adjust the focus point of the microscope and the apex of the cube corner to the same point. This cube corner is constructed from three separate round mirrors adjusted to angles of 90° with each other. Ideal adjustment of the focus point and the apex of the cube corner nearly completely eliminates the Abbé error. The interference fringes are detected by two detectors with 90° phase difference and counted by a direction-sensitive quadrature counter.

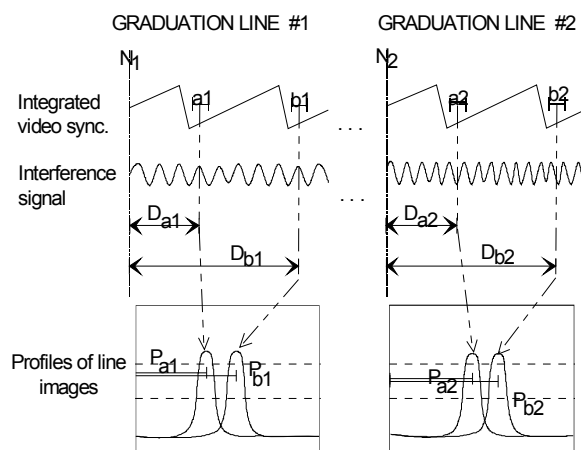


Figure 2. Analysis of the measurement data.

In measurement run, the carriage moves in one direction while the programme continuously monitors the counter reading. When the carriage is approaching a line, the programme slows down the speed of the carriage and just before passing over the line it stores the current counter reading (N_i ; figure 2), starting a synchronized sampling. In the sampling, one interference signal and an integrated video synchronisation signal, for determination of the field forming positions (a_i , b_i), are digitised, the graduation line image is stored, and the refractive index and temperature of the scale are calculated and stored. This set of samples is taken for each line after which a new run is started in the opposite direction. A single measurement of the decimetre lines of a 1 m scale takes approximately 15 minutes. The first approximation for the measured length is calculated as the distance between the positions where the graduation line fields are formed ($N_i - D_{ij}$).

Average profiles of the graduation lines are formed by summing picture element intensities of each row of the CCD. Each image of the CCD camera consists of two fields charged in 1 ms and with time separation of 20 ms. Thereafter, the centre points of the graduation lines (P_{a1} , P_{a2} , P_{b1} , P_{b2}) are determined from the slopes of the line profile and a correction term needed to superimpose the centre points is applied. The refractive index of air is determined by Edlen's formula updated by Bönsch et al. The line scale interferometer is capable of calibrating line separations from 10 μm to 1 m of good quality line standards, having line widths from 2 to 50 μm .

The measurements for comparison were done like for normal customer asking high accuracy calibration of good quality line standard. As specified in the protocol the width of the measuring section was adjusted to $50 \pm 2 \mu\text{m}$ and scale was supported from Airy points. The line spacings were measured in two different positions along the range of the stone rail. In both positions the scale was measured in normal and reversed orientation. Each measurement consisted of 5 runs. The averages of these 4 measurements are the results. Compressibility correction was calculated and applied.

Unfortunately the reference line was noticed to be non-ideal (fig 3). In separate test was studied what is the effect of this non-ideality. In test 10 first lines were measured normally and so that the defected area was excluded from the analysis. The difference was +12 nm with 6 nm STD. This correction was applied to the result.

Also lines 0.1; 0.4; 85; 90 and 95 mm were clearly non-ideal (see receipt confirmation from MIKES). For this reason the value of the uncertainty component "Influence of line detection algorithm with line quality" was raised to 20 nm for these lines. This approximately doubles their uncertainty.



Figure 3. Non-ideality in the reference line (pointed by red arrow).

References:

- A. Lassila, E. Ikonen, and K. Riski, Interferometer for calibration of graduated line scales with a moving ccd camera as a line detector, *Applied Optics* 1994, 33, 3600-3603.
- A. Lassila, Updated performance and uncertainty budget of MIKES' line scale interferometer, *In Proc. of euspen*, Glasgow, Scotland, May 31 – June 2, 2004, p 258-259.

MIRS Slovenia

Measurement setup

The line scale was measured on a Zeiss ULM 01-600 C 1D measurement machine by using laser interferometer HP 5528 A as a measurement system and Opto zoom microscope with CCD camera as a line detection system.

The scale is supported in Airy points by two metal half cylinders. Additional fixture is not necessary due to low movement speed (hand driven table).

The measurement setup is shown in Fig. 1

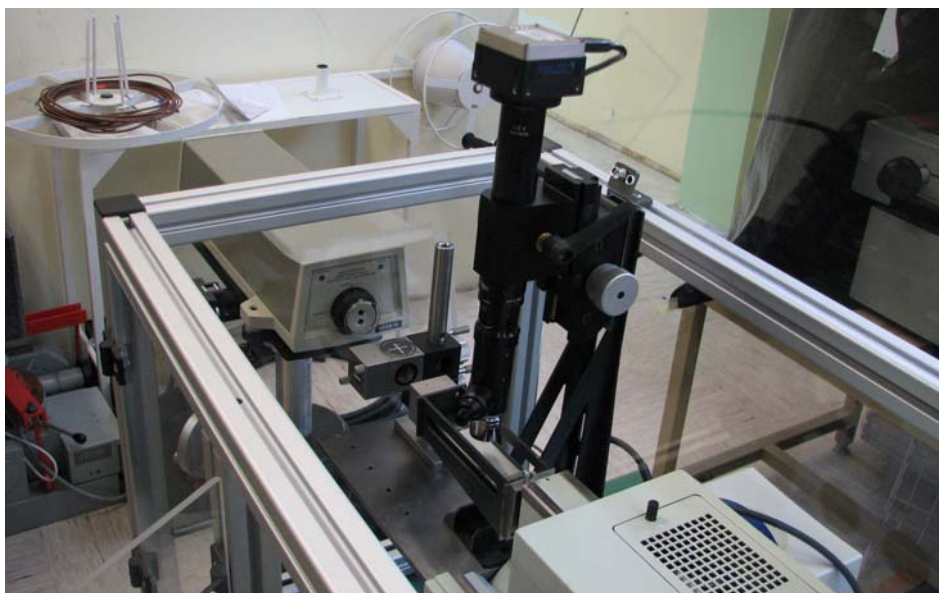


Fig. 1: Measurement setup

The centre of a line is detected by the video-positioning system consisting of a zoom microscope, CCD camera and a line detecting software, which was developed in the laboratory in the LabView environment.

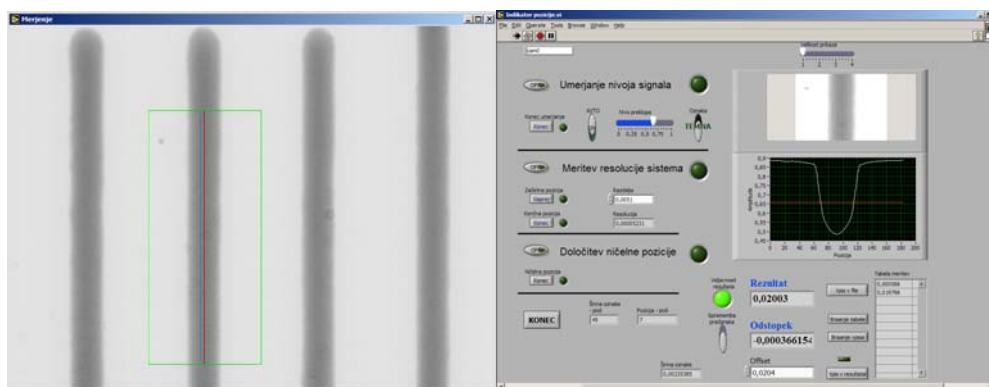


Fig. 2: Line detection software – screen masks

The material temperature is measured with a Zeiss termistor contact sensor (resolution 1 mK, standard uncertainty of calibration 2 mK) on the measuring table, while the air temperature is measured with Agilent temperature sensor with resolution of 10 mK.

Measurement procedure:

Each line position was measured from zero position (the system was positioned in zero point after each measurement). The whole procedure was repeated 10 times in a short time period. Arithmetic mean from those measurement represented measurement result, while the standard deviation represented the repeatability component of the measuring uncertainty. In order to evaluate reproducibility, the measurement was repeated in 5 different days with two different operators.

NCM Bulgaria

The measuring system consists of a comparator, laser interferometer (with light source He-Ne laser 633 nm, HP5529A), moving carriage with mounting on it reflector and (with light source laser diode) for location of scale marks, temperature measuring system, barometer and hygrometer.

The scale was placed horizontally on two supports at Airy points.

NML Ireland

Equipment Used:

Agilent 5519A Laser and SIP Horizontal Measuring Machine

Procedure:

The HP laser retro reflector is mounted to the end of the main bed of the SIP measuring machine, nearest the laser head. The HP interferometer is fixed to the longitudinal carriage of the SIP.

For line scales of nominal size greater than 10mm a transparent table is placed on the longitudinal carriage of the SIP measuring machine. This table is illuminated from below with a light source.

The glass scale under test is placed on the transparent table and aligned with the main axis (x axis) of the SIP using the adjustment screw on the transparent table.

The vertical microscope of the SIP is then aligned with the glass scale under test. An appropriate eyepiece and magnification is then selected to give optimum clarity to the glass scale under test, taking into account the line width and line quality of the line scale under test.

The central cross wire (the cross wires are imposed on the eyepiece of the SIP microscope) is aligned with the datum line of the glass scale. In this position the HP laser system is zeroed.

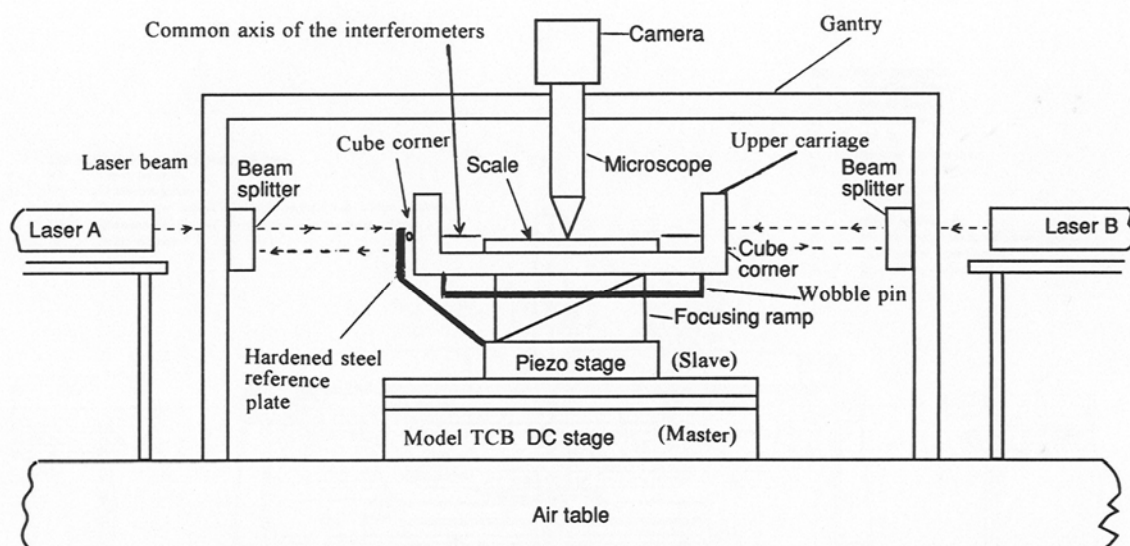
The carriage of the SIP is then moved until the second line of the glass scale is aligned with the cross wires. The distance moved is recorded from the display of the HP laser system.

This exercise is repeated at selected positions over the length of the glass scale. 5 repeat measurements are taken at each selected position along the scale and the average taken.

NPL United Kingdom

The NPL linescale machine consist of a 400mm range, interferometrically monitored, air-bearing stage that moves the scale to be measured under a nominally fixed optical probe. The probe consists of the NPL NanoVision image processing system.

Scale motion is measured by two co-linear independent laser interferometers, one being an NPL differential Jamin type with plane mirror and second being an HP Michelson type with cube-corner reflectors. The measurement is carried out in a laboratory atmosphere and a weather station monitors the refractive index of the air. Following the Abbe principle, the common axis of the interferometers lies in the plane of the scale to be calibrated and is co-linear with the line containing successive measuring points on the scale. Separation of the cube-corner / plane mirror reflectors (one flexure-mounted) is maintained by a fused silica 'wobble-pin'. The two beam splitter units are each flexure-mounted on the frame of the machine, separated from the measuring head by further silica wobble-pins.



A scale under examination is 'Airy point' mounted with the chrome uppermost and with no compression force on the scale. The scale is illuminated with reflected light. A combination of the two measurements obtained greatly reduces the chances of common-cause error in displacement-measurement and the configuration provides an indication of accuracy and repeatability.

The 2006 measurements were taken with the NPL 400mm machine in a temporary laboratory with poor environment conditions. The measurements were made without using an auto focusing routine.

The 2008 measurements were taken with the NPL 400mm machine in a dedicated laboratory in the New NPL building. The environment conditions here are much better. The measurements were made using an auto focusing routine and employing a second-generation version of NPL NanoVision video probe.



NSCIM Ukraine

The measurement of the scale intervals was carried out by the absolute method using the interference setup of the primary standard of the unit of length DETU 01-03-98, which is a horizontal comparator with Michelson dynamic laser interferometer and photoelectric microscope for fixing the centre of the measured scale marks. The photoelectric microscope (PEM) and the corner reflector of the measuring arm of the laser interferometer are rigidly fixed on the movable table of the comparator. The scale under measurement is installed in a special positioner on the stationary table of the comparator.

To create the required measurement conditions the interference setup is placed into a heat chamber with automatically maintained air temperature of (20 ± 0.05) °C.

The length of the scale intervals is determined in the wavelengths of the stabilized He-Ne laser radiation ($\lambda = 0.63 \mu\text{m}$) by means of reversible counting of the fringes kept within two automatic settings of the PEM to the tops of the image of the measuring scale marks. The equation is as follows,

$$L = N\lambda_0 / 16n + \alpha\Delta tL_H,$$

where N is the number of fringes (impulse number) kept within the measured scale interval; λ_0 is the wavelength of the laser source in vacuum; n is the air refractive index; α is the linear expansion factor of the scale material; Δt is the scale temperature deviation from 20 °C; L_H is the nominal length of the scale interval.

The air refractive index is calculated by the Edlen formula using the measured values of pressure, temperature and humidity. The temperature of the gauges and the air is measured with regard to the base of the interference setup using the platinum resistance thermometer, copper constant thermocouples and direct current bridge. The pressure and humidity are measured using standard devices.

The real value of the scale interval length is determined as the average value of the measured scale interval lengths in the direct and reverse motion of the PEM.

OMH Hungary

The measurements were done on the 3 m universal length measuring machine made by Zeiss, with the help of HP 5528 laser interferometer.

The environmental parameters were measured by independent calibrated measuring instruments. For the temperature measurements, 4 wires PT 100 thermoresistors were connected to Keithley type 196 multimeter. The readings were made automatically through HP-IB parallel interface. For the air temperature 2, for the material temperature 5 thermometers were used. The average of the 2 and the 5 values were used as air and material temperature.

The air pressure was measured by Wallace & Tiernan digital barometer Type Diptron 3, the data were taken also via HP-IB interface.

The air humidity was measured by a Digilog 60 capacitive digital humidity measuring instrument.

The correction factor was calculated by the EDLEN formula.

The data from the HP laserinterferometer were taken also via HP-IB interface.

The magnification of 100 X was used and the magnified image was seen on the SONY videomonitor through a videocamera. The image processing system generates digitally movable horizontal and vertical lines that serve to help to set the centre of the lines. The horizontal magnification was 1200 x.

The scale was placed on a steel base as the lines were standing vertically, 2/9L points were used.

The angle error of the carriage movement in vertical and horizontal plane (pitch and jaw) was measured by Agilent laserinterferometer in 0,1 sec resolution.

PTB Germany

The PTB performed the measurements reported here with its Nanometer Comparator. Here only a short description will be provided. Detailed descriptions have been published already elsewhere [1-3]. A schematic of the Nanometer Comparator is shown in Fig. 1.

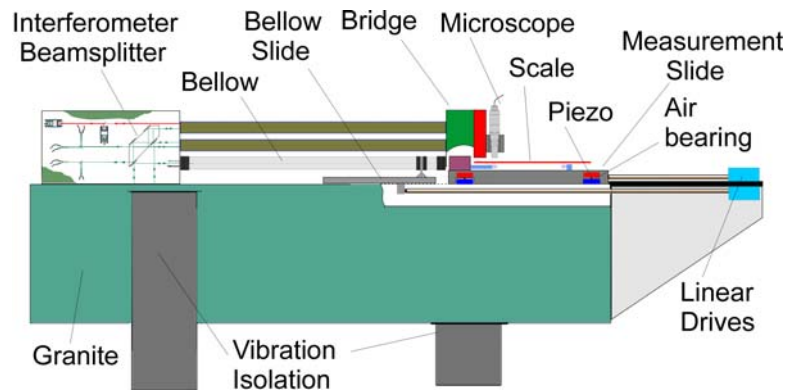


Figure 1: Schematic of the Nanometer Comparator

The Nanometer Comparator is equipped with a vacuum interferometer. An iodine-stabilized, frequency doubled Nd:YAG laser, which is operated according to the recommendations of the BIPM, serves as radiation source. The radiation is fed through polarisation maintaining fibres from the laser, which is located outside the measurement cabin, to the vacuum interferometer. The measurement slide is guided by air bearings and driven by a linear motor. Angular vacuum interferometers and piezo electric actuators integrated in the measurement slide are used in a closed loop to correct for the remaining angular deviations of the measurement slide. The z-axis actuators are also used to perform the z-axis fine motion required to determine the focus position of the sample. The sample is supported at its Airy points with a fixed and a movable roller. The fixed roller is supported by a height adjustable mount directly connected to the housing of the measurement reflector. The loose roller is put on a height stage mounted on the slide. A home-made optical microscope, which is shown schematically in figure 2, is used to detect the graduation lines of the scale. The housing was machined out of invar. The white light illumination is provided by a

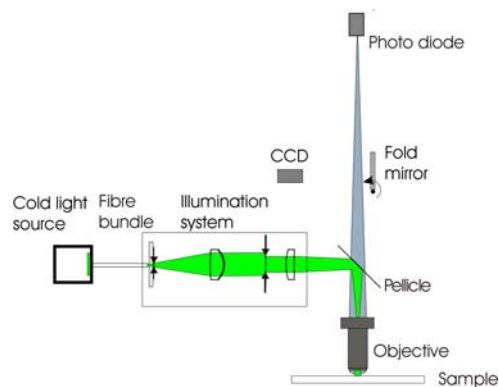


Figure 2: Schematic of the microscope

cold light source and guided to the microscope by an incoherent fibre bundle. The illumination optics has been designed to achieve a Köhler illumination. The light is directed through the objective towards the sample by a pellicle. Here a 50 x Nikon measurement objective with a

numerical aperture of 0.55 and a working distance of 16 mm was used. By means of a fold mirror the image of the line can be observed directly using a CCD camera. This feature is used to align the sample horizontally. During the measurements the light of the image is detected by a photo diode after it passes through a fixed slit. In the object plane the slit has the dimensions of $4\ \mu\text{m} \times 50\ \mu\text{m}$. The intensity profile of the line and the related positions were acquired simultaneously by means of a hardware trigger provided by a function generator. In order to restrict the data acquisition to a region closely located around the line only, a gate signal for the trigger was derived from the digital scales of the measurement slide. The following algorithm was used to determine the position of a line. First the intensity profile of the line was normalized so that all values are between zero and one. Straight lines are then fitted to the intensity displacement dependence in the intensity range between 0.4 and 0.6. From this the positions, where the intensity equals 0.5, are calculated for right and left edge. Finally the average of these two positions is calculated and considered as the position of the line.

The measurements were corrected for the deviation of the air pressure and the temperature from the normal conditions (1013.25 hPa and 20°C) using the linear coefficients of the compressibility and thermal expansion as given in the technical protocol of the comparison. Furthermore the influence of the residual gas in vacuum chamber of the interferometer on the wavelength was corrected for using a simplified Edlen equation.

b.) Measurement conditions and measurement uncertainty

Due to the different spacings between the lines to be measured the measurements were divided in two independent parts. First the lines of the first millimeter and then the lines over the whole scale were measured. The scale was measured in the first and again in the third week of January 2007. The scale was aligned to better than $0.1\ \mu\text{m}$ vertically and within $1\ \mu\text{m}$ laterally the day before the measurements were performed. The whole setup then was left to reach its thermal equilibrium over night. Before the measurements were performed the focus position of the scale was determined and the z-position of the scale was readjusted accordingly. Each day 5 data sets in forward and backward direction were collected for the two independent parts. The measurement speed of the short part was 0.1 mm/sec and that of the long part was 0.2 mm/sec. Then the scale was remounted in the reverse orientation. To obtain the final result the average results of each day were averaged again. The results of the uncertainty estimation are summarised in the table on the following pages.

The pilot laboratory was informed in a separate short report about the influence of the partly contaminated graduation on the measurement results of the PTB (report sent on Feb 8th 2007). The severe contamination of the sample leads in general to a considerable increase of the measurement uncertainty. At several lines (the position relative to the zero line are given in the table) an additional contribution was necessary to account for the experimentally observed scatter and the differences between the PTB mask comparator, which also has measured the scale, and the Nanometer Comparator. We like to mention here that neither the control measurements nor a comparison of these two instruments performed on the quartz scale used in the Nano 3 comparison performed parallel to the comparison showed any disagreements or variations, so that the observed larger variations of the results and differences between the instruments can be solely attributed to the contamination of the sample. In addition, a further comparison between the two instruments on a clean area of the scale also yielded a complete agreement within the observed experimental scatter, which was in the order of a few Nanometer.

References

- [1] J. Flügge, H. Dangschat, A. Spies, J. Tschirnich and H. Pieleles: "Concept of a interferometric length comparator with measurement uncertainties in the nanometer scale", Proceedings of 1st Euspen Conference, Bremen, Mai 1999, p. 227-230
- [2] J. Flügge, R. Köning and H. Bosse: "Status of the nanometer comparator at PTB", Proc. SPIE, Recent Developments in Traceable Dimensional Measurements, Jennifer E. Decker; Nicholas Brown; Eds., 2001, Vol. 4401, 275-283
- [3] J. Flügge, R. Köning and H. Bosse: "Achievement of sub nanometer reproducibility in line scale measurements with the Nanometer Comparator", to be published in the SPIE proceedings of the Advanced Lithography conference, held in San Jose in February 2007

SMU Slovakia

The line scale was calibrated on the setup consisting from the 1-D length measuring machine Abbe Zeiss (measuring range up to 200 mm) and the laser interferometer HP 5529B.

The frequency (vacuum wavelength) of HP HeNe 633 nm laser has been calibrated against the HeNe/I₂ 633 nm primary standard of SMU.

The line scale was laid upon the 150 mm gauge block placed horizontally (height of 9 mm) supported by two semicylindrical supports in the mutual distance corresponding to Bessel points related to 150 mm long artifact of rectangular shape – the reason was possibility to use clamp attaching the Pt resistance thermometer directly to the gauge block onto which the measured glass artifact was resting.

The extrapolated axis of calibrated scale intersected the axis of cube corner and thus the Abbe principle was kept.

The carriage bearing both measured line scale and cube corner was moving under the optical microscope. Due to bending of the artifact over the whole measured range just the limited magnification could be used – objective 10x, eyepiece 12,5x

The position of the line was observed in the area determined by two parallel lines (at the beginning and at the end of the scale) – as those as were not visible during the targeting on the measured lines, the height of observed area in the visual field was based on the subjective estimation.

The temperature of both the glass plate and air in the neighbourhood of the laser beam was measured by two Pt 100 thermometers (1 for scale, 1 for air), the air pressure was measured by the digital barometer DPi 141 and the relative humidity by the ALMEMO tester.

The scale was calibrated in two positions and the final result for each line is given by the arithmetic mean of two values corresponding to both positions of artifact (for every measured line, in each position the number of repeated measurements was equal)

The length values were corrected to 20 °C using the linear thermal expansion coefficient $5 \times 10^{-7} \text{ K}^{-1}$.

The pressure compressibility correction (negligible, cca -1 nm for 100 mm length) to 1013,25 hPa has been applied using the length compressibility factor - $8,9 \times 10^{-7} \text{ bar}^{-1}$.

ZMDM Serbia

The measurements were performed on a 1-D measuring machine (bench) with a total length of three meters (Zeiss type ULM 3000). Scale lines were detected using Zeiss optical microscope, mounted on a moving wagon of the measuring machine. A laser interferometer (HP 5526 A) was used to measure the displacement of the microscope.

Scale support: During measurements the line scale was supported on two roller bearings at Airy points without any clampings. Scale is aligned visually with the displacement axis of translation stage and measuring (laser) axis. Alignment is checked by comparing the focus and position of the end lines while displacing the translation stage from the line “0” up to the line “100”. This procedure is repeated several times.

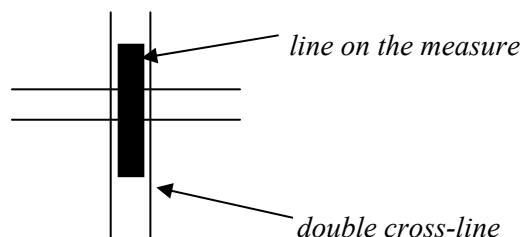
Measuring bench: The translation stage of the measuring bench consists of two parts. The main part is sliding on the bench and is used to coarsely move the microscope into desired position. The second part of the translation stage (which is mounted on the main part) is used for fine-setting the microscope onto the line. Everything is operated manually.

Measurement procedure: The line scale was measured by coarsely move the microscope to each scale line (using the main part of the translation stage) and then fine-tune on the line with second part of the translation stage.

Since the instrument is manually operated, the measurements are time-consuming. In order to control induced drifts, the microscope was moved to the zero-point after every 10 lines measurements for checking.

Line scale was measured in two orientations with overall microscope magnification 50x. In one orientation two repeating measurements – forward and backward - were made as one group for each run. The total number of runs for each orientation were 12 except for total length 100 mm and first 1 mm (20). Then scale were reinstalled in reverse orientation and the alignment is checked as mentioned above. The final result is the average of all these measurements.

The positions of the lines were determined by direct visual positioning of vertical double cross-line of the measuring microscope at the center of each line in reflected white light with green filter. Left and right edge of each line were detected visually as the same (50%) gap light intensity level between microscope double cross-line and left and right edge of the line.



GROUP 2

A*Star – NMC Singapore

The comparison was done using a laser line width measurement system (as shown in Figure 1 & 2) at the National Metrology Centre, Singapore. The system consists of five major parts: a main base with two working stages driven by separate linear motors for sample holding and positioning, a laser interferometer for displacement measurement, a photoelectric microscope for line edge detection, an electronics unit for system control and a PC for data acquisition and recording. The He-Ne laser used in the interferometer is Lamb-dip stabilized and its wavelength is corrected for temperature, humidity and atmospheric pressure.

The scale was placed so that the main inscriptions were uppermost and supported at the Airy points by stainless steel rollers. A lightly pinch was applied at the Airy points to avoid the scale shifting due to the movement of the working stage. The scale was viewed using transmitted light. The length of interval was measured along the longitudinal axis and at approximately mid-position of the scale.

Measurements were taken in two orientations. At each orientation, the scale was properly aligned and two repeated measurements were made.

For each measurement, it covered two independent measuring ranges: one from 0 to 1 mm and the other from 0 to 100 mm, both with a step of 0.1 mm. For the range from 0 to 1 mm, a closed reading was taken at the end of the measurement. For 0 to 100 mm, the measurement was divided into three sections: 0 to 50 mm, 40 to 90 mm and 80 to 100 mm in view of excess data collection. Adjustment factors at the overlapping intervals (40 to 50 mm and 80 to 90 mm) were considered in the calculation.

The average of the four measurements of the two orientations was reported as the final results. All results of measurement are referred to a temperature of 20 °C.



Figure 1: The laser line width measurement system

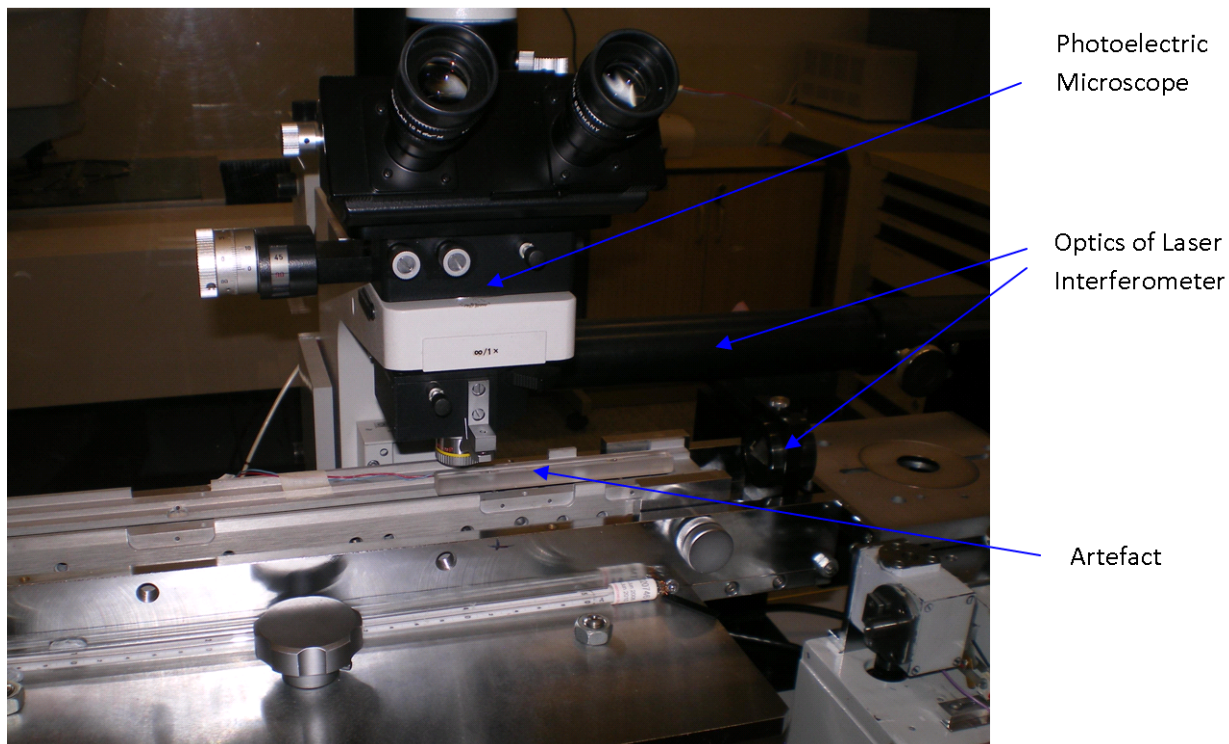


Figure 2: Enlarged view of the line edge detection unit

CEM Spain

Make and type of instrument

Custom-built length comparator CEM-TEK 1200 equipped with, two beams on flat mirrors, laser tracker and pseudo-Abbe measurement principle.

Light sources / wavelengths used or traceability path:

Stabilized Laser Source HP 5517C, $\lambda_0 = 632.991\ 365\ 64\ \text{nm}$, calibrated against He-Ne reference laser CEM-1 (national standard)

Method used to determine the refractive index of the air :

Measuring of ambient conditions and applying of Edlèn's formulae plus laser tracker (relative refractometer) for continuous updating of n value.

The laser is reseted in the first line (reference line position "0") using a reference standard (gauge block) calibrated by interferometry.

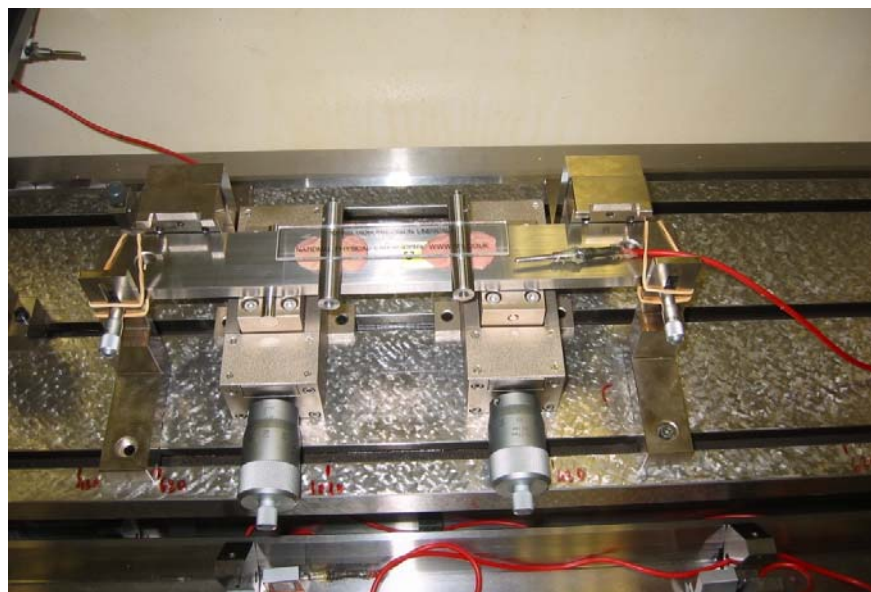
Optical system:

The detection of the line is made by automatic recognition by the optical system with the help of home made software.

Alignment:

With horizontal and vertical micrometers, by observing the two main lines of the scale (at the beginning and the end) and the central one, trying to maintain in focus. For those less-in-focus lines, the optical system posseses autofocus.





CENAM México

An optical microscope brand Leitz, model Libra 200, with 200x magnification was used.



The measurement range of the instrument is 150 mm x 100 mm, and the minimal division of the microscope scale is 0,1 μm

The lines edges were detected visually in a monitor connected to a CCD camera.

The distances between line centers were obtained by Micro/Measure Microscope Software and the temperature variation from the standard temperature was $\pm 0,4$ $^{\circ}\text{C}$.

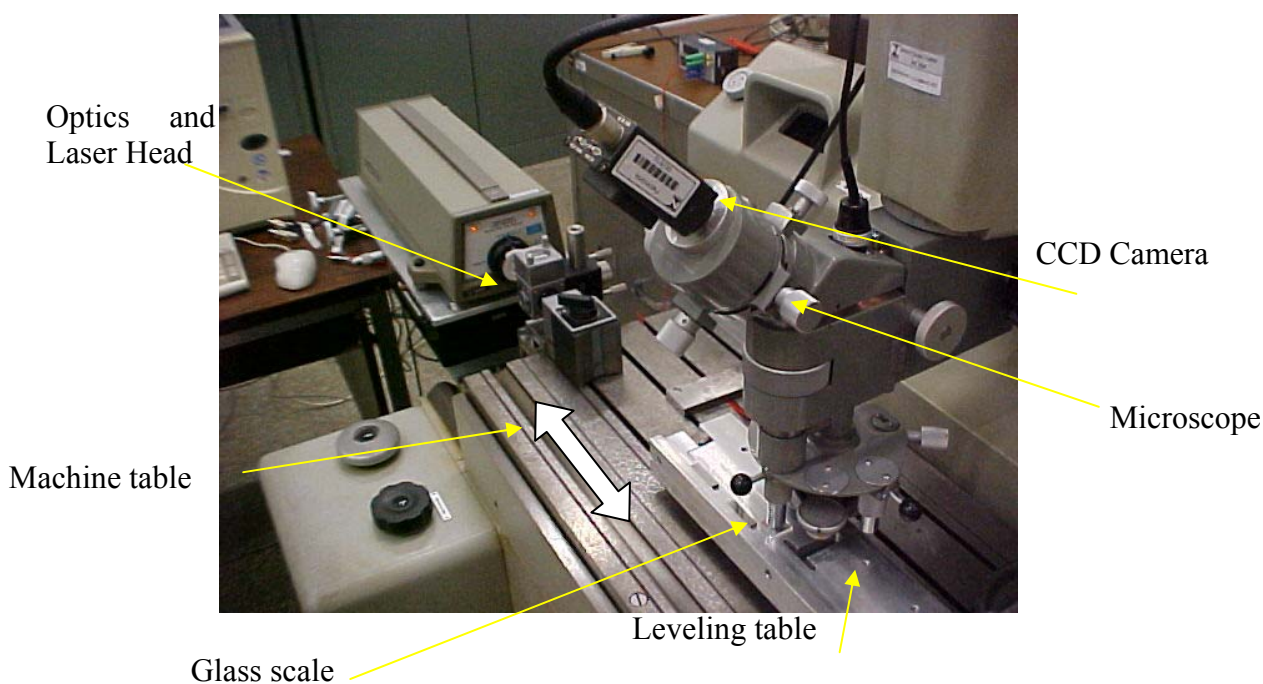
EIM Greece

The measurements were performed with the use of a Leitz universal measuring microscope with x100 total magnification. A Renishaw laser system was used for the measurements of the line scale displacement while the centers of the lines were estimated by the analysis of the digital images of the line scale at each measuring position. The air temperature, humidity and pressure were recorded during the measurement.

INMETRO Brazil

The scale was calibrated in a system composed by a microscope mounted in an optical CMM (Trioptic–SIP) whose table is able to move in one direction. The table movement is detected by an interferometric laser system. The scale was laid over a special table so that it could be leveled aligned to laser beam and focused appropriately. Due to limitations, the scale was not supported in Bessel points as recommended in the Protocol. The measurements were performed in the same points as that ones outlined in the Protocol taking as reference the “0” point. The temperature during the measurements was $(20\pm 0,6)$ °C, with a variation within 0,1 °C.

2 – System configuration



INRIM Italy

The measuring apparatus is based on a Moore Measuring Machine equipped with a laser interferometer and an optical probe. This latter consists of a optical microscope with a CCD-camera.

Tab. 1. Instrument identification.

| Instrument | Manufacturer | Model | Ser. No. |
|-----------------------------|--------------|--------------------------------|------------|
| Universal Measuring Machine | Moore | n. 3 | M245 |
| Laser interferometer | HP | 5518 | 3626A03700 |
| Microscope | Nikon | OPTIPHOT 100S | 628562 |
| Objective | Leitz | $\infty/0$ Plan 125X N.A. 0,80 | |
| CCD camera | Basler | FM 60955 | |

Measurement setup

The optical probe is used for the calibration of line standards. A rectangular window is created via software to simulate a probe; the “contact” is obtained from the image processing tool described below.

The window width corresponds to the ball tip diameter of a “contact” probe, whereas the window height determines the number of pixel rows activated (integration amplitude). By displacing the artefact (relative displacement between artefact and CCD camera), the window “penetrates” in the measurement area and defines the artefact edge position by measuring its distance from the window side (left or right, see Fig.1).

The optical probe is calibrated with reference to the laser interferometer. The pixel-size (about 0.08 $\mu\text{m}/\text{pixel}$, with a magnification of 125X) of the image window is obtained from the displacements measured with the laser interferometer when the window penetrates (of about 6 μm) the edge line from both left- and right-sides. In this way, the measurement runs are driven mostly as for the mechanical probe, except for the probe calibration which is based on the interferometer itself.

From the “contact” readings and the laser interferometer we determine the edge x-positions at the left- and right-sides of the line with an image window of about 32 μm width and 64 μm height. Then, the position of the centre of the line is obtained from the middle of the left- and right-edge positions.

Traceability is given by the wavelength of the laser interferometer.

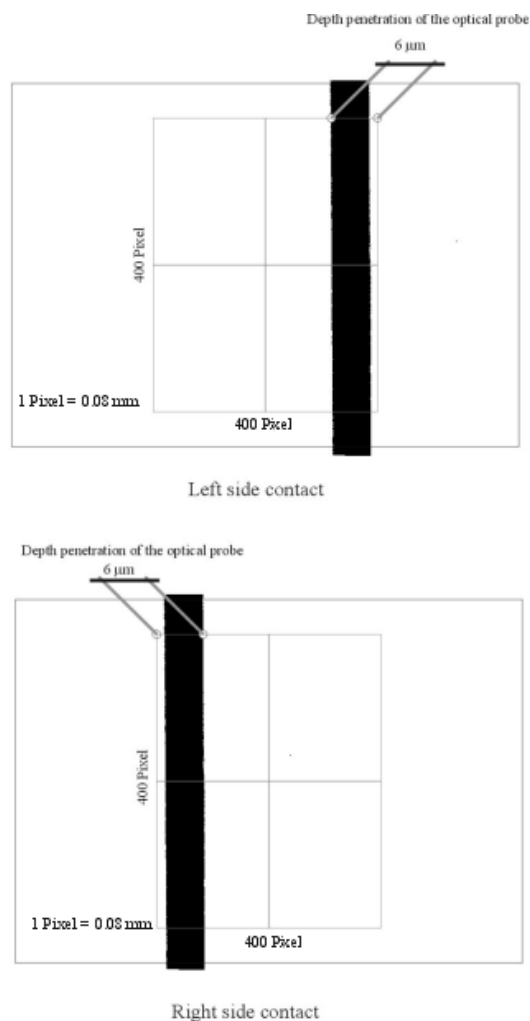


Fig. 1: The figure describes the way the position of the line was deduced from the image (a line of about $5\ \mu\text{m}$ width is shown in the image)

Measurement procedure

The equipment configuration from bottom up was: Moore carriage, vertical stage (height adapter up to Abbe condition in vertical), tilt and rotary stages, base support designed for the Airy support points of the linescale, linescale.

The applied procedure is the following:

The linescale is placed on the base support and is aligned (visually) with the measuring axis. Then, the alignment is improved by checking the focus and position of the line end on the video frame while displacing the artefact from the line „0“ up to the line „100“ and back (to be repeated several times).

With the automatic control of the Moore machine, no manual handling of the linescale is required to reset the equipment between each set of measurements.

The positions of the lines are then measured at the central section of the lines with a CCD image window length of about $80\ \mu\text{m}$.

The adopted measurement strategy is:

1. Every 5 mm line over 100 mm (31 runs);
2. Every 0.1mm line over first 1 mm (16 runs);

About half of the measurement runs have been performed with the linescale in the reversed orientation.

For each run the deviation from the nominal length is obtained from the average of forward and backward measurements of the line positions.

Ambient

Measurements have been carried out in a laboratory with air temperature control ($20 \pm 0.1^\circ\text{C}$). The table below gives the range of the ambient parameters during the measurement runs.

| | |
|-------------------------|------------------|
| Ambient air temperature | 19.96 – 20.08 °C |
| Pressure | 99.7 – 100.8 kPa |
| Humidity | ~ 50% |

Air refractive index is calculated using the revised Edlen's formula; the ambient parameters are measured by a precision thermometer, a Rosemount barometer and a Mitchell igrometer. The CO₂ content is assumed to be 400 ppm.

B) Tabular description of the measurement methods and instruments

Line detection

| Parameters | Parameters used for the measurement |
|--|---|
| Microscope type: | Nikon Optiphot 100S / Objective Leitz $\infty/0$ Plan 125X N.A. 0,80 |
| Light source | <i>Halogen lamp - Illuminator Intralux 4000</i> |
| Wavelength(s) | <i>White light</i> |
| window length | <i>64 μm</i> |
| window width | <i>32 μm</i> |
| Detection mode | <i>Image processing of the 2D CCD image video frame</i> |
| Detection principle | <i>Left- and right-side line edge detection to determine the centre line position</i> |
| Sampling frequency (image/interferometer) | <i>15 frames/second; synchronous reading of signal and interferometer</i> |
| Edge detection criterion | <i>50 % level dark-white light intensity</i> |
| Edge detection short term repeatability (1s) | <i>4 nm</i> |

Interferometric measurement

| Parameters | Parameters normally used for the measurement equipment | Achievable measurement uncertainty for measurands |
|--|--|---|
| Interferometer light source / wavelength | Stabilized He-Ne laser / 633 nm | $7 \cdot 10^{-9} \cdot L$ |
| Resolution of displac. Interferometer | 10 nm | 2,9 nm |
| Interferometer medium | Ambient air | |
| Refractive index: | calculated from ambient air parameters | $2,3 \cdot 10^{-8} \cdot L$ |
| => refractometer: | | |

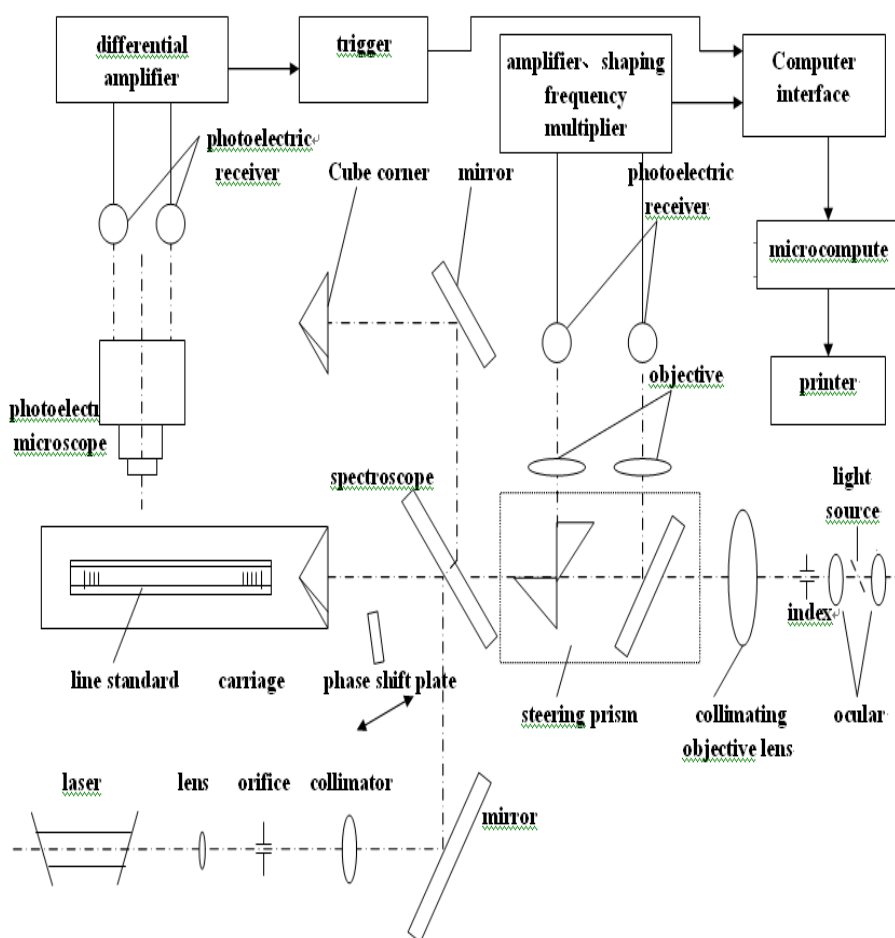
| | | |
|--------------------------|---------------------------------|--|
| => Edlen's formula: | revised Edlen's Formula | |
| Air temperature | 20±0,1°C, precision thermometer | |
| Air pressure | ~ 100 kPa, Rosemount barometer | |
| Air humidity | ~ 50%, Mitchell igrometer | |
| CO ₂ -content | Assumed to be 400 ppm | |

Other measurement conditions

| | | |
|--------------------|--|--|
| Parameters | Parameters normally used for the measurement equipment | |
| scale orientations | 0° and 180° | |
| kind of support | <i>Airy support base</i> | |
| clean room class | <i>Not classified – laboratory with filtered air</i> | |

NIM China

The line scale standards of No:2 was measured in Gauge Block and Line Scale Laboratory, Length Division, NIM. The comparator used for comparison measurement is made by NIM, which consists of He-Ne Laser with the wavelength 633 nm, main Interferometer, optical-electronic microscope, moving table, driving system, base, temperature measuring system, electronic part, computer and software. The interferometer is Mechelson type with resolution of 80 nm. The optical-electronic microscope uses dual slit to detect line position. Because the scale is transparent, the transmission light was used. Measurement starts from first line and continues till last line.



The principle diagram of Line Scale interference compactor

It took two weeks to finish total measurement. The kind of support is line contact. Four supports were used, whose positions were on the Bessel points marked on the scale. The scale was in series with the main beam path of interferometer with Abbe-error free. Scales were measured in two orientations. In one orientation two repeating measurements were made as one group. Then scale was reinstalled in reverse orientation and the instrument was readjusted such as focus and alignment and so on to eliminate possible system error. 48 groups of measurements were made, which means the Number of measurement of each scale is 96. The end result is the average of total measurement.

Measuring environment condition is as following:

| | |
|--------------------|------------------------|
| Measuring place: | normal laboratory room |
| Room temperature: | 20C±0.1C |
| Scale temperature: | 20C±0.1C |
| Humidity: | normal |
| Air pressure: | 1015.5Pa ± 3.0 Pa |

NIST USA

The 100 mm scale was measured with the NIST Line Scale Interferometer (LSI). The LSI consists of a scanning electro-optical line detector, a high precision one-axis motion system, and a high accuracy heterodyne interferometer for determining the displacement of the test artifact beneath the line detector. The wavelength of a stabilized helium-neon laser corrected for temperature, humidity, atmospheric pressure and CO₂ is used as the length standard. The instrument is housed in an environmental chamber in which all environmental properties are carefully monitored. The complete description of the design and operation of the NIST LSI is given in the Journal of Research of the National Institute of Standards and Technology Volume 104, Number 3, May-June 1999, .. *The NIST Length Scale Interferometer*. ..

Reflected light was used to obtain line images. The scale was measured in the horizontal position with scale face up and supported at the Airy points. The scale was laid on a flat glass surface, supported at left in the center at a single point with a 6 mm diameter, 0.1 mm thick paper pad and the scale was supported at the right at two points, at the edges of the scale with similar pads. This support was used to avoid slippage of the scale, due to inertia during measurement, and the three point support prevents a twisting force on the scale as well as allowing free expansion and contraction of the scale.

On the 100 mm scale there were two independent measurements. From zero to 1 mm with 0.1 mm steps and from zero to 100 mm with 5 mm steps.

Measurements were made from line center to line center using a graduation line segment of 50 μm long, in the center of the two horizontal alignment lines as indicated on page 11 fig.3 of the Technical Protocol document. Data was recorded by averaging 400 interferometer readings when the scale was stopped and servo-locked at each measured graduation line.

The environmental chamber and scale temperatures were held within ±0.005 °C of 20 °C during the measurements. The air temperature was measured close to the path of the interferometer laser beam and scale temperature was measured at three locations along the scale and the mean temperature was used for scale length corrections. The lengths are reported at a temperature of 20 °C (68 °F). A coefficient of linear thermal expansion of $5.1 \times 10^{-7} / ^\circ\text{C}$ for the quartz scale were used in normalizing the lengths to 20 °C. During measurements the average atmospheric pressure was 99825 Pa and the average relative humidity was 50 %.

Tabular description of the measurement methods and instrumentsLine detection

| Parameters | Parameters used for the measurement |
|---|---|
| Microscope type: | Scanning photoelectric microscope (See Ref. #1 p. 230) |
| Light source | White light |
| Wavelength(s) | $\approx .7$ to $.4 \mu m$ |
| Slit length (mask) | 0.08 mm |
| Slit width | 0.1 mm |
| Polarization | none |
| Coherence | NA |
| Aperture/magnification | 100 |
| Detection mode | Line image detected by photo multiplier |
| Detection principle | The left and right line edges are simultaneously detected and the line center derived by the servoing line detector circuit. (See Ref. #1 p. 230-231) |
| Detection velocity | 0 |
| Sampling frequency (image / interferometer) | 400 readings / sample |
| Edge detection criterion | Edges are detected at the 50 % intensity level. (See Ref. #1 p. 232) |
| Edge detection short term repeatability (1s) | 1 nm or less |

Displacement measurement

| Parameters | Parameters normally used for the measurement equipment | Achievable measurement uncertainty for measurands |
|---|---|--|
| Interferometer light source / wavelength | 0.6329913311 μm | 1.2×10^{-8} |
| Resolution of displacement Interferometer | 1 nm | |
| Interferometer medium | Air | |
| Refractive index: | | |
| => refractometer: | NA | |
| => Edlen's formula: | Revised 1994 | 2×10^{-8} |
| Air temperature | 20.000 $^{\circ}\text{C} \pm 0.005$ $^{\circ}\text{C}$ | 0.001 $^{\circ}\text{C}$ |
| Air pressure | 99000 to 101000 Pa | 4 Pa |
| Air humidity | 20 to 50 %R.H. | 1.2 % |
| CO ₂ -content | 400 ppm | 25 ppm |
| | | |
| Guide error | 1.5 arc sec / m | 0.1 arc sec |
| Abbe offset | Negligible | 0.2 mm |
| Alignment error: | 0.06 arc sec | |
| Interferometer | H.P. 10565 interferometer | 1 nm |
| Scale | 1 m length | 100 nm / m |

Other measurement conditions

| Parameters | Parameters normally used for the measurement equipment | Achievable measurement uncertainty for measurands |
|---|--|--|
| Scale temperature | 20.000 °C ± 0.005 °C | 0.001 °C |
| Number of repeat measurements in one scale position | 4 measurements | |
| Number of scale orientations | 2 orientations | |
| Kind of support | The scale is supported at the Airy points, on a wedge at one point and on a (one point supported) roller at the other point. | |
| Clean room class | Class 10000 | |

NMi-VSL Netherlands

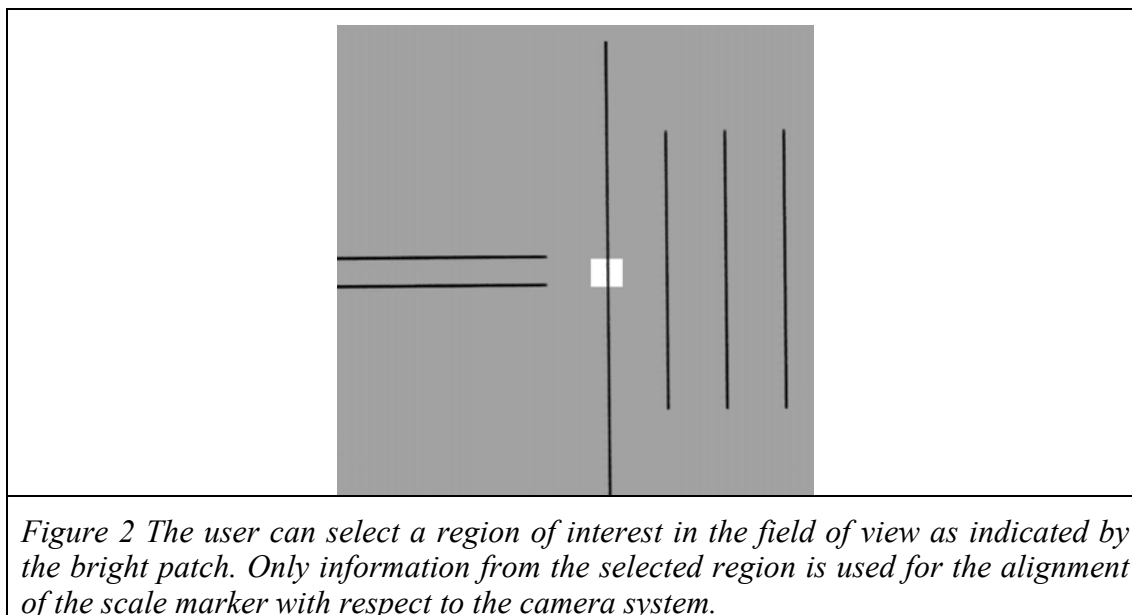
Measurement set-up.

The line scale has been measured with the set-up shown in figure 1. The set-up consists of a SIP 400 measuring machine of which only the 400 mm travel of one of the axis is used for line scale calibrations. The alignment procedure and actual measurement is performed by manually adjusting the positions.



Figure 1 Overview of the line scale calibration set-up. The line scale is positioned on a specially designed translation stage (1b) of a SIP 400 length measuring machine (1a). The structures on the scale are visualized using a video camera (2a) and a video monitor (2b). After data processing of the video signal (2c) several control signals are displayed (2d) and used for alignment of the scale with respect to the camera. The position of the scale relative to the camera is measured using a laser interferometer (3a,3b) and stored on a computer (3c). Ambient conditions are constantly monitored and up to 10 sensors can be using to record (4a,4b) the temperature of critical components.

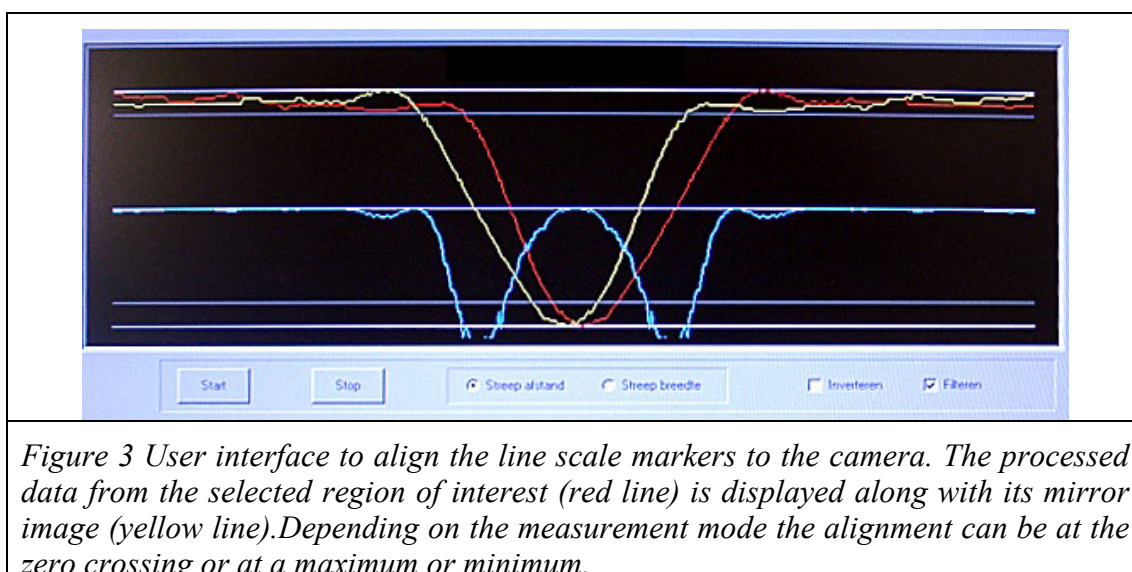
The original translation platform of the SIP 400 is replaced by a temperature controlled stage. The line scale and the retro mirror of the measurement arm are positioned onto an invar plate that is attached to the temperature controlled stage. The L-K7 line scale was supported on its Airy points.



The markers on the line scale are imaged using a CCD camera and a video monitor. A 1000 x magnification is used to image the L-K7 scale structures. In order to obtain a picture of sufficient quality additional illumination is required that is provided by optical fiber along the camera mount. To minimize heating of the scale, the amount of light is controlled to a minimum.

The SIP table with the line scale is translated manually while the movement of the table is measured by a laser interferometer.

The alignment of the scale markers to the video camera is performed by processing the camera signal with a frame grabber and a computer. In the field of view the user can select a region that will be used for the measurement, see fig. 2. The image in the selected region is processed by averaging all image lines, normalizing the result and displaying this averaged information and its mirror image on a computer screen. Accurate alignment on a line scale marker is performed by maximizing the overlap of the averaged information and its mirror image, see figure 3.



The alignment can be optimized by maximizing the overlap of the two signals. When the operator has adjusted the position of the scale to optimized alignment the data from the laser interferometer is transferred to a second computer.

The temperature of the air, line scale and SIP are continuously monitored during the calibration with a separate temperature measurement set-up. This set-up allows sequential recording of up to 10 temperature sensors. The temperature of the scale has been measured by positioning two thermistors on the scale surface above the Airy points. The thermistors were held by gravity without additional clamping. In order to keep the scale as clean as possible no thermally conductive paste was used to improve the thermal contact.

The alignment of the scale to the SIP is performed using the horizontal line structures at the left and right of the L-K7 scale. The alignment of the scale to the camera is optimized by matching the direction of the horizontal and vertical scale structures to software generated horizontal and vertical reference lines on the computer monitor. Final adjustments are optimized by rotating the line scale and/or camera and minimizing the vertical shift of the left and right horizontal lines while the scale is translated along its length.

Measurement procedure

The scale is measured both in the forward direction (0 mm to 100 mm) and in the backward direction. The center line position of the reference line (0 mm) is measured before each of the center line position of the line to be measured. During the acquisition the temperature of the air and of the scale, the air pressure and humidity are constantly monitored. These values are periodically updated when necessary (as judged by the operator) in the acquisition program for the laser interferometer. For this comparison the entire measurement has been repeated three times.

Analysis:

The analysis of the measurement data from the laser interferometer consists of averaging the values from the forward and backward series. The repeatability for a single measurement (forward and backward) is based on calculating the variance with respect to the average value for each position. The uncertainty due to the repeatability has been calculated from the square root of the averaged variances for three measurements.

NPLI India

The glass scale is fixed on sliding platform of universal measuring machine (UMM) Model – MUL -214 B (Make SIP- Switzerland). It is aligned along the 50 μ m wide parallel lines looking into locating microscope of UMM. A heterodyne laser interferometer (LI), Model - Universal calibrator 5529A, (Make Agilent-USA), is set on the sliding platform of UMM to obtain measurements of graduations of glass scale.

The edges of the desired nominal graduation are detected by looking into locating microscope. Repeatedly, laser Interferometer is initialized at zero mark on the glass scale, then the platform of UMM is moved to locate nominal graduation of the glass scale under the locating microscope of UMM. The corresponding readings are measured by the LI and evaluated to determine the deviation (dL) from each nominal length.

NRC Canada

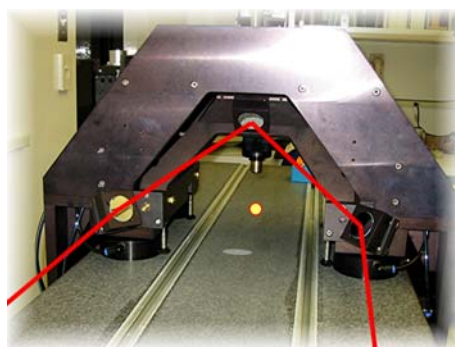
The scale was measured on the **NRC 4-metre Line Scale Comparator**. This instrument has a granite bed (L,W,H = 4500,500,800 mm) with top and side surfaces lapped flat & straight. The aluminum carriage rides the length of the bed on air bearing pucks and is constrained by opposing air pucks that press against both sides of the bed. An HP heterodyne laser interferometer measures the displacement of the carriage, and a motor drive can position the carriage to within 1 μm of a requested position from the host computer.



Line Scale Set-up & Viewing: A fixed CCD camera/microscope is mounted on the carriage looking vertically down to a focus point 100 mm above the bed. Line scales to be measured are supported at this elevation above the bed, and are fine adjusted to be level and in focus during set-up by manual elevating jack/tilting screws. The line scales are also moved sideways with respect to the focus point, to centre the linescale measurand axis to the focus-point trajectory made as the carriage moves along the bed. Special jigs with these adjustment motions hold a long scale comprised of a rigid beam at the Airy support points, whereas short scales on thin substrates, such as microscope micrometer scales, are placed flat on an elevated glass-plate platform that allows either transmitted or reflective illumination.



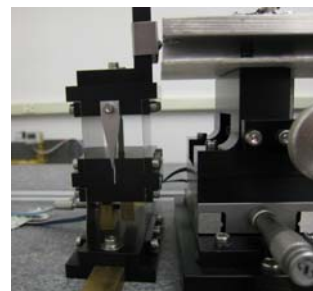
For K7, the NRC Airy-point fixtures were not suited to directly support the 100 mm scale on its Airy points, and so it was simply laid flat on the invar platform support and fixed with plastic putty at its sides.



Displacement Interferometer: The carriage displacement interferometer uses an 'open cube-corner' design that allows the interferometer measuring point to coincide with the microscope viewing point, and thereby minimize Abbe error due to carriage motion error. On the front of the carriage are 3 small plane mirrors arranged to form the open cube-corner retroreflector, with its vertex made to coincide to with the microscope focus point. The HP interferometer optics are organized at one end of the granite bed. The displacement-measuring beam is directed along one side of the bed to the carriage, where it makes the succession of

reflections off the 3 mirrors and retro-reflects back down the bed along the opposite side: the coming & going beam paths are separated by 200 mm, so that large line scale objects up to 4 metres long can be laid between them. At the interferometer end of the bed is a small stationary cube-corner prism that reverses the path of the measuring laser beam, sending it back to the

carriage, traversing the 3 mirrors, and then back into the interferometer optics where it mixes with the reference laser beam to form the interferometer displacement signal. Thus the measuring beam makes a double-pass to measure the carriage displacement along the bed. The interferometer reference beam is also turned by a retro prism, but it also makes a double pass up-and-down the bed, this time up the middle to a plane mirror on a flexure anchored to the bed and contacting the end of the line scale to be measured: in this way the interferometer reference (zero) is coupled to the zero of the line scale with the smallest material 'deadpath' between them, and automatically compensates for any mechanical shift of the scale during measurement.



For the K7 scale mounted to the invar plate, the interferometer reference-arm retro-reflector was made to spring-contact the end of the invar plate.

Displacement Corrections: Sensors measure the air temperature, pressure and humidity to correct the laser wavelength in air, and also measure the line scale and the granite bed temperature to correct for material thermal dilatation. An autocollimator monitors the carriage motion error (pitch and yaw) so that residual Abbe corrections can be applied to the carriage displacement measurements.

Data Collection: The host computer executes a script of positions to visit along the scale, via the carriage motor drive. At each position the carriage is stopped and allowed to settle, then the CCD microscope image is recorded (actually, an average of 10 successive video images), along with the interferometer reading of the actual carriage position (actually, an average of 30 or more readings taken during the video capture) as well as all the sensor and autocollimator readings, plus a time/date stamp. This allows fast collection of data to minimize drift, and then processor-intensive offline analysis of recorded data runs can be done repeatedly and at leisure, allowing exploration of changes to analysis model parameters.

Line Center Algorithm: The CCD camera captures the microscope image at high magnification (typically 250 nm/pixel), and so the 50 μm ROI (region-of-interest) 'slit height' for K7 corresponded to 200 CCD lines in the image. The NRC target-center algorithm is based on the mean of left and right edge detection. The left and right edge of the intensity profile along each CCD line in the ROI was determined using a dynamic 50% threshold criterion, and the mid-position is calculated. A straight line, with outlier rejection, was fitted through the 200 mid-position points that spanned the height of the ROI (rejecting edge roughness or contamination artifacts better than a simple average), and the mid-height position of the fitted line was reported as the effective line centre.

Camera as Null Detector: As much as possible, line centres were always determined at same central location in the CCD image for every scale line, so that measured location of each line on the line scale depended only on the carriage displacement measurement by laser interferometer, and not the magnification scale factor of the CCD image. This was accomplished by moving the carriage in five small (3 μm) successive steps about the expected carriage position that put the desired scale line in the nominal centre of the CCD image: the carriage position was measured at each step (via the laser interferometer) and the image recorded. In offline analysis, the line image center was determined for each step, expressed in camera pixel coordinates, and a trend line fitted through line-image position (in pixels) vs. carriage position (in millimetres), to calculate the effective carriage position corresponding to that line imaged at the exact center of the camera field (pixel 320.00 in a 640 pixel field). This was done for every scale line in the same way, so that most residual systematic errors would be common-mode constants that cancel when all line positions are expressed relative to the zero-line. The residuals about the 5-point line fit were

typically less than 2 nm, suggesting that the fitted line centre location was consistent and repeatable to better than 2 nm.

Data Run Design: The script, or list of required measurement positions, is created offline in MS Excel. For the K7 scale, the list consisted the 30 prescribed lines plus the zero line. After the 100 mm line measurement, the carriage was driven 5 mm further, before reversing direction and measuring the 31 lines in reverse order. After returning to measure the zero line, the carriage was driven an additional 2 mm backwards, and then driven forwards to re-measure the zero line a final time in the data run, taken in the same direction as the first measurement, so as to reveal the closing error under hysteresis conditions. Thus, a K7 data run consisted of $31 + 1 + 31 + 1 + 1 = 65$ lines. This describes data runs in the normal orientation of the scale (from 0 to the 100 mm line). A script was also designed for measuring the same lines when the scale was oriented in the reverse sense, starting a run at the 100 mm line and sequencing to the 0 line position, and then back to the 100 mm line (with the additional turn-around points as in the normal-orientation case.) Within a given data run, the forward-back repeatability of a given scale line location was the order of 20 nm, suggesting some drift problems, but differences the order of 100 nm were observed between normal and reversed orientation runs, as discussed below.

Data Runs for Reported Results: The results in the Table are the simple average of a normal-scale run, a reversed scale run and a 2nd normal scale run.

Observed Problems and Uncertainty: The NRC 4-metre Line Scale Comparator is still under development and has not yet achieved its expanded uncertainty performance goal of $U = Q[20 \text{ nm}, 0.2 \text{ ppm L}]$, where $Q[a,b]$ is the quadrature sum of a & b, and L is the distance between two scale lines (95% confidence interval). This uncertainty goal is the value expected when one applies a GUM model analysis to the customary influence factors for this type of comparator instrument, evaluated at the performance level of the modeled NRC instrument constituents.

However, during K7 data runs it was observed that after all corrections for environment, set-up and motion errors, there were still large differences between successive data runs and even larger between the normal and reverse data runs, calling for an increase in uncertainty to **$U = Q[80 \text{ nm}, 0.4 \text{ ppm L}]$** to account for the variations in the data runs. The source of the run-to-run and of the normal-to-reverse variations has not been identified yet, but may be due to failure to support the scale on the Airy points (causing unmodeled irregular bending distortions) and/or unmodeled thermal drift in the way the quartz scale is supported and fixed on the invar carrier, subject to illumination heating, and shifts/drifts in the coupling of the scale zero-line and the reference retro-reflector. NRC is investigating this aspect. Meanwhile, for the purpose of the K7 Report, NRC is not submitting a detailed GUM uncertainty model analysis while there exists such large rogue factors that dominate the performance.

NIMT Thailand

Principle of measurement:

Graduated scales of the glass scale are measured using line scale interferometer. The light source is, wavelength 633 nm passes through the vacuum chamber and bellow.

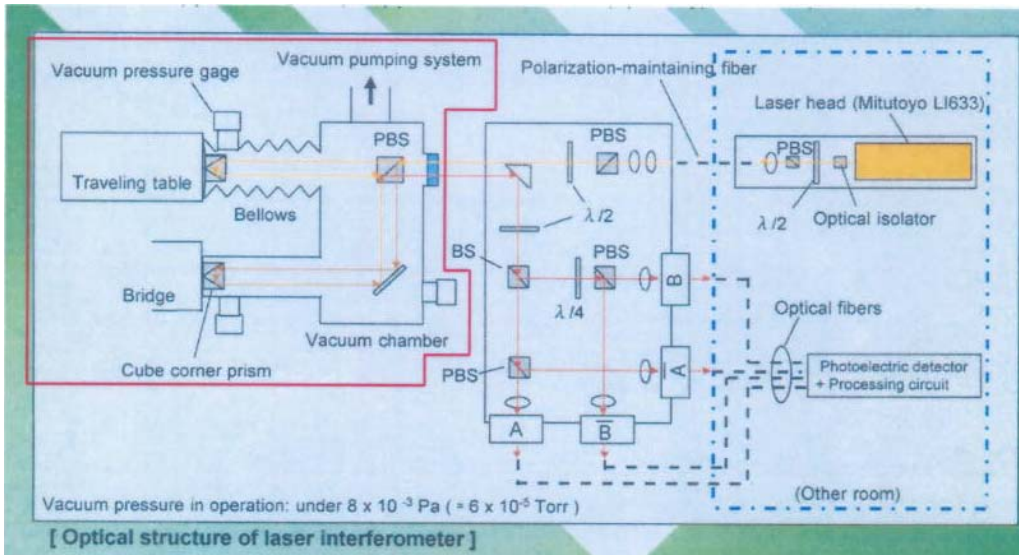


Fig I. Diagram of vacuum laser interferometer system

Resolution of the laser interferometer is approximately 0.8 nm (Referred to the manufacturer), which was calculated from $(633 \text{ nm} \times 1/2 \text{ (optical part)} \times 1/400 \text{ (electronic part)}) \cong 0.8 \text{ nm}$

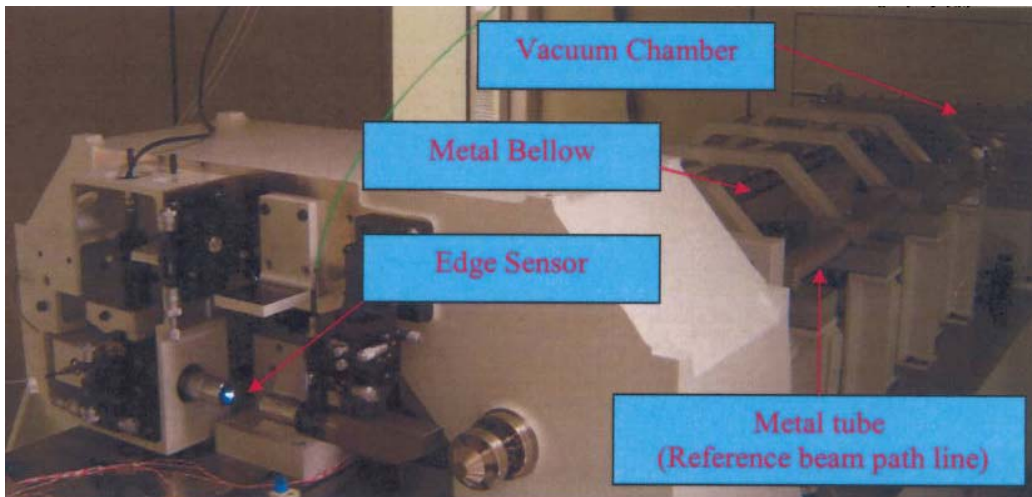


Fig2. The system of the laser interferometer

Graduated scales are detected by Edge sensor. Using triple slits system as show in Fig3.

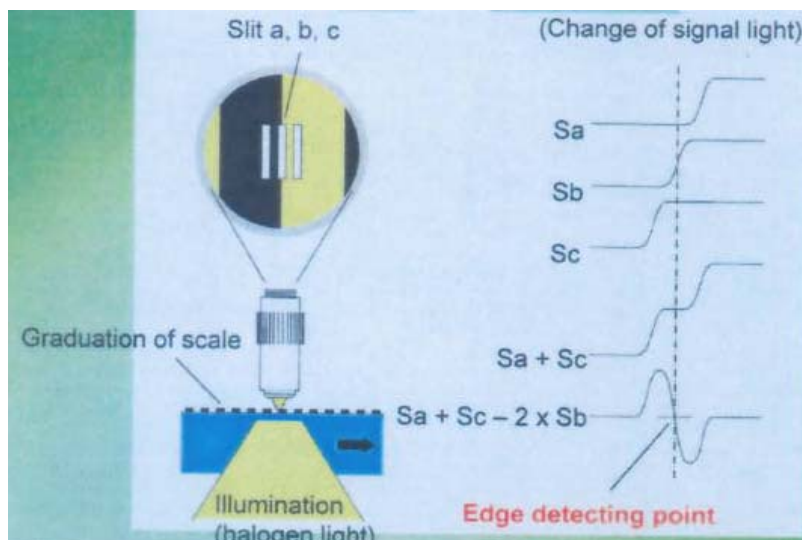


Fig3. Principle of Edge sensor

Resolution of Edge sensor is approximately 0.64 nm (Referred to the manufacturer).



Fig4. Edge sensor detection

Measurement setup:

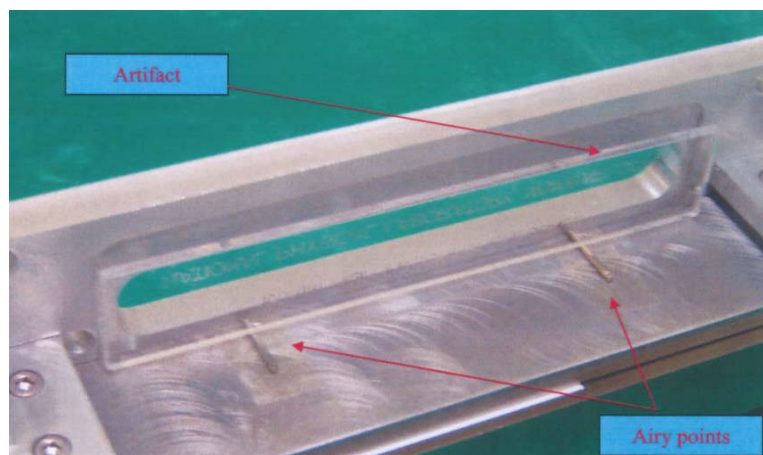


Fig5. Support and setting

Temperature measurement:

Due to artifact is small, the temperature is measured at the standard scale instead.

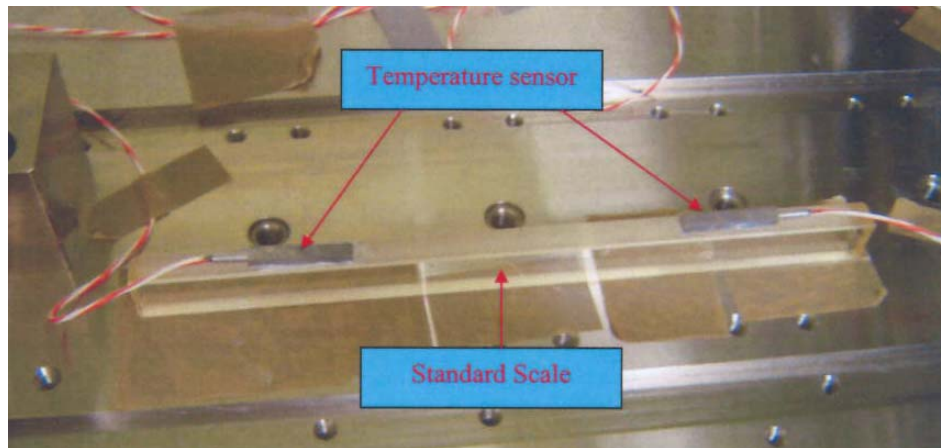


Fig6. Temperature measurement

Temperature measurement by:
Precision Thermometry Bridge with probe
Mfr: ASL, Model: F 300, Serial number: 00780303

VNIIM Rusia

An optical scheme of the comparator (Fig.1) consists of a laser polarization interferometer, a refractometer and a microscope. Parts of the laser interferometer and refractometer are fixed on a granite base. A carriage is moved over teflon supports at a distance of 1 m. As the carriage moves its rotation is not greater than $5 \mu\text{rad}$. Two reflectors of the interferometer and the confocal microscope are mounted on the carriage. The microscope focus is located on the measurement axis of the interferometer.

In the microscope there are a laser diode with a wave length of 540 nm and an objective with an aperture of 0.9. An illuminator of the microscope forms an illuminated strip with a width of $1 \mu\text{m}$. Light is reflected and forms the image in a photodiode. The length of the slot corresponds to $50 \mu\text{m}$ in the plane of a scale.

One of the two modes ($\Delta = 640 \text{ MHz}$) of the stabilized He/Ne laser is used in the interferometer, the second one is applied in the refractometer. A refractive index is measured in the process of pumping out a chamber of 1 m in length with air. Both the refractometer and interferometer have two photo diodes providing to shape the signals with a phase shift of 90° .

The scale is located on two piezo-supports. Focusing is controlled by a signal from the microscope. The measurement zone is closed by a thermal screen. Alongside the scale a platinum thermometer (10 Ohm) is located. The difference between the temperature of the scale and that of the platinum thermometer is measured with a set of differential thermocouples. The temperature inside a room is kept at a level of $20 \pm 0.1^\circ \text{C}$.

Output signals of the photo-detectors of the laser interferometer, refractometer and microscope enter the computer that is equipped with an analogue-to-digital converter with a multiplexing unit at its input.

A phase of the interference signal is calculated as *arctg* of the ratio of the signals of two photo-detectors. Parameters of the input signals are corrected. The coordinates of the scale graduation line centers are calculated at the time of joint processing of the microscope and interferometer signals. A center of gravity is calculated for that part of the graduation line profile, which is situated between the levels of 25 and 40 % of a maximum level of the signal.

Measurements are done in a dynamic mode. When the microscope is moving over the graduation line the speed of the carriage is decreased (0.05 mm/s).

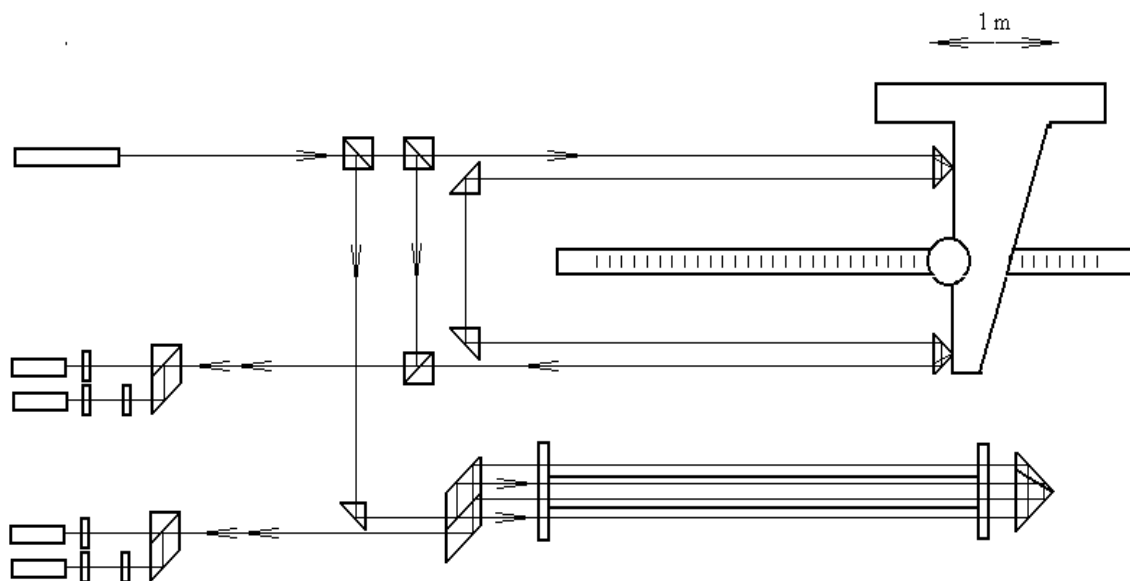


Fig.1 Optical scheme of the comparator.

Appendix 3: Reported uncertainty budgets

GROUP 1

BEV Austria

| Input quantity x_i | Distrib. | $u(x_i)$ unit | ν_i | $c_i = \partial dL / \partial x_i$ | u_i (dL) |
|---|----------|-------------------------|----------|---|-------------------------|
| p_{air} | N | 15 Pa | ∞ | $2.7 \cdot 10^{-9} \text{ Pa}^{-1} L$ | $0.04 \cdot 10^{-6} L$ |
| t_{air} | N | 0.15 °C | ∞ | $0.96 \cdot 10^{-6} \text{ °C}^{-1} L$ | $0.14 \cdot 10^{-6} L$ |
| c_{CO_2} | N | 300 ppm | ∞ | $0.14 \cdot 10^{-9} \text{ ppm}^{-1} L$ | $0.04 \cdot 10^{-6} L$ |
| n_{air} | N | $5 \cdot 10^{-8}$ | ∞ | 1 | $0.05 \cdot 10^{-6} L$ |
| t_{S} | N | 0.1 °C | ∞ | $0.5 \cdot 10^{-6} \text{ °C}^{-1} L$ | $0.05 \cdot 10^{-6} L$ |
| barometric compression δL_{κ} | N | $0.026 \cdot 10^{-6} L$ | ∞ | 1 | $0.026 \cdot 10^{-6} L$ |
| residual contributions δL_{res} | N | 5 nm | ∞ | 1 | 5 nm |
| line pos. & Abbe & orient. | N | 22 nm / 109 nm | 4 | 1 | 22 nm / 109 nm |
| <p>These errors can not easily be separated in our scheme. We use the standard deviation of 5 different calibrations (maximum of all lines) as explained on page 1 of this report.</p> <p>Values are for the 1 mm and 100 mm range, respectively.</p> | | | | | |
| | | | | | |

Since all contributions except the last one amount to only $Q[5 \text{ nm}, 0.17 \cdot 10^{-6} L]$ it is tempting to assume a constant, length independent measurement uncertainty. Since the calibration procedure is somewhat different for short range ($< 8 \text{ mm}$, mainly stage micrometers) and long range scales ($> 8 \text{ mm}$) we use two constant uncertainties. The smaller one is valid up to 1 mm, the second one from 5 mm to 100 mm.

Combined standard uncertainty: $u_c(L) = 23 \text{ nm} / 111 \text{ nm}$ (@ 1 mm / @ 100 mm)

Effective degree of freedom: $\nu_{\text{eff}}(dL) = 4 / 4$

Expanded uncertainty: $U_{95}(dL) = 65 \text{ nm} / 320 \text{ nm}$

CMI Czech Republic

| <i>Input quantity x_i</i> | <i>Distrib</i> | $u(x_i)$ | v_i | $c_i = \partial dL / \partial x_i$ | $u_i (dL) / \text{nm}$ |
|---|----------------|----------|-------|------------------------------------|------------------------|
| Resolution of edge detection | N | 1.5 nm | 1000 | 1 | 2 nm |
| Repeatability of edge detection | N | 5 nm | 30 | 1 | 5 nm |
| Interferometer resolution | N | 0.1 nm | 1000 | 1 | 0 nm |
| Interferometer nonlinearity | N | 1.0 nm | 100 | 1 | 1 nm |
| Interferometer dead path influences | N | 0.8 nm | 1000 | 1 | 1 nm |
| Drift influence | N | 0.8 nm | 100 | 1 | 1 nm |
| Influence of adjustment of measurement line + Nonlinearities of position sensing | N | 10 nm | 20 | 0.577 | 6 nm |
| Microscope axis - illumination alignment + defocusing | N | 5 nm | 10 | 1 nm/um | 5 nm |
| Influence of line edge detection algorithm, possible asymmetry of line profiles and shape | N | 10 nm | 20 | 1 | 10 nm |
| Microscope magnification (or other position deviation sensing device) | N | 0.1 nm | 20 | 138.0 nm/pix | 7 nm |
| repeatability of scale preparation (bending by fixing, cleaning, ...) | N | 12 nm | 3 | 0.577 | 7 nm |
| δl_{win} Influence of adjustment of measurement window or slit length | N | 5 nm | 5 | 0.707 | 4 nm |
| Errors due to Abbe offsets and pitch and yaw of translation stages at one position) | N | 1 nm | 1000 | 1 | 1 nm |
| total constant part of u | | | | | 17 nm |
| v_{eff} | | | 58 | | |

| | | | | | |
|--|---|----------|------|-------------|-----------------|
| Possible contributions from interferometric displacement measurement technique: | | | | | |
| λ_0 vacuum wavelength of light source used for displacement measurement | N | 5.0E-11 | 1000 | 1 | 5.0E-11 |
| n_{air} Index of refraction of air2 | N | 1.0E-08 | 1000 | | |
| t_{air} Air temperature | N | 1.0E-02 | 20 | 9E-7 /K | 9.0E-09 |
| p_{air} Air pressure | N | 5E-2 hPa | 1000 | 2E-7 /hPa | 1.2E-08 |
| RH_{air} Air humidity | N | 1.0E-02 | 1000 | 1E-8 /% | 1.0E-10 |
| c_{CO2} Air CO2 concentration | N | 100 ppm | 1000 | 1.5E-10/ppm | 1.5E-08 |
| δl_{Ai} Errors due to Abbe offsets and pitch and yaw of translation stages | N | 1.7E-07 | 1000 | 1 | 1.7E-07 |
| δl_{Si} Errors of scale alignment | N | 2.5E-09 | 1000 | 1 | 2.5E-09 |
| δl_{Ii} Cosine errors of interferometer alignment | N | 5.6E-09 | 1000 | 1 | 5.6E-09 |
| systematic distortion of measurement frame with movement | N | 5.0E-09 | 1000 | 1 | 5.0E-09 |
| Possible contributions from scale properties: | | | | | |
| α_Z, Cr Linear coefficient of thermal expansion of scale material | N | 0.0750 K | 1000 | 1E-6/K | 7.5E-08 |
| κ_Z, Cr Linear coefficient of compressibility of scale material | N | 750 Pa | 1000 | 9.0E-12 /Pa | 6.8E-09 |
| δ_{supp} Influence of support conditions | N | 2.3E-08 | 1000 | 1 | 2.3E-08 |
| total relative part of u | | | | | 1.92E-07 |
| v_{eff} | | | 1683 | | |

Combined constant part of standard uncertainty for one line position: $u_c=17$ nm
Combined constant part of standard uncertainty for one line distance from zero line, for three independent measurement (including removal and re-alignment) $u_c=14$ nm

Combined standard uncertainty $u_c(L)=Q[14;192*L]$ nm, L in m

Effective degree of freedom: $\nu_{eff} = 58 ; 1683$

Expanded uncertainty: $U_{95}(L) = Q[28;377*L]$ nm, L in m

DZM Croatia

| Input quantity x_i | Distrib. | $u(x_i)$ unit | ν_i | $c_i = \partial dL / \partial x_i$ | $u_i (dL) / \text{nm}, L \text{ in mm}$ |
|---|----------|--------------------------------|---------|--|---|
| Stage: | | | | | |
| Error due to Abbe offset in z ($a_p < 0.5 \text{ mm}$) and pitch, δl_{Ap} | R | 10 | 100 | 1 | 10 |
| Error due to Abbe offset in x, y ($a_y < 1 \text{ mm}$) and yaw, δl_{Ay} | R | 15 | 100 | 1 | 15 |
| Interferometer: | | | | | |
| Interferometer wavelength, $\delta \lambda$ | R | 0,03 | 100 | L | $0,03 \cdot L$ |
| Air temperature, t_{air} | R | $0,12 \text{ }^\circ\text{C}$ | 100 | $9,5 \cdot 10^{-7} L / ^\circ\text{C}$ | $0,112 \cdot L$ |
| Air pressure, p_{air} | R | 13 Pa | 100 | $2,7 \cdot 10^{-7} L / \text{Pa}$ | $0,035 \cdot L$ |
| Relative Humidity, RH_{air} | R | 0,06 | 100 | $8,5 \cdot 10^{-7} L$ | $0,050 \cdot L$ |
| Edlen equation uncertainty, δn_{air} | N | $2 \cdot 10^{-8}$ | 100 | L | $0,020 \cdot L$ |
| Interf. cosine error δl_{li} | R | $0,8L$ | 100 | 1 | $0,80 \cdot L$ |
| Scale: | | | | | |
| Scale temperature difference from $20 \text{ }^\circ\text{C}$, Δt_s | R | $0,036 \text{ }^\circ\text{C}$ | 100 | $5 \cdot 10^{-7} L / \text{K}$ | $0,018 \cdot L$ |
| Errors of scale alignment, δl_{si} | R | $0,55L$ | 27 | 1 | $0,55 \cdot L$ |
| Movement of scale due to bending, δl_{ai} | R | $0,2L$ | 100 | 1 | $0,2 \cdot L$ |
| Influence of line edge quality δE_{alg} | R | 10 | 49 | 1 | 10 |
| Measurement: | | | | | |
| Overall reproducibility, R | N | 55 | 27 | 1 | 55 |
| Interferometer resolution, δl_{res} | R | 6 | 100 | 1 | 6 |
| Reproducibility of line detection, S_E | N | 35 | 27 | 1 | 35 |
| Interferometer dead path influences, δl_{DP} | R | 30 | 100 | 1 | 30 |

Combined standard uncertainty:

$$u_c(L) = (75 + 0,5 \cdot L) \text{ nm}, L \text{ in mm}$$

Effective degree of freedom:

$$\nu_{\text{eff}}(dl) = 211, \quad L = 100 \text{ mm}$$

Expanded uncertainty:

$$U_{95}(dl) = (150 + 1 \cdot L) \text{ nm}, L \text{ in mm}$$

GUM Poland

| Input quantity x_i | Distrib. | $u(x_i)$ unit | ν_i | $c_i = \delta dL / \delta x_i$ | $u_i(dL) / \text{nm}$ |
|---|----------|-----------------------------------|---------|--|-----------------------|
| Line position sensing | | | | | |
| Repeatability of edge detection s_E | N | 130,0 nm | 7 | 1 | 130,0 |
| Reproduceability s_R | N | 1 | 7 | L | L |
| Influence of adjustment of measurement line $\delta_{l_{pos}}$ | N | 30,0 nm | 9 | 1 | 30,0 |
| Interferometric displacement measurement | | | | | |
| Vacuum wavelength of light source used for displacement measurement λ_o | N | $2,45 \cdot \lambda_o$ nm | 100 | L/λ_o | $0,00245L$ |
| Index of refraction of air n_{air} | N | $1 \cdot 10^{-8}$ | 100 | L | $0,010L$ |
| Air temperature t_{air} | N | 51,6 mK | 100 | $9,57 \cdot 10^{-7} \cdot L/K$ | $0,0494L$ |
| Air pressure p_{air} | N | 6,3 Pa | 100 | $2,68 \cdot 10^{-9} \cdot L/\text{Pa}$ | $0,0169L$ |
| Air humidity RH_{air} | N | 0,462 % | 100 | $8,67 \cdot 10^{-9} \cdot L/RH\%$ | $0,004L$ |
| Air CO ₂ concentration c_{CO2} | R | 57,7 ppm | 100 | $1,45 \cdot 10^{-10} \cdot L/\text{ppm}$ | $0,0084L$ |
| Interferometer resolution δ_{Res} | R | 2,9 nm | 100 | 1 | 2,9 |
| Interferometer nonlinearity δ_{NL} | R | 2,3 nm | 100 | 1 | 2,3 |
| Interferometer dead path influences δ_{DP} | R | 8,1 nm | 100 | 1 | 8,1 |
| Errors due to Abbe offsets and pitch and yaw of translation stages δ_{Ai} | R | 7,8 nm | 100 | 1 | 7,8 |
| Errors of scale alignment δ_{Si} | R | 1,2 nm | 100 | L | $0,0012L$ |
| Cosine errors of interferometer alignment δ_{Ii} | R | 18 nm | 100 | L | $0,018L$ |
| Scale properties | | | | | |
| Linear coefficient of thermal expansion of scale material α | R | $2,89 \cdot 10^{-8} / K$ | 100 | $L \cdot 0,14 K$ | $0,004L$ |
| The difference of the scale temperature t_s in °C during the measurement from the reference temperature of 20 °C Δt_s | N | 0,0173 K | 100 | $5 \cdot 10^{-7} \cdot L/K$ | $0,0087L$ |
| Linear coefficient of compressibility of scale material κ | N | $5,14 \cdot 10^{-13} / \text{Pa}$ | 100 | $L \cdot 1170 \text{ Pa}$ | $0,0006L$ |

| | | | | | | |
|---|-----------------|---|---------|-----|--|-----------|
| Variations of air pressure during measurement | Δp_s | N | 6,29 Pa | 100 | $8,9 \cdot 10^{-12} \cdot L/\text{Pa}$ | $0,0001L$ |
| Influence of support conditions | δ_{supp} | R | 0,6 nm | 100 | 1 | 0,6 |

Combined standard uncertainty: $u_c(L) = Q [134 ; 1,00 \cdot L]$ nm, L in mm

Effective degree of freedom: $\nu_{eff}(dl) = 181$ $L = 100$ mm

Expanded uncertainty: $U_{95}(dl) = Q [268 ; 2,00 \cdot L]$ nm; L in mm

INM Romania

| Input quantity x_i | Distrib. | $u(x_i)$ unit | ν_i | $c_i = \partial dL / \partial x_i$ | $u_i (dL) / \text{nm}$ |
|--|------------------------------|--|---------|--|------------------------|
| repeatability of the measurement | normal type A | 0.05 μm | 19 | 1 | 50 |
| thermal coefficient of expansion | rectangular | $0.5 \cdot 10^{-6} \text{K}^{-1}$ | 50 | $L \cdot \Delta t$ $\Delta t = 0,5 \text{ } ^\circ\text{C}$ | 250L |
| temperature: -calibration of thermometer - reading error | normal type B trapezoidal | 0.025 $^\circ\text{C}$ 0.003 $^\circ\text{C}$ | 8 | αL | 25L |
| comparator certificate | normal type B | 0.05+0.1L, μm | 10 | 1 | 50+100L |
| wavelength correction due to the environmental parameters | normal type B | 0.022L, μm | 50 | 1 | 22L |
| deviation of the flatness of the mirrors of retro-reflectors | rectangular | 0.08 μm | 50 | 1 | 46 |
| cosines angle | rectangular | 0.002L, μm | 50 | 1 | 2L |
| time of data acquisition | rectangular | 0.012 μm | 50 | 1 | 12 |
| Line scale alignment | rectangular | 0.02 μm | 50 | 1 | 20 |
| Rotation of the carriage | rectangular | 0.05 | 50 | 1 | 50 |
| | | | | | |

Combined standard uncertainty: $u_c(L) = [101,272L] \text{ nm};$

Effective degree of freedom: $\nu_{\text{eff}}(dl) = 100$

Expanded uncertainty: $U_{95}(dl) = [202,544L] \text{ nm}$

LNMC Latvia

| Input quantity x_i | Distrib. | $U(x_i)$ μm | ν_i | $c_i = \partial dL / \partial x_i$ | $u_i(dL) / \mu\text{m}$ |
|---|----------|------------------------|---------|------------------------------------|-------------------------|
| Reference scale $(0,03+2 \cdot 10^{-7}L)$ δl_s | N | 0,030 | >100 | 1 | 0,009 |
| Repeatability l_R | R | 0,7 | >100 | 1 | 0,7 |
| Scale resolution δl_X | R | 0,2 | >100 | 1 | 0,12 |
| Influence of focal length variation $\delta_{E_{\text{foc}}}$ | R | 0,3 | >100 | 1 | 0,17 |
| Eccentricity coil of helical grid δl_u | R | 0,2 | >100 | 1 | 0,12 |
| Difference in T between reference scale and comparator $T = \pm 0,3^\circ\text{C}$ $\alpha = (10,4 \cdot 10^{-6}) \delta t$ | R | 0,3 | >100 | $10,4 \cdot 10^{-6} L$ | 0,36 |
| Deviation of the laboratory T from the reference scale $T = (20 \pm 2)^\circ\text{C}$ $\pm 0,1 \cdot 10^{-6} \Delta t$ | R | 2 | >100 | $0,1 \cdot 10^{-6} L$ | 0,012 |
| Deviation of the laboratory T from the comparator $T = (20 \pm 2)^\circ\text{C}$ $\pm 0,1 \cdot 10^{-6} \Delta t$ | R | 2 | >100 | $0,1 \cdot 10^{-6} L$ | 0,012 |
| | | | | | |
| | | | | | |
| | | | | | |
| | | | | | |
| | | | | | |
| | | | | | |
| | | | | | |

Combined standard uncertainty: $u_c(L) = 0,823 \mu\text{m}$

Effective degree of freedom: $\nu_{\text{eff}}(dl) =$

Expanded uncertainty: $U_{95}(dl) = 1,647 \mu\text{m}$

METAS Switzerland

| Name and symbol x_i (unit) | distrib. | $u(x_i)$ | ν_i | for 100 mm | | const | rel. to L |
|---|----------|----------|---------|-----------------|---------------|---------------|--------------|
| | | | | $c_i = dl/dx_i$ | $u_i(dl) /nm$ | $u_i(dl) /nm$ | $u_i(dl) /L$ |
| Translation stage: | | | | | | | |
| Yaw of x-axis δ_{yaw} (μrad) | R | 3.36 | 100 | 5.77E-07 | 1.12 | 1.12 | |
| Pitch of x-axis δ_{pitch} (μrad) | R | 3.36 | 100 | 2.89E-07 | 0.56 | 0.56 | |
| Parameter: Abbe offset z δ_{Az} (mm) | R | 0.5 | | | | | |
| Parameter: Abbe offset x δ_{Ax} (mm) | R | 1 | | | | | |
| Interferometer: | | | | | | | |
| Vacuum wavelength λ_0 (nm) | N | 5E-06 | 10 | 1.58E-01 | 0.79 | | 7.9E-09 |
| Air temperature t_{air} ($^{\circ}C$) | N | 0.05 | 8 | 9.02E-05 | 4.51 | | -4.5E-08 |
| Air pressure p_{air} (mbar) | N | 0.05 | 4 | 2.68E-05 | 1.34 | | 1.3E-08 |
| Air humidity RH_{air} (%rel.) | N | 0.75 | 4 | 8.50E-07 | 0.64 | | -6.4E-09 |
| Air CO2 concentration c_{CO2} (ppm) | R | 60 | 4 | 1.38E-08 | 0.48 | | 4.8E-09 |
| Edlen equation n_{air} (rel.) | N | 1E-08 | 100 | 1.00E+02 | 1.00 | | 1.0E-08 |
| Interf. Deadpath δ_{DP} (mm) | N | 10 | 10 | 1.55E-07 | 1.55 | 1.55 | |
| Parameter: Change of n (1) | R | 3E-07 | | | | | |
| Interf. nonlinearity δ_{NL} (nm) | N | 3 | 10 | 1.00E-06 | 3.00 | 3.00 | |
| Interf. cosine error δ_b (μrad) | R | 130 | 10 | 6.50E-09 | 0.49 | | 4.9E-09 |
| Imaging: | | | | | | | |
| Microscope magnification Mag (%) | R | 0.2 | 10 | 1.15E+01 | 1.33 | 1.33 | |
| CCD orientation $\delta \alpha_{CCD}$ ($^{\circ}$) | R | 0.01 | 10 | 3.49E+01 | 0.20 | 0.20 | |
| Parameter: x-positioning d_{pos} (μm) | R | 2 | | | | | |
| Image distortion $\delta_{E_{img}}$ (%) | R | 0.05 | 10 | 6.00E+01 | 1.73 | 1.73 | |
| Parameter: half linewidth HLW (μm) | N | 6 | | | | | |
| Microscope focus stage: | | | | | | | |
| Focal length variation $\delta_{E_{foc}}$ (μm) | R | 0.2 | 10 | 1.00E-06 | 0.12 | 0.12 | |
| Microscope alignment xz $\delta_{E_{align}}$ ($^{\circ}$) | R | 0.12 | 10 | 3.49E-06 | 0.24 | 0.24 | |
| Ref. mirror alignment xz $\delta_{RMalign}$ ($^{\circ}$) | R | 0.03 | 10 | 6.98E-05 | 1.21 | 1.21 | |
| Pitch of z-axis zx $\delta_{E_{pitch}}$ ($\mu rad/\mu m$) | R | 0.015 | 10 | 7.62E-05 | 0.67 | 0.67 | |
| Roll of z-axis δE_{roll} ($\mu rad/\mu m$) | R | 0.01 | 10 | 4.00E-06 | 0.02 | 0.02 | |
| Parameter: focus-range dF (μm) | R | 4 | | | | | |
| Param.: Int. ref. beam offset (mm) | R | 19.05 | | | | | |

| Name and symbol x_i (unit) | distrib. | $u(x_i)$ | ν_i | for 100 mm | | const | rel. to L |
|---|----------|----------|---------|---|-----------------------|-------|-------------|
| | | | | $c_i = dl/dx_i$ | $u_i(dl) / \text{nm}$ | | |
| | | | | | | | |
| Scale properties: | | | | | | | |
| Scale alignment horiz. δ_{sh} (μrad) | R | 40 | 10 | 2.00E-09 | 0.05 | | 4.6E-10 |
| Scale alignment vert. δ_{sv} (μrad) | R | 100 | 10 | 5.00E-09 | 0.29 | | 2.9E-09 |
| Temperature deviation Δt_s (K) | N | 0.05 | 10 | 5.00E-05 | 2.50 | | 2.5E-08 |
| Thermal exp. coef. α_s (1/K) | R | 1E-07 | 10 | 7.00E+00 | 0.40 | | 4.0E-09 |
| Pressure variation s_{air} (mbar) | R | 0.1 | 10 | 8.90E-08 | 0.01 | | -5.1E-11 |
| Compressibility κ_s (1/bar) | R | 2E-07 | 10 | 6.50E+00 | 0.75 | | 7.5E-09 |
| Scale support δ_{supp} (nm/100mm) | N | 4 | 10 | 1.00E-06 | 4.00 | | 4.0E-08 |
| Measurement line def. δ_{pos} (μm) | R | 5 | 10 | 6.05E-07 | 1.75 | 1.75 | |
| Parameter: Line parallelity ($^\circ$) | R | 0.06 | | | | | |
| Line quality and evaluation δ_{eval} (nm) | R | 3 | 8 | 1.00E-06 | 1.73 | 1.73 | |
| Illumination inhomogeneity δ_{illum} (nm) | R | 2 | 4 | 1.00E-06 | 1.15 | 1.15 | |
| | | | | | | | |
| Measurement: | | | | | | | |
| Repeatability of line det. s_E (nm) | N | 6 | 16 | 1.00E-06 | 6.00 | 6.00 | |
| | | | | | | | |
| Total U_c (1S) | | | | | 10.5 | 7.9 | 6.9E-08 |
| Total U_{95} | | | | | 21.0 | 15.9 | 1.4E-07 |
| General expression: | | | | $U_{95} = Q(16 \text{ nm} ; 1.4E-07 * x)$ | | | |

In general for any length L :

$$u_c = Q(7.9 \text{ nm} , 6.9E-08 * L)$$

$$U_{95} = Q(16 \text{ nm} , 1.4E-07 * L)$$

with $Q(a,b) = (a^2 + b^2)^{1/2}$

For 100 mm:

Combined standard uncertainty: $u_c(L) = 10.5 \text{ nm}$

Effective degree of freedom: $\nu_{\text{eff}}(dl) = 70 \rightarrow k=1.99$

Expanded uncertainty: $U_{95}(dl) = 21.0 \text{ nm}$

MIKES Finland

| Input quantity x_i | Distrib. | $u(x_i)$ unit | ν_i | $c_i = \partial dL / \partial x_i$ | $u_i (dL) / \text{nm}$ |
|---|----------|---------------------|---------|------------------------------------|------------------------|
| Repeatability(all components of type A n=20) | Std. | 20.0 nm | 19 | 0.23 | 4.6 |
| Influence of line detection algorithm with line quality, δE_{alg} | Std. | 9 nm | 4 | 1 | 9.0 |
| Vacuum wavelength of laser, λ_0 | Std. | 4×10^{-9} | 100 | 1 L m | 4.0 L |
| Index of refraction of air, effect of equation, n_{air} | Std. | 10×10^{-9} | 100 | 1 L m | 10 L |
| Air temperature, t_{air} | Std. | 0.015 K | 4 | 960 L nm/K | 14 L |
| Dew point of air, DP | Std. | 0.200 K | 4 | 30 L nm/K | 6.0 L |
| Air pressure, p_{air} | Std. | 5.0 Pa | 4 | 2.7 L nm/Pa | 14 L |
| Air CO ₂ concentration, c_{co2} | Std. | 50 ppm | 4 | 0.2 L nm/ppm | 7.5 L |
| Linear coeff. of thermal expansion, α | Std. | 500 nm/m/K | 1 | 0.020 L Km | 10 L |
| Scale temp. difference from 20 °C, Δt_s | Std. | 0.010 K | 2 | 500 L nm/K | 5.0 L |
| Error due to Abbé offsets; pitch and yaw, δl_A | Std. | 3.0 nm/0.1m | 4 | 1 L | 30 L |
| Effect of diffraction of laser beam, | Std. | 8 nm | 2 | 1 L | 8.0 L |
| Errors of scale alignment, δl_s | Std. | 1 nm | 10 | 1 L | 1.0 L |
| Effect of compressibility, K | Rect. | 0.020 bar | 4 | 900 L nm/bar | 18 L |
| Effect of flatness dev. of the scale & microscope alignm., δh | Std. | 5 nm | 3 | 1 | 5.0 |
| | | | | | |

Combined standard uncertainty: $u_c(L) = Q[11.3; 45 L]$ nm, L in meters

Effective degree of freedom: $\nu_{\text{eff}}(L) = 12 \Rightarrow k=2.2$

Expanded uncertainty: $U_{95}(L) = Q[25; 99 L]$ nm, L in meters

For lines 0.1; 0.4; 85; 90 and 95 mm the uncertainty due to line quality is higher than in the above budget based on non-idealities seen in the visual inspection (see receipt confirmation report from MIKES). The estimated expanded uncertainties for these lines are 54; 54; 55; 55 and 55 nm respectively.

MIRS Slovenia

| Input quantity x_i | Distrib. | $u(x_i)$ | ν_i | $c_i = \partial dL / \partial x_i$ | $u_i(dL)$, nm, L in mm |
|--|----------|--|---------|---|--|
| wavelength drift, ΔL | R | $2,4 \cdot 10^{-9} \cdot L$ | 4 | 1 | $2,4 \cdot 10^{-9} \cdot L$ |
| Counting system | R | $5 \text{ nm} + 2,5 \cdot 10^{-8} \cdot L$ | 3 | 1 | $5 \text{ nm} + 2,5 \cdot 10^{-8} \cdot L$ |
| Correction factor | R | $2,5 \cdot 10^{-8} \cdot L$ | 3 | 1 | $2,5 \cdot 10^{-8} \cdot L$ |
| Wavelength correction for environmental influences, λ_{cor} | R | $2,8 \cdot 10^{-7} \cdot L$ | 3 | 1 | $2,8 \cdot 10^{-7} \cdot L$ |
| uncertainty of determination of the scale mark center, s | R | 26 nm | 100 | 1 | 26 |
| distance between the measurement and reference position in the video window, L_v | N | 25 nm | 100 | 1 | 25 |
| LI indication in reference position, $L_{L\text{ref}}$ | N | 25 nm | 100 | 1 | 25 |
| linear temperature expansion coefficient, α_m | R | $1,15 \cdot 10^{-6} \text{ }^\circ\text{C}^{-1}$ | 100 | $1 \text{ }^\circ\text{C}^{-1} \cdot L$ | $1,15 \cdot 10^{-6} \cdot L$ |
| temperature deviation, θ_m | N | $0,1 \text{ }^\circ\text{C}$ | 100 | $0,2 \cdot 10^{-6} \text{ }^\circ\text{C}^{-1} \cdot L$ | $0,2 \cdot 10^{-7} \cdot L$ |
| cosine error, e_{cos} | N | 0 | 100 | 1 | 0 |
| random error caused by uncontrolled mechanical changes, e_{ems} | N | 29 nm | 100 | 1 | 29 |
| measuring table inclination, e_a | R | 30 nm | 100 | 1 | 30 |

Combined standard uncertainty:

$$u_c(L) = (61 + 1,2 \cdot L) \text{ nm}, L \text{ in mm}$$

Effective degree of freedom:

$$\nu_{\text{eff}}(dl) = 520; L = 100 \text{ mm}$$

Expanded uncertainty:

$$U_{95}(dl) = (122 + 2,4 \cdot L) \text{ nm}, L \text{ in mm}$$

NCM Bulgaria

| Input quantity x_i | Distrib. | $u(x_i)/$ unit | ν_i | $c_i = \partial dL/\partial x_i$ | $u_i (dL)/$ nm |
|---|----------|-----------------------|---------|----------------------------------|----------------|
| Vacuum wavelength λ_0 | N | $8 \cdot 10^{-6}$ nm | 100 | L/λ | $13 \cdot L$ |
| Index of refraction of air n_{air} | - | $16 \cdot 10^{-8}$ | - | L/n | $160 \cdot L$ |
| Scale temperature Δt_s | - | 0,02 K | - | $\alpha \cdot L$ | $10 \cdot L$ |
| Linear coefficient of thermal expansion α_z | - | $4 \cdot 10^{-8}$ 1/K | - | $(t-20) \cdot L$ | $3 \cdot L$ |
| Cosine error δl_{li} | R | 230 μ rad | 5 | $0,4 \cdot L$ nm/ μ rad | $92 \cdot L$ |
| Error of scale alignment δl_{si} | R | 405 μ rad | 6 | $0,7 \cdot L$ nm/ μ rad | $284 \cdot L$ |
| Edge geometry influence δ_{Edef} | R | 23 nm | 4 | 1 | 23 |
| Influence of line edge detection algorithm δ_{Ealg} | R | 17 nm | 8 | 1 | 17 |
| Error due to Abbe offset δl_{Ai} | R | 40 nm | 5 | 1 | 40 |
| Influence of detection light wavelength $\delta l_{E\lambda}$ | N | 14 nm | 10 | 1 | 14 |
| Influence of focal length variation δ_{Efoc} | R | 35 nm | 6 | 1 | 35 |
| Influence of measurement in reversed orientation δl_{Rev} | R | 38 nm | 5 | 1 | 38 |
| Interferometer nonlinearity δl_{NL} | R | 15 nm | 5 | 1 | 15 |
| Repeatability of edge detection s_E | N | 24 nm | 20 | 1 | 24 |

Combined standard uncertainty: $u_c(L) = Q[78; 340 \cdot L]$ nm, L in m

Effective degree of freedom: $\nu_{\text{eff}}(d_i) =$ from 29 to 37

Expanded uncertainty: $U_{95}(dL) = Q[158; 690 \cdot L]$ nm, L in m ($k=2,03$)

NML Ireland

| Input quantity x_i | Distrib. | $u(x_i)$ unit | ν_i | $c_i = \partial dL / \partial x_i$ | $u_i (dL) / \text{nm}$ |
|----------------------------------|----------|---------------|----------|------------------------------------|------------------------|
| Calibration uncertainty of Laser | N | 20 | ∞ | 1 | 20 |
| | | | | | |
| Performance of Laser (1.7ppm) | R | 98.15 | ∞ | 1 | 98.15 |
| | | | | | |
| Laser System Resolution | R | 5.77 | ∞ | 1 | 5.77 |
| | | | | | |
| Temperature Corrections | R | 0.029 | ∞ | 750nm/°C | 216.51 |
| | | | | | |
| Cosine Error | R | 3.87 | ∞ | 1 | 3.87 |
| | | | | | |
| Line Scale Pitch & Yaw Error | R | 11.55 | ∞ | 1 | 11.55 |
| | | | | | |
| Repeatability | N | 700nm | 4 | 1 | 700 |
| | | | | | |
| | | | | | |
| | | | | | |
| | | | | | |
| | | | | | |
| | | | | | |
| | | | | | |

Combined standard uncertainty: $u_c(L) = 739.58 \text{ nm}$

Effective degree of freedom: $\nu_{\text{eff}}(dl) = 5$

Expanded uncertainty: $U_{95}(dl) = 1479.16 \text{ nm}$

NPL United Kingdom

| TYPE A UNCERTAINTIES | Magnitude | Magnitude assuming a Rectangular Distribution |
|-------------------------------------|-------------------------------|---|
| Thermal Expansion Of Microscope | 1.25 parts in 10 ⁸ | 3.61 parts in 10 ⁸ |
| Vibration | Contributes to St Dev | Contributes to St Dev |
| Positioning / Setting Repeatability | Contributes to St Dev | Contributes to St Dev |
| Focusing | Contributes to St Dev | Contributes to St Dev |

| TYPE B UNCERTAINTIES | Magnitude | Magnitude assuming a Rectangular Distribution |
|--|---|---|
| Laser Frequency | 1.3 parts in 10 ⁸ | 3.67 parts in 10 ⁹ |
| Refractive Index (Air Refractometer Value) | 8.8 parts in 10 ⁸ (or 2.0 parts in 10 ⁸) | 2.54 parts in 10 ⁸ (or 5.77 parts in 10 ⁹) |
| Angular Stability Of Stage | 1.5 parts in 10 ⁸ | 4.52 parts in 10 ⁹ |
| Thermal Expansion Of Scale | 1.5 parts in 10 ⁷ | 2.05 parts in 10 ⁷ |
| Alignment Of Lasers | 1.25 parts in 10 ⁷ | 3.61 parts in 10 ⁸ |
| Alignment Of Scale | 2.83/ L ² | 0.817/ L ² |

The Standard Uncertainty may now be expressed as:

$$\text{Standard Uncertainty} = \sqrt{\left((6.57 \times 10^{-8})^2 + \left(\frac{0.817}{L^2} \right)^2 \right) \times L^2 + (3.61 \times 10^{-9})^2 + \left(\frac{1.32}{\sqrt{3}} SD \right)^2}$$

hence;

$$\text{Standard Uncertainty} = \sqrt{\left(4.32 \times 10^{-15} + \frac{0.667}{L^4} \right) \times L^2 + 1.3 \times 10^{-17} + \left(\frac{1.32}{\sqrt{3}} SD \right)^2}$$

Therefore;

$$\text{Standard Uncertainty} = \sqrt{\left(4.32 \times 10^{-15} \times L^2 \right) + \frac{0.667}{L^2} + 1.3 \times 10^{-17} + \left(\frac{1.32}{\sqrt{3}} SD \right)^2}$$

Where L is the length of the scale or graticule in μm, and SD is the standard deviation of the measurements in μm.

NSCIM Ukraine

| Input quantity x_i | Distrib | $u(x_i)$ | ν_i | $c_i = \partial dL / \partial x_i$ | $u_i = c_i u_{x_i}$, nm |
|--|---------|------------------------------------|-------------------|---|---|
| Inaccuracy of measuring the order of interference | N | 14 nm | 10 | 1 | 14 |
| Wavelength reproduction error | R | $1.8 \cdot 10^{-9}$ | 100 | L | $0.002 \cdot 10^{-6} L$ |
| Inaccuracy of measuring the air parameters: pressure temperature humidity | R | 0.1 mm Hg 0.005 °C 0.1 mm Hg | 100 100 100 | $0.357 \cdot 10^{-6} L$ $0.927 \cdot 10^{-6} L$ $0.056 \cdot 10^{-6} L$ | $0.036 \cdot 10^{-6} L$ $0.005 \cdot 10^{-6} L$ $0.006 \cdot 10^{-6} L$ |
| Inaccuracy of measuring the scale temperature | R | 0.005 °C | 100 | αL $\alpha = 5 \cdot 10^{-7} 1/^\circ\text{C}$ | $0.003 \cdot 10^{-6} L$ |
| Inaccuracy of measuring the linear expansion factor of the scale | R | $5 \cdot 10^{-8} 1/^\circ\text{C}$ | 100 | $\Delta t L$ $\Delta t = 0.1^\circ\text{C}$ | $0.005 \cdot 10^{-6} L$ |
| Inaccuracy of the scale adjusting | R | $5.8 \cdot 10^{-4}$ rad | 100 | L | $0.17 \cdot 10^{-6} L$ |
| Abbe error | R | $9.6 \cdot 10^{-7}$ rad | 100 | 1 | 10 |
| Inaccuracy of determining the mark's centre | R | 10 nm | 100 | 1 | 10 |

Combined standard uncertainty: $u_c(L) = \sqrt{(20\text{nm})^2 + (0.17 \cdot 10^{-6} L)^2}$

Effective degree of freedom: $\nu_{\text{eff}}(dL) = 29$

Expanded uncertainty: $U_{0.95} = 2\sqrt{(20\text{nm})^2 + (0.17 \cdot 10^{-6} L)^2}$

OMH Hungary

| | Input quantity x_i | Distributio n | $u(x_i)$ unit | ν_i | $c_i = \partial dL / \partial x_i$ | $u_i(dL)$ [nm] |
|----|--|------------------|---------------|----------|------------------------------------|-------------------|
| 1 | λ_0 vacuum wavelength of HP 5528 laserinterfero | Normal | 6,0E-08*L | | 1 | 6,0E-08*L |
| 2 | Index of refraction of air n_{air} | Rectang. | 1,0E-08*L | ∞ | 1 | 1,0E-08*L |
| 3 | Air temperature t_{air} | Rectang. | 0,020 | ∞ | 1E-06*L | 2,0E-08*L |
| 4 | Air pressure P_{air} | Rectang. | 0,108 | ∞ | -3E-08*L | -3,23E-08*L |
| 5 | Air humidity RH_{air} (U=1,25%) | Normal | 0,169 | ∞ | 1E-08*L | 1,69E-10*L |
| 6 | Compensation factor of laserinterferometer | Rectang. | 0,058 | ∞ | 1E-08*L | 5,77E-08*L |
| 7 | Interferometer resolution δL_{Res} | Rectang. | 6 | ∞ | 1 | 6 |
| 8 | Interferometer dead path influences δL_{DP} | Rectang. | 11 | ∞ | 1 | 11 |
| 9 | Drift influence | Rectang. | 17 | ∞ | 1 | 17 |
| 10 | ABBE error in the xy plane | Rectang. | 23 | ∞ | 1 | 23 |
| 11 | ABBE error in the xz plane | Rectang. | 3 | ∞ | 1 | 3 |
| 12 | Cosine error of scale alignment in the xy plane | Rectang. | 3E-11 | ∞ | L | 3,32E-11*L |
| 13 | Cosine error of scale alignment in the xz plane | Rectang. | 6E-11 | ∞ | L | 5,89E-11*L |
| 14 | Cosine error of interferometer alignment | Rectang. | 3E-09 | ∞ | L | 3,12E-09*L |
| 15 | Linear expansion coefficient of the scale materia | Rectang. | 5,77E-07 | ∞ | -0,054*L | 1,8E-08*L |
| 16 | Difference of the scale temperature from the refe | Rectang. | 0,11 | ∞ | -5E-07*L | -5,53E-09*L |
| 17 | Length difference of scale position (standing or l | Rectang. | 5,00 | ∞ | 1 | 5 |
| 18 | Standard deviation max (*) | Normal | 94 | 19 | 1 | 94 |

*Note: In the line of 18: the maximum standard deviation is used (94 nm)

Combined standard uncertainty: $u_c(L) = Q[100; 9.4E-08 L]$ nm $L=[\text{nm}]$

Effective degree of freedom: $\nu_{\text{eff}}(dl) = 25 (L=100 \text{ mm})$ $k=2.11$

Expanded uncertainty: $U_{95}(dl) = Q[211; 2E-07 L]$ nm $L=[\text{nm}]$

PTB Germany

| name and symbol x_i (unit) | Dist. | x_i | for 100 mm | | const $u_i(dl)$ /nm | rel. to L $u_i(dl)*E9$ /L |
|---|-------|-----------------------|---|------------------|---------------------------|-----------------------------------|
| | | | $c_i = du(x_i)/dx_i$ | $u_i(dl)$ /nm | | |
| Translation stage: | | | | | | |
| Abbe offset $y, z, A_y, A_z = 1\text{ mm}, 2\text{ mm}$, Yaw and Pitch of x-axis $\delta_{yaw} (\mu\text{rad}) = 0.1$ and $\delta_{pitch} (\mu\text{rad}) = 0.1$ | R | 0.1 | 1 nm/urad | 0.06 | 0.14 | |
| | R | | 2 nm/urad | 0.12 | | |
| Interferometer: | | | | | | |
| Refractive Index (due to rest gas, in hPa) | R | 0.005 | 270 nm L/(m hPa) | 0.078 | | 0.78 |
| Vacuum Pressure (hPa) | R | 0.001 | 270 nm L/(m hPa) | 0.016 | | 0.16 |
| Interf. Deadpath L_{DP} (20 mm), pressure stab. during measurement 0.001 mbar | R | 20 | 270 nm L_{DP} /(m hPa) | 0.003 | 0.003 | |
| Interf. cosine error forw. beam δ_{θ_i} (μrad) back. beam | R | 15.2 | - | | 0.0003 | 0.003 |
| | | 30.54 | - | | | |
| Beam diffraction, $w_{\text{beam}} = 11\text{ mm}$ | R | 11 | - | 0.004 | | 0.04 |
| Vacuum wavelength λ_0 ($\Delta\lambda/\lambda = 1.4 \times 10^{-11}$) | R | 1.4×10^{-11} | L | 0.001 | | 0.01 |
| Wavefront deformation | N | 1×10^{-9} | L | 0.1 | | 1 |
| Nonlinearities (nm) | R | 0.1 | 1 | 0.06 | 0.06 | |
| Microscope: | | | | | | |
| Defocus (observed dependence): 27 nm / $3\ \mu\text{m}$, $\Delta x = 3 \times \Delta z^2\ \text{nm}/\mu\text{m}^2$, $\Delta z_{\text{max}} = 0.5\ \mu\text{m}$ | R | 0.5 | - | 0.45 | 0.45 | |
| Microscope mode dependence | R | 15 | 1 | | 8.7 | |
| Reference line | R | 15 | 1 | | 8.7 | |
| Scale properties: | | | | | | |
| Scale alignment horiz. $\Delta y = 0.5\ \mu\text{m}$, vert. $\Delta z = 0.5\ \mu\text{m}$ | R | 0.5 | - | 0.0004 | | 0.004 |
| | | 0.5 | | 0.0009 | | 0.009 |
| Scale alignment, position of support points, 1 mm interval | R | 1 | - | | 3.9 | |
| Unc. thermal exp. coef. $u_\alpha = 5 \times 10^{-8}/\text{K}$, $T_{\text{max}} - 20\ \text{C} < 0.06\ \text{K}$ | R | 5×10^{-8} | $0.06\text{L} \times \text{K}$ | 0.173 | | 1.73 |
| Temperature measurement, 10mK $\alpha = 5 \times 10^{-7}/\text{K}$ | R | 10 | $0.5 \times \text{L nm}/(\text{m K})$ | 0.29 | | 2.9 |
| Pressure measurement $u_{\text{pres}} = 0.6\ \text{hPa}$, $\chi = -8.9 \times 10^{-10}/\text{hPa}$ | N | 0.60 | $-0.89 \times \text{L nm}/(\text{m hPa})$ | 0.06 | | 0.6 |
| Unc. Compressibility $u_\kappa = 8.9 \times 10^{-11}/\text{hPa}$ ($\Delta p = 40\ \text{hPa}$) | R | 8.9×10^{-11} | 40hPa L | 0.21 | | 2.1 |

| name and symbol x_i (unit) | Dist. | x_i | for 100 mm | | const $u_i(dl)$ /nm | rel. to L $u_i(dl)*E9$ /L |
|--|---|-------|----------------------|------------------|---------------------------|-----------------------------------|
| | | | $c_i = du(x_i)/dx_i$ | $u_i(dl)$ /nm | | |
| Measurement: | | | | | | |
| Reproducibility (4 nm, n=9) | N | 1.33 | 1 | 1.33 | 1.33 | |
| Contamination at lines (0.2,0.4,0.5,0.7) | R | 60 | | | 29 | |
| Total $u_c(1\sigma)$ | | | 13 (31.8) nm | | | |
| Total U_{95} | | | 30.8 (75.4) | | | |
| General Expression | $U_{95} = 2.37 \times Q[13(32); 4.1E-9 \times L]$ | | | | | |

Effective degrees of freedom: 8

SMU Slovakia

| Input quantity x_i | Distrib. | $u(x_i)$ unit | ν_i | $c_i = \partial dL / \partial x_i$ | $u_i (dL) / \text{nm}$ |
|---|----------|------------------------------------|---------|---------------------------------------|------------------------|
| s_E repeatability of edge detection | N | 28 nm | 15 | 1 | 28 |
| $\delta_{E,def}$ edge geometry influence | R | 10 nm | > 100 | 1 | 10 |
| $\delta_{E,adj}$ influence of a djustment of measurement line | N | 10 nm | > 100 | 1 | 10 |
| $\delta_{E,foc}$ influence of focal length variation | N | 20 nm | > 100 | 1 | 20 |
| $\delta_{E,align}$ microscope axis align. | R | 15 nm | > 100 | 1 | 15 |
| $\delta_{E,rev}$ influence of measurement in reversed orientation | R | 22 nm | > 100 | 1 | 22 |
| λ_0 vacuum wavelength | N | 10^{-9} | > 1000 | L | $10^{-9} L$ |
| n_{air} refractive index of air ¹ incl correction to HP software error | N | $4 \cdot 10^{-5}$ | > 1000 | L | $4 \cdot 10^{-5} L$ |
| t_{air} air temperature incl. gradient and drift | R | 50 mK | > 100 | $-9,5 \cdot 10^{-7} \text{ K}^{-1} L$ | $4,8 \cdot 10^{-5} L$ |
| p_{air} air pressure incl. drift | R | 10 Pa | > 100 | $2,7 \cdot 10^{-9} \text{ Pa}^{-1} L$ | $2,7 \cdot 10^{-5} L$ |
| RH_{air} air humidity incl. gradient and drift | R | 3% | > 100 | $8,5 \cdot 10^{-9} \%^{-1} L$ | $2,6 \cdot 10^{-5} L$ |
| c_{CO_2} air CO ₂ concentration incl. drift | R | 0,02% (estimated, not measured) | - | $4,5 \cdot 10^{-7} \%^{-1} L$ | $9 \cdot 10^{-9} L$ |
| δ_{Res} interferometer resolution | R | 10 nm | > 1000 | $0,5 / \sqrt{3}$ | 3 |
| δ_{NL} interferometer nonlinear. | N | 6 nm | > 1000 | 1 | 6 |
| δ_{Ai} errors due to Abbe offsets and pitch and yaw of translation stages | R | 100 μrad | > 100 | - | $4 \cdot 10^{-9} L$ |
| δ_{Si} errors of scale alignment | R | 100 μrad | 10 | $(\gamma_i^2 / 2\Lambda_i) \cdot L$ | $4 \cdot 10^{-9} L$ |
| δ_{Ii} cosine errors of interferometer alignment | R | 250 μrad | 10 | $(\gamma_i^2 / 2\Lambda_i) \cdot L$ | $2,5 \cdot 10^{-5} L$ |
| $\alpha_{z,C}$ linear coefficient of thermal expansion | R | $2 \cdot 10^{-7} \text{ K}^{-1}$ | - | $ 20 - T_m \cdot L$ | $2,8 \cdot 10^{-5} L$ |
| $\Delta t_i = (t_i - 20)$ incl. gradient and drift | R | 100 mK | > 100 | $\alpha_z \cdot L$ | $5 \cdot 10^{-5} L$ |
| $\kappa_{z,C}$ linear coefficient of compressibility | R | 10^{-7} bar^{-1} | - | $u_p \cdot L$ | $4,5 \cdot 10^{-12} L$ |
| δ_{supp} influence of support conditions | R | 0,5 mm | 10 | - | 1 |

Combined standard uncertainty: $u_c(L) = \sqrt{46^2 + (0,094^2) \cdot L^2}$ nm (L in mm)

Effective degree of freedom: $\nu_{\text{eff}}(dl) \approx 500$

Expanded uncertainty: $U_{95}(dl) = \sqrt{92^2 + (0,19^2) \cdot L^2}$ nm (L in mm)

ZMDM Serbia

| Input quantity x_i | Distrib. | $u(x_i)$ unit | ν_i | $c_i = \partial dL / \partial x_i$ | $u_i (dL) / \text{nm}$ |
|---|----------|-----------------------------------|---------|------------------------------------|------------------------|
| Vacuum wavelength of laser, λ_0 | R | $4 \cdot 10^{-9}$ | 100 | 1 L | $4 \cdot 10^{-9} L$ |
| Interferometer resolution, δ_{Res} | R | 3 nm | 100 | 1 | 3 |
| Index of refraction of air, n_{air} | N | $1 \cdot 10^{-8}$ | 100 | 2 L | $1 \cdot 10^{-8} L$ |
| Air temperature, t_{air} | R | 0.1 °C | 8 | $9.5 \cdot 10^{-7} L$ | $9.5 \cdot 10^{-8} L$ |
| Air pressure, p_{air} | R | 30 Pa | 8 | $2.7 \cdot 10^{-9} L$ | $8.1 \cdot 10^{-8} L$ |
| Air humidity, RH_{air} | R | 3% | 5 | $1 \cdot 10^{-8} L$ | $3 \cdot 10^{-8} L$ |
| Air CO ₂ concentration, c_{CO_2} | R | 120 ppm | 5 | $1.5 \cdot 10^{-10} L$ | $2 \cdot 10^{-8} L$ |
| Linear coefficient of thermal expansion, α | N | $5 \cdot 10^{-7} \text{ °C}^{-1}$ | 10 | $0.2 L$ | $1 \cdot 10^{-7} L$ |
| Scale temperature difference, Δt_s | N | 0.1 °C | 8 | $5 \cdot 10^{-7} L$ | $5 \cdot 10^{-8} L$ |
| Interferometer alignment, δ_{Ii} | R | 200 μrad | 15 | $x_i^2/2 L$ | $4 \cdot 10^{-8} L$ |
| Scale alignment, δ_{Si} | R | 200 μrad | 10 | $x_i^2/2 L$ | $4 \cdot 10^{-8} L$ |
| Errors due to Abbe offsets and pitch and yaw, δ_{Ai} | R | 20 nm | 10 | 1 | 20 |
| Microscope axis alignment, δ_{Ealig} | R | 30 nm | 10 | 1 | 30 |
| Repeatability of center line detection | N | 80 nm | 20 | 1 | 80 |
| Drift influence (incl. deadpath) | R | 50 nm | 20 | 1 | 50 |
| | | | | | |
| | | | | | |
| | | | | | |
| | | | | | |
| | | | | | |
| | | | | | |
| | | | | | |
| | | | | | |

Combined standard uncertainty: $u_c(L) = Q[101; 0.19L]$ nm, L in mm

Effective degree of freedom: $\nu_{\text{eff}}(dl) = [42, 48L]$ L in m

Expanded uncertainty: $U_{95}(dl) = Q[202; 0.38L]$ nm, L in mm

GROUP 2**A*Star – NMC Singapore**

| Input quantity x_i | Distrib | $u(x_i)$ unit | ν_i | $c_i = \partial dL / \partial x_i$ | $u_i (dL) / \text{nm}$ |
|--|---------|--|---------|---|------------------------|
| Vacuum wavelength, λ_o | R | $3 \times 10^{-8} \lambda_o$ | 50 | L/λ_o | 0.03L |
| Interferometer resolution, δ_{Res} | R | 24 nm | 100 | 1 | 24 |
| Cosine errors of interferometer alignment, δ_{Ii} | R | 230 μrad | 50 | $400 \times 10^{-6} L/\text{rad}$ | 0.1L |
| Air temperature, t_{air} | R | 0.21 $^{\circ}\text{C}$ | 10 | $9.2 \times 10^{-7} L/^{\circ}\text{C}$ | 0.19L |
| Air pressure, p_{air} | R | 21 Pa | 10 | $2.9 \times 10^{-9} L/\text{Pa}$ | 0.061L |
| Air humidity, RH_{air} | R | 2.3 %rh | 10 | $8.9 \times 10^{-9} L/\%rh$ | 0.02L |
| Index of refraction of air, n_{air} | R | 2.4×10^{-7} | 10 | L | 0.24L |
| Edlen equation, n_{Edl} | R | 1×10^{-8} | 100 | L | 0.01L |
| Air CO ₂ concentration, c_{CO2} | R | 1×10^{-4} | 10 | $1.5 \times 10^{-4} L$ | 0.015L |
| Errors due to horizontal Abbe offsets ($\alpha_h \leq 1\text{mm}$), δ_{Aih} | R | 60 μrad | 50 | α_h | 60 |
| Errors due to vertical Abbe offsets ($\alpha_v \leq 0.5\text{mm}$), δ_{Aiv} | R | 60 μrad | 50 | α_v | 30 |
| Errors of scale alignment, δ_{Si} | R | 50 μrad | 100 | $50 \times 10^{-6} L/\text{rad}$ | 0.003L |
| Interferometer dead path, δ_{DP} | R | 32 nm | 50 | 1 | 32 |
| Thermal expansion coefficient of scale, $\alpha_{z, Cr}$ | R | $3 \times 10^{-8} \text{ }^{\circ}\text{C}^{-1}$ | 50 | $0.5L/^{\circ}\text{C}^{-1}$ | 0.015L |
| Temperature difference of the scale from 20 $^{\circ}\text{C}$, Δt_s | R | 0.2 $^{\circ}\text{C}$ | 10 | $5 \times 10^{-7} L/^{\circ}\text{C}$ | 0.10L |
| Repeatability of edge detection, s_E | N | 50 nm | 13 | 1 | 50 |
| Standard deviation of four repeat measurements, L_m | N | 65.5 nm | 3 | 1 | 65.5 |
| | | | | | |

Combined standard uncertainty: $u_c(dL) = [(115)^2 + (0.35L)^2]^{1/2}$, L in mm

Effective degree of freedom: $\nu_{\text{eff}}(dL) = 30$ at L = 100 mm

Expanded uncertainty: $U_{95}(dL) = [(230)^2 + (0.70L)^2]^{1/2}$ (k=2)

CEM Spain

| Input quantity x_i | Distrib. | $u(x_i)$ unit | ν_i | $c_i = \partial dL / \partial x_i$ | $u_i(dL) / \text{nm}$ |
|---|----------|---------------------------|---------|------------------------------------|-----------------------|
| Laser indication on reference line i | N | 22,2 nm | 9 | 1 | 22,2 |
| Laser indication on reference line 0 | R | 1,44 | >100 | 1 | 1,44 |
| Laser wavelength | N | 1,50e-09 | >100 | 1,58e+03 L | 2,37e-06 L |
| Index of refraction of air (initial reading of TRACKER) | N | 3,52e-08 nm | >100 | 1,00e+06 L | 0,035 L |
| Thermal coefficient of line scale | R | 5,77e-08 °C ⁻¹ | >100 | 1,00e+05 L °C | 5,77e-03 L |
| Temperature deviation of line scale from 20 °C | R | 0,116 °C | >100 | 0,5 L °C ⁻¹ | 0,058 L |
| TRACKER Accuracy (1) | R | 8,08e-08 L | >100 | 1 | 0,081 L |
| Optics (2) | R | 3,7 nm | >100 | 1 | 3,7 nm |
| Dead path | R | 8,1 nm | >100 | 1 | 8,1 nm |
| Comparator misalignment (maximum for flat mirrors) (2) | R | 2,89e-08 L | >100 | 1 | 2,89e-02 L |
| Misalignment of the line scale | R | 1,02e-07 nm | >100 | 1 | 1,02e-01 L |
| Optic set of line position | N | 15,3 nm | 49 | 1 | 15,3 nm |

(1) "Achieving Maximum Accuracy and Repeatability with the Agilent 5527A/B Laser Position Transducer System", Product Note.

(2) Optics and Laser Heads for Laser-Interferometer Positioning Systems, Product Overview, Agilent Technologies.

Combined standard uncertainty: $u_c(L) = Q [28.43; 0.15 \text{ L/mm}] \text{ nm}$

Effective degrees of freedom: $\nu_{\text{eff}}(dl) = 42$

Expanded uncertainty: $U_{95}(dl) = Q [60; 0.3 \text{ L/mm}] \text{ nm}$

CENAM México

| Input quantity, x_i | Distribution | $u(x_i)$ | ν_i | $c_i = \frac{\partial dL}{\partial x_i}$ | $u_i^2(dL)$ nm | |
|---|--------------|-------------|---------|--|-------------------|---------|
| | | | | | Independent | $*L^2$ |
| Repeatability of edge detection | N | 120 | 11 | $(1 + \alpha_{\text{scale}} * \Delta T)$ | 14 293 | |
| Microscope magnification | R | 52 | 12 | 1 | 2 700 | |
| Microscope axis alignment | R | $4,4^{-7}$ | 100 | L | | 0,19 |
| Line edge detection | R | 29 | 100 | 1 | 833 | |
| Microscope calibration | R | 5,77 | 100 | $(1 + \alpha_{\text{micro}} * \Delta T)$ | 1 168 | |
| Linear coefficient of thermal expansion of microscope scale | R | $4,62^{-7}$ | 100 | $\Delta T * L$ | | 0,034 |
| Difference of the microscope temperature | R | 0,29 | 100 | $\alpha_{\text{micro}} * L$ | | 3,4 |
| Linear coefficient of thermal expansion of scale | R | 4^{-8} | 100 | $\Delta T * L$ | | 0,00026 |
| Difference of the scale temperature | R | 0,29 | 24 | $\alpha_{\text{scale}} * \Delta T$ | | 0,026 |

Combined Standard Uncertainty: $u_c(L) = \sqrt{18994 + 3,8 * L^2}$

$u_c(L)$ in nm

L in mm

EIM Greece

| Input quantity x_i | Distrib. | $u(x_i)$ unit | ν_i | $c_i = \partial dL / \partial x_i$ | $u_i (dL) / \text{nm}$ |
|----------------------------------|----------|--------------------------|---------|------------------------------------|------------------------|
| Displacement Measurement | R | 1ppm | 50 | 1 | l |
| <i>Artifact Temperature</i> | R | 0.15 °C | 50 | $a * l$ | $0.075 * l$ |
| <i>Zero Line center estimate</i> | R | 0.200 μm | 50 | 1 | 200 |
| <i>Line center estimate</i> | R | 0.200 μm | 50 | 1 | 200 |
| <i>Scale alignment</i> | R | $1.25 \cdot 10^{-9} * l$ | 50 | 1 | $0.001 * l$ |
| | | | | | |
| | | | | | |
| | | | | | |
| | | | | | |
| | | | | | |

L in mm

Combined standard uncertainty: $u_c(L) = \sqrt{283^2 + L^2}$ (nm), L in mm

Effective degree of freedom: $\nu_{\text{eff}}(dl) = 123$ for $dl=100$ mm

Expanded uncertainty: $U_{95}(dl) = 2 * u_c(L)$

INMETRO Brazil1. L from 0 mm to 55 mm

| Input Quantity x_i | Distrib. | $U(x_i)$ unit | ν_i | $c_i = \partial dL / \partial x_i$ | $u_i (dL) / \text{nm}$ |
|-------------------------------|----------|-----------------|---------|------------------------------------|------------------------|
| Repeatability | N | 19 nm | 9 | 1 | 19 nm |
| Resolution | R | 1 nm | | 1 | 0,577 nm |
| Variation in indication | R | 2 nm | | 1 | 1,155 nm |
| Laser alignment | R | 0,0001 nm | | 1 | 0,00005 nm |
| Dead length | R | 1 nm | | 1 | 0,788 nm |
| Errors of scale alignment | R | 0,02 nm | | 1 | 0,012 nm |
| Edge detection | T | 130 nm | | 1 | 53,072 nm |
| focal length variation | R | 50 nm | | 1 | 46,189 nm |
| Air temperature | N | 0,017 °C | | 9,28E-07 (1/°C) | 0,434 nm |
| Air pressure | N | 10,9 (Pa) | | 2,68E-09 (1/Pa) | 0,806 nm |
| Escale temperature | N | 0,010 °C | | 5,00E-07 (1/°C) | 0,137 nm |
| Thermal expansion coefficient | N | 0,000001 (1/°C) | | 5,46E-01 (°C) | 15,015 nm |
| Partial vapor pressure | N | 16,374 (Pa) | | 3,71E-10 (1/Pa) | 0,167 nm |
| ----- | ----- | ----- | | ----- | ----- |

Combined standard uncertainty:

$$u_c(dl) = 63 \text{ nm} ; 0\text{mm} \leq L \leq 55\text{mm}$$

Effective degree of freedom:

$$\nu_{\text{eff}}(dl) = \infty$$

Expanded uncertainty:

$$U_{95}(dl) = 126 \text{ nm}$$

2. L above 55 mm mm to 100 mm

| Input quantity x_i | Distrib. | $u(x_i)$ unit | ν_i | $c_i = \partial dL / \partial x_i$ | $u_i(dL) / \text{nm}$ |
|-------------------------------|----------|-----------------|---------|------------------------------------|-----------------------|
| Repeatability | N | 10 nm | 9 | 1 | 10 nm |
| Resolution | R | 1 nm | | 1 | 0,577 nm |
| Variation in indication | R | 20 nm | | 1 | 11,547 nm |
| Laser alignment | R | 0,0001 nm | | 1 | 0,00005 nm |
| Dead length | R | 1nm | | 1 | 0,788 nm |
| Errors of scale alignment | R | 0,02 nm | | 1 | 0,012 nm |
| edge detection | T | 200 nm | | 1 | 81,650 nm |
| focal length variation | R | 50 nm | | 1 | 28,868 nm |
| Air temperature | N | 0,017 °C | | 9,28E-07 (1/°C) | 0,789 nm |
| Air pressure | N | 10,9 (Pa) | | 2,68E-09 (1/Pa) | 1,465 nm |
| Escale temperature | N | 0,010 °C | | 5,00E-07 (1/°C) | 0,250 nm |
| Thermal expansion coefficient | N | 0,000001 (1/°C) | | 5,46E-01 (°C) | 27,30 nm |
| Partial vapor pressure | N | 16,374 (Pa) | | 3,71E-10 (1/Pa) | 0,303 nm |
| ----- | ----- | ----- | | ----- | ----- |

Combined standard uncertainty: $u_c(dl) = 92 \text{ nm}; 55\text{mm} < L \leq 100\text{mm}$

Effective degree of freedom: $\nu_{\text{eff}}(dl) = \infty$

Expanded uncertainty: $U_{95}(dl) = 184 \text{ nm}$

INRIM Italy

| name and symbol x_i | distrib. | $u(x_i)$ unit | ν_i | $c_i = \partial dl / \partial x_i$ | $u_i(dl) / \text{nm}$ L in mm |
|---|----------|------------------------------------|---------|------------------------------------|------------------------------------|
| edge detection repeatability between series | N | 40 nm | 30 | 1 | 40 |
| interferometer digital resolution | R | 2,9 nm | 100 | 1 | 2,9 |
| vacuum wavelength | N | 5 fm | 100 | L | $7 \cdot 10^{-3} \cdot L$ |
| air refractive index | N | $2,3 \cdot 10^{-8}$ | 100 | L | $23 \cdot 10^{-3} \cdot L$ |
| interferometer non-linearity | R | 1 nm | 50 | 1 | 1 |
| interferometer deadpath | R | 2,4 nm | 100 | 1 | 2,4 |
| linear coefficient of thermal expansion (α) of scale | N | $2 \cdot 10^{-8} \text{ K}^{-1}$ | 50 | $(t_s - 20) \cdot L$ | $1 \cdot 10^{-3} \cdot L$ |
| difference of the scale temperature from the reference temperature during measurement | N | 0,013 K | 50 | $\alpha \cdot L$ | $6,5 \cdot 10^{-3} \cdot L$ |
| linear coefficient of compressibility (k) of the scale material | N | $1 \cdot 10^{-12} \text{ Pa}^{-1}$ | 50 | $(101325 - p) L$ | $1 \cdot 10^{-3} \cdot L$ |
| variations of air pressure during measurement | N | 0,3 kPa | 50 | $k \cdot L$ | $2,7 \cdot 10^{-3} \cdot L$ |
| Abbe offsets and pitch and yaw of translation stages | R | | 100 | | 7 |
| Imperfect alignment of scale (laser) with respect to meas. direction | R | | 100 | | $50 \cdot 10^{-3} \cdot L$ |
| imperfect alignment in direction and height of the linescale | R | | 15 | | $26 \cdot 10^{-3} \cdot L$ |
| Microscope axis alignment and straightness of translation stage | R | | 10 | | $15 + 0,18 \cdot L$ |

Formula or expression of uncertainty shall be given in the same way as for MRA C:

Combined standard uncertainty: $u_c(dl) = 48 \text{ nm} \quad (L=100 \text{ mm})$

Effective degree of freedom: $\nu_{\text{eff}}(dl) = 50$

Expanded uncertainty: $U_{95}(dl)/\text{nm} = Q[90, 0.4 L] ; L$ in mm
 $= 98 \text{ nm} \quad (L=100 \text{ mm})$

NIM China

| Input quantity x_i | Distrib | $u(x_i)$ unit | i_i | $c_i = \partial dL / \partial x_i$ | $u_i (dL) / \text{nm}$ |
|---------------------------|---------|---|----------|---|--------------------------|
| \ddot{e}_0 | R | $1.73 \times 10^{-8} \ddot{e}_0$ | 50 | dL / \ddot{e}_0 | $1.73 \times 10^{-8} dL$ |
| n_{air} | N | 1×10^{-8} | 12.5 | dL | $1.00 \times 10^{-8} dL$ |
| t_{air} | R | $0.0115 \text{ }^\circ\text{C}$ | 12.5 | $0.930 \times 10^{-6} dL \text{ }^\circ\text{C}^{-1}$ | $1.07 \times 10^{-8} dL$ |
| RH_{air} | R | 23.09 Pa | 12.5 | $0.371 \times 10^{-9} dL \text{ Pa}^{-1}$ | $0.86 \times 10^{-8} dL$ |
| C_{CO_2} | N | 60×10^{-6} | 6500 | $1.45 \times 10^{-4} dL$ | $0.87 \times 10^{-8} dL$ |
| P_{air} | R | 15 Pa | 12.5 | $2.683 \times 10^{-9} dL \text{ Pa}^{-1}$ | $4.03 \times 10^{-8} dL$ |
| S_E | N | 0.48 | 39 | $\ddot{e}_0 / 8$ | 38 |
| \ddot{A}_{t_s} | R | $0.0058 \text{ }^\circ\text{C}$ | 12.5 | $5.0 \times 10^{-7} dL \text{ }^\circ\text{C}^{-1}$ | $0.29 \times 10^{-8} dL$ |
| $\dot{a}z, cr$ | N | $1.17 \times 10^{-8} \text{ }^\circ\text{C}^{-1}$ | 50 | $0.026 \text{ }^\circ\text{C} \times dL$ | $0.03 \times 10^{-8} dL$ |
| $\ddot{a}l_{\text{DP}}$ | R | 0.8nm | 2 | 1 | 1 |
| $\ddot{a}l_{\text{Res}}$ | R | 3nm | ∞ | 1 | 3 |
| $\ddot{a}E_{\text{alig}}$ | R | 12nm | 12.5 | 1 | 12 |
| $\ddot{a}E_{\text{res}}$ | R | 0.289 | ∞ | $\ddot{e}_0 / 8$ | 23 |
| $\ddot{a}l_{\text{Ai}}$ | R | 6nm | 12.5 | 1 | 6 |
| $\ddot{a}l_{\text{NL}}$ | R | 12nm | 12.5 | 1 | 12 |
| $\ddot{a}l_{\text{li}}$ | R | $3.6 \times 10^{-10} dL$ | 12.5 | 1 | $0.04 \times 10^{-8} dL$ |
| $\ddot{a}l_{\text{Si}}$ | R | $2.4 \times 10^{-10} dL$ | 12.5 | 1 | $0.03 \times 10^{-8} dL$ |
| D | R | 0.0116mm | 50 | $1 \times 10^{-7} dL \text{ mm}^{-1}$ | $0.12 \times 10^{-8} dL$ |

D -Diameter of diaphragm for incidence light

Combined standard uncertainty: $u_c = \sqrt{(48 \text{ nm})^2 + (4.80 \times 10^{-8} dL)^2} = 48.3 \text{ nm} \approx 49 \text{ nm}$

Effective degree of freedom: $i_{\text{eff}}(dL) = 95$

Expanded uncertainty: $U_{95}(dL) = 98 \text{ nm}$

NIST USA

Description of the measurement uncertainty

Results of the measurements are given on the following pages of this report. The length values are the mean of eight measurements and the expanded uncertainty is

$$U_{95} = k u_c$$

and the combined standard uncertainty is

$$u_c = \sqrt{(u_i^2 + u_j^2)}$$

where u_i is the type-A standard uncertainty and u_j is the type-B standard uncertainty. A coverage factor $k=2.36$ was used which gives for the reported value a level of confidence of 95 percent.

The u_i uncertainty was derived from the measurement result and includes several input quantities which cannot be separated. These uncertainties include those contributed by laser interferometer polarization mixing, scale surface and graduation lines quality, measurement repeatability, line edge detection and line center derivation, measured length difference between normal and reverse scale orientation, measured length deviation due to sudden pressure changes during interferometer readings, and vibrational noise in the measurement system, just to mention a few.

The u_i standard uncertainty is one standard deviation of the mean value and is computed from the formula

$$u_i = \frac{\sqrt{\sum \frac{d^2}{N-1}}}{\sqrt{N}}$$

where d is the deviation of a single measurement from the mean, $N-1$ is the number of degrees of freedom (7) and N is the number measurements (8).

We measured the scale in two interval groups. In group one we measured from 0 to 1 mm at each 0.1 mm interval. In group two we measured from 0 to 100 mm at each 5 mm interval. In each interval group the u_i values are reported as the RMS values of all u_i values within that group.

The u_j standard uncertainty was derived from the sum of several estimated systematic uncertainties present in the measurement system:

$$u_j = \sqrt{(u_{\lambda_0}^2 + u_{n_{ref}}^2 + u_{t_s}^2 + u_{t_r}^2 + u_p^2 + u_{rh}^2 + u_{co_2}^2 + u_{align}^2 + u_{\alpha}^2)}$$

Description of the measurement uncertainty (cont.)

where the estimated systematic uncertainties are

| | |
|-------------|---|
| λ_0 | the vacuum wave length of the laser (20 nm/m) |
| n_{tpf} | the refractive index equation (20 nm/m) |
| t_a | the air temperature in the interferometer path (less than 1 nm/m) |
| t_s | the scale temperature (1 nm/m for quartz or Zerodur) |
| p | the atmospheric pressure in the laboratory (20 nm/m) |
| rh | the Relative Humidity in the measuring chamber (10 nm/m) |
| co_2 | the carbon dioxide in the laboratory (10 nm/m) |
| $align.$ | the interferometer and scale alignments (20 nm/m) |
| α | the expansion coefficient of the scale (less than one nm/m) |

$u_j = 50 \text{ nm / m}$ was used in the measurements

Measurement results for: #2, 100 mm Quartz Scale, Group #1 intervals

| Nominal length L (mm) | Measured deviation dL (nm) | Nominal length L (mm) | Measured deviation dL (nm) |
|--------------------------|-------------------------------|--------------------------|-------------------------------|
| 0 | 0, per definition | 0.6 | 4.9 |
| 0.1 | 36.0 | 0.7 | -15.1 |
| 0.2 | 1.2 | 0.8 | 18.2 |
| 0.3 | 16.7 | 0.9 | -11.3 |
| 0.4 | 4.4 | 1.0 | 30.3 |
| 0.5 | -11.2 | | |

All length deviation values are referred to the position of the zero reference line, thus the uncertainty of determination of the reference line position has to be taken into account for the uncertainty estimation of the measured deviations from nominal lengths.

Combined standard uncertainty: $u_c(dL) = [(3.1 \text{ nm})^2 + (5 \times 10^{-8} \times L)^2]^{1/2}$

Effective degree of freedom: $\nu_{\text{eff}}(dL) = 7$

Expanded uncertainty: $U_{95}(dL) = [(3.1 \text{ nm})^2 + (5 \times 10^{-8} \times L)^2]^{1/2} \times [2.36]$

Measurement results for: #2, 100 mm Quartz Scale, Group #2 intervals.

| Nominal length L (mm) | Measured deviation dL (nm) | Nominal length L (mm) | Measured deviation dL (nm) |
|--------------------------|-------------------------------|--------------------------|-------------------------------|
| 0 | 0, per definition | 55 | -131.7 |
| 5 | 20.7 | 60 | -153.1 |
| 10 | 24.9 | 65 | -111.2 |
| 15 | -19.4 | 70 | -129.0 |
| 20 | 27.3 | 75 | -146.2 |
| 25 | -116.6 | 80 | -125.3 |
| 30 | -145.8 | 85 | -125.4 |
| 35 | -119.3 | 90 | -313.4 |
| 40 | -119.3 | 95 | -266.3 |
| 45 | -183.1 | 100 | -249.6 |
| 50 | -110.8 | | |

All length deviation values are referred to the position of the zero reference line, thus the uncertainty of determination of the reference line position has to be taken into account for the uncertainty estimation of the measured deviations from nominal lengths.

$$\text{Combined standard uncertainty: } u_c(dL) = [(3.7 \text{ nm})^2 + (5 \times 10^{-8} \times L)^2]^{1/2}$$

$$\text{Effective degree of freedom: } v_{\text{eff}}(dL) = 7$$

$$\text{Expanded uncertainty: } U_{95}(dL) = [(3.7 \text{ nm})^2 + (5 \times 10^{-8} \times L)^2]^{1/2} \times [2.36]$$

NMi-VSL Netherlands

| Input quantity x_i | Distrib. | $u(x_i)$ unit | ν_i | $c_i = \partial dL / \partial x_i$ | $u_i (dL) / \text{nm}$ |
|--|----------|------------------------------------|---------|--|------------------------------|
| Interferometer resolution | R | 0,4 nm | inf | 1 | 0,4 nm |
| Repeatability edge detection | N | 12 nm | 93 | 1 | 12,0 nm |
| Wavelength | | | | | |
| Laser | R | $3,1 \cdot 10^{-9}$ | inf | L | $3,1 \cdot 10^{-9} \cdot L$ |
| Air temperature | R | 0,051 K | inf | $9,6 \cdot 10^{-7} \text{ K}^{-1} \cdot L$ | $4,9 \cdot 10^{-9} \cdot L$ |
| Air pressure | R | 22 Pa | inf | $2,7 \cdot 10^{-9} \text{ Pa}^{-1} \cdot L$ | $5,8 \cdot 10^{-8} \cdot L$ |
| Air humidity | R | 2,0 %RH | inf | $8,5 \cdot 10^{-9} \text{ %RH}^{-1} \cdot L$ | $1,7 \cdot 10^{-8} \cdot L$ |
| CO ₂ content | R | 58 ppm | inf | $1,5 \cdot 10^{-10} \text{ ppm}^{-1} \cdot L$ | $8,4 \cdot 10^{-9} \cdot L$ |
| Edlen equation | R | $1,0 \cdot 10^{-8}$ | inf | L | $1,0 \cdot 10^{-8} \cdot L$ |
| Dead path ($L_{dp}=10 \text{ mm}$) | | | | | |
| Air temperature drift | R | 0.051 K | inf | $9,6 \cdot 10^{-7} \text{ K}^{-1} \cdot L_{dp}$ | 0,5 nm |
| Air pressure drift | R | 5.8 Pa | inf | $2,7 \cdot 10^{-9} \text{ Pa}^{-1} \cdot L_{dp}$ | 0,2 nm |
| Air humidity drift | R | 1.7 %RH | inf | $8,5 \cdot 10^{-9} \text{ %RH}^{-1} \cdot L_{dp}$ | 0,1 nm |
| CO ₂ content drift | R | 58 ppm | inf | $1,5 \cdot 10^{-10} \text{ ppm}^{-1} \cdot L_{dp}$ | 0,1 nm |
| Alignment | | | | | |
| Scale to SIP 400 | R | $4,2 \cdot 10^{-10}$ | inf | L | $4,2 \cdot 10^{-10} \cdot L$ |
| Laser to SIP 400 | R | $1,0 \cdot 10^{-10}$ | inf | L | $1,0 \cdot 10^{-10} \cdot L$ |
| Interferometer optics | R | 0,1 nm | inf | 1 | 0,1 nm |
| Material temperature | | | | | |
| Scale | R | 0,087 K | inf | $5,0 \cdot 10^{-7} \text{ K}^{-1} \cdot L$ | $4,3 \cdot 10^{-8} \cdot L$ |
| Expansion coefficient | R | $1,4 \cdot 10^{-7} \text{ K}^{-1}$ | inf | 0,015 K | $2,2 \cdot 10^{-9} \cdot L$ |
| Local heating | R | 0,194 K | 150 | $5 \text{ nm} \cdot \text{K}^{-1}$ | 1,0 nm |
| Abbe error | R | 17,3 nm | inf | 1 | 17,3 nm |

Combined standard uncertainty: $u_c(L) = 21 \text{ nm} + 9,0 \cdot 10^{-8} \cdot L$

Effective degree of freedom: $\nu_{\text{eff}}(dl) = 890$

Expanded uncertainty: $U_{95}(dl) = 42 \text{ nm} + 1,8 \cdot 10^{-7} \cdot L$

NPLI India

| <i>Source of uncertainty</i> | x_i | $\pm u(x_i)$ | ν_i | $c_i = \partial L_i / \partial x_i$ | $\pm u_i(dL_i)$ <i>nm</i> |
|------------------------------|-----------------------------------|-------------------------------------|----------|--|------------------------------|
| Edge detection | 0 nm | 144 nm | 16.5 | 1 | 144 |
| Alignment | 0 nm | 0.288 μ rad/m | Infinite | L | 288 L |
| Thermal Expansion | $5 \times 10^{-7} \text{ K}^{-1}$ | $2.8 \times 10^{-8} \text{ K}^{-1}$ | Infinite | $L \text{ m} \times 0.5 \text{ K}$ | 14 L |
| Temperature variation | 0 °C | 0.28 K | Infinite | $L \text{ m} \times 5 \times 10^{-7} \text{ K}^{-1}$ | 140 L |
| Laser interferometer | 100 mm | 50 nm/m | Infinite | $L \text{ m}$ | 50 L |
| Repeatability | 0 | 187 nm | 20 | 1 | 187 |
| | | <i>veff.</i> | 36 | | |
| | | <i>t distribution</i> | 2 | $u_c(dL)$ | 239 |

Combined standard uncertainty (k=1) $u_c(dL) = \pm [(236)^2 + (324L)^2]^{1/2}$

Combined standard uncertainty (k=1) $u_c(dL) = \pm 239 \text{ nm}$ at $L = 100 \text{ mm}$

NRC Canada

No budget was reported. Only report in the form of tabular values for single measurement points was sent:

$U = 80 \text{ nm}$ (at 0,1 mm) to 89 nm (at 100 mm)

The following explanation was given:

“The NRC long-bed comparator was still under development at the time of measurement and an uncertainty model was not developed at that time. The cited uncertainty was based on repeatability & reproducibility data, plus allowances for some instrument problems we were suspecting at the time.”

NIMT Thailand

| Input quantity x_i | Distrib | $u(x_i)$ unit | ν_i | c_i | u_i (dL)/ nm | |
|--|-------------|--------------------|----------|-------------|----------------|----------------|
| l_s | Normal | 5.00E-10 λ | ∞ | l/λ | | 5.00E-10 l |
| δl_d | Rectangular | 7.84E-09 λ | ∞ | l/λ | | 7.84E-09 l |
| $\delta l_{stability}$ | Rectangular | 1.27E-10 λ | ∞ | l/λ | | 1.27E-10 l |
| δl_{ip} | Rectangular | 1.67E-09 λ | ∞ | l/λ | | 1.67E-09 l |
| δl_{is} | Rectangular | 0.231 nm | ∞ | 1 | 0.231 | |
| δl_{ind} | Normal | 5.814 nm | 5 | 1 | 5.814 | |
| δl_{rep} | Normal | 18.000 nm | ∞ | 1 | 18.000 | |
| δl_{abbe} | Rectangular | 7.136 nm | ∞ | 1 | 7.136 | |
| δl_{mis} | Rectangular | 2.89E-09 l | ∞ | 1 | | 2.89E-09 l |
| δl_{cos} | Rectangular | 4.41E-11 l | ∞ | 1 | | 4.41E-11 l |
| δl_{edge} | Rectangular | 0.185 nm | ∞ | 1 | 0.185 | |
| δl_{α} | Rectangular | 2.89E-07 | ∞ | 2.0E-01 l | | 5.77E-08 l |
| $\delta l_{\Delta t}$ | Normal | 1.00E-02 | ∞ | 5.0E-07 l | | 5.00E-09 l |
| δl_{drift} | Rectangular | 1.15E-02 | ∞ | 5.0E-07 l | | 5.77E-09 l |
| $\delta l_{stability}$ | Rectangular | 1.15E-02 | ∞ | 5.0E-07 l | | 5.77E-09 l |
| $\delta l_{difference}$ | Rectangular | 1.73E-02 | ∞ | 5.0E-07 l | | 8.66E-09 l |
| $\delta l_{\alpha \Delta t}$ | Rectangular | 2.89E-09 | ∞ | l | | 2.89E-09 l |
| $\delta l_{\alpha drift(\Delta t)}$ | Rectangular | 3.33E-09 | ∞ | l | | 3.33E-09 l |
| $\delta l_{\alpha stability(\Delta t)}$ | Rectangular | 3.33E-09 | ∞ | l | | 3.33E-09 l |
| $\delta l_{\alpha difference(\Delta t)}$ | Rectangular | 5.00E-09 | ∞ | l | | 5.00E-09 l |
| δl_{uuc} | Rectangular | 5.77E-11 l | ∞ | 1 | | 5.77E-11 l |
| δl_{op} | Rectangular | 2.56E-09 l | ∞ | 1 | | 2.56E-09 l |
| $\delta l_{compression}$ | Rectangular | 5.14E-07 l | ∞ | 1 | | 5.14E-07 l |
| | | | | | 408.81 | 2.68E-13 l^2 |
| u_c | | | | | 20.22 | 5.17E-07 l |
| $U(l_x)$ | | | | $k=2$ | 40.44 | 1.03E-06 l |
| | | | | | 41.0 | 1.03E-06 l |

Combined standard uncertainty: $u_c(L) = Q[20.5, 0.517 \cdot L]$ nm L indication in mm
 Effective degree of freedom: $\nu_{eff}(dL) = 9893.8$
 Expanded uncertainty: $U_{95}(dL) = Q[41, 1.03 \cdot L]$ nm L indication in mm

VNIIM Russia

| name and symbol x_i | dist rib. | $u(x_i)$ unit | ν_i | $c_i =$ $\partial dl / \partial x_i$ | $u_i(dl) / \text{nm}$ |
|---|--------------|-------------------------|---------|---|-----------------------|
| <i>Length independent</i> | | | | | |
| δ_{Edef} Edge geometry influence (roughness, parallelism) | N | 9 nm | 10 | 1 | 9 |
| δ_{Eloc} Influence of focal length variation | N | 1 μm | 5 | 0.002 | 2 |
| δ_{Ealig} Microscope axis alignment | R | 1 mrad | >100 | δ_{Estr} | 1 |
| δ_{Res} Interferometer resolution | N | 0.1 nm | 5 | 1 | 0.1 |
| δ_{NL} Interferometer nonlinearity | N | 1 nm | 5 | 1 | 1 |
| δ_{Ai} Errors due to Abbe offsets and pitch and yaw of translation stages | R | 0.2 mm | >100 | δ_{Erot} | 1 |
| <i>Length dependet</i> | | | | | |
| λ_0 vacuum wavelength of light source used for displacement measurement | N | 3E-8 | 10 | L | 3E-8 * L |
| n_{air} Index of refraction of air | N | 1.3E-7 | 10 | L | 1.3E-7 * L |
| δ_{Ii} Cosine errors of interferometer alignment | R | 0.1 mrad | >100 | $(\delta_{Ii}/2)$ $*L$ | 5E-9 * L |
| δ_{Si} Errors of scale alignment | R | 0.02 mrad | >100 | $(\delta_{Si}/2)$ $*L$ | 4E-10 * L |
| α Linear coefficient of thermal expansion of scale material | N | 0.01 K | 10 | $\alpha * L$ | 5E-9 * L |
| $\Delta t_s = (t_s - 20)$ is the difference of the scale temperature t_s in °C during the measurement from the reference temperature of 20 °C | N | 3E-8 K ⁻¹ | 10 | $(t_s - 20)$ $*L$ | 3E-9 * L |

Combined standard uncertainty: $u_c(dl) = 10 \text{ nm} + 1.5 * 10^{-7} * L$ (from 10 nm to 25 nm)

Effective degree of freedom: $\nu_{\text{eff}}(dl) = 22$

Expanded uncertainty: $U_{95}(dl) = 20 \text{ nm} + 3 * 10^{-7} * L$ (from 20 nm to 50 nm)